



THE UNIVERSITY *of* EDINBURGH

This thesis has been submitted in fulfilment of the requirements for a postgraduate degree (e.g. PhD, MPhil, DClinPsychol) at the University of Edinburgh. Please note the following terms and conditions of use:

This work is protected by copyright and other intellectual property rights, which are retained by the thesis author, unless otherwise stated.

A copy can be downloaded for personal non-commercial research or study, without prior permission or charge.

This thesis cannot be reproduced or quoted extensively from without first obtaining permission in writing from the author.

The content must not be changed in any way or sold commercially in any format or medium without the formal permission of the author.

When referring to this work, full bibliographic details including the author, title, awarding institution and date of the thesis must be given.

Bioassay-guided phytochemical study of indigenous medicinal plants of Ethiopia

Ketema Tolossa Gutu

Thesis submitted in partial fulfilment of the requirements for
the degree of Doctor of Philosophy

University of Edinburgh

2017



Declaration

I declare that this thesis is my own composition, and the research contained within it is my own work, except where acknowledged. The work that has been described in this thesis has not been submitted for any other degree or professional qualification.

Ketema Tolossa Gutu

Acknowledgments

Over the past three-and-a-half years, I have received support and encouragement from a number of individuals/organizations. Understandably, my words and statements indicated below cannot cover all of the contributions.

I wish to express my sincere gratitude to Professor Stephen Fry (Edinburgh Cell Wall Group, University of Edinburgh) and Professor Jos Houdijk (Monogastric Science Research Centre/Disease Systems Team, SRUC), my supervisors, for their willingness to accept me as their PhD student, allowing me to do my research in their labs under multidisciplinary settings, their continuing follow up, advice, critical comments on conference abstracts, thesis chapters and overall guidance.

I owe special thanks to Professors Ensermu Kelbessa and Sebsebe Demisse School of Biological Sciences and Mr. Melaku Wondafrash from the National Herbarium for enthusiastic help in identification of plant samples.

My thanks also goes out to all members of ECWG and IMPS (University of Edinburgh) and Disease Systems Team and Monogastric Science Research Centre (SRUC) for their friendly support and help whenever and wherever assistance was required.

I would like to thank Dr Ian Sadler and Dr Lorna Murray (School of Chemistry, University of Edinburgh) for the NMR experiments and Dr Logan Mackay (School of Chemistry for the MS experiments. The staffs of the March building (University of Edinburgh) are thanked for the excellent husbandry of the mice. I gratefully acknowledge the funding from BBSRC/DFID (UK AID) and Scottish Government (CIDLD project) and SRUC's International Engagement Strategy for the studentship that made these studies possible. I am also thankful to financial support from

Worshipful Company of Woolmen for co-funding the second field trip for sample collection and from SRUC Trust Fund for providing the unique opportunity to attend and present at the biannual meeting of the International Society for Ethnopharmacology, in Petra, Jordan.

Dr. Spiridoula Athanasiadou is thanked for her help in inoculating the donors, advising me on RTCA software, analysing RTCA data using R software and being my co-supervisor. My fellow PhD student Sokratis Ptochos is thanked for training me on how to recover eggs and larvae and how to set up both EHI and LMI assays. Professor Gary Loake, my co-supervisor also deserves special thanks for his critical comments on my 10 month report to enrich my PhD project plan.

The great administrative support of Mrs Sheila Davidson, Carol Virtue and Audrey Johnson deserves special appreciation for their kindness and help in all aspects. Professor Adugna Tolera is thanked for the cause for my PhD study and encouraging me and my family during my PhD study. Thank you! Sister Hirut, Mimi, Dhunfa and Reta for visiting my family and encouraging them in my absence.

The traditional healers, Noh and Boru are thanked for sharing their indigenous knowledge and willingness to get the plant samples for this study. In particular, Mr. Boru deserves my special gratitude and appreciation for traveling six days on foot with me in search of *Adenia* sp. and saved me not to be bitten by Cobra snake in such scorching sun in a very low land pastoral area where there is no access to roads.

My mother (Kumeshi), brother (Geremew) and sisters (Kebebush, Zewditu and Derebu) and my nephews (Wayessa and Diribe) are thanked for their unconditional love, prayers and support.

Above all, my extraordinary gratitude goes to my beloved wife, Kassech (Chaltu), for her love, understanding, pray and encouragement. Chale, your spiritual strength and confidence in taking many responsibilities in my absence and letting me to concentrate on my work deserves a special heartfelt thanks and admiration. Thank you Chale koo! Waaqayyo saa'eebisu. I know things were not as easy as we thought. The question of long journey (at least for both of us) is going to be answered soon with the help of God. Looking forward to hug you and Yerosan, our lovely son, a blessing from God!

Abstract

In many developing countries, farmers and pastoralists still rely on their indigenous knowledge, practices and locally available plants to control nematode parasitic infections, both in livestock and humans. The overall aim of my thesis was to undertake bioassay-guided phyto-chemical study of extracts and their constituents from Ethiopian anti-parasitic plants used by healers to control gastrointestinal nematode parasites in livestock to validate their ethno-medicinal use and to characterise and identify their active ingredients.

As a first experiment (Chapter Three), four types of crude extracts (water, 70% methyl-alcohol, absolute methanol and acetone) of four indigenous Ethiopian medicinal plants (*Adenia* species, *Cissus ruspolii*, *Ipomoea eriocarpa* and *Euphorbia thymifolia*) were screened against *Teladorsagia circumcincta* egg hatching *in vitro*, not only as a first step to validate the traditional healers claim but also to choose the most promising plant extract(s) for further phyto-chemical studies. The egg hatching inhibition (EHI) test results revealed that the anti-parasitic properties of these plants depended on plant species, dose, and solvent polarity. The water extracts of both *C. ruspolii* and *Adenia* sp. exhibited largest, up to 100% EHI but also larval migration inhibition activities, and were selected for further studies. The second experiment (Chapter Four) assessed the nature of active constituents in these extracts by physico-chemical methods. It was observed that the major constituents of both plant extracts responsible for the EHI activities are likely highly polar, water-soluble, small and moderately heat-labile molecules. The third and fourth experiments (Chapters Five and Six) consisted of separating *Cissus ruspolii* and *Adenia* sp. water extracts into discrete fractions by gel-permeation chromatography, EHI tests of Bio-Gel P-2

fractions followed by thin layer chromatography (TLC) profiling of these fractions to detect separated spots (in day light, under UV-light or after staining with various staining reagents) and also to see how elution patterns of separated spots affected by column parameters. The EHI tests on the fractions obtained revealed that the active constituents of *C. ruspolii* and *Adenia* sp. water crude extracts were eluted into few fractions based on their molecular sizes. The TLC profilings of these fractions identified spot patterns of active and inactive fractions, which allowed pooling of active constituents based on their EHI and TLC profiling into three pools for each plant. The fifth experiment (Chapter Seven) was to isolate and purify compounds from these pools using various preparative planar and column chromatographic methods. Sequential applications of column chromatography followed by preparative thin layer chromatography isolated and purified five active compounds from *C. ruspolii* and two active compounds from *Adenia* sp. The sixth experiment (Chapter Eight) was to characterize and propose/elucidate structures of compounds from the active fractions using chromatographic, analytical and spectroscopic methods. In this regard, the structures of two oleanane type triterpenoid saponins isolated from one of active fractions of *Adenia* sp. were proposed based on their mass spectrometry (MS) and nuclear magnetic resonance (NMR) data with support of compounds property, TLC and literature. Similar outcomes for *C. ruspolii* were not achieved due to lack of sufficient sample to run ^{13}C -nuclear magnetic resonance spectroscopy and distortionless enhancement by polarization transfer (DEPT), contamination of some purified compounds with ill-characterised substance from the preparative TLC matrix and in some cases mass spectrometry (MS) and nuclear magnetic resonance (NMR) data did not support each other. The last experiment (Chapter Nine) was to

assess anthelmintic efficacy and safety of *C. ruspolii* and *Adenia* sp. crude water extracts in *Heligmosomoides bakeri* infected mice. This *in vivo* test revealed that both plant extracts exhibited significant reduction in worm burdens and worm egg excretion, with moderate effects on haematology and organ weights at tolerated dosages.

In conclusion, both *in vitro* and *in vivo* data revealed that *Adenia* sp. and *C. ruspolii* have anthelmintic properties, thus validating traditional healer claims and supporting ethno-medicinal use. The bioassay-guided phytochemical study resulted in the isolation of a number of active compounds from these plants, for some of which a structure has been proposed.

List of Abbreviations

ASPA	<i>Adenia</i> sp. pool A
ASPALH-20	<i>Adenia</i> sp. pool A LH-20
ASPB	<i>Adenia</i> sp. pool B
ASPC	<i>Adenia</i> sp. Pool C
BAW	Butanol-acetic acid-water
CB	Chlorobutanol
CMA	Chloroform-methanol-acetic acid
CRPA	<i>Cissus ruspolii</i> pool A
CRPALH-20	<i>Cissus ruspolii</i> pool A LH-20
CRPB	<i>Cissus ruspolii</i> pool B
CRPBLH-20	<i>Cissus ruspolii</i> pool B LH-20
CRPC	<i>Cissus ruspolii</i> pool C
CRPCLH-20	<i>Cissus ruspolii</i> pool C LH-20
C	Carbon
C ₁₈	Reversed phase C-18 column
CID	Collision induced ionization
¹³ C-NMR	¹³ Carbon nuclear magnetic resonance
COSY	Correlation spectroscopy
1D	One dimensional
2D	Two dimensional
EHl	Egg hatching inhibition
FEC	Faecal egg count

FECR	Faecal egg count reduction
EPAW	Ethylacetat-pyridine-acetic acid-water
H	Proton
HMBC	Heteronuclear multiple bond correlation
HSQC	Heteronuclear spin quantum coherence
¹ H-NMR	Proton nuclear magnetic resonance
HVPE	High voltage paper electrophoresis
Hz	Hertz
LMI	Larval motility inhibition
<i>m/z</i>	Mass-to-charge ratio
NMR	Nuclear magnetic resonance
NOESY	Nuclear over hauser enhancement spectroscopy
MS	Mass spectrometry
PBS	Phosphate buffer saline
PSM	Plant secondary metabolites
PC	Paper chromatography
PE	Paper electrophoretogram
PTLC	Preparative thin layer chromatography
RTCA	Real time cell analyser
RP DSC-18	Reverse phase discovery C ₁₈ column
TFA	Trifluoroacetic acid
TWC	Total worm count
TWCR	Total worm count reduction

List of Tables

Table 1.1.	List of some <i>in vivo</i> studies of medicinal plants with purported anthelmintic properties.	20
Table 3.1.	Plant extract colour and yield from four Ethiopian plants with claimed anthelmintic properties.	73
Table 4.1.	Molecular size separation of constituents of water extracts by membrane dialysis.	91
Table 5.1.	The summary of effects of sample volumes loaded and column parameters on elution position of V_o , V_i and active pooled fractions of <i>C. ruspolii</i> runs 1-4.	120
Table 6.1.	The summary of effects of sample volumes loaded and column parameters on elution position of V_o and V_i and active pooled fractions of <i>Adenia</i> sp. runs 1-3.	137
Table 7.1.	Overall summary of chromatographic characterization and EHI tests of Sephadex LH-20 purified pooled fractions from CRPB.	176
Table 7.2.	Summary of spot colour and R_F -values of major constituents of Bio-Gel P-2 active pooled fractions of <i>C. ruspolii</i> and <i>Adenia</i> sp. examined under UV-light and after stained with universal reagents.	190
Table 9.1.	The effect of plant extracts on FEC (epg) at dissection.	268
Table 9.2.	The effect of plant extracts on total RBC and WBC differential blood counts at dissection.	275

List of Figures

Figure 1.1.	Life cycle representing gastrointestinal nematodes (order <i>Strongylida</i>) of small ruminants; adapted from Roeber <i>et al.</i> (2013) with permission.	6
Figure 1.2.	Chemical structures of representative conventional anthelmintics. Levamisole (a), ivermectins (b) and albendazole (c).	8
Figure 1.3.	Mevalonic acid pathway of terpenes biosynthesis. The phosphorylated intermediates, isopentenyl pyrophosphate (IPP) and dimethylallyl pyrophosphate (DMAPP) are combined to make monoterpenes (C ₁₀), sesquiterpenes (C ₁₅) and larger terpenes.	11
Figure 1.4.	The shikimic and malonic acids pathways of plant phenolics biosynthesis. In higher plants most phenolics compounds are derived at least in part from phenylalanine, a product of the shikimic acid pathway. Formulae in brackets indicate the basic arrangement of carbon skeletons: C ₆ indicates a benzene ring, and C ₃ is a three-carbon chain.	14
Figure 1.5.	<i>C. ruspolii</i> collected from Denbyte, Hamer District, and South Nation and Nationalities and People Regional State (SNNPRS) located at 03°43'54.6" N, 36°45'36" E and 1613 m altitude.	30
Figure 1.6.	<i>Adenia</i> sp. collected from Muktano, near to Sololo district, Ethio-Kenyan border located at 03°54'19.8" N, 38°56'29" E and 900 m altitude.	31
Figure 1.7.	<i>Ipomoea eriocarpa</i> collected from Beneta, Maalee district, and South Nation and Nationalities and People Regional State (SNNPRS) located at 03°43'36.2" N, 36°35'21" E and 1291 m altitude.	32
Figure 1.8.	<i>Euphorbia thymifolia</i> collected from Qarsa Danbi, Borana Zone, Oromia Regional State located at 03°45'20" N, 38°22'40" E and 1094 m altitude.	34
Figure 1.9.	Overall approach of my PhD project.	35
Figure 2.1.	Larval suspension preparation using baermannisation.	45
Figure 2.2.	The flow chart of larval motility monitoring by real time cell analyser.	47

Figure 2.3.	Bioassay guided fractionation of <i>C. ruspolii</i> water extract.	51
Figure 2.4.	Bioassay guided fractionation of <i>Adenia</i> sp. water extract.	52
Figure 2.5.	Flow diagram of isolation and purification of compounds A and B from <i>Adenia</i> sp. water extract.	58
Figure 3.1.	Schematic representation of crude extracts preparation by maceration.	69
Figure 3.2.	Schematic representation of parasite eggs recovery and EHI test.	70
Figure 3.3.	Schematic representation of the real time cell analyser setup used for the larval motility test.	70
Figure 3.4.	Mean of egg hatch inhibition (EHI) with standard error of the mean (n=3) of crude extracts. <i>Adenia</i> sp. (a), <i>Cissus ruspolii</i> (b), <i>Euphorbia thymifolia</i> (c) and <i>Ipomoea eriocarpa</i> (d). — Acetone — Methanol — 70% MeOH — Water.	76
Figure 3.5.	Egg hatch inhibition (EHI) with standard error of the mean of water crude extracts (n=3) of <i>Adenia</i> sp. (a) and <i>C. ruspolii</i> (b).	78
Figure 3.6.	Larval motility readouts of alive and dead larvae over 48 h with after 24 h the addition of <i>C. ruspolii</i> water extracts (a), <i>C. ruspolii</i> 70% MeOH extracts (b), <i>Adenia</i> sp. water extracts (c), and <i>Adenia</i> sp. acetone extracts (d). Legends are displayed in each figure; software settings could not be amended in order to use same legends in each graph.	81
Figure 4.1.	EHI of <i>T. circumcincta</i> incubated with low and high molecular weight membrane dialysis products. <i>Adenia</i> sp. (a) and <i>C. ruspolii</i> (b); negative control (H ₂ O).	92
Figure 4.2.	EHI and chromatograms of heat treated <i>Adenia</i> sp. water extract. Boiled full strength (BF) and one-fifth of BF (1/5 BF) and non-boiled full (NBF) and 1/5 NBF strengths. Chromatograms: thymol stained (b), molybdate (c) and ninhydrin (d). Chlorobutanol (0.05% w/v) and deionized water (H ₂ O) were used as negative controls. TLC was done only for the sample incubated at 100°C for 60 min.	94

Figure 4.3.	EHI and chromatograms of heat treated <i>C.ruspolii</i> water extract. The same condition as in Fig. 4.2. EHI (a) TLC under UV-366 nm (b); stained with ninhydrin (c) and thymol (d). BF and NBF stand for boiled and non-boiled samples at full and 1/5 dilutions.	95
Figure 4.4.	EHI and chromatograms of solvent partitioned fractions of <i>Adenia</i> sp. water extract. Butanol (BuOH), ethylacetate (EtOAc), H ₂ O _{Bu} (water from BuOH-H ₂ O solvent system), H ₂ O _{Et} (water from EtOAc-H ₂ O solvent system). EHI (a); thymol stained (b) and molybdate (c).	97
Figure 4.5.	EHI and chromatograms of solvent partitioned fractions of <i>C. ruspolii</i> . water extract. Butanol (BuOH), ethylacetate (EtOAc), H ₂ O _{Bu} (water from BuOH-H ₂ O solvent system), H ₂ O _{Et} (water from EtOAc-H ₂ O solvent system). EHI (a); thymol stained (b) and molybdate (c) under UV-366nm (d).	98
Figure 5.1.	The gel permeation chromatography (GPC) separation set up (SEC image search: https://www.medicinescomplete.com).	106
Figure 5.2.	TLC equipment and development set up.	107
Figure 5.3.	Flow diagram of Bio-Gel P-2 fractionation of <i>C. ruspolii</i> (run-4).	109
Figure 5.4.	EHI of Bio-Gel P-2 water fractions of <i>C. ruspolii</i> (run-1). Void volume (V ₀), included volume (V _i); 0.05% w/v chlorobutanol and deionized water are negative controls, <i>C. ruspolii</i> crude extract used as positive control.	111
Figure 5.5.	Chromatograms of Bio-Gel P-2 fractions (1-18) of <i>C. ruspolii</i> (run-1). Thymol stained (a), molybdate (b), ninhydrin (c), iodine (d) and before staining under UV-light at 366 nm (e). Marker mixture (MM): D-glucose (Glc), sucrose (Sucr), Leucine (Lue) and Ferulic acid. Fractions with EHI activitiy are labelled red.	112
Figure 5.6.	EHI of <i>C. ruspolii</i> Bio-Gel P-2 fractions (run-2). At full (■), 0.2 (■), 0.04 (■), 0.008 (■) strengths. <i>C. ruspolii</i> crude extract (positive control); chlorobutanol (0.05% w/v) and deionized water (H ₂ O) as negative controls. CRPA, CRPB, CRPC are <i>C. ruspolii</i> active pooled fractions.	114
Figure 5.7.	Chromatograms of Bio-Gel P-2 fractions (1-37) of <i>C. ruspolii</i> (run-2). Molybdate stained fractions 1-37 (a) and fractions 19-37 examined before staining under UV-light at 366 nm (b). Void volume (V ₀) and included volume (V _i). Fractions with EHI activity are underlined.	114

Figure 5.8.	R _F values of separated spots on TLC vs elution behaviour (K _{av} –values) on Bio-Gel P-2 column of <i>C. ruspolii</i> active pooled fractions. CRPA (—), CRPB (—), CRPC (—) are active pooled fractions. TLC was developed in BAW (4:1:1 v/v/v). This simple mapping done based on merging of chromatograms of runs 1 and 2.	115
Figure 5.9.	Chromatograms of Bio-Gel P-2 fractions of <i>C. ruspolii</i> (run-3). Developed in BAW (4:1:1 v/v/v) examined under UV-light at 366 nm (a, e and f) and 254 nm (b) and molybdate stained and heated at 105°C for 30 min. (c and d); void volume (V ₀) and included volume (V _i); CRPA, CRPB and CRPC are <i>C. ruspolii</i> pooled fractions; A, B, C and D are separated spots of crude (CRD) extract.	117
Figure 5.10.	Chromatograms of Bio-Gel P-2 fractions of <i>C. ruspolii</i> (run-4). Developed in BAW (4:1:1 v/v/v) and molybdate stained and heated at 105°C for 30 min. (a); examined under UV-light before molybdate staining at 366 nm (b) and 366 nm BW (c). Void volume (V ₀) and included volume (V _i). CRPA, CRPB and CRPC are <i>C. ruspolii</i> pooled fractions; crude extract (CRD).	119
Figure 6.1.	Flow diagram of Bio-Gel P-2 fractionation of <i>Adenia</i> sp. (run-2).	129
Figure 6.2.	EHI of Bio-Gel P-2 fractions of <i>Adenia</i> sp. (run-1). Void volume (V ₀) and included volume (V _i). Crude extract (positive control), chlorobutanol (0.05% w/v) and deionized water (H ₂ O) as negative controls.	131
Figure 6.3.	TLC profiles of Bio-Gel P-2 fractions (1-18) of <i>Adenia</i> sp. Stained with thymol (a), ninhydrin (b) iodine vapour (c). molybdate (d). Marker mixture (MM): D-glucose (Glc), sucrose (Sucr), luecine (Lue) and ferulic acid. Fractions with EHI activity are underlined.	132
Figure 6.4.	EHI tests of <i>Adenia</i> sp. Bio-Gel P-2 fractions (run-2). At full (■), 0.2 (■), 0.04 (■), 0.008 (■) strengths. <i>Adenia</i> sp. crude extract (positive control), chlorobutanol (0.05% w/v) and deionized water (H ₂ O) as negative control. ASPA, ASPB, ASPC are <i>Adenia</i> sp. pooled fractions.	133
Figure 6.5.	Molybdate stained chromatogram of Bio-Gel P-2 fractions of <i>Adenia</i> sp. (run-2). ASPA, ASPB, ASPC are <i>Adenia</i> sp. active pooled fractions.	134

Figure 6.6.	R _F -values of separated spots on TLC vs elution behaviour (K _{av} –values) on Bio-Gel P-2 column of <i>Adenia</i> sp. active pooled fractions. ASPA (—), ASPB (—), ASPC (—) are active pooled fractions. TLC was developed in BAW (4:1:1 v/v/v). This simple mapping done based on merging of molybdate stained chromatograms of run-1 and 2.	136
Figure 6.7.	Molybdate stained chromatograms of Bio-Gel P-2 fractions of <i>Adenia</i> sp. (run-3). Developed in BAW (4:1:1 v/v/v) dried and heated at 105°C for 30 min.; ASPA, ASPB and ASPC stand for <i>Adenia</i> sp. pooled fractions; A-G are separated spots of crude (CRD) extract.	137
Figure 7.1.	Adsorption and hydrogen bonding between compound and silica gel sorbent surface.	142
Figure 7.2.	Reversed phase C ₁₈ (modified silica stationary phase).	143
Figure 7.3.	Paper chromatogram of active pooled fractions of <i>C. ruspolii</i> and <i>Adenia</i> sp. Marker mixture (MM) contained caffeic and ferulic acids. Chromatogram under UV-light at 366 nm before exposed to ammonia vapour (a) and after being exposed to ammonia vapour (b). Blue and yellow spots are fluorescent compounds in CRPC.	146
Figure 7.4.	EHI of ASPC fractions eluted from paper chromatogram. First run (a) and repeated experiment (b).	148
Figure 7.5.	PTLC and TLC chromatograms of <i>C. ruspolii</i> extract and recovered bands. PTLC of crude extract at 366 nm (a) molybdate stained recovered bands (b) recovered fluorescent bands at 366 nm (c) molybdate stained fluorescent bands (d).	149
Figure 7.6.	Chromatograms of C ₁₈ fractions of <i>C. ruspolii</i> crude extract. Under UV-light at 366 nm (a) 366 nm BW (b) 254 nm (c) after molybdate stained (d). The 20, 40, 60 and 80 show percentages of methanol in the gradient eluents used.	151
Figure 7.7.	PTLCs of CRPC examined under UV-light at 366 nm. PTLC thickness 1 mm (a) and 0.5 mm (b). Fr-6 (a) corresponds to blue band (b) and Fr-10 (a) corresponds to yellow band (b).	152

Figure 7.8.	EHI of PTLC purified bands from active pooled fractions of <i>C. ruspolii</i> : CRPA (a), CRPB (b), CRPC (c) and pH of the recovered bands from CRPC (d). The band above the solvent front (Band-14) was used as negative control and crude extract as positive control. EHI tests of <i>C. ruspolii</i> (run-2) supernatants. At full (■), 0.5 (■), 0.25 (■), 0.125 (■) strengths. <i>C. ruspolii</i> crude and zolvix (positive control); chlorobutanol (0.05% w/v) and PBS as negative control.	154
Figure 7.9.	EHI tests of PTLC purified bands of active pooled fractions of <i>Adenia</i> sp. ASPA (a), ASPB (b), ASPC (c) and egg suspension incubated with recovered supernatant (d). At full (■), 0.5 (■), 0.25 (■), 0.125 (■) strengths. <i>Adenia</i> sp. crude and zolvix (positive control); chlorobutanol (0.05% w/v) and PBS as negative control.	156
Figure 7.10.	Vanillin stained chromatograms of Sephadex LH-20 water fractions from CRPA. A, B, C and D are separated spots.	158
Figure 7.11.	Vanillin stained chromatogram of Sephadex LH-20 fractions from CRPA. CRPA used as marker at full and diluted lower strengths. A, B and C are separated spots.	159
Figure 7.12.	Vanillin stained chromatogram of C ₁₈ purified fractions from CRPA. Chromatogram heated at 120°C for 3 h. 10 and 20 show 10% and 20% MeOH fractions. H ₂ O stands for water fractions. A, B, C are separated spots. The numbers 13-20 are Sephadex LH-20 water fractions of CRPA.	160
Figure 7.13.	Chromatogram of C ₁₈ water sub fractions (1-5) and 10 and 20% MeOH gradient pooled fractions from CRPA. A, B, C are separated spots.	161
Figure 7.14.	PTLC strips of C ₁₈ water fractions of CRPA. B-1 to B-5 show separated bands of fractions. The numbers 14, 16, and 17 are Sephadex LH-20 fractions.	162
Figure 7.15.	Vanillin stained chromatograms of supernatants recovered from PTLC purified bands from ASPA Sephadex LH-20 water fractions 14, 16 and 17. Arrows show spots of purified compounds. Chromatogram heated in oven at 120°C for 30 min. (a) and 3 h (b). Arrows and circles show purified compounds.	163
Figure 7.16.	EHI of PTLC purified compounds from CRPA with controls. PTLC matrix (band above the solvent front), 0.5PBS, H ₂ O and 0.05% chlorobutanol are negative controls; zolvix, crude, CRPA and water fractions of LH-20 and C ₁₈ fractions are positive controls. B ₁ , B ₃ , B ₄ and B ₅ are purified bands from LH-20 water fractions 14, 16 and 17.	164

Figure 7.17.	Molybdate stained chromatogram of Sephadex LH-20 water fractions from CRPB with crude extract (CRD) as marker. A, B, C show major separated spots of CRPB.	165
Figure 7.18.	Molybdate stained chromatogram of Sephadex LH-20 water fractions from CRPB (re-run) with CRPB as marker. A, B, C are major separated spots.	166
Figure 7.19.	The pH of Sephadex LH-20 water fractions of CRPB.	166
Figure 7.20.	EHI of Sephadex LH-20 fractions of CRPB and controls. De-ionized water and 0.5PBS (negative controls) and CRPB and Zolvix (positive control).	167
Figure 7.21.	Molybdate stained chromatogram of Sephadex LH-20 fractions (49-64) from CRPB. First run (a), re-run (b). Arrows show smears (a) and blue stained (b) in fractions (56-58).	168
Figure 7.22.	Mean percentage EHI of Sephadex LH-20 pooled fractions of CRPB. First run EHI (a) and repeated EHI (b). Eggs incubated with pooled fractions at full strengths (c and d) and eggs incubated with 0.5 PBS (e, negative control). Zolvix and CRPB were used as positive controls.	168
Figure 7.23.	Chromatogram of Sephadex LH-20 purified pooled fractions from CRPB and markers. Under UV-light at 366 nm (a), 254 nm (b), 254 BW (c) and in day light (d). Oleic acid, β -sitosterol, quercetin are markers. CRPB as control. The circled spot shows quercetin dihydrate. BW is black and white background.	170
Figure 7.24.	Iodine stained chromatogram of Sephadex LH-20 purified pooled fractions from CRPB and markers. β -sitosterol, oleic acid, quercetin and CRPB are markers. A, B, C and D are separated spots of CRPB.	171
Figure 7.25.	Vanillin re-stained chromatogram of Sephadex LH-20 purified pooled fractions from CRPB and markers. β -sitosterol, oleic acid, quercetin and CRPB are markers. Chromatogram heated at 120°C for 30 min. Arrows show purified spots.	172
Figure 7.26.	Molybdate stained chromatogram of Sephadex LH-20 purified pooled fractions from CRPB and markers. β -sitosterol, oleic acid, quercetin and CRPB are markers. Chromatogram was heated at 105°C for 3 h. Arrows show spots of purified compound.	172

Figure 7.27.	Antimony (III) chloride stained chromatogram of Sephadex LH-20 purified pooled fractions from CRPB and markers. Chromatogram heated at 100°C for 5 min. β -sitosterol, oleic acid, quercetin and CRPB are markers.	173
Figure 7.28.	Vanillin stained chromatograms of Sephadex LH-20 pooled fractions from CRPB and markers. β -sitosterol, oleic acid, quercetin and CRPB are markers. Chromatogram was developed in BuOH-HOAc-H ₂ O (4:1:1 v/v/v), dried and heated at 120°C for 30 min. (a) and 3 h (b).	174
Figure 7.29.	Vanillin stained chromatograms of Sephadex LH-20 purified compound(s) from CRPB and markers. Chromatogram was developed in CHCl ₃ -MeOH-HOAc (10:2:1 v/v/v), dried and heated at 120°C for 30 min. (a) and 3 h (b). Arrows show purified compound.	175
Figure 7.30.	Vanillin stained chromatograms and PTLC strips of purified compound(s) from CRPB. Both chromatograms were heated at 120°C for 3 h. Arrows and circles show purified compounds.	177
Figure 7.31.	Mean percentage EHI tests of PTLC purified compounds from CRPB and controls. PBS, H ₂ O, 0.05% CB (negative controls) and monepantel (positive control).	178
Figure 7.32.	Chromatograms of Sephadex LH-20 water fractions from CRPC and marker: Under UV-light 366 nm (a); vanillin stained and heated at 120°C for 30 min. (b). CRPC used as marker.	179
Figure 7.33.	Chromatograms of Sephadex LH-20 water fractions from CRPC: at UV-366 nm (a) vanillin stained and heated at 120°C for 30 min. (b).	179
Figure 7.34.	Chromatograms of Sephadex LH-20 water fraction-13 from CRPC further purified on C ₁₈ column. Chromatogram examined at 366 nm (a) vanillin stained and heated at 120°C for 30 min. (b).	180
Figure 7.35.	Chromatogram of CRPC replicates at UV-366 nm (a) at 366 nm BW (b). BW stands for black and white background at 366 nm.	182
Figure 7.36.	PTLC and TLC chromatograms of Sephadex LH-20 pooled fractions 12 and 14 from CRPC. Chromatograms were examined at UV-366 nm. B-1 and B-2 are separated bands.	182

Figure 7.37.	The EHI tests of PTLC purified compound(s) from CRPC. Crude extract, CRPC and Zolvix (positive controls); PBS, H ₂ O and 0.05% CB (negative controls). B-1 and B-2 are purified bands.	183
Figure 7.38.	Vanillin stained chromatograms of Sephadex LH-20 fractions from ASPA. Chromatogram heated at 120°C for 30 min.(a) 3 h (b). A to E are separated spots.	185
Figure 7.39.	Vanillin stained chromatograms of C ₁₈ water and methanol gradient fractions of ASPA. Chromatogram heated at 120°C for 30 min. (a) 3 h (b). A to E are separated spots.	186
Figure 7.40.	Vanillin stained chromatograms and PTLC strip of C ₁₈ fraction-2 from ASPA Sephadex LH-20 fraction-9. Chromatogram heated at 120°C for 30 min. (a) and 3 h (b). A and B are purified compounds.	188
Figure 7.41.	Vanillin stained chromatograms of white pellet recovered from ASPA Sephadex LH-20 pooled fraction (21-28). Chromatogram heated at 120°C for 30 min. (a) and 2 h (b).	188
Figure 7.42.	The EHI tests of PTLC purified compounds A and B from ASPA with both positive and negative controls.	189
Figure 7.43.	Molybdate stained chromatograms of <i>C. ruspolii</i> water crude extract and phosphates. Chromatogram in day light (a) after heating in oven at 120°C for 30 min (b) 3 h (c).	191
Figure 7.44.	The molybdate stained chromatograms of <i>C. ruspolii</i> water extract with markers. Sodium dihydrogen phosphate dihydrate and sodium pyrophosphate are markers: in day light (a) heated at 120°C for 30 min. (b) and 3 h (c).	191
Figure 7.45.	Molybdate stained electrophoretograms of <i>C. ruspolii</i> and sodium dihydrogen phosphate dihydrate at pH 2. Electrophoretogram before exposure to sun light (a) after exposure to sunlight (b).	192
Figure 7.46.	Molybdate stained electrophoretograms of <i>C. ruspolii</i> water crude extract and sodium dihydrogen phosphate dihydrate at pH 6.5. Electrophoretograms before exposure to sun light (a) after exposure to sunlight (b).	193
Figure 7.47.	Mean intensity of molybdate stained spots of standard sodium dihydrogen phosphate dihydrate versus their concentration.	194
Figure 7.48.	The plot of [Pi] vs volume of crude extract loaded onto PC.	195

Figure 8.1.	1D- ¹ H-NMR spectra of compound A (<i>Adenia</i> sp.) and blank. Spectrum of compound A (a) and of a control from a blank plate (b) (sample source is detailed in section 2.10 and Figure 2.5).	220
Figure 8.2.	1D- ¹ H-NMR spectra of compound B (<i>Adenia</i> sp.) and control. Spectrum of compound B (a), spectrum of control from blank plate (b) (sample source is detailed in section 2.10 and Figure 2.5).	220
Figure 8.3.	2D-COSY spectra of compound A (a) and compound B (b) from ASPA.	223
Figure 8.4.	MS spectrum of a mixture containing A and B of <i>Adenia</i> sp. (C ₁₈ water fraction-1) with characteristic ionic species and their unique molecular weight. The two major and closely migrating constituents of ASPA: Arrows show compound A (a) and compound B (b) to be selected by the first MS as precursor ions for CID mode of fragmentation in MS/MS spectrometry.	224
Figure 8.5.	MS spectrum of mass selected ions. Compound A (a) and compound B (b) from <i>Adenia</i> sp. selected by the first MS as precursor ions for CID mode of fragmentation in MS/MS spectrometry. The mass difference between A and B is 78.140 g/mole. Arrows show the mass selected ions.	225
Figure 8.6.	MS/MS spectrum of compound A (<i>Adenia</i> sp.) based on a selected parent ion mass. The diamond (♦) shows the mass of the presumed molecular ion (M ⁺) of compound A with m/z = 881.6748 g/mole; the most intense fragment peak derived from this, with [M+1] ⁺ at m/z 491.4047, is the base peak.	226
Figure 8.7.	MS/MS spectrum of compound B (<i>Adenia</i> sp.) based on the selected parent ion mass. The diamond (♦) shows the mass of molecular ion (M ⁺) of compound B with m/z = 803.5357 g/mole; the most intense fragment peak derived from this, with [M+1] ⁺ at m/z 413.2648, is the base peak.	227
Figure 8.8.	Proposed structures of compounds A and B (<i>Adenia</i> sp.) based on Scenario I.	229
Figure 8.9.	Chemical structures of oleanolic acid (a) and ursolic acid (b).	231
Figure 8.10.	The chemical formulae and proposed structures of triterpenoid aglycones, with (a) the aglycone of compound A and (b) the aglycone of compound B (<i>Adenia</i> sp.).	234

Figure 8.11.	Scenario I: Chemical formula and proposed structure of trisaccharide sugar moiety common to both compounds A and B (<i>Adenia</i> sp.).	235
Figure 8.12.	Proposed structures of compounds A and B (<i>Adenia</i> sp.) based on MS spectral data and chromatograms of TFA hydrolysates.	236
Figure 8.13.	Thymol stained chromatograms of TFA hydrolysed C ₁₈ water fractions 3 and 4 of ASPA. (a) developed in EPAW (6:3:1:1); (b) developed in BAW (2:1:1). Marker mixture: galactronic acid (GalA), glucuronic acid (GlcA), galactose (Gal), glucose (Glc), mannose (Man), arabinose (Ara), xylose (Xyl), unknown sugar (may be quinovose) and rhamnose (Rha).	237
Figure 8.14.	Proposed structure for compound A (<i>Adenia</i> sp.) and possible positions to accommodate more sugars.	239
Figure 8.15.	1D- ¹ H-NMR of compound A (<i>C. ruspolii</i>) and authentic β-cyclodextrin. Proton resonance signals of compound A after MS analysis (a), before MS analysis (b), authentic β-cyclodextrin (c).	242
Figure 8.16.	The DEPT-135 spectrum of compound A (<i>C. ruspolii</i>).	243
Figure 8.17.	1D- ¹ H-NMR of compound A (<i>C. ruspolii</i>).	244
Figure 8.18.	The COSY spectrum of compound A (<i>C. ruspolii</i>).	245
Figure 8.19.	The HSQC spectrum of compound A (<i>C. ruspolii</i>).	245
Figure 8.20.	The simulated molecular formula suggested for compound A (<i>C. ruspolii</i>).	246
Figure 8.21.	MS spectra of β-cyclodextrin (21a) and compound A in <i>C. ruspolii</i> (21b).	247
Figure 8.22.	¹ H-NMR spectrum of compound C (<i>C. ruspolii</i>).	251
Figure 8.23.	TOCSY irradiation of <i>C. ruspolii</i> compound C. The arrow shows the irradiation point and a, c, d, e, f, h, w and x are sequentially irradiated signals.	252
Figure 8.24.	2D-COSY spectra of compound C (<i>C. ruspolii</i>).	253
Figure 8.25.	HSQC spectrum of <i>C. ruspolii</i> compound C.	255

Figure 8.26.	Tentatively suggested structures of compound C present in <i>C. ruspolii</i> . Rhamnose attached to unknown non-sugar moiety (a), α -rhamnose attached to 1,2,3,4-tetrahydroxy-tetrahydrofuran (b) or β -rhamnose attached to 1,2,3,4-tetrahydroxy-tetrahydrofuran (c).	255
Figure 9.1.	Flow diagram of dose and dose frequencies of plant extracts. <i>Adenia</i> sp. (a) and <i>C. ruspolii</i> (b).	264
Figure 9.2.	The effect of extracts on egg out in mice infected with <i>H. bakeri</i> . Orally treated with water (—), <i>C. ruspolii</i> (—), <i>Adenia</i> sp.(—) or ivermectin (—) on days 0 (grouping and inoculation), 22 (before treatment), 29 (three days after first treatment) and 36 (at dissection or three days after second treatment).	269
Figure 9.3.	The effect of extracts on total worm burden in mice infected with <i>H. bakeri</i> .	270
Figure 9.4.	The effect of extracts on male and female <i>H. bakeri</i> in mice.	271
Figure 9.5.	The effect of extracts on mice body weight infected with <i>H. bakeri</i> . Orally treated with water (◆), <i>C. ruspolii</i> (▲), <i>Adenia</i> sp.(■) or ivermectin (×) on days 0 (grouping and inoculation), 22 (before treatment), 29 (three days after first treatment) and 36 (at dissection or three days after second treatment).	272
Figure 9.6.	The effect of extracts on organ weight in mice infected with <i>H. bakeri</i> . After oral treatment with water, <i>C. ruspolii</i> , <i>Adenia</i> sp. or ivermectin. Small intestine (a), liver (b), spleen (c) and kidney (d).	274

Table of Contents

Chapter One: General introduction and literature review

1.1.	Gastrointestinal nematodes in livestock	1
1.2.	Gastrointestinal nematode infection and epidemiological factors in small ruminants	2
1.3.	Life cycle of gastrointestinal nematodes of small ruminants	5
1.4.	Control methods of nematode infections in small ruminants	7
1.5.	Conventional anthelmintic drugs, mode of actions and anthelmintic resistance	7
1.6.	Plant secondary metabolites	9
1.7.	Terpenes and their roles in plants	10
1.8.	Phenolic compounds and their role in plants	13
1.9.	Nitrogen-containing compounds and their role in plants	17
1.10.	Medicinal plants as alternative or complementary anti-parasitic agents	18
1.11.	Anti-parasitic properties of plant secondary metabolites	22
1.11.1.	Alkaloids and other nitrogen containing compounds	22
1.11.2.	Essential oils and terpenoids	23
1.11.3.	Tannins	24
1.11.4.	Flavonoids and polyphenols	25
1.11.5.	Glycosides and saponins	26
1.12.	<i>In vitro</i> and <i>in vivo</i> validation of anti-parasitic plant extracts	27
1.13.	The classification, distribution, description and uses of the four plant species used in this study	28
1.13.1.	<i>Cissus ruspolii</i>	29
1.13.2.	<i>Adenia</i> sp.	30
1.13.3.	<i>Ipomoea eriocarpa</i>	31

1.13.4.	<i>Euphorbia thymifolia</i>	33
1.14.	Thesis hypotheses and objectives	35
1.14.1.	Overall hypotheses	35
1.14.2.	Specific objectives	36
Chapter Two: Materials and methods		
2.1.	List of materials and equipment	38
2.2.	List of solvents	38
2.3.	List of chemicals, reagents, pharmaceuticals and marker compounds	38
2.4.	Preparation of plant materials	39
2.4.1.	Selection	39
2.4.2.	Collection and identification	40
2.4.3.	Drying and grinding	40
2.4.4.	Preparation of crude extracts	41
2.5.	<i>In vitro</i> experiments	41
2.5.1.	Egg hatching inhibition test	41
2.5.1.1.	Egg recovery	41
2.5.1.2.	Egg suspension preparation	42
2.5.1.3.	Egg hatch inhibition (EHI) tests	42
2.5.2.	Larval motility inhibition test	44
2.5.2.1.	Larval suspension preparation (Baermann technique)	45
2.5.2.2.	RTCA monitoring of LMI activities of crude extracts	47
2.6.	Physico-chemical characterization of water extracts	48
2.6.1.	Membrane dialysis	48

2.6.2.	Heat stability testing	49
2.6.3.	Solvent partition	49
2.7.	Bioassay-guided size-fractionations	49
2.7.1.	Preparation of water extracts	49
2.7.2.	Fractionations of water extracts on gel-permeation chromatography	50
2.8.	Inorganic phosphate assessment in crude water extract of <i>C. ruspolii</i>	52
2.8.1.	TLC development and molybdate staining of <i>C. ruspolii</i> crude extract	52
2.8.2.	TLC development for serially diluted $\text{NaH}_2\text{PO}_4 \cdot 2\text{H}_2\text{O}$ and <i>C. ruspolii</i> extract	53
2.8.3.	1D-high voltage paper electrophoresis at pH 2.0 and pH 6.5	53
2.8.3.1.	Sample preparation, loading, and paper electrophoretogram development	53
2.8.3.2.	Staining reagent preparation and electrophoretogram staining protocol	54
2.9.	Chemical and chromatographic profiling of Bio-Gel P-2 fractions	54
2.9.1.	Sample preparations, loading, TLC development and staining	54
2.9.2.	Staining reagent preparations and staining procedures	55
2.9.2.1.	Molybdate reagent	55
2.9.2.2.	Iodine vapour	55
2.9.2.3.	Thymol reagent	56
2.9.2.4.	Ninhydrin reagent	56
2.9.2.5.	Antimony(III) chloride reagent	56
2.9.2.6.	Antimony(III) chloride-acetic acid reagent	56
2.9.2.7.	Vanillin reagent	57

2.10.	Isolation, purification and TLC profiling of compounds from pooled active Bio- Gel P-2 fractions	57
2.10.1.	Isolation and purification of compounds on Sephadex LH-20	58
2.10.2.	Further purification of LH-20 fractions on RP C ₁₈ column	59
2.10.3.	Further purification of compounds on preparative TLC	60
2.10.3.1.	Purification of C ₁₈ water fraction of ASPALH-20-9 by PTLC	60
2.10.3.2.	Purification of C ₁₈ water fractions of CRPALH-20 by PTLC	61
2.10.3.3.	Purification of C ₁₈ water and methanol fractions of CRPB	61
2.11.	NMR and MS analysis methods	61
2.12.	<i>In vivo</i> mice model experiment	62
2.12.1.	Animals and housing	63
2.12.2.	Preparation of infective L ₃ larvae of <i>H. bakeri</i>	63
2.12.3.	Mice handling during oral gavage	64
2.12.4.	Animal infection protocol	64
2.12.5.	Plant extracts and ivermectin stock solution preparation	64
2.13.	TFA hydrolysis of putative triterpene glycosides A and B from <i>Adenia</i> sp.	65
Chapter Three: <i>In vitro</i> screening of anti-parasitic activity of extracts from four Ethiopian medicinal plants		
3.1.	Abstract	66
3.2.	Introduction	67
3.3.	Materials and methods	69
3.3.1.	Extract preparation	69
3.3.2.	EHI and LMI assay	69
3.3.3	Calculations and statistics	71
3.4.	Results	72

3.4.1.	Yields of crude extracts	72
3.4.2.	EHI assays of crude extracts	74
3.4.3.	LMI assays of selected crude extracts	78
3.5.	Discussion	82
Chapter Four: Physico-chemical studies and EHI properties of crude extracts		
4.1.	Abstract	85
4.2.	Introduction	86
4.3.	Materials and methods	89
4.3.1.	Membrane dialysis	89
4.3.2.	Heat stability testing	89
4.3.3.	Solvent partition	89
4.3.4.	Thin layer chromatography	90
4.3.5.	Egg hatch inhibition	90
4.3.6.	Statistics	90
4.4.	Results	91
4.4.1.	Molecular sizes of constituents of extracts and their EHI assays	91
4.4.2.	Effect of heat on EHI properties of crude extracts	93
4.4.3.	Solvent partition of active constituents of crude extracts	96
4.5.	Discussion	99
Chapter Five: Bioassay-guided fractionation and chromatographic profiling of <i>C. ruspolii</i> water extract		
5.1.	Abstract	104
5.2.	Introduction	105
5.3	Materials and methods	108

5.3.1.	Crude extract preparation	108
5.3.2.	Gel-permeation chromatography	108
5.3.3.	Egg hatch inhibition	110
5.3.4.	Thin-layer chromatography	110
5.3.5.	Calculations and statistics	110
5.4.	Results	111
5.4.1.	EHI of <i>C. ruspolii</i> Bio-Gel P-2 fractions	111
5.4.2.	Chromatographic profiling of <i>C. ruspolii</i> Bio-Gel P-2 active fractions	115
5.5.	Discussion	121
Chapter Six:	Bioassay-guided fractionations of <i>Adenia</i> sp. extract and chromatographic characterisation of resultant fractions	
6.1.	Abstract	126
6.2.	Introduction	127
6.3	Materials and methods	128
6.3.1.	Crude extract preparation	128
6.3.2.	Gel-permeation chromatography	128
6.3.3.	Egg hatch inhibition	129
6.3.4.	Thin-layer chromatography	129
6.3.5.	Calculations and statistics	130
6.4.	Results	131
6.4.1.	Bio-Gel P-2 fractions of <i>Adenia</i> sp.	131
6.4.2.	Chromatographic profiling of <i>Adenia</i> sp. Bio-Gel P-2 active fractions	135
6.5.	Discussion	138

Chapter Seven: Isolation and purification of compounds from active pooled fractions of *C. ruspolii* and *Adenia* sp.

7.1.	Abstract	140
7.2.	Introduction	141
7.3.	Materials and methods	144
7.4.	Results	146
7.4.1.	Paper chromatographic profiling of pooled active fractions	146
7.4.2.	PTLC isolation and TLC profiling of <i>C. ruspolii</i> extract	149
7.4.3.	<i>C. ruspolii</i> extract purification on C ₁₈ column	150
7.4.4.	PTLC profiling of CRPC	151
7.4.5.	EHI tests of partially purified bands on PTLC from active pooled fractions of <i>C. ruspolii</i>	152
7.4.6.	EHI tests of partially purified bands from active fractions of <i>Adenia</i> sp.	155
7.4.7.	Isolation of constituents of <i>C. ruspolii</i> active fractions and their EHI tests	157
7.4.7.1.	Isolation and purification of CRPA constituents on Sephadex LH-20 column chromatography	157
7.4.7.2.	Further purification of fractions 13-20 from CRPA on RP C ₁₈ column	159
7.4.7.3.	Further purification of C ₁₈ water fractions of CRPA on PTLC	161
7.4.7.4.	The EHI tests of purified compounds from CRPA	163
7.4.8.	Isolation of constituents from CRPB and their EHI tests	164
7.4.8.1.	Isolation and purification of CRPB (Run-4) on Sephadex LH-20	164
7.4.8.2.	Chromatographic characterization of Sephadex LH-20 purified active pooled fractions of CRPB	169
7.4.8.2.1.	Visualization in day light and under UV-light	170

7.4.8.2.2.	Iodine vapours staining	171
7.4.8.2.3.	Re-staining of iodine stained chromatogram with vanillin reagent	171
7.4.8.2.4.	Molybdate staining	172
7.4.8.2.5.	Antimony (III) chloride staining	173
7.4.8.2.6.	Vanillin in conc. H ₂ SO ₄ staining	174
7.4.8.3.	Further purification of C ₁₈ purified compound(s) on PTLC	176
7.4.8.4.	The EHI tests of PTLC purified compound (s) from CRPB	177
7.4.9.	Isolation of active constituents from CRPC and their EHI tests	178
7.4.9.1.	Isolation and purification of CRPC on Sephadex LH-20 column chromatography	178
7.4.9.2.	Further purification of blue fluorescent compound on C ₁₈ column	180
7.4.9.3.	Further purification of blue fluorescent compound on PTLC	182
7.4.9.4.	The EHI tests of PTLC purified compounds from CRPC	183
7.4.10.	Isolation of active compounds from <i>Adenia</i> sp. active pooled fractions	184
7.4.10.1.	Isolation and purification of ASPA on Sephadex LH-20 column	184
7.4.10.2.	Further purification of water fraction from ASPA on C ₁₈ column	186
7.4.10.3.	Further purification of C ₁₈ water fraction on PTLC	187
7.4.10.4.	EHI tests of isolated and purified compounds from ASPA	189
7.4.11.	Qualitative characterization and semi-quantitative determination of yellow stained component of <i>C. ruspolii</i> extract	190
7.4.11.1.	Chromatogram profiling of yellow stained constituent of <i>C. ruspolii</i> extract	190
7.4.11.2.	HVPE analysis for P _i in <i>C. ruspolii</i> aqueous extract	192
7.4.11.3.	Semi-quantitative determination of the level of yellow stained constituent of <i>C. ruspolii</i> crude extract by colorimetric method	193
7.5.	Discussion	196

7.5.1.	PC isolation and profiling of active pooled fractions of <i>C. ruspolii</i> and <i>Adenia</i> sp.	196
7.5.2.	PTLC isolation and TLC profiling of <i>C. ruspolii</i> water crude extract	197
7.5.3.	<i>C. ruspolii</i> water crude extract purification on C ₁₈ column	198
7.5.4.	PTLC profiling of CRPC and EHI test	198
7.5.5.	EHI tests of partially purified bands from active fractions of <i>C. ruspolii</i>	199
7.5.6.	EHI tests of partially purified bands from active fractions of <i>Adenia</i> sp.	201
7.5.7.	Isolation of compounds from active pooled fractions of <i>C. ruspolii</i>	202
7.5.7.1.	Isolation and purification of compounds from <i>C. ruspolii</i> pool A (CRPA)	202
7.5.7.2.	Isolation and purification of compounds from CRPB	202
7.5.3.3.	Isolation and purification of compounds from CRPC	207
7.5.8.	Isolation and purification of compounds from <i>Adenia</i> sp. pool A (ASPA)	208
7.5.9.	The EHI tests of isolated compounds from <i>C. ruspolii</i> pooled fractions	209
7.5.10.	EHI tests of isolated and purified compounds from ASPA	210
7.5.11.	Qualitative characterization and semi-quantitative determination of yellow stained component of <i>C. ruspolii</i> extract	212

Chapter Eight: Analytical and spectroscopic characterization of some anthelmintic compounds isolated from *Adenia* sp. and *C. ruspolii*

8.1.	Abstract	215
8.2.	Introduction	217
8.3.	Materials and methods	219

8.4.	Results and Discussion	220
8.4.1.	1D- ¹ H-NMR spectra of compounds from <i>Adenia</i> sp. pool A (ASPA)	220
8.4.2.	2D-COSY NMR spectra of compounds from <i>Adenia</i> sp. pool A (ASPA)	222
8.4.3.	MS spectra of compounds from <i>Adenia</i> sp. pool A (ASPA)	223
8.4.4.	Interpretation of MS spectra to propose structures of compounds A and B from ASPA	228
8.4.4.1.	Scenario I: Proposed structures of compounds A and B based on MS/MS and NMR spectra	229
8.4.4.2.	Scenario II: Proposed structures of compounds A and B based on MS/MS, NMR spectra and sugar analysis by TLC	236
8.4.5.	General information on compounds from <i>C. ruspolii</i> and their NMR and MS data	241
8.4.5.1.	Attempts to propose/elucidate compound A based on NMR data	242
8.4.5.2.	The MS data of compound A	246
8.4.5.3.	Attempt to propose the structure of CRPALH-20-13 (compound C)	249
 Chapter Nine: Preliminary evaluation of anthelmintic activities of <i>C. ruspolii</i> and <i>Adenia</i> sp. aqueous extracts against <i>Heligmosomoides bakeri</i> in a mouse model		
9.1.	Abstract	257
9.2.	Introduction	259
9.3.	Materials and methods	260
9.3.1.	Animals and housing	260
9.3.2.	Mice handling during oral gavage	261
9.3.3.	Experimental infection	261
9.3.4.	Plant extracts and anthelmintic stock solution preparation	262
9.3.5.	Experimental design	262

9.3.6.	Body and organ weights measurements	264
9.3.7.	Blood sampling and determination of haematological parameters	265
9.3.8.	Faecal sampling and faecal egg counts (FEC)	265
9.3.9.	Post-mortem worm count	266
9.3.10.	Calculations and statistics	266
9.4.	Results	268
9.4.1.	Anthelmintic effects of water crude extracts of plants used in this study	268
9.4.1.1.	Effect of extracts on FEC	268
9.4.1.2.	Effect of extracts on adult <i>H. bakeri</i>	269
9.4.2.	Body weight measurement	271
9.4.3.	Organ weight measurement	272
9.4.4.	Effects of extracts on haematological parameters	275
9.5.	Discussion	276
Chapter Ten: Overall discussion, conclusions and future work		
10.1.	Introduction	282
10.2.	Effects of crude extracts on nematode egg hatching and larvae motility	283
10.3.	Effects of crude extract physico-chemical treatments on EHI properties	285
10.4.	Bioassay-guided fractionations of crude extracts and chromatographic profiling of Bio-Gel P-2 fractions	288
10.5.	Isolation and purification of compounds from active pooled fractions	291
10.6.	Proposed structures of compounds isolated from active fraction(s)	293
10.7.	<i>In vivo</i> validation of water crude extracts in mice	294

10.7.1.	The effect of extracts on FEC and TWC	295
10.7.2.	The effect of extracts on body weight, organ weight and haematological parameters	296
10.8.	Conclusions	298
10.9.	Future directions	300
11.	References	302
12.	Publications	346

Chapter One: General introduction and literature review

1.1. Gastrointestinal nematodes in livestock

Livestock production systems are key components of world-wide agriculture; it has been estimated that 30% of the world's economic output comes from this sector (Lamy *et al.*, 2012). This sector is increasingly organized in long market chains employing approximately 1.3 billion people globally and directly supporting the livelihoods of 600 million smallholding farmers in developing countries (Thornton, 2010). In both developed and developing countries, livestock are used as sources of raw materials for leather industry, human food (e.g. meat, fat, milk, cheese and eggs) and fibre for clothing (e.g. sheep, goats). Livestock species also play very important additional economic and socio-cultural roles for the wellbeing of rural households in developing countries. Thus, they are used not only as food supply and source of income, but also asset saving, source of employment, soil fertility building, transport, agricultural traction, agricultural diversification and its sustainable production (Siegmond-Schultze *et al.*, 2007). In Africa, the number of cattle and/or small ruminants owned is symbolic of an individual's wealth and status in the society.

Livestock parasitic infections are one of the major constraints for both small- and large-scale farmers. In particular, helminthosis is a serious problem causing significant economic losses and threatening food security in various ways (Williams *et al.*, 2014). These losses can be manifested by lowered fertility, reduced work capacity and breeding efficiency, involuntary culling, a reduction in food intake and weight gain, reduced immunity to other pathogens, lower milk production, treatment costs, and mortality in heavily parasitized animals (Kumsa *et al.*, 2007; Mavrot *et al.*,

2015). Their impact is even greater in sub-Saharan Africa (Ademola and Eloff, 2011). For instance, livestock production is an integral part of the Ethiopian agriculture and shares about 40% of the total agricultural economic output. However, gastrointestinal nematode parasite infections in livestock are very prevalent due to the availability of a wide range of agro-ecological factors suitable for diversified hosts and parasite species (Abebe *et al.*, 2011). The severities of infections also vary considerably depending on local environmental conditions, such as humidity, temperature, rainfall, vegetation, and management practices (Regassa *et al.*, 2006)

1.2. Gastrointestinal nematode infection and epidemiological factors in small ruminants

The epidemiology of gastrointestinal nematode infections is influenced by many factors such as management systems used for animals, climatic, host and parasitic factors (Blackie, 2014). Firstly, high stocking rates and intensive management with little or minimal rotational grazing, are associated with high contamination of the environment with nematode eggs or larvae and thus makes the infective stages to be more accessible to susceptible animals (Stadaliènè *et al.*, 2014). Anthelmintic treatments reduce the prevalence and severity of gastrointestinal nematodes and significantly influence their epidemiology. However, indiscriminate use of anthelmintics may result in development of resistant nematode strains and this problem is increasing in importance across in sub-Saharan region (Ntonifor *et al.*, 2013; Lemma and Abera, 2013).

Secondly, moisture and temperature are the two most important climatic conditions influencing survival, development, dissemination, and availability of free living stages of helminths in the environment (Blackie, 2014). Higher worm burdens and

outbreaks of parasitic gastroenteritis in small ruminants in sub-Saharan Africa are encountered during or immediately after the end of rainy season (Chiejina and Behnke, 2011). Temperature also influences the development of nematode larvae, with the optimal temperature for the development of *Trichostrongylid* larvae being 20-30°C. Some *Trichostrongylid* larvae are known to be resistant to desiccation and this ability enables them to survive under both extremely high and low temperatures. (Ellenby, 1968). Gastrointestinal nematodes can also survive harsh climatic conditions by hypobiosis (arrested development of parasitic L₃ larvae within the host or the parasitic L₃ larvae remains ensheated in the host until favourable climatic conditions established). In the absence of hypobiosis, nematodes survive in the hosts during hot and dry season as adults. In general, the humid tropical climate is favourable for the survival, development and transmission of gastrointestinal nematodes throughout the year (Rossanigo and Grunner, 1995).

Thirdly, the incidence rate and severity of infection with gastrointestinal nematodes can also be influenced by host factors such as age, breed, nutrition, physiological state and presence or absence of inter-current infection: other diseases that intervene during the course of parasitic infection (Gana *et al.*, 2015). Kids and lambs are more susceptible than non-reproducing adults. There is also a general tendency showing that worm burdens decrease with increasing age. This may be related to the ability of adults with well-developed immune system to fight nematode infections better than young animals. Some breeds of small ruminants are known to be having some degree of genetic resistance to gastrointestinal nematode infections. The physiological status of the animal also influences its susceptibility to gastrointestinal nematode infections. For instance, hormonal changes during late pregnancy and lactation lower the

resistance of the host to nematodes and consequently results in the establishment of higher worm burdens. The stress associated with lambing and kidding results in non-specific immunological loss of resistance that is modulated by hormones such as glucocorticoids and increases the fecundity of female worms whereas oestrogens have been found to be responsible for the resistance of female hosts to gastrointestinal nematodes (Kusiluka and Kambarage, 1996; Coyne *et al.*, 1991). Poor nutrition also lowers the resistance of the animal thus enhancing the establishment of worm burdens and increasing the pathogenicity of the parasites. In many countries of sub-Saharan Africa, malnutrition during the dry season has been found to lower the resistance of small ruminants to *H. contortus* infection and results in heavy mortality (Blackie, 2014). Inter-current infections and other stress factors also enhance the establishment of higher worm burdens (Molento *et al.*, 2011).

In general, the phylum Nematoda (roundworms) includes many parasites that are of major socio-economic importance. Grazing ruminants such as sheep are usually parasitized by one or more nematode species (order *Strongylida*) which can cause parasitic gastroenteritis (Roeber *et al.*, 2013). Different species of *Strongylid* nematodes can vary considerably in their pathogenicity, geographical distribution and susceptibility to anthelmintic drugs. Mixed infections involving multiple genera and species are common, and generally have greater impact on the host than mono-specific infections depending upon the species and number of parasites (Roy *et al.*, 2004). The most economically important species are those found in the abomasum and small intestine, and include *Haemonchus*, *Teladorsagia*, *Cooperia*, *Ostertagia*, *Bunostomum*, *Trichostrongylus* and *Nematodirus* species. Depending on the number, species and burden of parasitic nematodes, common signs of parasitic gastroenteritis

include anorexia (loss of appetite), reduced weight gain or weight loss, diarrhoea, reduced milk production and in the case of blood-feeding species anaemia (Jatau *et al.*, 2011)

1.3. Life cycle of gastrointestinal nematodes of small ruminants

Almost all economically important gastrointestinal nematodes of small ruminants have a direct life cycle. Sexually matured adults are residing either in abomasum or small intestine. The fertilized females in gastrointestinal tract produce eggs that excreted in faeces. The size of the trichostrongyloidea eggs ranges from 70-150 μm . These eggs are usually hatched within 24-48 h. After hatching, the first stage larvae (L_1) feed on bacteria and undergo two moults to develop into the infective, non-feeding and ensheathed third-stage larvae (L_3) via L_2 in the environment (faeces or soil). The sheath (cuticular layer) protects the L_3 stage from environmental conditions and enhances its survival but prevents the free living L_3 stage from feeding. Hosts are get infected by ingestion of the free living stage (L_3 ; Figure 1.1). The parasitic L_3 stage loses its protective sheath and become a histotropic (tissue) phase prior to its transition to the L_4 and pre-adult stages. The exsheathment usually occurs proximal to predilection site. Under adverse environmental conditions, L_3 of many gastrointestinal nematodes such as *Haemonchus* and *Teladorsagia* undergo a period of arrested development (hypobiosis). Although the trigger mechanisms remain unclear, hypobiotic larvae resume their activity and development when conditions are more favourable for their survival, e.g. during lambing season (Gibbs, 1986). The impact of endo-parasitic infections is influenced by the number and species of worms, health and immunological state of the host. Moreover, external factors such as climate, pasture type, stress, stocking rate, management and/or diet

also exacerbate the condition. In particular, young, immuno-compromised adults and those animals exposed to high L₃-contaminated environment are prone to heavy worm burdens (Roeber *et al.*, 2013).

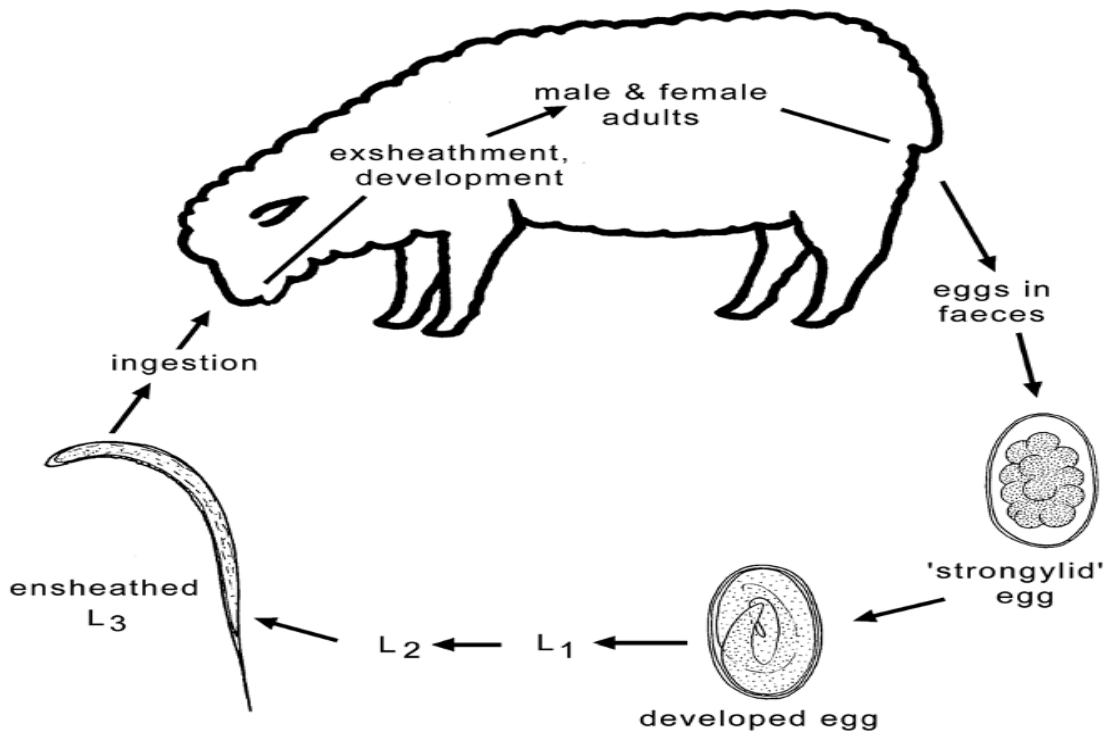


Figure 1.1. Life cycle representing gastrointestinal nematodes (order *Strongylida*) of small ruminants; adapted from Roeber *et al.* (2013) with permission.

The L₁, L₂ and L₃ are free-living in the environment where as L₄ and adult stages are parasitic in the gastrointestinal tract of the host (Taylor *et al.*, 2007).

1.4. Control methods of nematode infections in small ruminants

There are at least seven methods used in gastrointestinal parasite control strategies. These include use of conventional anthelmintic drugs (mainly the benzimidazoles, macrocyclic lactones and imidazothiazoles groups), animal vaccination, selective breeding, improvement of feed quality, grazing management, biological control methods and last but not least phytotherapy, which includes medicinal plants used in ethno-veterinary medicine by traditional healers (Molan *et al.*, 1999; Howell, 2009; Hrcckova *et al.*, 2013). The focus of my thesis is on the latter, and will be introduced below, after briefly describing mode of actions for conventional anthelmintic drugs and the problem of drug resistance development.

1.5. Conventional anthelmintic drugs, mode of actions and anthelmintic resistance

Conventional anthelmintics are drugs that used to treat the parasitic stages of worms in the host to prevent the discharge of eggs and larvae into the environment. Effective treatment of endo-parasitic infections with drugs requires a thorough understanding of the life cycle, physiology, biochemistry, and key target sites such as tegument or cuticle of worms (Hrcckova *et al.*, 2013).

Nicotinic agonists such as levamisole (Figure 1.2a) are selectively acting on nicotinic acetylcholine receptors of nematode muscle cells and induce muscle contractions by blocking ion channels. This ion channel blockage results in worm paralysis followed by worm expulsion (Williamson *et al.*, 2007). Macrocyclic lactones such as ivermectins (Figure 1.2b) are also involved in the opening of the GABA-dependent chloride channels, which leads to complete paralysis and immobilization of worms (Martin and Pennington, 1989).

Benzimidazoles are also other classes of anthelmintics that bind to intracellular β -tubulin, thus inhibiting the formation of microtubules in parasites that lead to disruption of cell homeostasis. For instance, albendazole (Figure 1.2c) is blocking glucose uptake in larval and adult stages of susceptible parasites, and thus decreasing ATP formation (Martin, 1997).

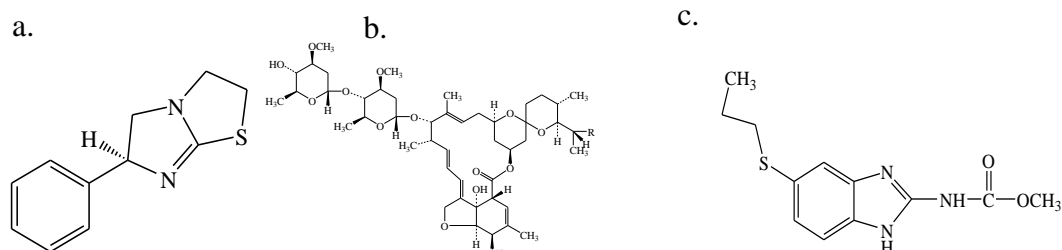


Figure 1.2. Chemical structures of representative conventional anthelmintics. Levamisole (a), ivermectins (b) and albendazole (c).

Anthelmintic resistance is the heritable ability of parasites to tolerate a normally effective dose of an anthelmintic. Parasites are considered resistant if more than 5% survive a normal dose of a single anthelmintic (<http://www.scops.org.uk> dated June 2016). Resistance to conventional anthelmintics in small ruminants is rapidly increasing, especially in warm and humid climatic regions because of intensive and indiscriminate uses of de-wormers, under-dosing, and lack of anthelmintic class change over years (Bersissa and Ajebu, 2008; Domke *et al.*, 2012; Kumsa *et al.*, 2007). Therefore, alternative parasite control methods are required, which includes phytotherapy or plant-based parasite control. The basis of the latter resides in anti-parasitic properties of plant secondary metabolites.

1.6. Plant secondary metabolites

In natural habitats, plants are surrounded by a large number of potential enemies, including a wide variety of bacteria, viruses, fungi, nematodes, mites, insects but also mammals and other herbivorous animals (Agrawal *et al.*, 2002; Hancock *et al.*, 2015). Plants respond to their enemies through an intricate and dynamic defence system that includes structural barriers, toxic chemicals, and attraction of natural enemies of the target pests. Firstly, plants use their first line of defence that involves plant surface such as cuticle (a waxy outer layer) and periderm (secondary protective tissue). These plant cell wall components provide passive barriers to bacterial and fungal entry. Secondly, higher plants have a characteristic capacity to synthesize large diverse array of organic molecules known as plant secondary metabolites (PSMs) or natural products (War *et al.*, 2012). These chemical protections play a decisive role in the resistance of plants against a wide variety of pathogens and herbivores (Wink, 1988). Primary metabolites are found across the plant kingdom, but PSM have a distinct distribution, which is the basis of chemotaxonomy (Wink, 2015). Unlike primary metabolites, they are only found in one plant species or related group of species. Many PSM have important ecological functions in plants. They protect them against being eaten by herbivores or being infected by microbial pathogens, but are also involved in attraction of pollinators and seed-dispersing animals, agents of plant–plant competition and plant–microbe symbioses (Wink, 2012). These PSMs can be divided into three major chemically distinct groups: terpenes, phenolics, and nitrogen-containing compounds (Mazid *et al.*, 2011).

1.7. Terpenes and their roles in plants

Terpenes or terpenoids constitute the largest class of secondary metabolites (Tholl, 2015). Most of the diverse substances of this class are insoluble in water (Anulika *et al.*, 2016). They are synthesized from acetyl-CoA or its glycolytic intermediates. They are derived from the branched five-carbon skeleton isopentene known as isoprene units. Although extensive metabolic modifications make it difficult to recover C₅ residues, terpenes are classified based on the number of C₅ units they contain (Singh *et al.*, 2015; Martin *et al.*, 2003), and are thus known as monoterpenes (two C₅ units), sesquiterpenes (three C₅ units), diterpenes (four C₅ units), triterpenes (six C₅ units), tetraterpenes (eight C₅ units), and polyterpenoids (more than eight C₅ units). Terpenes are biosynthesized from primary metabolites in the mevalonic acid and methylerythritol phosphate pathways. In the mevalonic acid pathway, three molecules of acetyl-CoA are joined together stepwise to form a six carbon intermediate (mevalonic acid) and then mevalonic acid is further pyrophosphorylated, decarboxylated, and dehydrated to yield isopentenyl diphosphate (Figure 1.3). In the methylerythritol phosphate pathway, isopentenyl diphosphate can also be formed from intermediates of glycolysis or the photosynthetic carbon reduction cycle via a separate set of reactions called the methylerythritol phosphate pathway that operates in chloroplasts and other plastids. Isopentenyl diphosphate and its isomer, dimethylallyl diphosphate are the activated 5-carbon building blocks of terpene biosynthesis that join together to form the larger, aforementioned molecules (Dewick, 2002).

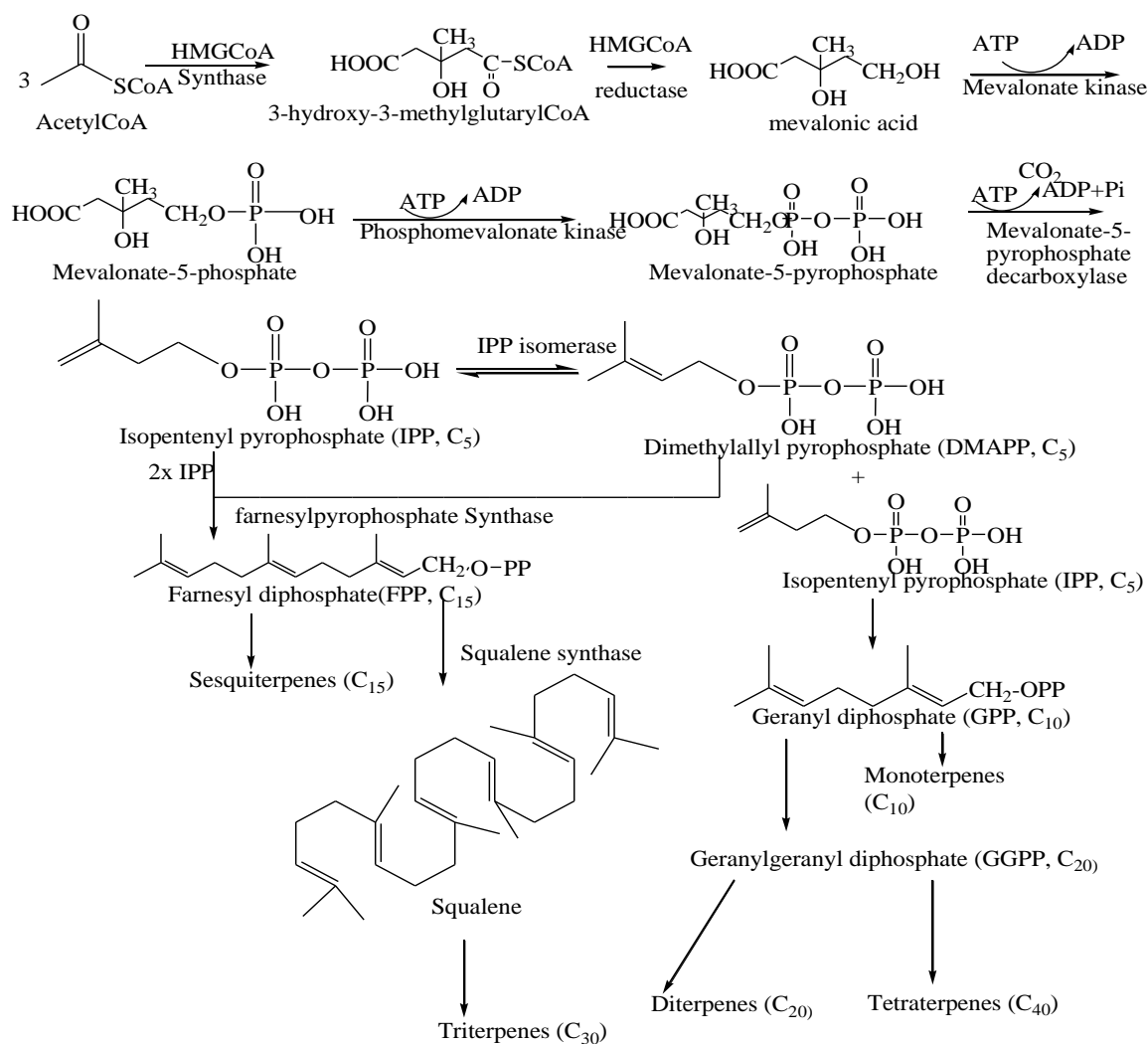


Figure 1.3. Mevalonic acid pathway of terpenes biosynthesis. The phosphorylated intermediates, isopentenyl pyrophosphate (IPP) and dimethylallyl pyrophosphate (DMAPP) are combined to make monoterpenes (C₁₀), sesquiterpenes (C₁₅) and larger terpenes.

Some terpenes have roles in growth and development. For instance, gibberellins (diterpenes) and brassinosteroids (triterpenes) are important classes of plant hormones with growth-regulating functions. Sterols are triterpene derivatives that are essential components of cell membranes that stabilise by interacting with phospholipids. Carotenoids are tetraterpenes that function as accessory pigments in photosynthesis and protect photosynthetic tissues from photo-oxidation. The

hormone abscisic acid is a sesquiterpene produced by degradation of a carotenoid precursor. Long-chain polyterpene alcohols known as dolichols function both as carriers of sugars in cell wall and glycoprotein synthesis. Terpene-derived phytols (side chains of chlorophyll) are used to anchor certain molecules in membranes (Tholl, 2006).

The vast majority of terpenes, however, are secondary metabolites presumed to be involved in plant defences. They are toxins and feeding deterrents to many herbivorous insects and mammals and thus play important defensive roles in the plant kingdom (Mazid, 2011). For instance, monoterpene esters (pyrethroids) from *Chrysanthemum* species have shown significant insecticidal activity (Haouas, 2008). Many plants also contain essential oils (mixtures of volatile monoterpenes and sesquiterpenes) with insect repellent properties. Complex group of triterpenes such as limonoids from *Azadirachta indica* are well known for their powerful feeding deterrent properties to herbivores (Jilani and Saxena, 1990). The phytoecdysones (plant steroids with the same basic structure to insect moulting hormone) disrupt moulting and other developmental processes often with lethal consequences upon ingestion by insects. These steroids were found to have a defensive function against plant-parasitic nematodes (Soriano *et al.*, 2004).

Saponins and glycosides are naturally occurring chemical compounds found in a wide variety of higher plants (Francis *et al.*, 2002). Glycoside is a molecule in which a sugar is bound to a non-carbohydrate moiety, usually small organic molecules. They play numerous important roles in living organisms. Many plants store chemicals in the form of inactive glycosides, which are activated by enzyme hydrolysis. Saponins are chemically glycosides, which are composed of a lipid-

soluble aglycone consisting of either a sterol or a triterpenoid with different water-soluble sugar residues. Saponins with sterol group in their structure also have surfactant properties and can particularly affect eukaryotic organisms that contain steroids in their cell membranes (Osbourn *et al.*, 2011).

1.8. Phenolic compounds and their role in plants

Plants produce nearly 10,000 phenolic compounds that are chemically heterogeneous and either soluble in organic or aqueous solutions, or are insoluble polymers (Wink, 2015). Phenolic plant secondary metabolites serve as defences against herbivores and pathogens, in mechanical support, in attracting pollinators and seed dispersers, in absorbing harmful ultraviolet radiation, or in reducing the growth of nearby competing plants (Bhattacharya, 2010). They are biosynthesized by several different routes of biosynthetic pathways. However, the two major pathways dedicated in phenolic compounds biosynthesis are the shikimic acid and the malonic acid pathways (Figure 1.4). The shikimic acid pathway participates in the biosynthesis of most plant phenolics. It converts simple carbohydrate precursors derived from glycolysis and pentose phosphate pathways into the three aromatic amino acids: phenylalanine, tyrosine, and tryptophan (Ghasemzadeh, 2011).

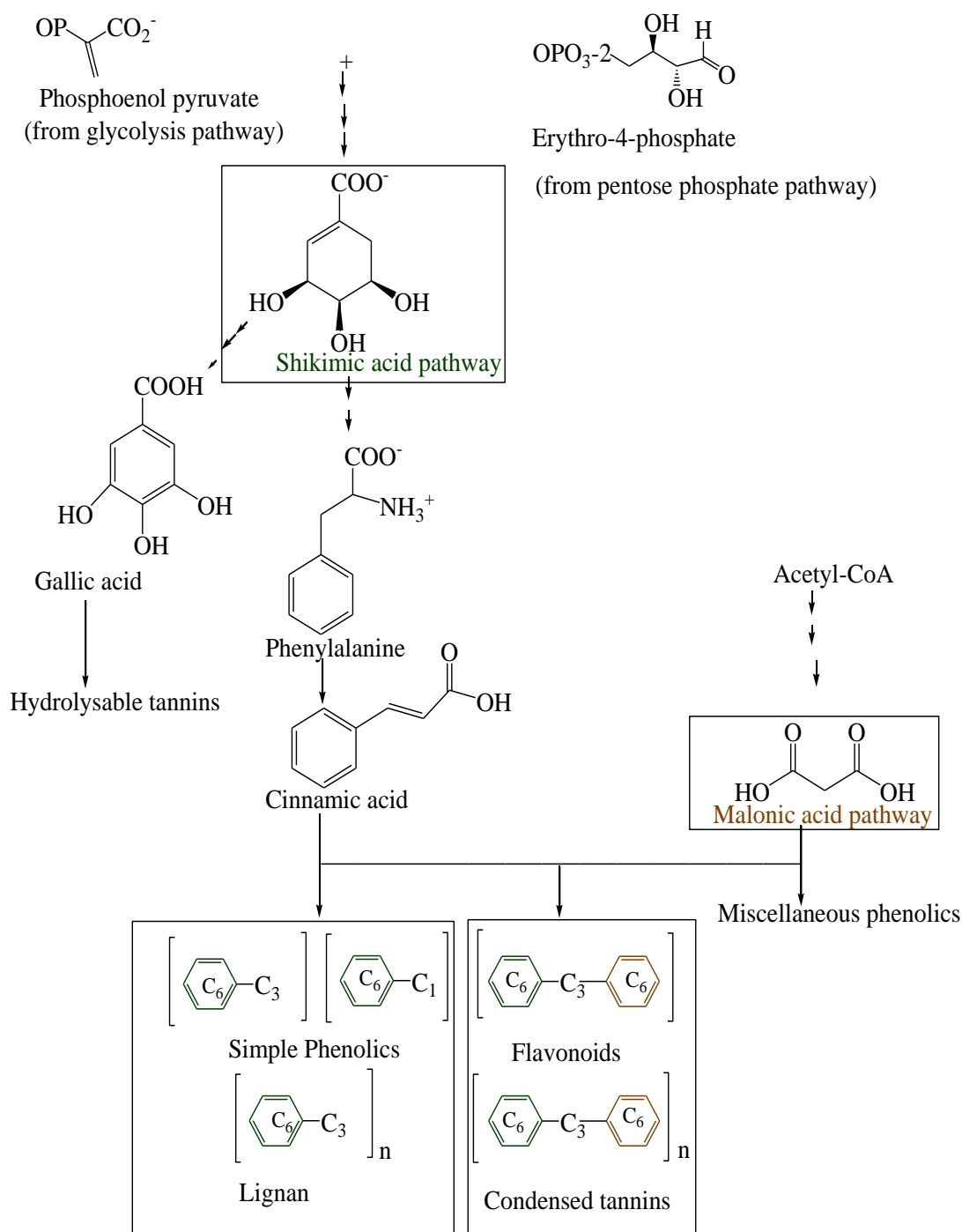


Figure 1.4. The shikimic and malonic acids pathways of plant phenolics biosynthesis. In higher plants most phenolics compounds are derived at least in part from phenylalanine, a product of the shikimic acid pathway. Formulae in brackets indicate the basic arrangement of carbon skeletons: C_6 indicates a benzene ring, and C_3 is a three-carbon chain.

Many simple phenolic compounds have important roles in plants as defences against insect herbivores and fungi. For instance, the activated furanocoumarin (psoralen) exhibits photo-toxicity to insect herbivores due to its ability to insert itself into the double helix of DNA and bind to the pyrimidine bases thus blocking transcription and repair and leading eventually to cell death (Berenbaum, 1995).

The flavonoids are one of the largest classes of plant phenolics. The basic carbon skeleton of a flavonoid contains 15 carbons arranged in two aromatic rings connected by a three-carbon bridge that results from the shikimic acid and the malonic acid biosynthetic pathways as shown in Figure 1.4. Flavonoids are classified primarily on the basis of the degree of oxidation of the three-carbon bridge as anthocyanins, flavones, flavonols, and isoflavones. The majority of flavonoids exist naturally as glycosides because both hydroxyl groups and sugars increase the water solubility of flavonoids. However, other substituents such as methyl ethers or modified isopentyl units make flavonoids lipophilic (hydrophobic). Different types of flavonoids perform very different functions in the plant, including pigmentation and defence (Treutter, 2006).

Some flavonoids are coloured pigments of plants that provide visual cues that help to attract pollinators and seed dispersers (Tanaka *et al.*, 2008). Flavones and flavonols generally absorb light at shorter wavelengths than anthocyanins and protect cells from excessive UV-B radiation (Mierziak *et al.*, 2014). UV-B radiation is known to induce mutations in the DNA and oxidative stresses in plants (Gill *et al.*, 2015). These effects have the potential to damage cellular macromolecules and result in poor growth under normal conditions (Saewan and Jimtaisong, 2013). Flavonoids that are secreted into soil by legume roots are mediating the interaction of legumes

and rhizobacteria (nitrogen-fixing symbionts) and also play regulatory role in plant development as modulators of polar auxin transport (Grunewald *et al.*, 2009).

Next to cellulose and hemicellulose, the most abundant organic substance in plants is lignin, a highly branched polymer of phenylpropanoid groups. Besides providing mechanical support, lignin has significant protective functions in plants. Its physical toughness deters herbivores. Lignification also blocks the growth of pathogens and is a common response to infection or wounding (Hijwegen, 1963).

A second category of plant phenolic polymers with defensive properties are the tannins (Driver and Bilgener, 1989). This group of PSMs includes many water-soluble phenolic compounds with a great diversity, which can be divided into two major groups: the hydrolyzable and the condensed tannins (Waterman, 1999). Condensed tannins are polyphenols (proanthocyanidins) with high molecular weight from 500 to 20,000 kDa, which consist mainly of oligomers or polymers of monomeric units of flavan-3-ols (catechin and epicatechin). Depending on hydroxyl functional groups they are classified into sub-classes: the prodelphinidins, procyanidins, prorobetinidins, profisetinidins etc. (Mueller-Harvey, 2006). Tannins are toxic to many herbivores and act as feeding repellents to a great variety of animals. The defensive properties of most tannins are due to their toxicity, which is generally attributed to their ability to bind proteins non-specifically. It has long been thought that plant tannins bind proteins in the guts of herbivores by forming hydrogen bonds between their hydroxyl groups and electronegative sites on the proteins (Bunglavan and Dutta, 2013). Plant tannins also serve as defences against microorganisms which help prevent fungal and bacterial decay.

1.9. Nitrogen-containing compounds and their role in plants

A large variety of PSMs have nitrogen as part of their structure. These include alkaloids, amides, cyanogenic glycosides, glucosinolates, and non-protein amino acids (Miyagawa, 2009). Alkaloids are among nitrogen containing PSM known for their anti-herbivore and medicinal properties. Most nitrogenous secondary metabolites are synthesized from common amino acids. Alkaloids are a large family of more than 15,000 nitrogen-containing PSMs which are found in approximately 20% of vascular plant species (Fürstenberg-Hägg *et al.*, 2013). The nitrogen atom in these compounds is usually part of a heterocyclic ring (a ring that contains both nitrogen and carbon atoms). As a group, alkaloids are best known for their ranges of pharmacological effects at low concentration on vertebrate animals. As their name would suggest, most alkaloids are alkaline. At the pH values commonly found in the cytosol (pH 7.2) or the vacuole (pH 5–6), the nitrogen atom is protonated, which means that alkaloids are positively charged and are generally water soluble. Alkaloids are usually synthesized from lysine, tyrosine or tryptophan. However, the carbon skeleton of some alkaloids also contains a component derived from the terpene pathway. On a cellular level, the mode of action of alkaloids in animals is quite variable. Many alkaloids interfere with components of the nervous system, especially neurotransmitters. Others affect membrane transport, protein synthesis or miscellaneous enzyme activities (Macel, 2011).

Various nitrogenous protective compounds other than alkaloids are found in plants. Two groups of these substances are cyanogenic glycosides and glucosinolates. These are not themselves toxic but when the plant is crushed are readily broken down and release poisons, some of which are volatile (Zagrobelny *et al.*, 2004). Many

cyanogenic plants release hydrogen cyanide (HCN) in sufficient quantities to be toxic and then tend to be avoided by herbivores. A second class of plant glycosides are called glucosinolates from which the aglycone can break down to release defensive substances such as isothiocyanates and nitriles. These defensive products function as toxins and herbivore repellents (Hopkins *et al.*, 2009).

Plants and animals incorporate the same 20 amino acids into their proteins. However, many plants also contain unusual amino acids, called non-protein amino acids (e.g. canavanine and azetidine-2-carboxylic acid) that are not incorporated into proteins. Instead, these amino acids are present in a free form and act as defensive substances that range from interference with the uptake of amino acids to the disruption of translation (Bell, 2003).

1.10. Medicinal plants as alternative or complementary anti-parasitic agents

The use of medicinal plants and their preparations in the management and treatment of diseases started with life. Medicinal plant preparations that have been used by indigenous peoples for centuries for the treatment of a variety of health problems both in livestock and humans are often referred to as ethno-veterinary or ethno-medicinal remedies (FAO, 2002). In many parts of the developing world, small-scale and subsistence farmers rely on traditional methods of deworming that include the administration of remedies derived from plants (Mirzaei *et al.*, 2013). Table 1.1 shows some examples of such plants, and which parasites and hosts are targeted. It also provides some examples where medicinal plants have been studied in mice as a model, as also done in this thesis (Chapter Nine). It is known that medicinal plants contain valuable chemical compounds (bioactive PSMs) that could offer alternative

means to the problems of modern synthetic drugs, such as chemical residue, environmental toxicity and development of drug resistance (Shai *et al.*, 2009; Tandon *et al.*, 2011). As such, plant based medicines have become an indispensable mainstay, and will continue to form an integral part of the primary health care systems across the world, particularly in financial resource poor developing countries (Hoareau, 1999; Amin *et al.*, 2009). Thus, the use of plants and plant-derived natural compounds as primary and alternative sources of medicine against various ailments, such as those due to parasite infections, continues (Salifou *et al.*, 2013).

Table 1.1. List of some *in vivo* studies of medicinal plants with purported anthelmintic properties.

Plant	Parasite species	Host	References
<i>Albizia anthelmintica</i>	<i>H. contortus</i>	Sheep	Githiori, 2004
<i>Coriandrum sativum</i>	<i>H. contortus</i>	Sheep	Egualé <i>et al.</i> , 2007
<i>Iris kashmiriana</i>	Natural challenge	Sheep	Khan <i>et al.</i> , 2016
<i>Entada leptostachya</i>	Natural challenge	Sheep	Kimani <i>et al.</i> , 2014
<i>Prosopis juliflora</i>			
<i>Ferula costata</i>	Natural challenge	Sheep	Kakar <i>et al.</i> , 2013
<i>Prosopis juliflora</i>	Natural challenge	Sheep	Mutembei <i>et al.</i> , 2015
<i>Entada leptostachya</i>			
<i>Peganum harmala</i>	<i>H. contortus</i>	Goats	Intisar <i>et al.</i> , 2015
<i>Cratylia mollis mollis</i>	Natural challenge	Goats	Mendonça-Lima <i>et al.</i> , 2016
<i>Embelia schimperi</i>	<i>Hymenolepis nana</i> & <i>Necator americanus</i>	Mice	Debebe <i>et al.</i> , 2015
<i>Codiaeum variegatum</i>	<i>Hymenolepis microstoma</i>	Mice	Wilar <i>et al.</i> , 2014
<i>Albizia anthelmintica</i>	<i>H. polygyrus</i>	Mice	Githiori, 2004
<i>Aframomum sanguineum</i>	<i>H. polygyrus</i>	Mice	Githiori <i>et al.</i> , 2003
<i>Ziziphus spina-christi</i>	<i>Allolobophora caliginosa</i>	Mice	Alzahrani <i>et al.</i> , 2016

The African continent is one of the richest continents in biodiversity. It abounds in plants of economic and medicinal importance which, when developed could reduce expenditure on imported drugs to meet primary health care needs of both livestock and humans (Adamu *et al.*, 2013). Several medicinal plants have been used as

anthelmintic agents in the treatment of gastrointestinal nematode infection in African developing countries, especially to control the nematode *Haemonchus contortus* (Githiori, 2004; Adamu *et al.*, 2013). There have also been many other different studies that utilized plant extracts because of prior reports of medicinal effects or known to contain phytochemicals such as condensed tannins with anthelmintic properties against different nematodes (Molan *et al.*, 2010; Bauri *et al.*, 2015). The majority of these studies utilized a number of economically important gastrointestinal nematode parasites such as *Haemonchus contortus*, *Ostertagia (Teladorsagia) circumcincta*, *Ostertagia ostertagi*, *Trichuris ovis*, *Trichuris globulosa*, *Chabertia ovina*, *Thelazia skrjabini*, *Bunostomum trigonocephalum*, *Nematodirus filicollis*, *Nematodirus oiratianus*, *Cooperia cuticei*, *Marshallagia marshalli*, *Gaigeria pachyscelis*, *Skrjabinema ovis* and *Gongylonema pulchrum* (Regassa *et al.*, 2006; Sissay *et al.*, 2007). The use of medicinal plants as primary, alternative or complementary anti-parasitic agents can be explained from at least two major perspectives. In one hand, inaccessibility and/or unaffordability by low income communities leads to a very limited use of conventional anthelmintics in small holder farmers and pastoral systems. On the other hand, the side effects associated with the synthetic anthelmintic drugs (such as chemical residue and toxicity) and development of resistance against these drugs pose serious threat to both human and livestock health in the rest of the world (Hrckova *et al.*, 2013). As a result, there is a renewed interest for people to rely on their traditional knowledge, practices and locally available materials (mainly plants and by-products of other processes) for the management of diseases of their domestic animals (Giday and Teklehaymanot, 2013).

1.11. Anti-parasitic properties of plant secondary metabolites

Before commercial anthelmintics were introduced into the world market, worm infections were controlled using medicinal plants with the belief that PSMs that protect plants against nematodes infections also protect animals from similar pathogens (Qadir *et al.*, 2010). Indeed, worms that infect plants and animals including humans have very similar physiology and biochemistry (Jasmer *et al.*, 2003). These anti-parasitic PSMs can be divided, on the basis of their molecular formulae and structural motifs, into several classes and the most abundant include essential oils, flavonoids, alkaloids, saponins, glycosides, tannins, sesquiterpene lactones, lactones with peroxidic structure, amides, and proteins with enzymatic activity such as proteolytic enzymes.

1.11.1. Alkaloids and other nitrogen containing compounds

Plant extracts with optimum alkaloid content have been reported as having nematocidal potential or vermifuge properties by paralyzing larvae/adult nematodes. These alkaloids may interfere with neurotransmitter molecules or regulatory enzymes involved neuromuscular system of nematodes (Wink, 2015). Some plants also contain proteolytic enzymes such as cysteine proteinases that act on the nematodes cuticle (Stepek *et al.*, 2006). For instance, daily administration of papaya latex (250 mg/kg body weight) to mice infected with *Heligmosomoides bakeri* for seven days resulted in 97% reduction in faecal egg counts (FEC; Behnke *et al.*, 2008) by day 25 post-therapy. Similarly, Buttle *et al.* (2011) reported that enzymes present in papaya latex possess potent anthelmintic activity capable of clearing the adult parasitic nematode *H. contortus* from the ovine abomasum.

Amides are also small organic substances containing nitrogen in their molecule. They are found in plants in much lower concentration than other PSMs (Onguéné *et al.*, 2013), where they usually play a role in the defence against insects or fungi, but also have anti-parasitic properties. For instance, *Piper tuberculatum* that belongs to the genus *Piper* is widely distributed throughout the tropical and subtropical regions of the world. The amide piperlongumine, found in root extract of this plant, was reported to have anthelmintic activity against *Schistosoma mansoni* (de Moraes *et al.*, 2012). The mechanisms of actions of amides may be related to their tegumental alterations, decrease motor activity of adult worms, and impact on worm fecundity and larval development (Magalhães *et al.*, 2012).

1.11.2. Essential oils and terpenoids

The hydrophobicity of essential oils enables them to pass through the cell membrane and disrupt the structure and affect its fluidity (Turina *et al.*, 2006). This extensive change in membrane fluidity/permeability results in membrane damage followed by leakage of intracellular materials, induction of oxidative stress and bioenergetics failure that cause parasite death (Pessoa *et al.*, 2002). For instance, essential oils from *Eucalyptus staigeriana* and *Ocimum gratissimum* showed significant total worm burden and FEC reductions in ruminants and rodent models (Macedo *et al.*, 2010). The PSMs in forage plants such as chicory known for their anthelmintic activities are sesquiterpene lactones (Foster *et al.*, 2011). Plant extracts from the genus *Artemisia* (*Asteraceae*) have been used for a long time in traditional Chinese medicine for treatment of parasitic infections both in humans and livestock (Willcox *et al.*, 2004). Its anti-parasitic activity is attributed to the unique bioactive sesquiterpene lactone with an endoperoxide bridge (artemisinin) that damage nematode membrane and

induce oxidative stress (Ferreira *et al.*, 2010). In a recent study of Squires *et al.* (2011), artemisinin was tested for efficacy against *H. contortus* in a gerbil model. A number of studies using sesquiterpene lactones from various legume forages and medicinal plants confirmed their anthelmintic effects on both pre-parasitic (eggs to L₃) and parasitic stages (L₄ and adults) of gastrointestinal nematodes (Pena-Espinoza *et al.*, 2015).

1.11.3. Tannins

Condensed tannins, especially the prodelphinidins and procyanidins, have long been recognised as having anti-parasitic properties (Diaz *et al.*, 2010; Hoste *et al.*, 2012; Sandoval-Castro *et al.*, 2012). These authors pointed out that bioactive tanniniferous plants represent a valuable option as an alternative to commercial anthelmintic drugs for the control of gastro-intestinal nematodes as consumption of these plants has been associated with reductions in nematode numbers, worm fecundity, and nematode egg excretion (Hoste *et al.*, 2012). Condensed tannin-rich legume forages have been reported as having beneficial effects on the host physiology and its ability to maintain homeostasis under parasitic challenge (Juhnke *et al.*, 2014). They have also nematocidal effects that result in substantial decrease in FEC due to their significant effect on female worm fecundity (Paolini *et al.*, 2003). For instance, condensed tannin-rich wattle drench to small ruminants significantly reduced worm burden, FEC and egg hatching (Max, 2010; Ferreira *et al.*, 2013). Condensed tannin-rich extracts also interfere with hatching of eggs and larval motility and significantly inhibited the exsheathment process of third-stage larvae (Azando *et al.*, 2011). Martin (1997) reported that tannins would have similar mode of actions as synthetic phenolic anthelmintics on various stages of small ruminant nematodes. This is

because conventional phenolic anthelmintics such as oxyclozanide, niclosamide, and nitroxylnil interfere with energy generation in helminth parasites by uncoupling oxidative phosphorylation, consequently leading to depletion of parasite adenosine triphosphate (ATP). Another report also suggested the tannins ability to bind to glycoproteins on the cuticle of parasites and cause significant cuticle tissue damage (Hoste *et al.*, 2006). Studies on condensed tannins from various legume forages and medicinal plants confirmed as having anthelmintic effects on both pre-parasitic (eggs to L₃) and parasitic stages (L₄ and adults) stages of gastrointestinal nematodes (Athanasiadou *et al.*, 2001; Athanasiadou and Kyriazakis, 2004; Williams *et al.*, 2014).

1.11.4. Flavonoids and polyphenols

Flavonoids and polyphenols inhibit key enzymes of glycolysis and glycogenolysis of nematodes, resulting in bioenergetics failure that causes parasite death (Bauri *et al.*, 2015). In helminths, nitric oxide has been suggested to have many physiological roles as a neurotransmitter at neuromuscular junctions and in control of embryogenesis (Pfarr *et al.*, 2001). Flavonoids also disturb calcium cation homeostasis and nitric oxide activity in the parasites (Das *et al.*, 2009). The disturbances in Ca²⁺ homeostasis and nitric oxide activity in nematodes due to these phytochemicals induce rapid muscular paralysis, inhibit mobility followed by parasite death. A combination of flavonoids and polyphenols such as condensed tannins (procyanidins) also synergistically inhibits L₃ exsheathment of *H. contortus* (Klongsiriwet *et al.*, 2015).

1.11.5. Glycosides and saponins

Glycosides and saponins are detected in many higher plants used in the ethno-medicine at various concentrations. To date, several compounds of these phytochemical groups have been isolated from plants, and show very promising anthelmintic activities (Das *et al.*, 2012; Esposito *et al.*, 2013). For instance, oral administration of a saponin-rich extract from *Acacia auriculiformis* at 200 mg/kg body weight significantly reduced adult worm count in mice infected with *H. bakeri*. (Nandi *et al.*, 2004). Sinha *et al.* (1997) showed experimentally that these saponins enhance the cell membrane lipid peroxidation. Nandi *et al.* (2004) also reported that the conjugated unsaturated system of selected saponins would be involved in the formation of free radicals, which induce membrane damage through peroxidation of membranes in helminths. An important crop plant in Brazil, locally known as Sisal (*Agave sisalana*), is composed of about 60% liquid containing mostly sapogenins (aglycone portion of saponins) that demonstrated significant anthelmintic activity on L₁ stage of gastrointestinal nematodes (Botura *et al.*, 2013). Steroidal saponins are considered to be the active ingredients of sisal extract, which have detergent properties similar to those of polyene antibiotics (Osbourn, 1996). According to Francis *et al.* (2002), saponins present in *A. sisalana* showed anthelmintic activities due to the intercalation of the hydrophobic portions of the saponins in cell membranes that resulted in the formation of pores in the tegument of helminths. *Calendula officinalis* and *Beta vulgaris* are plants native in countries with temperate climate and their saponin components (ursanes and oleananes) showed strong anthelmintic activities on development of free-living stages of *Heligmosomoides bakeri* by interfering with the function of major membrane transporters for

xenobiotics, P-glycoprotein (Doligalska *et al.*, 2011), which plays a crucial role in the distribution, metabolism, excretion and absorption of toxic molecules (Lespine *et al.*, 2012). The oleanane type glucuronides inhibited egg hatching and moulting of larvae and also changed their morphology (Doligalska *et al.*, 2011). In nematodes, the bioavailability of drugs is modulated by physical and biochemical barriers such as cuticle and intestinal epithelium (Kerboeuf *et al.*, 2010). The function of these barriers depends on specific membrane transport systems such as P-glycoprotein, and nematode resistance to anti-parasitic treatment may be mediated by P-glycoprotein-related pathways (Kaschny *et al.*, 2015). The anthelmintic activity of these saponins could be attributed to the molecular structure of oleanane type of glucuronides, which is based on a 30-carbon skeleton comprising five fused six-membered rings. For instance, when a saponin (oleanolic acid) is glycosylated at both C-3 and C-28, it induces a permeability change in cuticle and cell membranes of *H. bakeri* (Doligalska *et al.*, 2011). An increase in level of P-glycoprotein has also been observed in nematode strains resistant to anthelmintic treatment (Kerboeuf *et al.*, 2003).

1.12. *In vitro* and *in vivo* validation of anti-parasitic plant extracts

For the purpose of my thesis, *in vitro* studies (in test tubes or on culture plates) refer to the technique of performing a given procedure using non-parasitic life stages (eggs, free living L₃ larvae) in a controlled environment outside the host animal. In contrast, *in vivo* (within the living organism) studies refer to experimentation using a whole, living organism as opposed to a partial or dead organism (Mbaya *et al.*, 2014), and in my thesis this would be using the mouse as host animal. An overview of the *in vitro* and *in vivo* methodologies used for my thesis is presented in Chapter

Two. Wherever possible, *in vitro* studies should be followed by *in vivo* testing because it is better suited for observing the overall effects of an experiment on a living subject and offer conclusive insights about the outcome of an experiment (Ramazani *et al.*, 2010). Therefore, to validate the claimed anti-parasitic properties of medicinal plant extracts, *in vitro* and *in vivo* bioassays are needed. *In vitro* bioassays such as egg hatch test, larval migration inhibition, larval feeding inhibition, larval exsheathment inhibition, larval development test and adult motility test provide a preliminary screening for efficacy of plants, which can provide a basis for *in vivo* trials. The *in vivo* evaluation is carried out to assess efficacy by determination of FEC reduction (FECR), total worm count reduction (TWCR), and possible toxicity (effect on blood biochemical and haematological parameters) of medicinal plant extracts, usually in ruminants and rodent models (Carvalho *et al.*, 2012).

1.13. The classification, distribution, description and uses of the four plant species used in this study

Plant material to be investigated for anti-parasitic properties can be selected on the basis of some specific ethno-medicinal uses, chemotaxonomic data or randomly (Ngarivhume, 2015). Extracts prepared from selected plant materials on the basis of ethno-medicinal uses are more likely to contain biologically active components of medicinal interest (Hemalatha *et al.*, 2013). Alternatively, if species/genera related to the plant under investigation are known to contain specific compounds, then the plant itself is expected to contain similar compounds (Singh, 2016). Thus, the use of literature databases early in the selection process can provide some preliminary information on type of natural products already isolated from the plant and the extraction methods employed to isolate them (Ntie-Kang *et al.*, 2013). In Ethiopia,

there are a large number of medicinal plants and plant species utilized by ethno-veterinary medicine practitioners to control ecto- and endo-parasite infections in livestock (Eugale *et al.*, 2007; Tomass *et al.*, 2013; Tolossa *et al.*, 2013; Lulekal *et al.*, 2014). In our study, the following four medicinal plants were selected based on their priorities in ethno-medicinal uses as claimed by traditional healers.

1.13.1. *Cissus ruspolii*

C. ruspolii (Figure 1.5) belongs to the family *Vitaceae*. It is a herbaceous climber or creeper to 1.5 m long from a woody rootstock and grown in dry juniperus forest, woodland, bushland, on rocky slopes and on red sandy to loamy soil. It is found in tropical Africa mainly in east and central Africa such as Ethiopia, South Sudan and Kenya (<http://www.ville-ge.ch/musinfo/bd/cjb/africa/details> dated June 2017). The genus *Cissus* consists of about 350 species of which, at least, a dozen is used globally in traditional medicine to treat different ailments. For instance, *C. rotundifolia*, *C. populnea*, *C. ibuensis* and *C. quadrangularis* are claimed as traditional medicine to treat parasitic diseases such as trypanosomiasis and bacterial infections (Aguoru *et al.*, 2014). In Congo, *C. rubiginosa* is used as anti-dysentery and anti-diarrhoea agent (Fernandes and Banu, 2012).

In Ethiopia, *C. quadrangularis* leaf and aerial parts are used for treatment of blackleg in cattle by Afar pastoral communities (Giday and Teklehaymanot, 2013). *C. ruspolii* (Figure 1.5) is also traditionally claimed as having anti-parasitic properties against both human and livestock helminths by the Hamar and Maale ethnic groups (Tolossa *et al.*, 2013). Some species in this genus are known to contain PSMs such as

triterpenes, tannins, flavonoids, alkaloids, stilbenes, steroids, coumarin and saponins (Shah, 2011).

To my knowledge, there has been no bioactivity and phytochemical study of this plant. Therefore, this is the first bioassay-guided phytochemical study to validate its anti-parasitic properties and to elucidate the structure of active compound(s) responsible for the claimed and observed activities.



Figure 1.5. *C. ruspolii* collected from Denbyte, Hamer District, and South Nation and Nationalities and People Regional State (SNNPRS) located at 03°43'54.6" N, 36°45'36" E and 1613 m altitude.

1.13.2. *Adenia* sp.

The genus *Adenia* belongs to the family *Passifloraceae*. It comprises about 95 species of which about 60 are found on the African mainland, 20 in Madagascar and 15 in Asia (Hearn, 2006). Different species of the genus *Adenia* have many uses in traditional medicine throughout Africa. For instance, an infusion or decoction of root, stem or leaves of *A. cissampeloides* is used for the treatment of gastrointestinal complaints, intestinal worms (root part), malaria and also claimed for dressing of

wounds and sores (Schmelzer and Gurib-Fakim, 2008). The major phytochemical constituents of the genus *Adenia* are triterpenoids, glycosylated flavonoids, alkaloids, cynogenic compounds, and saponins (Patel *et al.*, 2011).



Figure 1.6. *Adenia* sp. collected from Mukitano, near to Sololo district, Ethio-Kenyan border located at 03°54'19.8" N, 38°56'29" E and 900 m altitude.

In Ethiopia, the plant *Adenia* sp. (Figure 1.6) locally known as Wandilee is traditionally claimed as having anthelmintic properties both in human and livestock by the Borana Oromo pastoralists living around the Ethio-Kenyan border. It is also claimed for its wound healing properties.

1.13.3. *Ipomoea eriocarpa*

The genus *Ipomoea*, with approximately 500-600 species, comprises the largest number of species within the *Convolvulaceae* family (Bhellum, 2012), which comprise nearly 1650 predominantly tropical species. More than ~95% species of *Ipomoea* are found throughout tropical and subtropical regions of the world. Several of those species have been used as ornamental plants, food, medicines or in religious

ritual. These species are used in different parts of the world for the treatment of several diseases, such as, diabetes, hypertension (Ludvik *et al.*, 2004), dysentery, constipation, fatigue, arthritis, rheumatism, hydrocephaly, meningitis, kidney ailments and inflammations (Ferreira *et al.*, 2006). Some of these species also showed antimicrobial, anthelmintic, anti-inflammatory, and anticancer activities. Alkaloids, phenolics compounds, lignan, triterpenes and glycolipids are the most common biologically active constituents from these plant extracts (Meira *et al.*, 2012).

In Ethiopia, *Ipomoea eriocarpa* (Figure 1.7) is mostly grown as hedge and also claimed for its anthelmintic properties against gastrointestinal nematodes in livestock by agro-pastoral communities of Maalee ethnic groups (Tolossa *et al.*, 2013).



Figure 1.7. *Ipomoea eriocarpa* collected from Beneta, Maalee district, and South Nation and Nationalities and People Regional State (SNNPRS) located at 03°43'36.2" N, 36°35'21" E and 1291 m altitude.

1.13.4. *Euphorbia thymifolia*

The family *Euphorbiaceae* consists of about 322 genera and 8,900 species around the world in both arid and humid tropics. The plants are found as herbs, shrubs, stunted succulents, and tall canopy trees. Many plant species of *Euphorbiaceae* family are traditionally used for treatment of various ailments including gastrointestinal complaints, tape worm, bloody diarrhoea and dysentery (Özbilgin and Saltancitoğlu, 2012). In Tanzania, decoctions of *E. micrantha* are used to treat skin diseases, intestinal parasites, yellow fever malaria (Moshi *et al.*, 2012). Plants in the family *Euphorbiaceae* are well known for the chemical diversity and have been shown to possess flavonoids, saponins, diterpenes, phorbol esters, lectins, and triterpenoids. Compounds isolated from extracts of the genus *Euphorbia* perform many different biological activities, including cytotoxic, antimicrobial, anti-viral, hepatoprotective, anti-inflammatory, anticancer and antioxidant activities (Özbilgin and Saltancitoğlu, 2012; Dahare and Jain, 2010). In Ethiopia, some *Euphorbia* species such as *Euphorbia thymifolia* (Figure 1.8) have been used to treat gastrointestinal problems, ascariis, gonorrhoea, ringworm, impotence, and rabies by different tribes in different districts of the country (Mesfin *et al.*, 2009).



Figure 1.8. *Euphorbia thymifolia* collected from Qarsa Danbi, Borana Zone, Oromia Regional State located at 03°45'20" N, 38°22'40" E and 1094 m altitude.

The reported traditional medicinal uses of these plants for gastrointestinal complaints might indeed refer to the direct anthelmintic action on the target parasite and its parasitic stages, or boosting the immune response of the host that supports parasite elimination. Screenings of plants highly utilized and claimed by traditional healers are important either to search for bioactive compound(s) that can be formulated or used as lead compound to synthesize new drugs or used as marker compound(s) to standardize the crude extracts as phytomedicine used by traditional healers and communities (Kinghorn *et al.*, 2011). Such a search for bioactive compound(s) requires bioassay-guided phytochemical study, as was the overall approach of my PhD project (Figure 1.9).

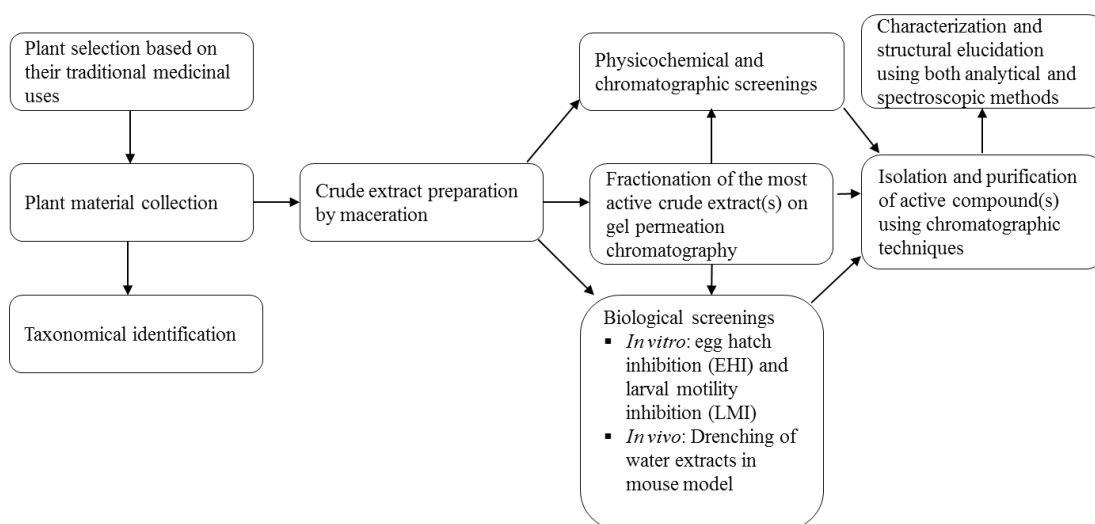


Figure 1.9. Overall approach of my PHD project.

1.14. Thesis hypotheses and objectives

The aim of my PhD thesis study was to undertake bioassay-guided phyto-chemical study of extracts and constituents from Ethiopian anti-parasitic plants used by healers to control gastrointestinal nematode parasites in livestock in order to validate their ethno-medicinal uses.

This aim was addressed through a series of three overall hypotheses and seven specific objectives as described below.

1.14.1. Overall hypotheses

Here the three hypotheses aimed to be tested were:

1. Extracts prepared from selected plants based on their ethno-medicinal uses in livestock will show anthelmintic activity *in vitro* against the free living stages of small ruminant nematodes such as *T. circumcincta*.

2. The major active phytochemical groups isolated from active fractions of these selected plants may belong to plant secondary metabolites known for their anthelmintic activity, such as tannins, flavonoids, saponins and alkaloids.
3. Extracts from selected plants that show anthelmintic activity *in vitro* will show anthelmintic activity *in vivo*.

1.14.2. Specific Objectives

The overall aim of my thesis has been addressed through a series of following seven specific objectives.

1. To conduct *in vitro* eggs hatch inhibition (EHI) and larval motility inhibition assays of four medicinal plant crude extracts using standard anthelmintic evaluation methods on *Teladorsagia circumcincta* eggs and L₃ to validate the claimed activity and to choose the most promising plants and extracts for further phytochemical studies.
2. To assess the nature (molecular size, heat stability and polarity) of active constituents of selected plant extracts by physico-chemical methods followed by EHI assays of treated fractions to determine the effects of these treatments on extract active constituents.
3. To separate the active extracts into discrete fractions by gel-permeation chromatography and assess the EHI to quickly home in on those fractions containing active anti-parasitic compounds.
4. To characterize fractions and isolated compounds under UV-light and using various staining reagents.
5. To isolate and purify compounds from active pooled fractions using various preparative planar and column chromatographic methods.

6. To characterize and propose/elucidate structures of compounds responsible for the observed activities using chromatographic and spectroscopic methods.
7. To assess efficacy by determination of faecal egg count reduction, total worm count reduction and safety (effect on blood haematology) of crude extracts of medicinal plants in mice model.

These specific objectives form the basis of the individual experimental chapters presented below, following an overview of the general Materials and Methods used throughout my thesis.

Chapter Two: Materials and methods

2.1. List of materials and equipment

The following materials and equipment were used for plant material processing, extraction, fractionation and purification steps as well as during the *in vivo* and *in vitro* bioassays: centrifuge (Thermo Scientific Heraeus Multifuge 3RS+, Loughborough, UK), freeze dryer (Edwards Freeze Dryer Super Modulyo, UK), rotary evaporator (Buchi-300, Buchi UK Ltd, Oldham, UK), digital analytical balance (Sartorius BP 210D, Poole, UK), high voltage paper electrophoresis (Laborate LTD, London, UK), stomacher (Seward Stomacher®80 Lab System), stereomicroscope (Meiji and Leica, VTech LTD, Stirling, Scotland), incubator (LEEC Ultrasonic type temperature and humidity controls, LEEC Limited, Nottingham, UK), and real time cell analyser (RTCA, ACEA, Bioscience Inc., San Diego, USA).

2.2. List of solvents

The following solvents were used for crude extract preparations, fractionations and chromatographic purification and/or chromatograms developments: de-ionized water, acetone, methanol, acetic acid, butanol, ethyl acetate, pyridine, ethanol, chloroform, trifluoroacetic acid (TFA), concentrated H₂SO₄, and formaldehyde. Analytical grade solvents were obtained from Sigma Aldrich (Sigma Aldrich Co Ltd, Irvine, UK)

2.3. List of chemicals, reagents, pharmaceuticals and marker compounds

The following chemicals, reagents, pharmaceuticals and authentic marker compounds were used either as antimicrobial for crude extract preparation,

preparation of staining reagents, as marker compounds or positive control pharmaceuticals: 1,1,1-trichloro-2-methyl-2-propanol hemihydrate, thymol (2-isopropyl-5-methyl-phenol), ninhydrin (2,2-dihydroxyindane-1,3-dione), iodine crystal, ammonium molybdate tetrahydrate, vanillin, antimony(III) chloride, Lugol's reagent (iodine and potassium iodide solution), ferulic acid, caffeic acid, D-glucose, sucrose, mannose, galactose, arabinose, xylose, fucose, rhamnose, ribose, galacturonic acid, glucuronic acid, leucine, β -sitosterol, quercetin, oleic acid, formaldehyde were obtained from BDH and Sigma Aldrich, UK. Monepantel (Zolvix; Novartis, Rutherford, UK and ivermectin oral suspension (Oramec®) (Merial Animal Health Ltd, Harlow, UK) were the anthelmintics used as positive controls in the *in vitro* and *in vivo* studies, respectively. Zolvix was used as a positive control in EHI tests; as it is a broad spectrum anthelmintic against sheep parasites such as *T. circumcincta*, i.e. the model parasite used in my *in vitro* experiments, the expectation was that it would be very effective. This was confirmed in the studies; at tested concentration it showed virtually 100% egg hatch inhibition.

2.4. Preparation of plant materials

2.4.1. Selection

The plant materials used in this study were selected on the basis of their ethno-medicinal uses as claimed by traditional healers against gastrointestinal nematodes (Tolossa *et al.*, 2013) with the assumption that they therefore most likely contain biologically active constituents with anti-parasitic properties (Karayil *et al.*, 2014; Atanasov *et al.*, 2015; Ngarivhume *et al.*, 2015). The four plants selected were *C. ruspolii*, *Adenia* sp., *E. thymifolia* and *I. eriocarpa*.

2.4.2. Collection and identification

The whole plant or a particular plant part can be collected depending on where the metabolites of interest accumulate. Hence, aerial (leaves, stems, flowering tops, fruits seeds, stem bark) and underground (bulbs, rhizomes, tubers, roots) parts can be collected separately (Gajbhiye *et al.*, 2015). For my PhD project, *C. ruspolii* and *Adenia* sp. (roots) and *I. eriocarpa* and *E. thymifolia* (aerial parts) were collected as these parts are used by the traditional healers and communities. Plant samples for crude extract preparation were collected in polyethylene bags, tied with rubber bands and transported to Animal Nutrition Laboratory, Hawassa College of Agriculture, Hawassa, Ethiopia on the same day and immediately processed for drying. Any features relating to collected specimens such as local name of the plant, the identity of the part collected, place and date of collection were recorded as part of a voucher (a dried specimen pressed between sheets of paper) and deposited in National Herbarium, Addis Ababa University, Ethiopia for future reference. *C. ruspolii*, *I. eriocarpa* and *E. thymifolia* were botanically identified at species levels whereas *Adenia* sp. was identified only at genus level by group of plant taxonomists in the School of Biological Sciences, Addis Ababa University, Ethiopia.

2.4.3. Drying and grinding

The collected plant materials were brushed to remove soils and other debris and then grated into small pieces. The grated samples were evenly distributed to facilitate homogenous drying on clean plastic sheet in a room with adequate ventilation at temperature of 25°C (Asami *et al.*, 2003; Rocha *et al.*, 2011). A mechanical grinder (mill) was used to shred the grated and dried plant materials to 1-mm particle sizes to

improve the subsequent extraction by rendering the sample more homogenous, increasing the surface area and facilitating the penetration of solvent into cells.

2.4.4. Preparation of crude extracts

The powdered plant materials (5 g) (run-1) were macerated (Azwanida, 2015) in 100 ml (each) of acetone, absolute methanol (MeOH), 70% MeOH or de-ionized water with continuous stirring at room temperature for 72 h. Supernatants were filtered through four layers of mira cloth, centrifuged, dried on rotary evaporator (organic extracts) or in freeze dryer (water extract) and weighed and stored at -20°C until used.

2.5. *In vitro* experiments

2.5.1. Egg hatching inhibition test

2.5.1.1. Egg recovery. The helminth eggs were recovered by a saturated salt floatation technique (Dryden *et al.*, 2005) with modification. The only modification was the amount of faecal samples processed to recover as many eggs as possible to set up series of egg hatch test at a time; 1 g in 10 ml proportionally increased to 30 g in 300 ml of tap water to prepare faecal slurry. Eggs used in this study were collected from male donor sheep (Suffolk × Scottish Mule) aged 8-10 months which were mono-specifically infected with *T. circumcincta*. They were housed indoors on a concrete floor, bedded with shavings, fed grass nut and commercial concentrate pellets and had free access to potable water. They were maintained in clean and well ventilated room. Their body condition was monitored every day. The room was closed in the night and opened in the morning. They were restrained before faecal sampling where faecal samples were collected from rectum using a gloved finger and

a plastic bag. Resulting faecal samples were homogenised in tap water using a stomacher. The resultant faecal slurry was filtered using sieves of different mesh sizes (38, 70, 120, and 250 μm) transferred to plastic test tubes of 50-ml capacity and then centrifuged at $470 \times g$ for 5 minutes. The supernatant was removed using a water aspirator. The sediment (residue) was stirred with stick rod to break the residue and release the eggs. The saturated salt (NaCl) solution ($\rho \geq 1.2 \text{ g/ml}$) was added to the stirred samples and centrifuged again at $470 \times g$ for 5 minutes. The floated eggs were recovered by clamping the plastic test tube with forceps near to the lower meniscus of the solution and then poured over a sieve with pore size of 38 μm to recover parasite eggs.

2.5.1.2. Egg suspension preparation. The egg suspension recovered was washed with de-ionized water to remove any remaining faecal and undigested food particulates. The purified egg suspension was transferred to a glass beaker, and 5 μl was transferred to a grid culture plate to determine egg density per 5 μl under a stereomicroscope to calculate the volume of egg suspension to be placed in each well so that each well contains at least 200 eggs.

2.5.1.3. Egg hatch inhibition (EHI) tests

The EHI tests were conducted according to World Association for the Advancement of Veterinary Parasitology (WAAVP) guidelines (Coles *et al.*, 1992; Coles *et al.*, 2006). The EHI test is the generic name for a series of tests developed to detect anthelmintic drug resistance by gastrointestinal nematodes or to screen plant extracts with anthelmintic properties against gastrointestinal nematode eggs (Demeler *et al.*, 2012; Álvarez-Sánchez *et al.*, 2002). The eggs were used for this test within 1 h of

faecal collection. The dried and powdered extracts of the four solvent systems were re-dissolved separately in de-ionized water to prepare stock solutions (10 mg/ml) and the lower concentrations (3 mg/ml and 1 mg/ml) were prepared by serial dilutions. The test was conducted using culture plates with 24 wells (Thermo Fisher Scientific, Poole, UK). In the test, 500 µl of egg suspension (that contained at least 200 eggs) and an equal volume of plant extract were incubated at 25°C and 90% RH for 48 h. Egg hatching process was then stopped with Lugol's reagent after 48 h. The sample in each well was separately withdrawn using a micropipette into 2-ml Sarstedt tube, centrifuged and then the supernatant was removed using a water aspirator. The concentrated samples were transferred to a microscopic slide using Pasteur pipette and then hatched larvae (L₁) and unhatched eggs counted under a dissecting microscope at 10 × magnification. The percentage of EHI was then calculated as number of eggs counted divided over the sum of eggs and larvae counted, times 100. The same procedure and incubation conditions were also used to bioassay the preparative thin layer chromatography purified compounds from three active pooled fractions of *C. ruspolii*: *Cissus ruspolii* pool A (CRPA), *Cissus ruspolii* pool B (CRPB) and *Cissus ruspolii* pool C (CRPC) and one active pooled faction of *Adenia* sp. pool A (ASPA). For the final EHI tests, all the preparative TLC purified compounds, their corresponding crude extracts and chromatographic fractions (such as Bio-Gel P-2, Sephadex LH-20, RP C-18) were assayed at 20% (v/v) of their respective stock solution for EHI using 96 wells culture plate where 100 µl of egg suspension containing at least 100 eggs was incubated with 100 µl plant sample. The 96 wells culture plates were used due to small test sample sizes. The assays were conducted in triplicate for each tested sample. Any sample with mean EHI activity

greater than 70% is considered as having a high and biologically relevant activity (Githiori *et al.*, 2003); here activity between 50 to 70% is considered moderate, whilst those less than 40% are considered low. In addition, outcomes were statistically assessed for deviation from the negative control, where $P < 0.05$ was considered significant.

2.5.2. Larval motility inhibition test

The larval motility inhibition (LMI) test is also used to estimate the percentage of paralyzed infective third stage larvae (L_3) when incubated in a serial dilution of anthelmintics or bioactive plant extracts with anthelmintic properties. Like EHI test, LMI is also used to assess anthelmintic resistance by gastrointestinal nematodes (Álvarez-Sánchez *et al.*, 2002). The test protocol consists of incubation of larval suspension containing at least 3000 L_3 in serial concentration of anthelmintic drugs, extracts or fractions with anthelmintic properties. Currently, the larval motility inhibition assay can be monitored by real-time cell analyser (RTCA) automated equipment as described by Smout *et al.* (2010), Atienzar *et al.* (2011) and Storey *et al.* (2014).

2.5.2.1. Larval suspension preparation (Baermann technique)

Figure 2.1. shows the larval suspension preparation steps.

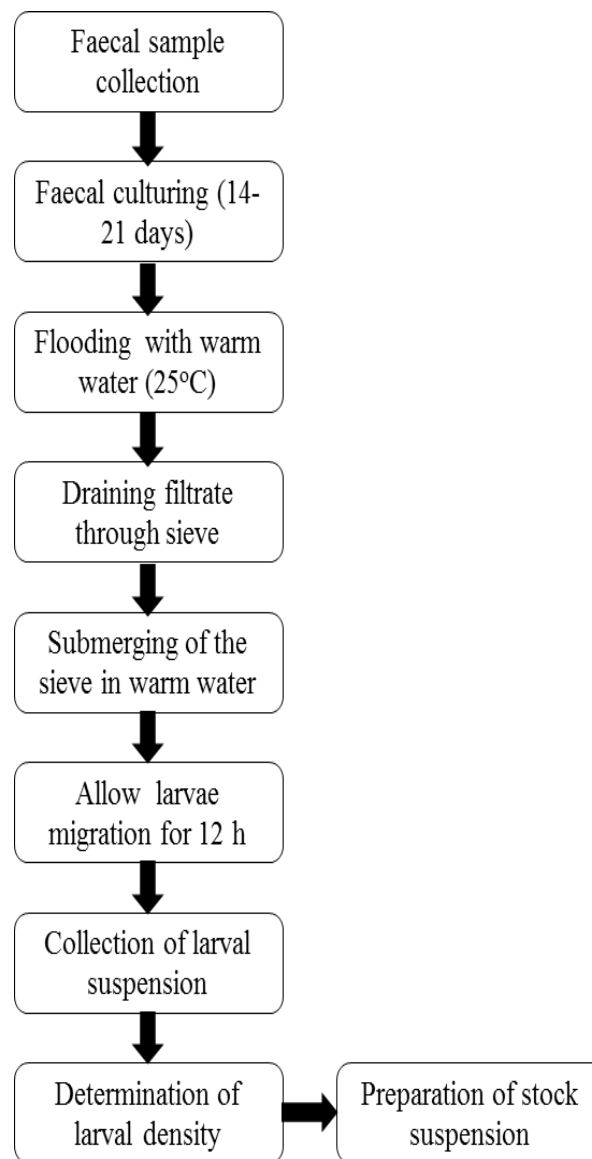


Figure 2.1. Larval suspension preparation through baermannisation.

A faecal sample was collected from donor sheep by putting on harness with bags. The faecal samples were cultured in standard culture room (i.e. separate room with adjustable temperature regulation facility and well-spaced shelves) for 14-21 days. Then, the cultured faecal samples were flooded with warm water, kept overnight and

then filtered the next day. The filtrates were drained through dental napkin sieves. The dental napkin sieves carrying larvae were submerged in big plastic funnel filled with warm water for 12 h to allow larvae migration. The larvae suspensions were collected into culture bottles by opening the stop cock of the funnels from the bottom, concentrated by sedimentation or centrifugation and removal of supernatants. Larval density was determined by counting the number of larvae in 5 μ l of concentrated larval suspension under a microscope. Five replicates (5 μ l each) dispensed onto grid culture plate, larvae counted under microscope and then the average was taken as larvae density in 5 μ l. Then, the volume of larvae suspension to be dispensed into each well was calculated based on the larval density.

2.5.2.2. RTCA monitoring of LMI activities of crude extracts

The RTCA flow diagram is shown in Figure 2.2.

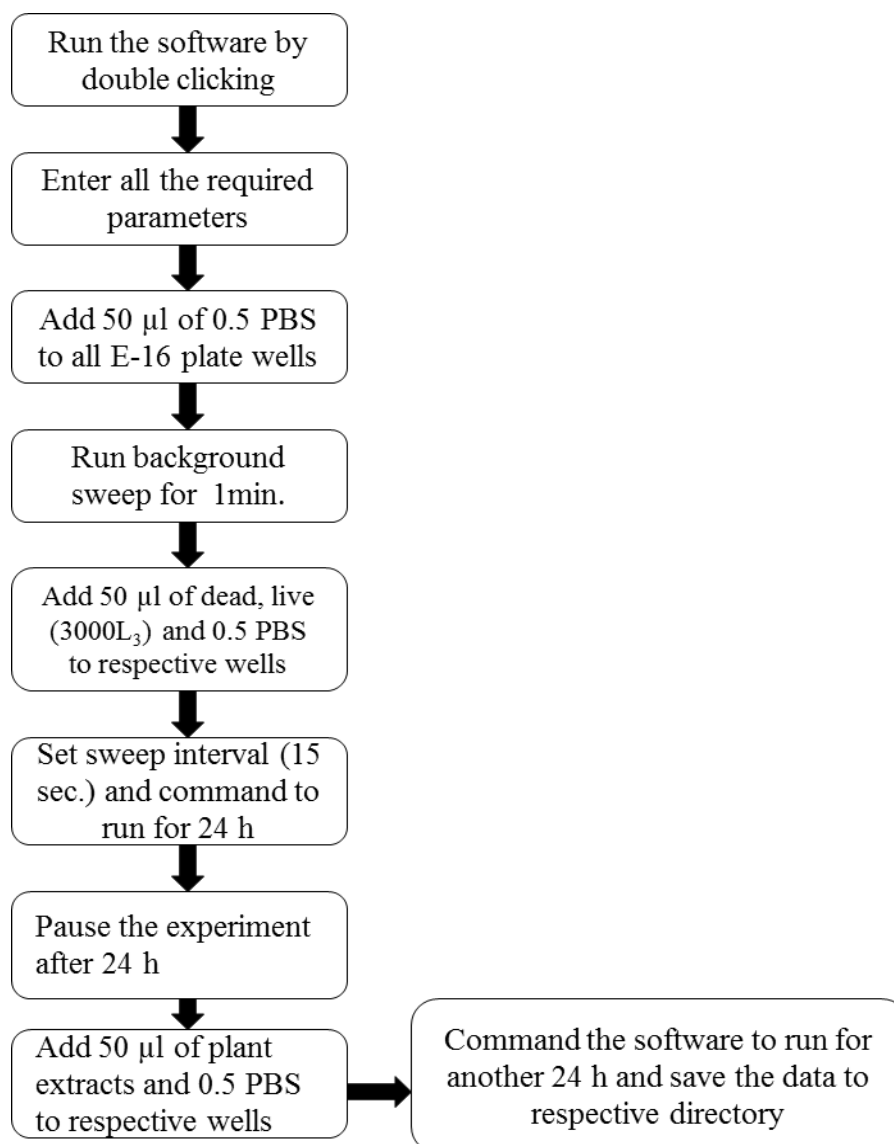


Figure 2.2. Larval motility monitoring by real time cell analyser.

Firstly, phosphate buffered saline, 0.5 PBS (50 µl each) was added to each well of an E-16 plate, placed back onto its port and the RTCA run for one minute to achieve a background reading, referred to as a sweep. Secondly, 50 µl of live and dead larvae (containing at least 3000 L₃ each) and the same volume of 0.5 PBS were added to the

respective wells as per the experimental set up. The E-16 plate was placed back to its port, sweep interval set at 15 seconds and RTCA software set to run for 24 h. The experiment was paused after 24 h, plant extracts or 0.5 PBS (50 µl each) added to the respective wells as per the experiment design and set up, the software commanded to run for another 24 h and then the cell index of each well saved to the directory folder automatically. Then a graph of the mean motility of worms over time for each well was extracted using R software. The RTCA runs on an xCelligence software system (Atienzar *et al.*, 2011).

2.6. Physico-chemical characterization of water extracts

2.6.1. Membrane dialysis

Membrane dialysis tubing was prepared according to the manufacturer's instructions. Thus, dialysis tubing (Medicel membrane Ltd, Greenwich, London, UK) with 19 mm diameter and 12-14000 Da molecular weight cut-off was cut to desired length and then submerged in tap water for 10 minutes and rinsed thoroughly with de-ionized water to remove glycerine or sodium azide preservative. Samples (10 ml with 10 mg/ml) were loaded into dialysis tubing tied both side with strings and submerged into an external de-ionized water (50 ml) placed in measuring cylinder (first dialysis) with gentle stirring on magnetic stirrer plate for 24 h at 4°C. The external water solution of the first dialysis was collected, dried in freezer and labelled as 'small molecules'. The tubing was transferred to a beaker containing 2 l of de-ionized water (for further dialysis) for another 24 h under the same conditions. The new external water solution was discarded and the sample in membrane tubing recovered, dried in freeze dryer and labelled as 'large molecules'. Both samples were stored at -20°C pending EHI tests.

2.6.2. Heat stability testing

Three water crude extracts per plant (2 ml @ 10 mg/ml each) were prepared for *C. ruspolii* and *Adenia* sp. and boiled in a water bath at 100°C for 0, 10 or 60 minutes. The samples were cooled naturally to room temperature and stored at -20°C until use for bioassay. Only the water extract was tested for thermal stabilities of its constituents. Water is the crude extract that showed the highest activity in the first study (see Chapter Three) and also traditional healers use water as a vehicle to drench their animals.

2.6.3. Solvent partition

The water extracts of *C. ruspolii* and *Adenia* sp. (4 ml @ 10 mg/ml each) were taken separately. The pH of extracts was adjusted to nearly neutral (pH~7) using 0.025 M NaOH. The pH of the sample solutions was monitored using universal indicator paper. The extracts (2 ml per plant) were shaken with 2 ml of butan-1-ol or ethyl acetate, and then centrifuged at $2057 \times g$ for 10 min. The upper (organic) and lower (water) phases were dried in Speed Vac and stored at -20°C until use for bioassay.

2.7. Bioassay-guided size-fractionations

2.7.1. Preparation of water extracts

Powdered root samples (50 g each; run-2) of *C. ruspolii* and *Adenia* sp. were macerated separately in 1 L of de-ionized water containing 0.05% (w/v) chlorobutanol to inhibit microbial growth. The macerated samples were stirred continuously at room temperature for 72 h. The supernatants were filtered through mira cloth, which is specifically designed for quick filtration of gelatinous materials.

Then, the filtrate of *Adenia* sp. was centrifuged at $2057 \times g$ for 10 min in an Eppendorf centrifuge model 5810R while that of *C. ruspolii* centrifuged at $41837 \times g$ for 30 min. in a DuPont centrifuge SA-600. For homogeneity of extracts, the clear supernatants from all tubes of the same plant were pooled, then divided into 50-ml aliquots and stored frozen at -20°C . An additional 10 ml was freeze dried and the product weighed (60 mg for *C. ruspolii* and 84.5 mg for *Adenia* sp.).

2.7.2. Fractionations of water extracts on gel-permeation chromatography

A 3.5-ml portion (6 mg/ml for *C. ruspolii* and 8.45 mg/ml for *Adenia* sp.) of the clarified extract (run-1) was passed through a glass column containing 70 ml bed volume of Bio-Gel P-2, eluted with de-ionized water. Fifty-five 4-ml fractions were collected using a BIO-RAD model 2110 automatic fraction collector. The column used for fractionation of *Adenia* sp. extract was washed with de-ionized water for 24 h and then used for fractionation of *C. ruspolii* extract. All fractions were tested for their EHI properties at full strength as described above (section 2.5.1.3). After the active fractions had been identified, thin layer chromatography (TLC) was developed for all fractions and stained with various reagents to assess correlations between the EHI properties of the active fractions and stainable constituents in them. Similarly, 6.6 ml portion of the clarified extracts (run-2) was passed through a glass column containing 132 ml bed volume of Bio-Gel P-2 and eluted with de-ionized water. Sixty 4-ml fractions were collected. TLCs were developed for all fractions and stained with molybdate reagent. Those Bio-Gel P-2 fractions of run-2 with the same chromatogram profiles as the active fractions of run-1 were bio-assayed for their EHI properties at full strengths and serially diluted lower strengths as described above (see section 2.5.1.3). Figures 2.3 and 2.4 show the flow diagram of Bio-Gel P-2

fractionations of *Cissus ruspolii*. and *Adenia* sp. water extracts respectively.

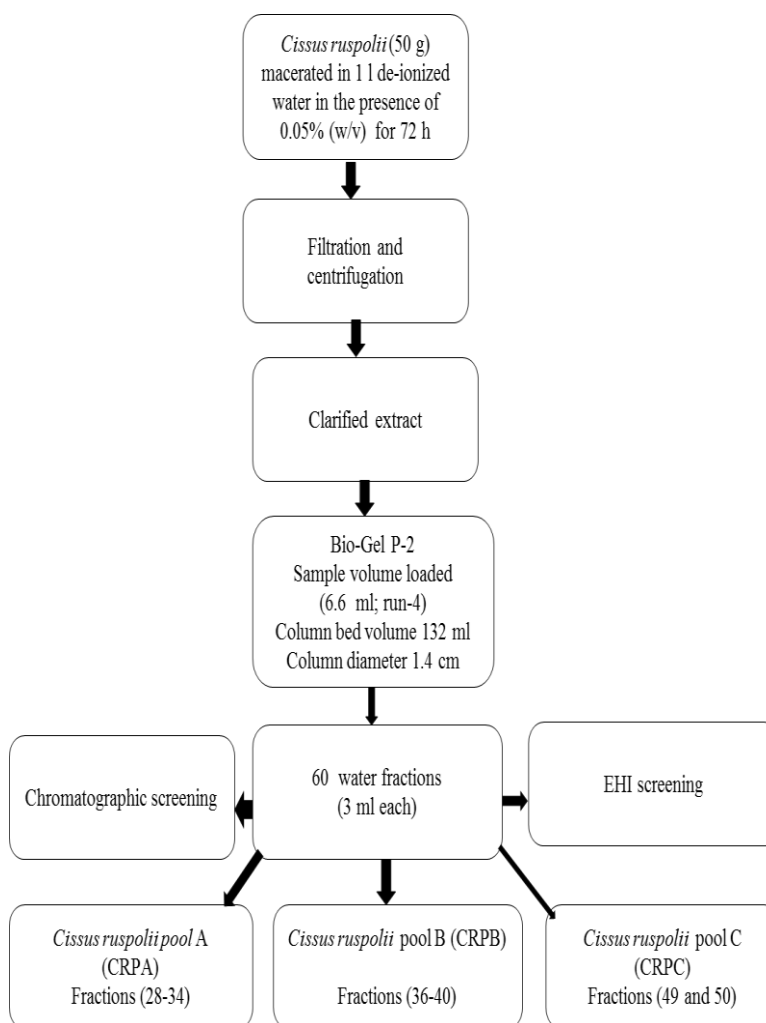


Figure 2.3. Flow diagram of Bio-Gel P-2 fractionation of *C. ruspolii* water extract, resulting in three active pooled fractions.

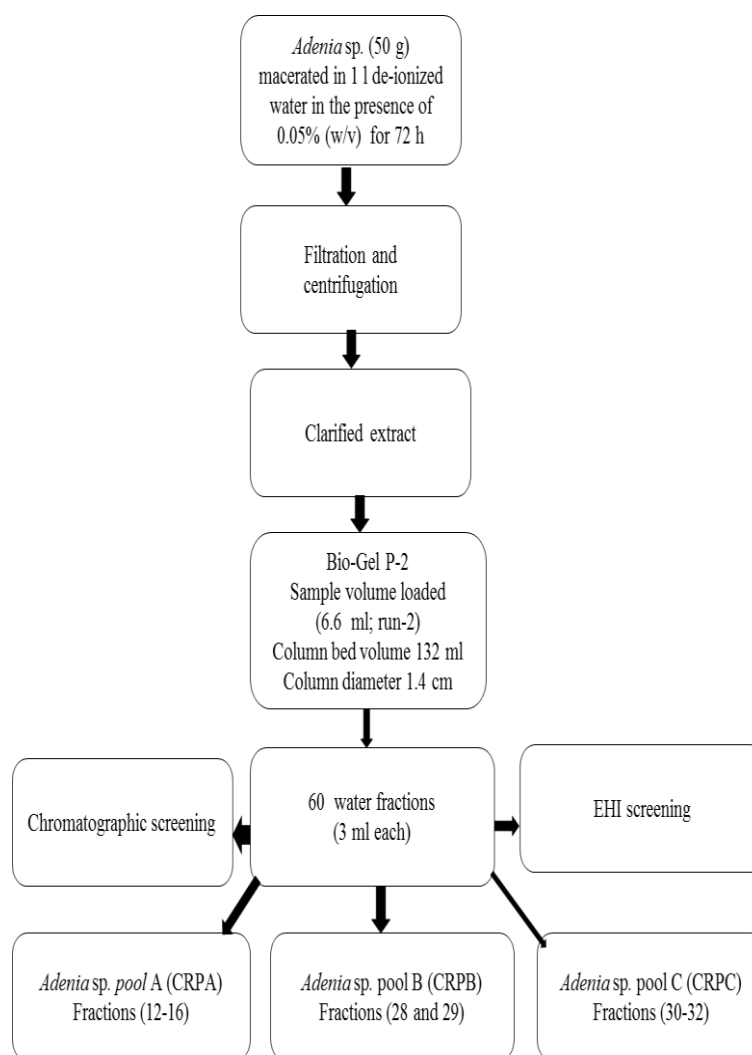


Figure 2.4. Flow diagram of Bio-Gel P-2 fractionation of *Adenia* sp. water extract, resulting in three active pooled fractions.

2.8. Inorganic phosphate assessment in crude water extract of *C. ruspolii*

2.8.1. TLC development and molybdate staining of *C. ruspolii* crude extract

The authentic markers sodium dihydrogen phosphate dihydrate, sodium pyrophosphate, ATP, 3-phosphoglyceric acid, and D-glucose-6-phosphate, at 15 µg/10 µl each in 2:1:1 v/v/v butanol-acetic acid-water (BAW) and water crude extract of *C. ruspolii* (3 µl) were loaded on to a silica-gel TLC plate with F₂₅₄ fluorescent indicator. The TLC was developed in BAW (4:1:1 v/v/v), dried, stained

with molybdate (see section 2.9.2.1), scanned, heated at 105°C for 30 min. and re-scanned, and finally re-heated at 105°C for 4 h and again re-scanned.

2.8.2. TLC development for serially diluted $\text{NaH}_2\text{PO}_4 \cdot 2\text{H}_2\text{O}$ and *C. ruspolii* extract

Crude extract (3 μl) and a dilution series of $\text{NaH}_2\text{PO}_4 \cdot 2\text{H}_2\text{O}$ (1.9–15 μg) were analysed by TLC as in section 2.8.1.

2.8.3. 1D-high voltage paper electrophoresis at pH 2.0 and pH 6.5

2.8.3.1. Sample preparation, loading, and paper electrophoretogram development

A dilution series of $\text{NaH}_2\text{PO}_4 \cdot 2\text{H}_2\text{O}$ (P_i) (0.5–128 μg) and *C. ruspolii* water crude extract (2–16 μl) were loaded onto two identical Whatmann No.1 papers (42× 57 cm). A trace of Orange G was also loaded between neighbouring spots as guide marker to monitor uniform migration of loaded samples. The papers were wetted with electrophoresis buffer, pH 2.0 (formic acid/acetic acid/water, 1:4:45 v/v/v) or pH 6.5 (pyridine/acetic acid/water, 1:33:300 v/v/v) and electrophoresed in tanks filled with immiscible coolants (white spirit for pH 2.0 and toluene for pH 6.5) at 4.5kV (approximately 110 mA) for 30 min. Both developed paper electrophoretograms (PEs) were dried in an oven overnight, and fluorescent phytochemicals were visualized under UV lamp (at 366 nm) without and with exposure to ammonia vapour.

2.8.3.2. Staining reagent preparation and electrophoretogram staining protocol

Phosphates were stained with molybdate. Ammonium molybdate tetrahydrate in 36% (w/v) concentrated HCl and 70% (w/v) perchloric acid mixed with acetone and stirred with a magnetic stirrer until the remaining precipitate completely dissolved and clear solution was achieved. Then, paper electrophoretogram were stained with the molybdate reagent by dipping, dried in fume hood for 10 min., examined visually for any yellow/blue spot formation and then scanned. Again, the same paper electrophoresis were exposed to natural sun light outside of the building for 10 min and examined for any additional spot formation, or colour change (yellow to blue) and then re-photographed.

2.9. Chemical and chromatographic profiling of Bio-Gel P-2 fractions

2.9.1. Sample preparations, loading, TLC development and staining

A 200- μ l portion of each Bio-Gel P-2 fraction was dried in Speed Vac. Dried samples were reconstituted in 10 μ l of either 50% MeOH or BAW (2:1:1 v/v/v), 3 μ l of which was loaded on to TLC with fluorescent indicator at 254 nm. TLCs were run in BAW (4:1:1 v/v/v), dried, examined under UV lamp at 366 nm, captured by digital TLC imaging (Doc.It) and/or stained with various reagents (see section 2.9.2) and scanned using Epson colour scanner 1200 series (Seiko Epson Corporation, Poole, UK).

2.9.2. Staining reagent preparations and staining procedures

2.9.2.1. Molybdate reagent

The 10% (w/v) ammonium molybdate dihydrate in sulphuric acid solution was mixed with acetone in 1:3 ratios by volume. Chromatograms were dipped quickly through this reagent, dried, heated at 105°C for 30 min. and scanned. It is a universal reagent that reacts with a range of phytochemical groups with hydrogen or electron donating properties that form coloured complexes with molybdate and/or reduce Mo (VI) to Mo (IV) such as 3-hydroxy flavonoids (Malešev and Kunti, 2007; Uddin *et al.*, 2014; Ghareeb *et al.*, 2013).

2.9.2.2. Iodine vapour

Iodine crystals (1 g) were placed in a TLC tank. Chromatograms were stained with iodine vapour then placed in plastic file and scanned. Iodine is a very useful universal reagent and most but not all of its reactions are reversible. The use of iodine as vapour enables the detection of separated substances rapidly and economically before final characterization with group specific reagents. Where lipophilic constituents are present on developed and dried chromatogram, the iodine molecules concentrate in the substance spots and give brown chromatographic zones on a yellow background. Moreover, iodine vapour is a universal reagent and its reversible reactions occur with a wide range of organic lipophilic molecules, such as hydrocarbons, fats, waxes, some fatty acids and esters, steroids, antioxidants, detergents, emulsifiers, antibiotics and many miscellaneous organic substances (Joshi, 2012). All relatively lipophilic compounds such as steroids give yellow–brown spots with iodine vapour (De *et al.*, 2010).

2.9.2.3. Thymol reagent

Chromatograms were quickly dipped through 0.5% (w/v) thymol in ethanol containing concentrated H₂SO₄, dried in fume hood, heated at 105°C for 30 min. and scanned. Thymol is used to detect sugars and glycosides (Jork *et al.*, 1990).

2.9.2.4. Ninhydrin reagent

Chromatograms were quickly dipped through 0.5% (w/v) ninhydrin in acetone, dried, heated at 105°C for 30 min. and scanned. It is used to detect amino acids, amines, amino sugars and alkaloids with free primary and secondary amine functional groups (Dykes and Rooney, 2006).

2.9.2.5. Antimony(III) chloride reagent

The chromatogram was stained by dipping through 10% (w/v) of antimony(III) chloride in chloroform, dried in fume hood, examined under UV-lamp at 254 nm and 366 nm, scanned and documented. This is to detect the presence of flavonoids (Jork *et al.*, 1990).

2.9.2.6. Antimony(III) chloride-acetic acid reagent

The chromatogram was stained by dipping through 9% (w/v) of antimony(III) chloride - glacial acetic acid in chloroform, dried in fume hood, examined under UV-lamp and scanned. Then, the same chromatogram heated in oven at 100°C for 5 min. and scanned again (Jork *et al.*, 1990). It is used to stain cardiac glycosides and saponins.

2.9.2.7. Vanillin reagent

The chromatograms were stained by dipping through 6% (w/v) of vanillin in absolute ethanol containing concentrated H_2SO_4 . (2.5 ml for this particular percentage). Vanillin in sulphuric acid is a universal reagent that stains a range of organic compounds such as plant secondary metabolites containing nucleophile group(s) that react(s) with the aldehyde functional group in vanillin (Dykes and Rooney, 2006).

2.10. Isolation, purification and TLC profiling of compounds from pooled active Bio-Gel P-2 fractions

Figure 2.5 shows the overall steps of isolation and purification of compounds A and B from *Adenia* sp. water extract.

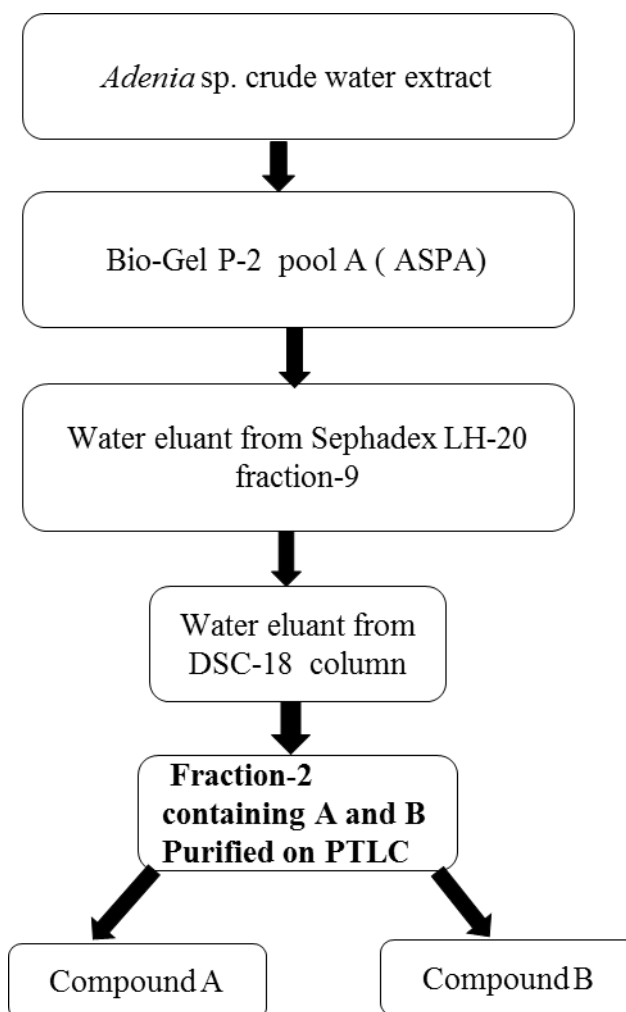


Figure 2.5. Flow diagram on isolation and purification of compounds A and B from *Adenia* sp. water extract.

2.10.1. Isolation and purification of compounds on Sephadex LH-20

Sephadex LH-20 is obtained by alkylation of the hydroxyl groups of Sephadex G-25. Derivatization adds lipophilicity that still retains the hydrophilic characteristics of the gel. Sephadex LH-20 has bead size of 25-100 μm that operates over 2-13 pH ranges. The gel swells in polar solvents such as water, methanol and tetrahydrofuran. In gel filtration mode, using a single polar solvent, compounds are separated according to their sizes where as in partition mode, using solvent mixture, compounds are

separated based on their difference in affinity for stationary or mobile phases (Ghisalbert, 2008).

In this study, Sephadex LH-20 slurry was prepared in water as per the manufacturer's recommendation (1 g of Sephadex LH-20 powder in 4 ml of solvent). The glass column was packed with slurry of 106 ml bed volume. The column was conditioned by passing approximately 1 L of de-ionized water for 48 h. The pooled Bio-Gel P-2 active fractions of *C. ruspolii* and *Adenia* sp. were concentrated from 10 ml down to 6 ml by removing some of the water in the Speed Vac. An aliquot (1 ml) sample was stored at -20°C (to be used as marker for TLC development, to determine the concentration of the pool and control for EHI assays). The concentrated active pooled fractions (5 ml each) of *C. ruspolii* and *Adenia* sp. were loaded onto the column. Eighty fractions (4 ml each) were collected using a methanol gradient: de-ionized water, 20%, 40%, 60%, and 80% MeOH and absolute methanol. Thirty fractions for deionized water and ten fractions (each) for the remaining solvent systems were collected.

2.10.2. Further purification of LH-20 fractions on RP C₁₈ column

A reversed phase discovery C-18 (C₁₈) column (Supelco, Sigma Aldrich, 5 cm × 4.6 mm, 3 μm) was conditioned by use of absolute methanol followed by de-ionized water (5x1 ml each). Samples (3 ml each) were loaded on to the column. The elution was done with de-ionized water followed by methanol step-wise eluents. For de-ionized water, 10% and 20% methanol fractions, five 1 ml sub-fractions per solvent were collected, and for the 40%, 60%, 80% and absolute methanol five 5 ml sub-fractions were collected.

2.10.3. Further purification of compounds on preparative TLC

2.10.3.1. Purification of C₁₈ water fraction of ASPALH-20-9 by PTLC

The C₁₈ water fraction-2 (see Figure 2.5) from ASPALH-20-9 (533 µl; 0.13 mg) was dried in a Speed Vac, re-dissolved in 40 µl of BAW (2:1:1 v/v/v), and a portion (32 µl) was loaded as an 8-cm streak onto a non-fluorescent TLC with plastic backings (Merck, Germany; 20 cm x 20 cm dimension and 0.1-0.25 mm thickness); 32 µl de-ionized water was loaded onto a different part of the same plate. Preparative TLC was developed in BAW (4:1:1 ratio by volume) twice and dried; a 1-cm strip was cut off and stained with vanillin-concentrated H₂SO₄ (see section 2.9.2.7). The vanillin stained strip was used to locate and mark (with pencil) the position of separated bands on the rest of the PTLC. The marked target band with 3 cm band width containing two very close migrating compounds was subdivided into six smaller bands (0.5 cm each), numbered from bottom top as bands 1-6 (i.e. B-1, B-2, B-3, B-4, B-5 and B-6). Each sub-band was scraped off the PTLC separately, divided into two and mixed with 2 ml of de-ionized water (1 ml added to each), centrifuged at $2057 \times g$ for 30 minutes and supernatants (1 ml each) collected in separate in vials per sub-band. From supernatants 1 and 2 of each sub-band, 50 µl was dried in Speed Vac, re-dissolved in 8 µl BAW (2:1:1 v/v/v) and the whole 8 µl was loaded on to TLC with fluorescent indicator at 254 nm, developed in BAW (4:1:1 v/v/v), stained with vanillin and heated at 120°C for 5 minutes and 3 h. Based on their degree of purity and TLC profiles, the slow moving (B_{1/1}) and the relatively fast moving pooled bands (supernatant of band-3 subfraction-1 (B_{3/1}) and supernatant of band-4 subfraction-1 (B_{4/1}) fractions were dried in Speed Vac. and labelled as compound A (0.016 mg) and B (0.027 mg), respectively. Parallel bands from the de-ionized water

zone were eluted, dried and used as negative controls for NMR analysis.

2.10.3.2. Purification of C₁₈ water fractions of CRPALH-20

Non-fluorescent TLC plates were washed with acetone/acetic acid/water (4:1:1 v/v/v) on a rocker for 2 h and dried in a fume hood. About 3.8 ml (each) *C. ruspolii* pool A Sephadex LH-20 (CRPALH-20) fractions 14, 16 and 17 were dried in a Speed Vac (0.017, 0.011, 0.009 mg respectively), re-dissolved in 144 µl (per sample) of BAW (2:1:1 v/v/v), loaded (8 µl/cm) onto washed non-fluorescent plate, developed twice in BAW (4:1:1 v/v/v) and dried. Chromatogram development, staining of separated bands, band markings, band numberings, supernatant recoveries were similarly done as shown in section 2.9.3.2.

2.10.3.3. Purification of C₁₈ water and methanol fractions of CRPBLH-20

PTLC purifications, chromatograms development, staining and supernatants recoveries of C₁₈ pooled fractions of CRPBLH-20 (water of 49-51 and 56-58 and 20% MeOH of 56-58), 4.2 ml (each) were done as described in section 2.9.3.1 and 2.9.3.2. The dried sample weighed 0.012 mg (49-51), 0.078 mg (56-58) and 0.01 µg (for 20% MeOH of 56-58).

2.11. NMR and MS analysis methods

NMR experiments were done on a Bruker Avance-500 spectrometer (Bruker, Rheinstetten, Germany) equipped with sample exchangers with DCH (dual cryoprobe optimised for ¹³C/¹H) with ¹H at 500 MHz; ¹³C at 125 MHz and deuterated water (D₂O) as solvent. ¹H-NMR, ¹H-¹H correlation (COSY), 1D total correlation (TOCSY), distortionless enhancement by polarization transfer (DEPT) spectra were

recorded using standard Bruker pulse sequences. System control and data evaluation was done with the XWINNMR software package version 2.6 (Bruker, Rheinstetten, Germany).

Mass spectra were also generated on Bruker 12 T SolariX instrument for Fourier transforms ion cyclotron resonance mass spectrometry (FT-ICR MS). This instrument was equipped with electrospray ionization (ESI), atmospheric pressure photoionization (APPI) and matrix-assisted laser desorption/ionization-time-of-flight (MALDI-TOF) ion sources with collision induced dissociation (CID) mode of fragmentation on MS/MS spectrometry. The mass spectrometer operating conditions included a capillary voltage of +8 v (positive ionization mode). The source temperature and desolvation gas temperature were set at 150 and 450°C, respectively. Spectra were recorded in positive mode. Full-scan spectra were acquired over the range of m/z 100–2000. In the second MS, the most intense ions from the first MS spectrum were selected for the collision-induced dissociation. System control and data evaluation was done with the Bruker Compass data analysis 4.2 (Bruker, Rheinstetten, Germany). NMR spectra were generated by Dr. Ian Sadler and Dr. Lorna Murray, and MS spectra by Dr. Logan MacKay, all of School of Chemistry, UoE.

2.12. *In vivo* mice model experiment

In vivo validation of bioactive crude extract or fraction of medicinal plant origin involves the use of a naive animal model, inoculated with target pathogenic organism, check for infection establishment, administration of the substance, and then check efficacy and toxicity of sample administered by collecting and analysing biological samples. Because the overall success rate of active target compound

during clinical development depends on preclinical data, validated and predictive model and target animals used during preclinical research are pivotal to bridge the translational gap to the clinic research and success of the new chemical entity (Denayer *et al.*, 2014).

2.12.1. Animals and housing

A total of 32 female C57BL/6 mice (8 weeks old; 17-22 g body weight) were obtained from The University of Edinburgh Animal House, Edinburgh, UK. These mice are characterised as poor responders as they are maintaining the infection for many weeks. They also appeared to experience sufficient performance penalties during parasitism, which makes them appropriate model organisms for livestock. Animals were housed in groups of four, in plastic cages containing wood-chip bedding and adapted for one week in the animal house prior to usage. The room was maintained at a temperature of ($21\pm 2^{\circ}\text{C}$) with relative humidity of ($45\pm 5\%$) under a 12 h light/dark cycle. All animals had *ad libitum* access fresh tap water and a standard pelleted mouse diet (RM3; SDS, Witham, UK), formulated to supply 202 g/kg digestible protein and 12.2 MJ/kg digestible energy. Animals were cared for in accordance with the guideline to the care and use of experimental animals (NRC, 2011). The experimental protocol was reviewed and approved by SRUC Ethical Review Body (AE ED 28/2016) and The University of Edinburgh Veterinary Services (249-KB-16), and conducted under Home Office licence authority (PPL 60/4395).

2.12.2. Preparation of infective L₃ larvae of *H. bakeri*

The infective larvae of *H. bakeri* used were kindly donated by Dr Amy Buck (University of Edinburgh). Briefly, the life cycle of the parasite was maintained in C57BL/6 × CBA F₁ mice (Jenkins and Behnke, 1977), faeces collected 14 days post infection, cultured at room temperature for 8-14 days, and then infective larvae L₃ of *H. bakeri* were harvested through baermannisation. The final concentration was set at 1000 L₃ per ml and checked by a second person. Mice inoculation was done on the same day of larval harvesting.

2.12.3. Mice handling during oral gavage

Larval suspension, plant extracts and controls were administered directly into the stomach of mice via oral gavage. In this procedure, a bulb tipped gastric gavage needle mounted to a tuberculin (1 ml) syringe was used to deliver larvae into the stomach. The mice was gently restrained (grasped by the loose skin of the neck and back) to immobilize the head. Then, the mice were maintained in an upright (vertical) position and the gavage needle was passed along the side of the mouth. Following the roof of the mouth, through gravity, the needle was advanced into the oesophagus and then toward the stomach. After the needle was passed to the correct length, the samples were injected.

2.12.4. Animal infection protocol

Each mouse was inoculated with 200 *H. bakeri* L₃ by oral gavage with 0.2 ml larval suspension (day 0). This infection model has been previously used to establish chronic, sub-clinical parasitic infection in this mouse model, and consistent with a minimum possibility of accidental over-challenging (Athanasiadou *et al.*, 2015)

2.12.5. Plant extracts and ivermectin stock solution preparation

Freeze dried water extracts *Adenia* sp. and *C. ruspolii* (550 mg each) were separately dissolved in 10 ml of deionized water to prepare a stock solution with 55 mg/ml concentration. The anthelmintic stock was prepared by adjusting the dose (mg/kg BW) based on the 2.5 ml of 0.08% ivermectin per 10 kg BW recommended for sheep drench using the average body weight of mice used in the experiment. The required concentrations were prepared by serial dilution for both plant extracts and ivermectin. Both ivermectin and plant extracts were dissolved in water.

2.13. TFA hydrolysis of putative triterpene glycosides A and B from *Adenia* sp.

Reversed phase C₁₈ water fractions 3 and 4 assumed to contain compounds A and B (0.5 ml) were dried separately in Speed Vac and weighed. The dried samples (0.07 mg each) were re-dissolved in 2 M TFA (300 µl) and heated at 120°C for 1 h. The mixture was cooled to room temperature and then dried in Speed Vac to remove TFA. Water (50 µl) was added and re-dried to completely remove the TFA. The re-dried sample was again re-dissolved in 30 µl of water and portions (2 and 8 µl) were loaded on to each of two non-fluorescent TLC plates with monosaccharide marker mixtures (2 µg each). The first and the second TLCs were developed in ethylacetate-pyridine-acetic acid-water, EPAW (6:3:1:1 v/v/v/v) and BAW (2:1:1 v/v/v) respectively. Both TLCs were developed twice, dried in fume hood, and stained with thymol (see section 2.9.2.3).

Chapter Three: *In vitro* screening of anti-parasitic activity of extracts from four Ethiopian medicinal plants

3.1. Abstract

A series of *in vitro* EHI tests were conducted on four Ethiopian medicinal plant crude extracts, using a standard anthelmintic evaluation method and *T. circumcincta* eggs. This was carried out, not only to underpin the claimed medicinal properties of these plants, but also to choose the most promising plant(s) and extract(s) for further anthelmintic and phytochemical studies. Highly significant plant type-, solvent polarity- and dose-dependent EHI were observed. Broadly, EHI properties of plant extracts increased with increasing extract doses, although these increases differed in magnitude between the type of plant and solvent polarity used for extraction. At 10 mg/ml concentration, the 70% MeOH extract of *C. ruspolii* and the water extracts of both *C. ruspolii* and *Adenia* sp. completely inhibited egg hatching. *E. thymifolia* extracts obtained in all solvent systems showed less than 30% EHI activity at highest concentration. For *I. eriocarpa*, only the 70% MeOH extract at 10 mg/ml showed greater than 70% EHI. On the basis of these results, LMI properties were evaluated for selected *C. ruspolii* and *Adenia* sp. crude extracts. The 70% MeOH extract of *C. ruspolii* and water extracts of both *C. ruspolii* and *Adenia* sp. showed a significant inhibitory effect ($P < 0.05$) on the motility of *T. circumcincta* larvae at 10 mg/ml. In conclusion, these *in vitro* experiments not only support the view that the ethno-medicinal plants studied possess anthelmintic properties, but also informed the choice of using water extracts from *C. ruspolii* and *Adenia* sp. as the plant extracts for further bioassay-guided phytochemical studies.

3.2. Introduction

Infections by gastrointestinal nematode parasites are among the most common and economically important diseases of grazing livestock (Kabaka *et al.*, 2013; Jurasek *et al.*, 2010). They are a worldwide problem, manifested by reduced weight gain, meat production and milk yield arising from anorexia, anaemia, diarrhoea and oedema, and in severe cases mortality, particularly in young, aged and immunosuppressed animals (Kabaka *et al.*, 2012). Control of gastrointestinal nematode parasites in small ruminants is generally achieved by use of anthelmintics in combination with grazing management. However, frequent use of conventional anthelmintics over many years has resulted in the inevitable development of drug resistance against benzimidazole, imidazothiazole and ivermectin, which have long been the three main broad spectrum families of anthelmintics (Fleming *et al.*, 2006). The development of drug resistance (Shalaby, 2013), but also concern about potential drug residues in animal products, inaccessibility of anthelmintics in rural developing countries, and continuing economic losses due to parasite infections have all necessitated a search towards an alternative parasite control strategy (Rahman *et al.*, 2006).

One of such alternative methods of worm control is the use of medicinal plants (Hrckova *et al.*, 2013). Although considered an alternative for farmers in the developed countries, in many parts of the developing world, small-scale and subsistence farmers have long relied on medicinal plants as their traditional methods of deworming (Mirzaei *et al.*, 2013). Plants may contain valuable chemical compounds in the form of bioactive PSM that could offer alternatives to the modern synthetic drugs (Shai *et al.*, 2009; Tandon *et al.*, 2011). In recent years, there have been many *in vitro* and *in vivo* studies into bioactivities of natural products of plant

origin against parasites, microbes and other pathogens (Adamu *et al.*, 2013; Githiori, 2004; Kennedy and Wightman, 2011; Molan *et al.*, 2010; McLaughlin *et al.*, 1998). Such use of plants and plant-derived natural compounds as (part of) herbal preparations will continue to play major roles in health care systems of many developing countries across the world as the preferred remedies against various ailments, including parasite infections (Salifou *et al.*, 2013; Ogugua *et al.*, 2013). In Ethiopia, there are a large number of medicinal plants used by ethno-veterinary medicine practitioners to control ecto- and endoparasite infections in livestock (Eugale *et al.*, 2007; Tomass *et al.*, 2013; Tolossa *et al.*, 2013; Lulekal *et al.*, 2014). The objective of this chapter was to screen four indigenous Ethiopian medicinal plants claimed by traditional healers for their anti-parasitic properties using the sheep nematode *T. circumcincta* as a model in a series of *in vitro* studies, and to choose the most promising plant(s) and extract(s) for further phytochemical studies.

3.3. Materials and methods

3.3.1. Extract preparation

Extract preparation was done by maceration (see section 2.4 for details and Figure 3.1 for a schematic representation). In summary, powdered plant materials were extracted by maceration, under continuous stirring, using four solvent systems (acetone, MeOH, 70% MeOH and de-ionized water) for 72 h at room temperature. The supernatants were filtered using four layers of mira cloth, centrifuged, dried by rotary evaporator (organic extracts) or freeze dryer (water extract), weighed, and then stored at -20°C pending bioassay.

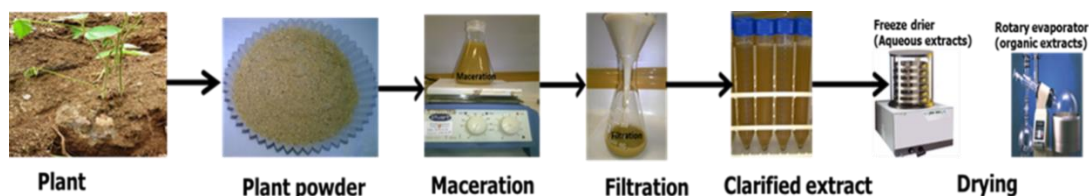


Figure 3.1. Schematic representation of crude extracts preparation by maceration.

3.3.2. EHI and LMI test

Preparation of parasite eggs suspensions and EHI assays were carried out as detailed earlier (see section 2.5 and Figure 3.2 for a schematic illustration). In summary, *T. circumcincta* eggs were obtained from donor sheep faeces using saturated salt flotation technique. The EHI assays were done by incubating the parasite egg suspension with plant extracts using 24-well culture plates at 25°C and 90% RH. Incubation was stopped by Lugol's reagent after 48 h. The total numbers of unhatched eggs and hatched first-stage larvae were counted microscopically. The

0.05% chlorobutanol and de-ionized water were used as negative control. No positive control used.

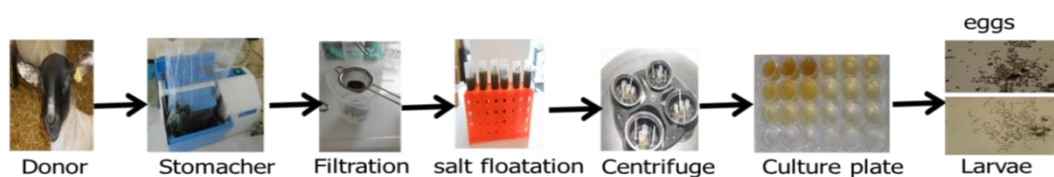


Figure 3.2. Schematic representation of parasite eggs recovery and EHI test.

Larval motility inhibition tests were carried out through RTCA as described previously (see section 2.5.2 for detail and Figure 3.3 for schematic representation). In summary, motility of *T. circumcincta* L₃ was monitored for 24 h before plant extracts or PBS was added followed by another 24 h of motility monitoring. Readouts were compared with data from wells containing dead larvae with or without extract, and blanks. The test was done only once on the same batch of larvae on the same day in triplicate. The dead larvae used as positive control in this project were obtained from stock. However, larvae can be killed at -80°C in freezer or using 10% formalin then thorough washing with normal saline followed by de-ionized water and then the larvae dose adjusted to required concentration.



Figure 3.3. Schematic representation of the real time cell analyser (RTCA) setup used for the larval motility test.

3.3.3. Calculations and statistics

The EHI data were expressed as a percentage, i.e. the number of eggs counted as a percentage of the total of the number of eggs and larvae counted. These data were arcsine transformed prior to 4×4×3 factorial analysis through ANOVA in order to examine the effect of plant, solvent, concentration and their interactions, and are reported as back-transformed means with standard errors.

The LMI data was extracted and analysed by R software to convert the cell index as function of time before and after adding of plant extracts monitored and recorded by RTCA software to mean motility as function of time. Mean motility is the average motility of larvae obtained from three equivalent well readings. For instance, the mean motility of live worms incubated with a given dose level of plant extract is the average of live larvae motility readings obtained from three E-16 well plate. The larval motility is monitored automatically by RTCA and displayed as cell index versus time (hr) and the mean motility as function of time is extracted by R software. Then, the effects of plant extracts on the larval motility were visually inspected by comparing the mean motility plot of the live larvae before and after adding plant extracts as well as by comparing the live larvae with plant extract plot vs dead worms with plant extract and live larvae with PBS plots.

3.4. Results

3.4.1. Yields of crude extracts

Table 1 shows the yields and colours of crude extracts of *I. eriocarpa*, *E. thymifolia*, *C. ruspolii* and *Adenia* sp. prepared by maceration in the four solvent systems used. The extract yields were dependent on polarities of solvent systems employed in extraction. Except for *I. eriocarpa*, the yields more or less increased with increasing solvent polarities. For instance, the yields in 70% MeOH and de-ionized water were greater than in the less polar solvents acetone and absolute methanol. However, 70% MeOH and water solvent systems had comparable yields followed by absolute methanol.

The difference between water, 70% MeOH, MeOH and acetone is the difference in polarity, which related to their extractive power. Water is the most polar followed by 70% MeOH. Acetone is the least polar. For *Adenia* and *Cissus*, the water and 70% MeOH have high extractive power to capture the most polar and active constituents of these plants than the relatively low polar solvents such as acetone and methanol.

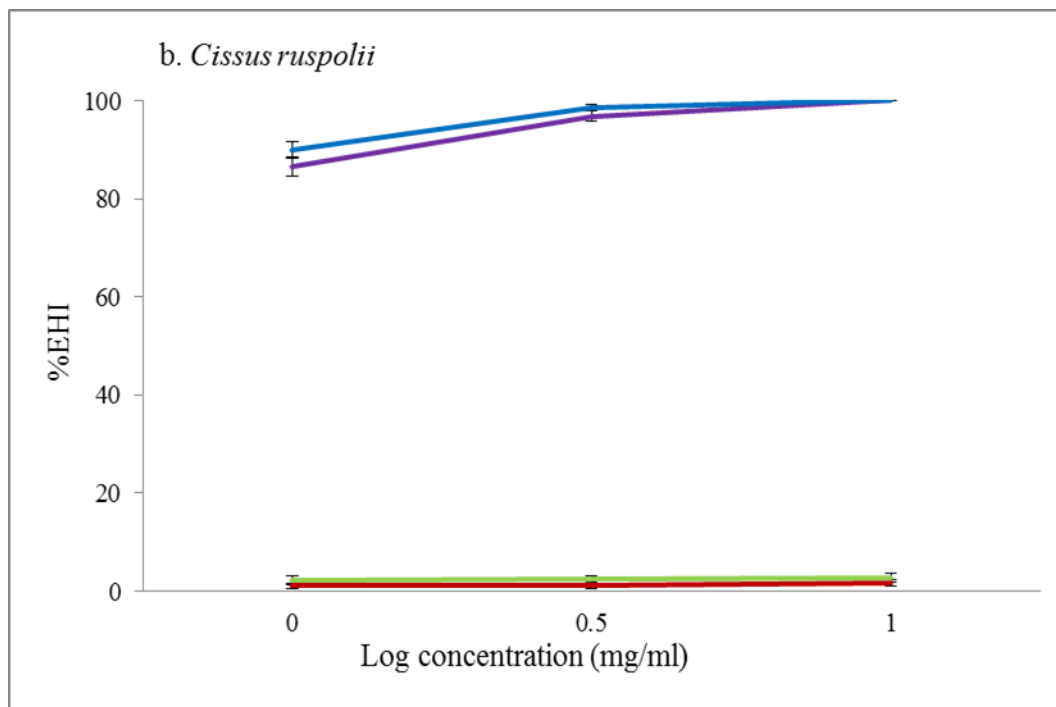
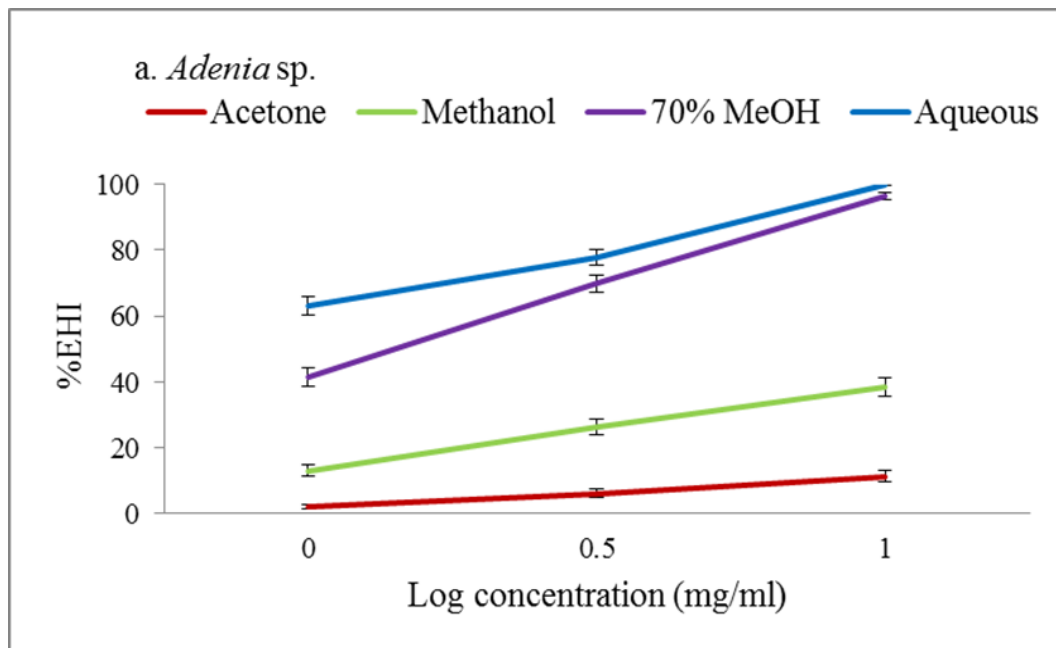
All acetone extracts were yellow coloured in day light except for *Adenia* sp. that coloured milky/creamy. Absolute methanol extracts were generally brown coloured for all plants. The 70% MeOH extracts were brown coloured except for *Adenia* sp. that coloured yellow. The water extracts of *E. thymifolia*, and *Adenia* sp. were generally yellow coloured whereas those of *I. eriocarpa* and *C. ruspolii* extracts were brown coloured.

Table 3.1. Plant extract colour and yield from four Ethiopian plants with claimed anthelmintic properties.

Plant	Solvent	Extract colour	Extract yield (%)
<i>I. eriocarpa</i>	Acetone	Bright yellow	1.4
	Methanol	Light brown	0.6
	70% MeOH	Brown	5.2
	De-ionized water	Light yellow	9.2
<i>E. thymifolia</i>	Acetone	Light yellow	3.4
	Methanol	Light brown	0.8
	70% MeOH	Dark brown	8.0
	De-ionized water	Yellow	8.0
<i>Adenia</i> sp.	Acetone	Milky/creamy	0.4
	Methanol	Brown	11.6
	70% MeOH	Yellow	12.6
	De-ionized water	Bright yellow	9.6
<i>C. ruspolii</i>	Acetone	Yellow	2.4
	Methanol	Brown red	8.4
	70% MeOH	Dark brown	10.8
	De-ionized water	Brown	11.6

3.4.2. EHI tests of crude extracts

The EHI results of the four medicinal plant extracts carried out at various concentrations are shown in Figure 3.4. Highly significant three-way interactions between plant, solvent and concentration were observed ($P < 0.001$), indicating that whilst EHI increased with increasing extract concentration, these increases differed in magnitude between the plant-solvent combinations used. As such, the EHI assay results showed that the anti-parasitic properties of extracts of all solvent systems were dose dependent except for acetone and methanol extracts of *C. ruspolii*. At 10 mg/ml, 70% MeOH of *C. ruspolii* and water extracts of both *C. ruspolii* and *Adenia* sp. completely inhibited egg hatching. *E. thymifolia* extracts of all solvent systems at all tested concentrations showed less than 30% EHI activities. For *I. eriocarpa*, only the 70% MeOH extract at 10 mg/ml showed greater than 70% EHI (Figure 3.4). The lack of a strong dose response for water and 70% MeOH *Adenia* sp. and *C. ruspolii* implies that the two plants are highly active even at the lowest dose (1 mg/ml). Only negative controls (0.05% (w/v) chlorobutanol and water) were used. The graphs show dose dependency of plant extracts. The negative controls do not have dose levels like plant extracts and the log of 0 does not exist, so therefore negative control results were not shown on the graph.



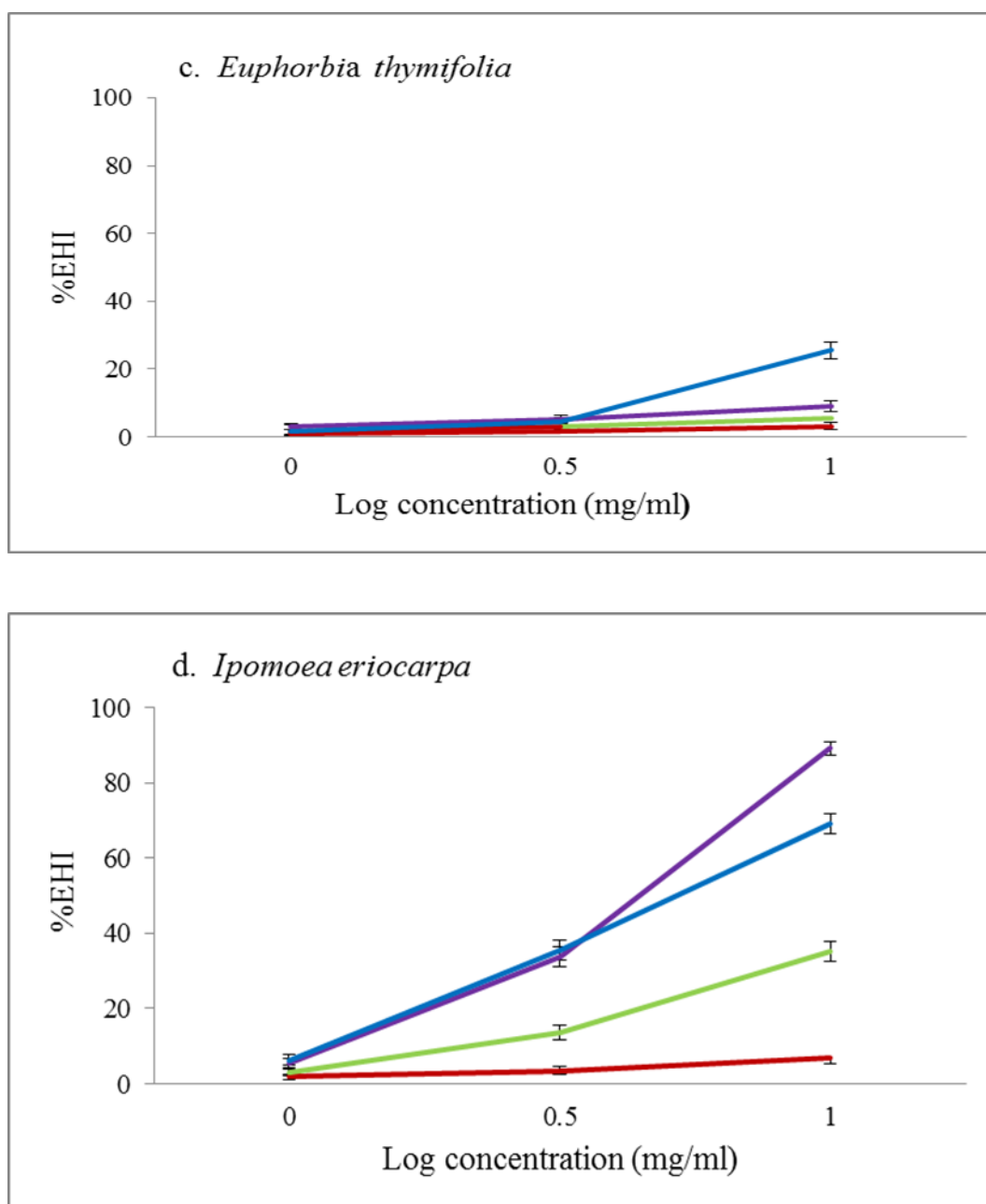


Figure 3.4. Mean of egg hatch inhibition (EHI, %) with standard error of the mean (n=3) of crude extracts. *Adenia* sp. (a), *C. ruspolii* (b), *Euphorbia thymifolia* (c) and *Ipomoea eriocarpa* (d). — Acetone — Methanol — 70% MeOH — Water.

Since the first series of EHI informed the choice to use water extracts of *C. ruspolii* and *Adenia* sp. for further study in this PhD, additional samples were collected from Ethiopia during December 2013 (Year 2) of the study. Year 1 is the plant sample

collected in December 2012, extracted by maceration method and tested for its EHI properties in May 2013 (see Figure 3.4). Year 2 is the plant sample collected in December 2013, extracted by maceration at the same time in parallel with the one year old sample (Year 1) and both tested in parallel for their EHI properties (see Figure 3.5). This allowed assessing the degree of consistency of yield and anti-parasitic activity over time, by comparing yield and EHI of Year 2 samples with those collected during December 2012, i.e. Year 1 samples.

The difference in EHI properties of *C. ruspolii* between Year 1 and Year 2 might be related to differences in year of collection. The difference in efficacy due to year of collection could be associated with environmental and edaphic factors that affect the chemical profile of medicinal plants from year to year.

The EHI test results of both Year 1 and Year 2 samples, bio-assayed at full and their serially diluted lower concentrations, are shown in Figure 3.5. In here, EHI is plotted against the log-transformed concentrations, arising from serial dilutions of the full strength extracts. Natural hatch rate is the percentage of unhatched eggs after incubation with deionized water for 48 h. In this work, the egg hatch tests were done in an incubator working at 25°C and 90% RH. The natural hatching rates for eggs incubated in deionized water were varied between 0 and 2.5%.

The dried weight of Year 1 and 2 samples recovered were 8.67 and 8.45 mg/ml for *Adenia* sp. and 6.17 and 6.00 mg/ml for *C. ruspolii* respectively. The EHI efficacies of Year 1 and Year 2 samples of both plants showed very similar dose dependent EHI activities (Figure 3.5), although at full strength and second dilution, Year 1 *C. ruspolii* appeared slightly more effective than its Year 2 counterpart.

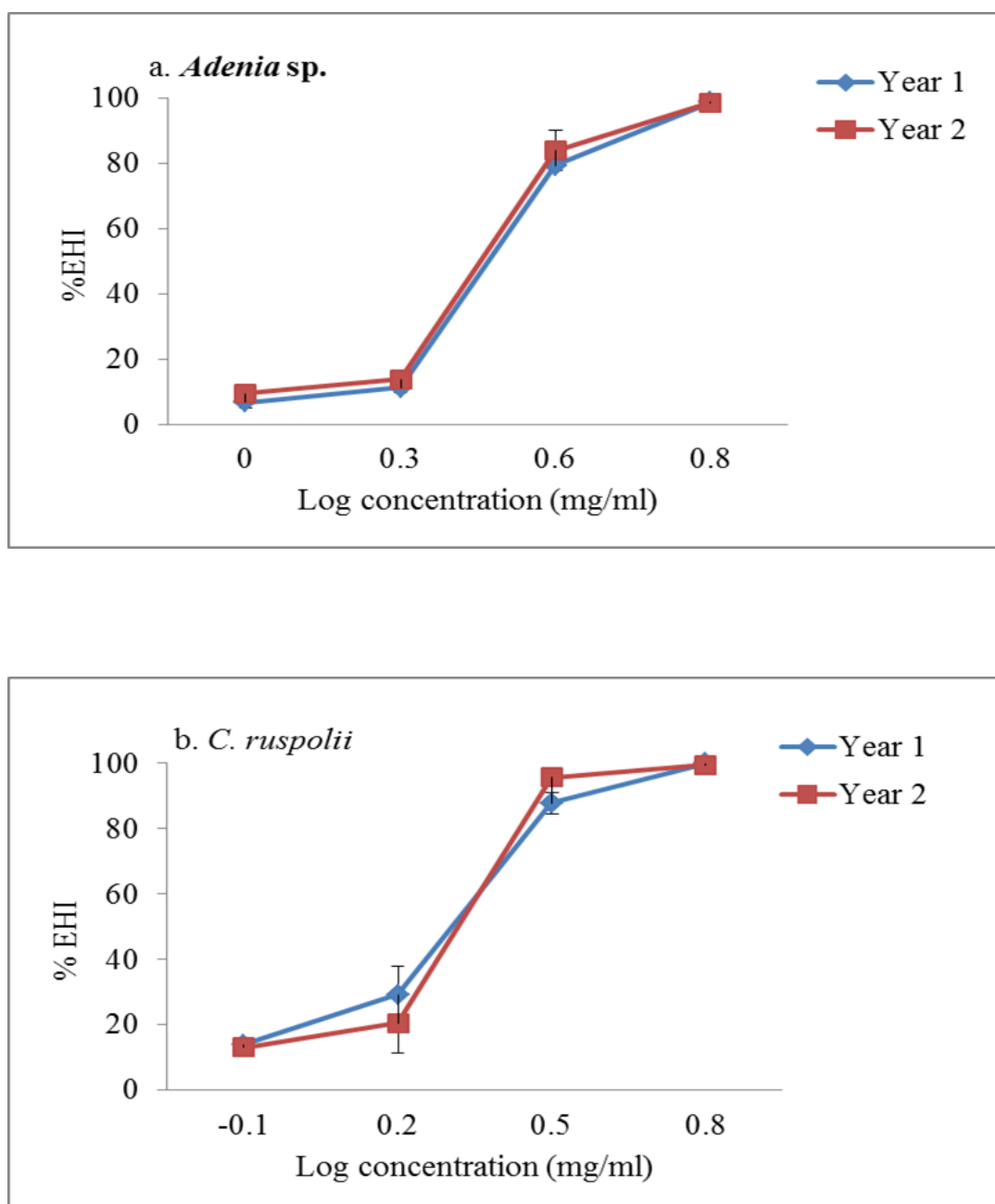
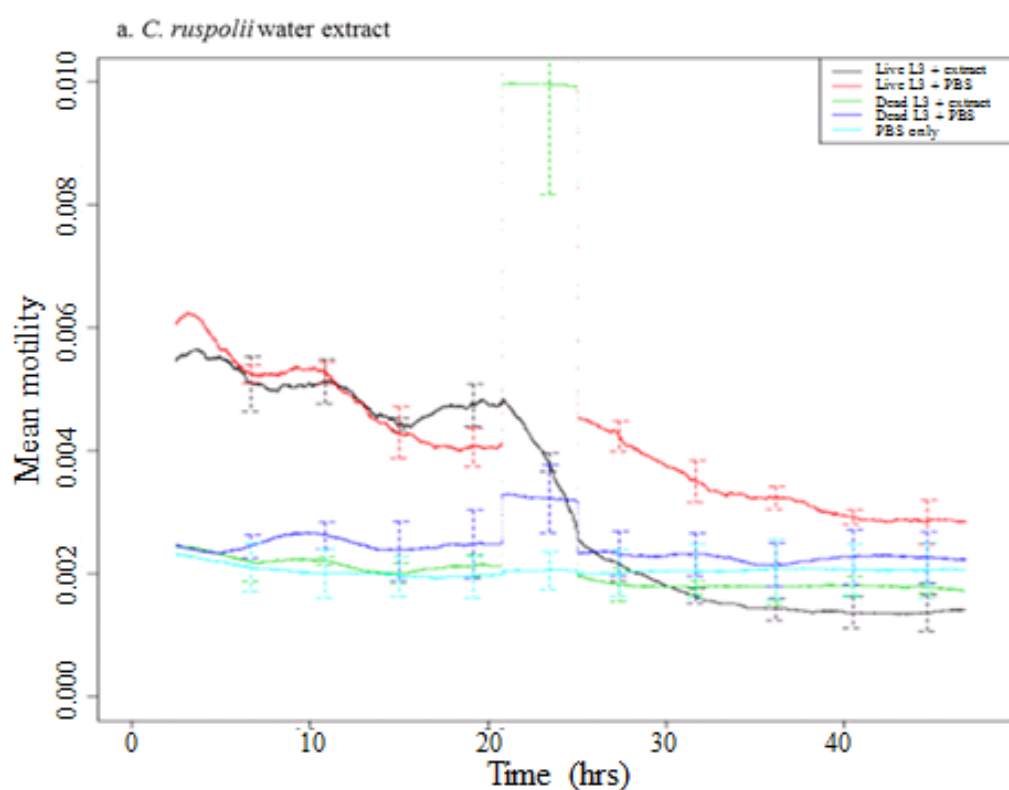


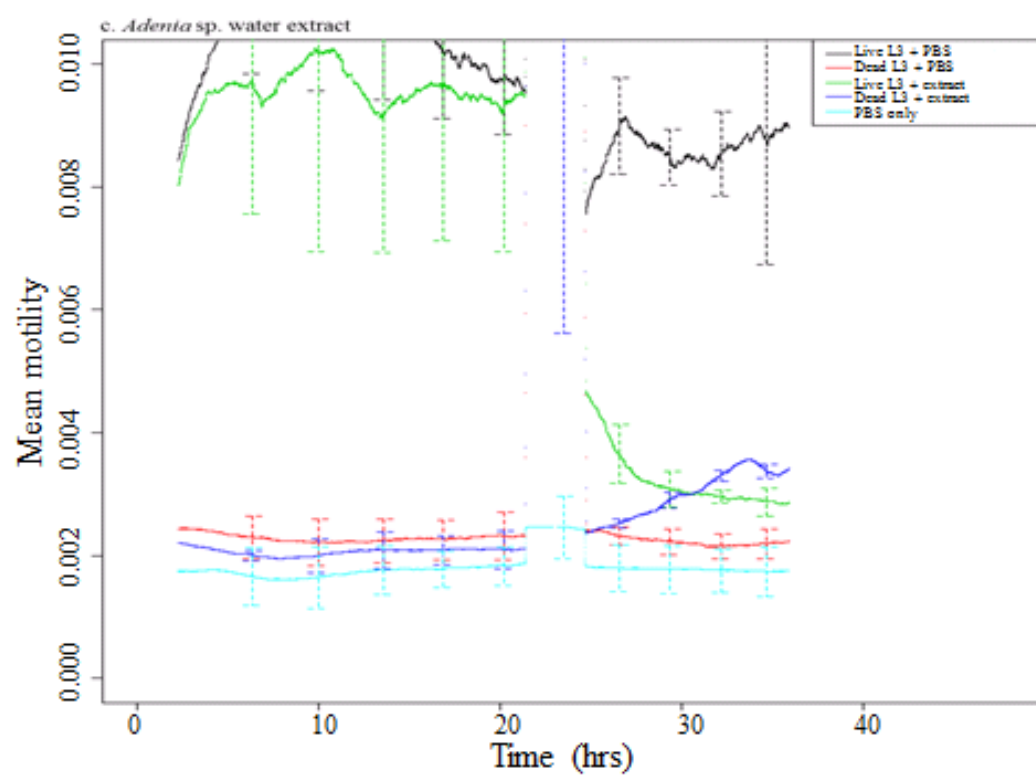
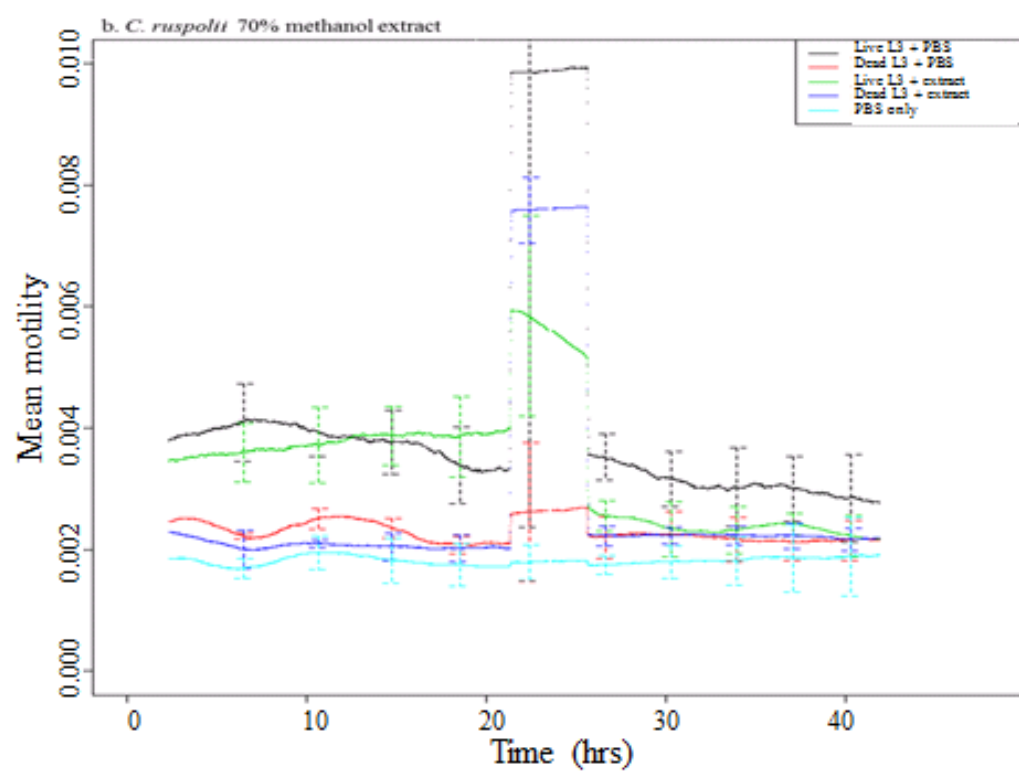
Figure 3.5. Egg hatch inhibition (EHI) with standard error of the mean of water crude extracts (n=3) of *Adenia* sp. (a) and *C. ruspolii* (b) collected in different years.

3.4.3. LMI tests of selected crude extracts

To further screen anthelmintic properties of *C. ruspolii* and *Adenia* sp., selected extracts of both plants at a concentration of 10 mg/ml were used to assess the impact

on *T. circumcincta* L₃ motility (Figure 3.6). The LMI test results showed that water and 70% MeOH extracts of *C. ruspolii* (Figures 3.6a and 3.6b respectively) and water extract of *Adenia* sp. (Figure 3.6c) significantly reduced L₃ motility at 10 mg/ml compared to controls (PBS with worms) and reached same readouts as for positive control wells, i.e. dead worms with plant extracts and PBS only. The signal drifting after addition of *Adenia* sp. water extract in wells containing dead worms could be due to foamy nature of the extract that resulted in the formation of bubbles. The larvae incubated in PBS (negative control) showed a constant increase in mean motility throughout all experiments. In contrast, the acetone extract of *Adenia* sp. (Figure 3.6d) did not show larval motility inhibition.





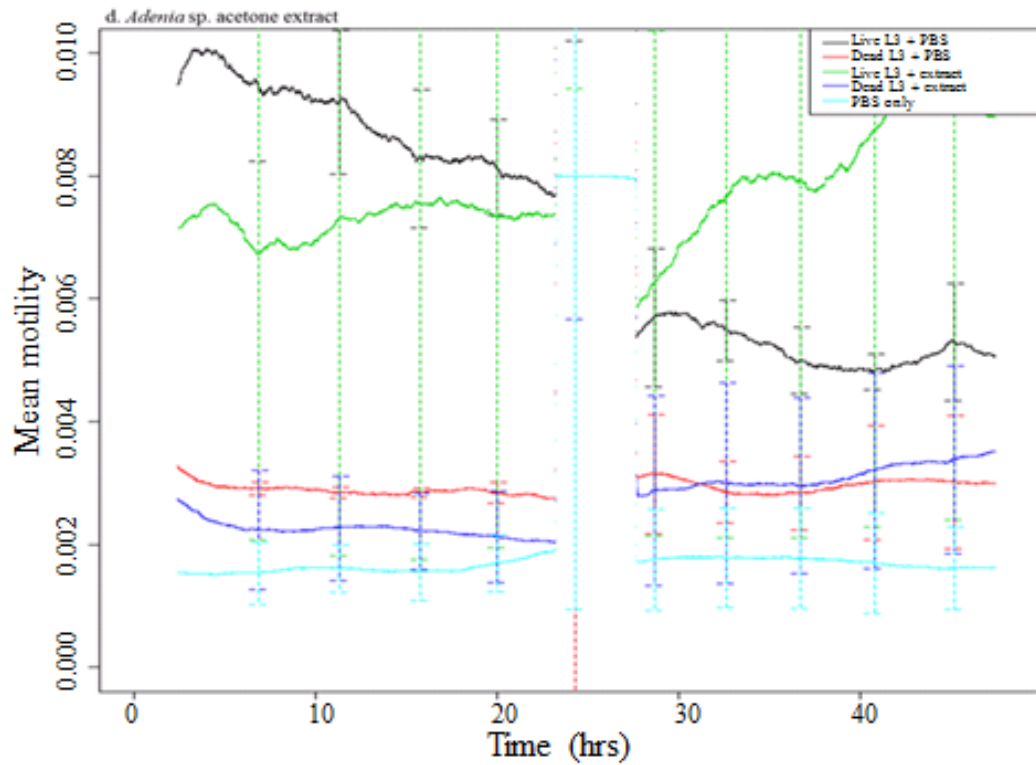


Figure 3.6. Larval motility readouts of alive and dead larvae over 48 h with after 24 h the addition of *C. ruspolii* water extract (a), *C. ruspolii* 70% MeOH extract (b), *Adenia* sp. water extract (c), and *Adenia* sp. acetone extract (d). Legends are displayed in each figure; software settings could not be amended in order to use same legends in each graph.

3.5. Discussion

Deionized water and 70% MeOH extracts had greater yields than the less polar solvents. This yield difference could be due to the difference in extractive power (polarity) of solvents and solubility incompatibilities of plant constituents. Extract yield could also be affected by many other factors such as the methods of extraction, temperature, pH, and extraction time (Dent *et al.*, 2013) although apart from pH, these factors were controlled. The very small difference in extract yields from batch to batch implies that year of collection had no significant impact on the yield of extract. Since sample collection in both Year 1 and 2 were done in the same season, and the EHI results were virtually similar, it cannot be excluded that yields and anti-parasitic activity may be rather constant between years but whether this would also be the case between seasons needs to be further assessed.

Flavonoids, anthocyanins and nitrogen containing compounds such as betalains and carotenoids are just some of the categories of plant pigments (Młodzińska, 2009). The similarities or differences in colour of crude extracts of various solvent systems are attributed to their phytochemical constituents that absorb and reflect similar or different colours in day light. The similarity in colour of crude extracts of different solvent systems might be due to the solubility of the same or different phytochemical groups forming that characteristic colour. For instance, crude extracts rich in flavonoids (Młodzińska, 2009) and some nitrogen containing compounds such as alkaloids (Tanaka *et al.*, 2008) usually appeared as yellow coloured in day light.

The EHI test is one of many *in vitro* anti-parasitic screenings used to investigate medicinal plant claims for their anti-parasitic properties. The test is based on the

ovicidal effect or embryo development inhibition (Álvarez-Sánchez *et al.*, 2002). The EHI properties of the four plant extracts tested were clearly dependent on dose, type of plant and polarity of solvent system employed in extract preparations. For instance, the relatively low EHI properties of acetone and methanol extracts of *C. ruspolii* could be due to insolubilities of constituents in de-ionized water that was used to reconstitute plant extracts for EHI. Our findings are in agreement with the observation that yield and biological activities of plant extracts are mainly dependent on the types of extraction methods and polarities of solvents employed (Murugan and Parimelazhagan, 2014; Kotze, 2012).

The LMI test is another bioassay carried out to assess anthelmintic properties, and estimates the degree of L₃ paralysation when incubated with plant extracts. The LMI observed by 70% MeOH of *C. ruspolii* and water extracts of *Adenia* sp. could be due to the effect of PSMs that either paralyze or kill the larvae. The interference of extracts with larval stage (L₁ or L₃) motility may contribute to a gradual decrease in pasture contamination with infective stages (Lorimer *et al.*, 1996). Reduction in motility may also affect the parasite life cycle within the animal, as following exsheathment, L₃ require migrating to their final niche in the gut, in case of *T. circumcincta* the abomasum. The *in vitro* LMI has been used to evaluate the nematocidal effects of other plant extracts (Álvarez-Sánchez *et al.*, 2002). Khan *et al.* (2016) reported that the water and methanolic extracts of *Iris kashmiriana* rhizome resulted in 85% and 100% mean LMI against *H. contortus* L₃ respectively. Williams *et al.* (2016) also reported that MeOH extract of the chicory (*Cichorium intybus*) cultivar Spadona showed potent anthelmintic activity against larval stages of swine parasites *Ascaris suum* and *Oesophagostomum dentatum* whereas extracts from a

second cultivar Puna II showed less activity against *A. suum* and no activity towards *O. dentatum*. Egualé *et al.* (2011) also reported that water extracts of *Leonotis ocymifolia*, *L. martinicensis*, *Albizia schimperiana* and *Senna occidentalis* induced 100%, 99.85%, 99.31%, and 96.36% *H. contortus* larval development inhibition, respectively. It was also reported that an ethanolic leaf extract of *Moringa oleifera* at 5 mg/ml showed 99% *H. contortus* EHI and 98% and 100% mortality of *H. contortus* L₁ and L₂ larvae, respectively (Tayo *et al.*, 2014). Through the EHI and LMI screenings used here, evidence is provided that medicinal plants selected based on their ethno-medicinal use indeed have anti-parasitic properties, at least *in vitro*. This finding is consistent with the general assumption that extracts prepared from selected plant materials on the basis of ethno-medicinal uses are most likely to contain biologically active components of medicinal interest (Hemalatha *et al.*, 2013).

In conclusion, roots of *C. ruspolii* and *Adenia* sp. and aerial parts of *I. eriocarpa* and *E. thymifolia* were collected based on their ethno-medicinal uses. These plant samples were processed and extracted in four solvent systems by maceration method. Our EHI and LMI findings support the view that the four medicinal plants have anti-parasitic properties and thus contribute to a validation of their ethno-medical uses. Based on these *in vitro* experiments, *C. ruspolii* and *Adenia* sp. water extracts were chosen for further bioassay guided phytochemical studies and *in vivo* testing of anthelmintic properties and side-effects.

Chapter Four: Physico-chemical studies and EHI properties of crude extracts

4.1. Abstract

Physico-chemical study of extracts and bioassays of the resulting products is required to inform the optimal method of separation, so to choose appropriate purification techniques and to understand conditions under which these processes could be carried out without affecting the active constituents responsible for the targeted activity. The objective of this study was to treat crude extracts by physico-chemical methods and to determine the effects of treatments on EHI properties of these extracts. Thus, the active constituents of *C. ruspolii* and *Adenia* sp. water extracts were characterized by membrane dialysis, thermal stability testing and solvent partition. Membrane dialysis showed that small molecules of both plant samples had significantly greater EHI activities than their large molecule counterparts, tested at 12 and 11 mg/ml respectively. This effect was stronger for *C. ruspolii* than for *Adenia* sp. ($P < 0.001$). At 10 mg/ml, EHI activities decreased slightly but significantly with increased boiling time for both plants ($P < 0.001$). Active principles of *Adenia* sp. and *C. ruspolii* extracts partitioned very similarly, partly into lower-polarity solvents (ethyl acetate or butan-1-ol) but the majority remained in the water phase as shown by EHI activities ($P < 0.001$). In summary, the major constituents of both plant extracts responsible for the EHI activities observed are most likely highly polar, water-soluble, small and moderately heat-labile molecules.

4.2. Introduction

Bioactive phytochemicals are PSMs eliciting pharmacological or toxicological effects in man and animals. The phytochemical study of medicinal plant constituents begins with the process of crude extract preparation followed by various separation techniques (Tiwari *et al.*, 2011). However, crude natural product extracts are generally extremely complicated mixtures of several compounds possessing varying chemical and physical properties (Hossain *et al.*, 2013). Isolation of compounds in a pure state from such complex mixture is considered the most difficult and time-consuming step in natural product research (Bart, 2011). Moreover, appropriate techniques and conditions should be selected and employed to protect and stabilize the bioactive constituents (Colegate and Molyneux, 2007). The fundamental strategy for separating these compounds is based on their physico-chemical properties (Bigoniya *et al.*, 2011; Michelle *et al.*, 2013) that can be exploited to initially know the nature of the various chemical groups present (Visht and Chaturvedi, 2012). The general features of a molecule that are helpful to ascertain the isolation process include molecular size, charge, heat stability, solubility (i.e. hydrophobicity or hydrophilicity) and acid–base properties. The success or failure of the extraction and isolation processes is then monitored by an appropriate bioassay.

The general principle of stability testing of crude extracts is to provide evidence on how the quality of active constituents of extracts varies with time under the influence of a variety of environmental factors such as temperature, humidity, and light (Amr and Al-Tamimi *et al.*, 2007). In particular, the heat stability testing refers to the ability of a bioactive substance to retain at least 80% of its functional activity when incubated at 100°C for an hour (Srivastava *et al.*, 2010). A common problem

associated with the isolation and purification of bioactive compounds of plant origin is thermal instability. The thermal instability of the active compound(s) in the extract can be confirmed by chemical, physical or biological assay methods (Srivastava *et al.*, 2010). In biological assay, thermal instability of active constituents of extracts can be confirmed by heating the extract at different temperature for specified time intervals followed by bioactivity evaluation for the claimed activity. Any reduction or loss of activity confirms the presence of thermo-labile bioactive compounds in the crude extract (Sarker *et al.*, 2006). Thus, heat stability testing of crude extracts is very important to identify the likelihood of degradation of active constituents, degradation pathways, and intrinsic stability of active constituents and to validate the stability indicating power of the test methods and extraction procedures used (Hsieh *et al.*, 2011).

Solvent partition is also a physico-chemical technique that involves the use of two immiscible solvents between which compounds are distributed according to their partition coefficients (Dai and Mumper, 2010). A partition coefficient (K) is the ratio of the concentration of the constituent in the organic phase divided by the concentration in the water phase. This partition coefficient is dependent on the nature of the constituents analysed, organic solvent used, temperature and the degree of polarity of the constituents in the crude extract (Iloki-Assanga *et al.*, 2015; Saeidian and Rashidzadeh, 2013). Thus, a number of factors must be considered in evaluating the use of potential solvents for solvent partition process, including capacity for partitioning of the target compound(s), selectivity for the desired compound over other components, miscibility with the water phase, and property difference from

target compounds to allow for adequate separation and recovery (McPartland *et al.*, 2013).

Therefore, the objective of this study was to assess the molecular size, heat-stability and polarity of active constituents of extracts followed by bioassay and TLC profiling of physico-chemically treated fractions. The three physico-chemical techniques employed in this study were membrane dialysis, thermal stability testing and solvent partition, respectively.

4.3. Materials and methods

4.3.1. Membrane dialysis

A detailed description of the membrane dialysis used is given in section 2.6.1. In summary, samples were loaded into dialysis tubing and placed in external de-ionized water (first dialysis) with gentle stirring for 24 h at 4°C. The external water solution recovered, dried and labelled as ‘small molecules’. The tubing was then transferred to larger volume of external deionized water for further dialysis for another 24 h. The remaining sample in the tubing was then recovered, dried and labelled as ‘large molecules’.

4.3.2. Heat stability testing

A detailed description of the heat stability testing is given in section 2.6.2. Briefly, three water crude extracts per plant for *C. ruspolii* and *Adenia* sp. extracts were treated as non-boiled (0 min.) or incubated in a water bath at 100°C for 10 or 60 min. Samples were then dried and bio-assayed.

4.3.3. Solvent partition

The full methodology used for the solvent partition technique is presented in section 2.6.3. Briefly, the water crude extracts of *Cissus ruspolii* and *Adenia* sp. were shaken with either butan-1-ol or ethyl acetate, and then centrifuged at $2057 \times g$ for 10 min. The upper (organic) and lower (water) phases were then recovered, dried and then bio-assayed.

4.3.4. Thin layer chromatography

Section 2.9 describes in detail the TLC development and staining used. In short, the test samples (200 µl) from the physico-chemical testing were dried in Speed Vac, reconstituted in 40 µl of 50% MeOH, loaded onto the TLC (10 µl), and developed in BAW (4:1:1 v/v/v). Resulting chromatograms were stained with thymol, molybdate and ninhydrin.

4.3.5. Egg hatch inhibition

All physico-chemically treated products were bio-assayed for their EHI activities against *T. circumcincta* eggs in triplicate, as described in section 2.5.1.3. Resulting EHI percentage, i.e. the number of eggs counted as a percentage of the total of the number of eggs and larvae counted are graphically presented as means \pm standard error of the means (SEM).

4.3.6. Statistics

The EHI data were arcsine transformed prior to statistical analysis. The latter consisted of ANOVA in order to examine the effect of plant species and the product types generated within each approach used.

4.4. Results

4.4.1. Molecular sizes of constituents of extracts and their EHI assays

The aim of the membrane dialysis experiment was to separate the constituents of water crude extracts based on molecular sizes. The amount of samples taken for membrane dialysis, the proportions of low and high molecular weight fractions recovered and amount of low molecular weight lost during further dialysis are shown in Table 4.1.

Table 4.1. Molecular size separation of constituents of water extracts by membrane dialysis.

Plant	Initial weight (mg)	Low molecular weight (mg)	High molecular weight (mg)	Low molecular weight lost (mg)
<i>C. ruspolii</i>	100	25	56	19
<i>Adenia</i> sp.	100	22	48	30

During the first dialysis process, recovery of low molecular weight constituents from *C. ruspolii* (25 mg) was slightly greater than that from *Adenia* sp. (22 mg). In contrast, the total low molecular weight proportion of *Adenia* sp. (52 mg) was slightly larger than that of *C. ruspolii* (44 mg) when allowance was made for the low molecular weight material evidently lost during the further dialysis processes. The amount of low molecular weight fractions lost in *Adenia* sp. during further dialysis was greater (30 mg) compared to *C. ruspolii* (19 mg). Both low and high molecular weight molecules recovered were tested for their EHI properties. The EHI test results

of low and high molecular weight constituents of both plant samples are shown in Figure 4.1.

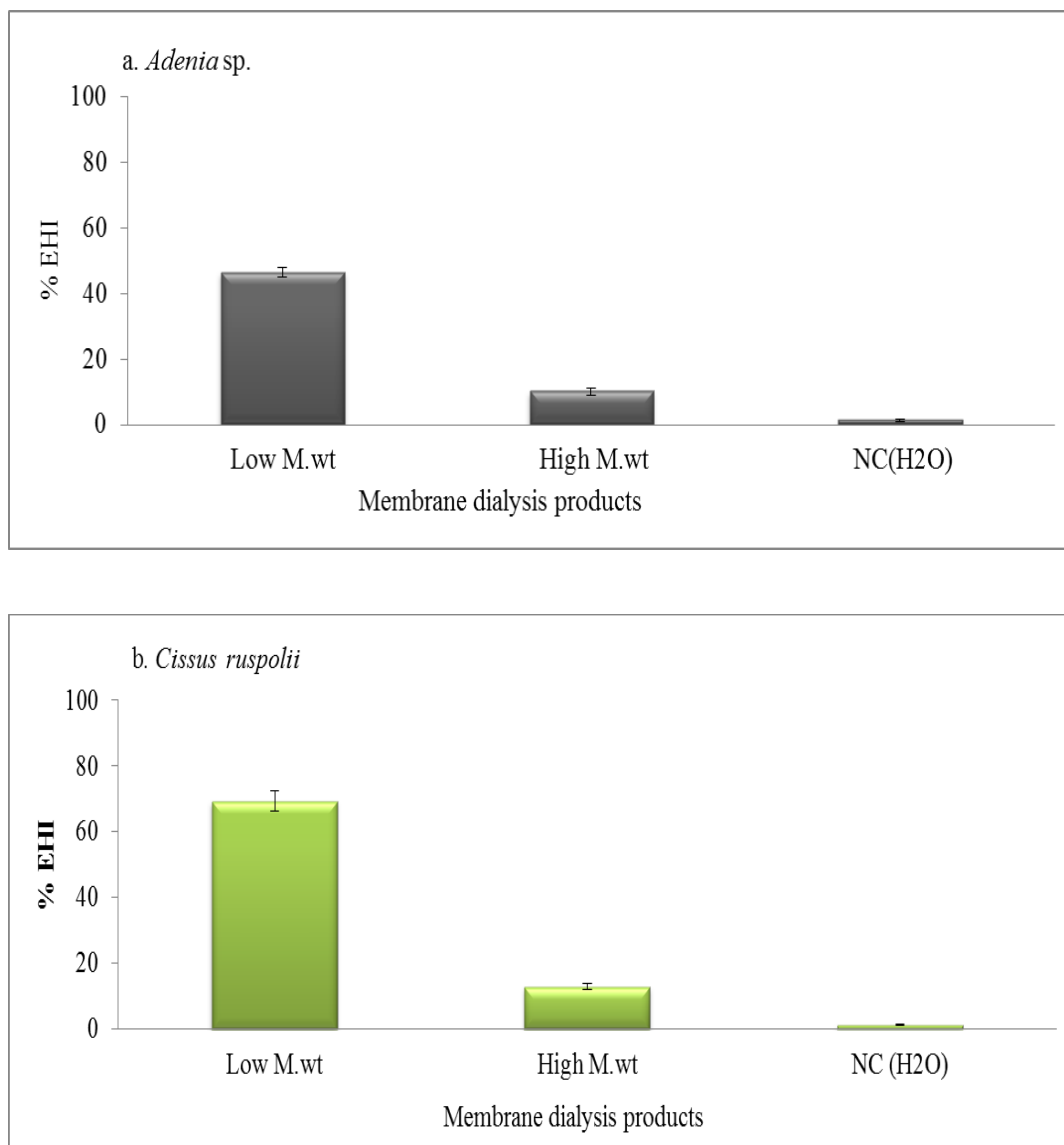


Figure 4.1. Egg hatch inhibition (EHI) of *T. circumcincta* incubated with low and high molecular weight membrane dialysis products. *Adenia* sp. (a) and *C. ruspolii* (b); water was used as negative control (NC).

The low molecular weight fraction of both extracts showed greater EHI efficacy than high molecular weight fraction ($P < 0.001$). At tested concentrations, the low molecular weight molecules of *C. ruspolii* and *Adenia* sp. exhibited 65 and 48% EHI

properties respectively. Even though the efficacy was significantly reduced, high molecular weight constituents of both plants did show some EHI activity, as it was significantly greater than EHI observed on the negative controls ($P < 0.001$).

4.4.2. Effect of heat treatment on EHI properties of crude extracts

This experiment was carried out to provide evidence on how efficacies of active constituents of crude extracts withstand heat. The EHI assay results and their corresponding TLC profiles of extracts after heat treatments are shown in Figures 4.2 and 4.3.

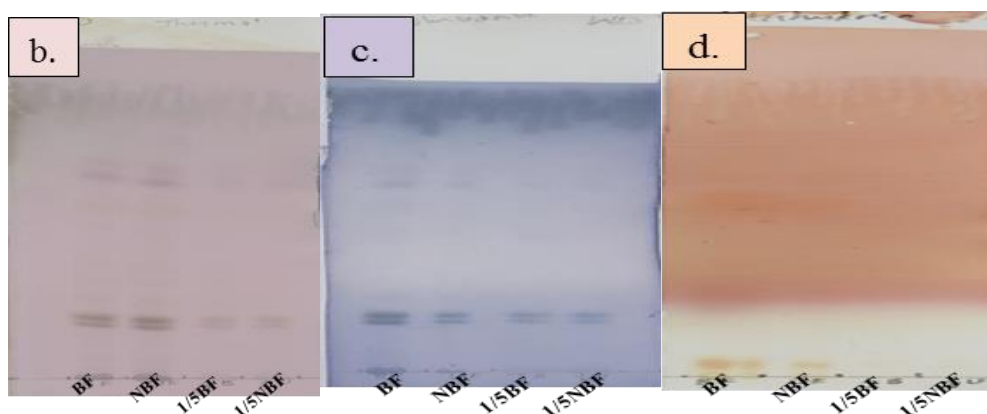
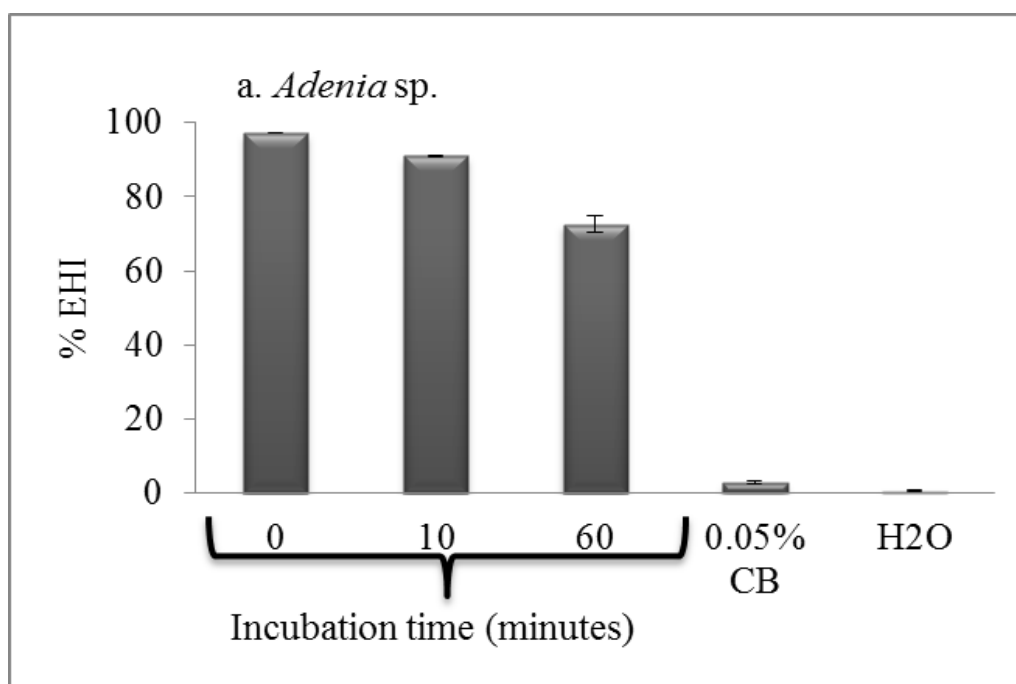


Figure 4.2. Egg hatch inhibition (EHI) and chromatograms of heat-treated *Adenia* sp. water extract. Boiled full strength (BF) and one-fifth of BF (1/5 BF) and non-boiled full (NBF) and 1/5 NBF strengths. Chromatograms: thymol stained (b), molybdate (c) and ninhydrin (d). Chlorobutanol (0.05% w/v) and deionized water (H₂O) were used as negative controls. TLC was done only for the sample incubated at 100°C for 60 min.

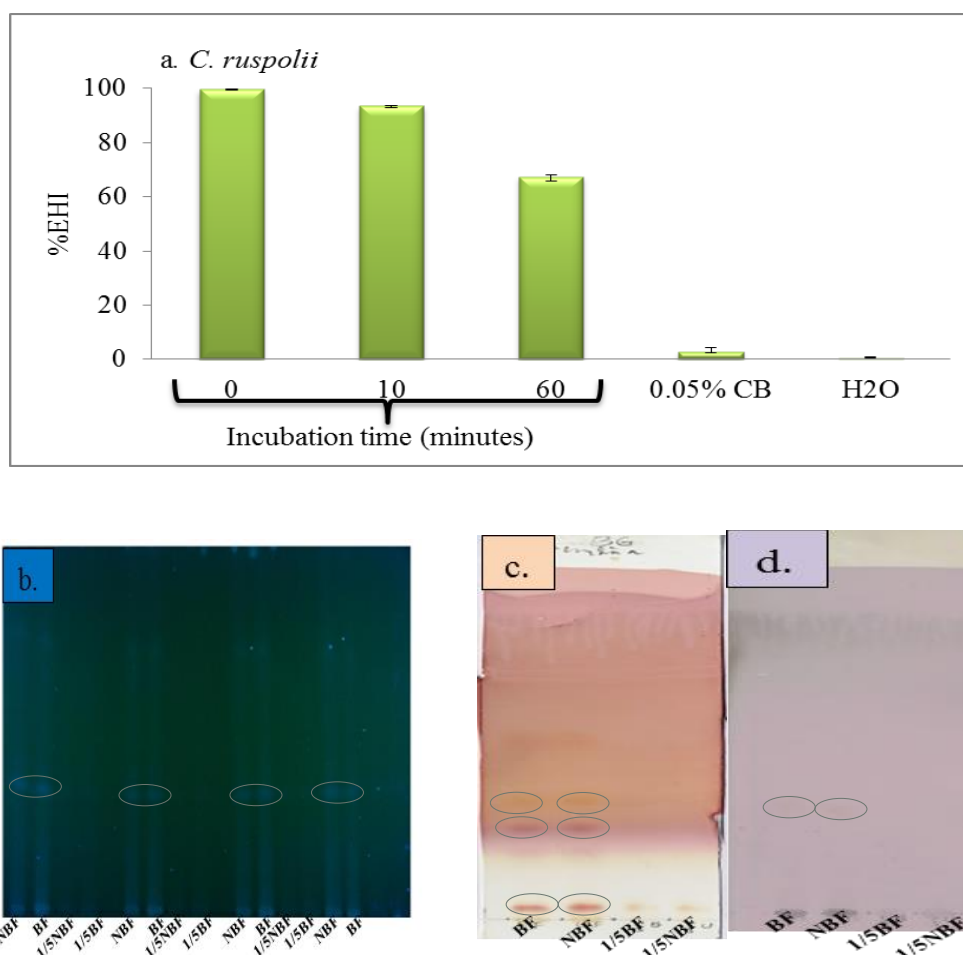


Figure 4.3. Egg hatch inhibition (EHI) and chromatograms of heat treated *C.ruspolii* water extract.

The same condition as in Fig. 4.2. EHI (a) TLC under UV-366 nm (b); stained with ninhydrin (c) and thymol (d). BF and NBF stand for boiled and non-boiled samples at full and 1/5 dilutions.

The EHI properties of extracts significantly decreased with increased heating time for both plant extracts ($P < 0.001$; Figures 4.2 and 4.3). The slow migrating and major spots of *Adenia* sp. were heavily stained with both thymol (Figure 4.2b) and molybdate (Figure 4.2c) staining reagents. Similarly, two spots of *C. ruspolii* fluoresced blue under UV-light at 366 nm (Figure 4.3b); four other spots heavily stained with ninhydrin (Figure 4.3c) and only one spot faintly stained with thymol (Figure 4.3d), respectively.

4.3.3. Solvent partition of active constituents crude extracts

This experiment was designed to partition the constituents of water extracts of both plants between water and organic medium based on their relative hydrophilic and amphiphilic properties and to test the recovered fractions for their EHI properties. Both extracts contained constituents with hydrophobic and hydrophilic properties as exhibited in their EHI and TLC profiles (Figures 4.4 and 4.5).

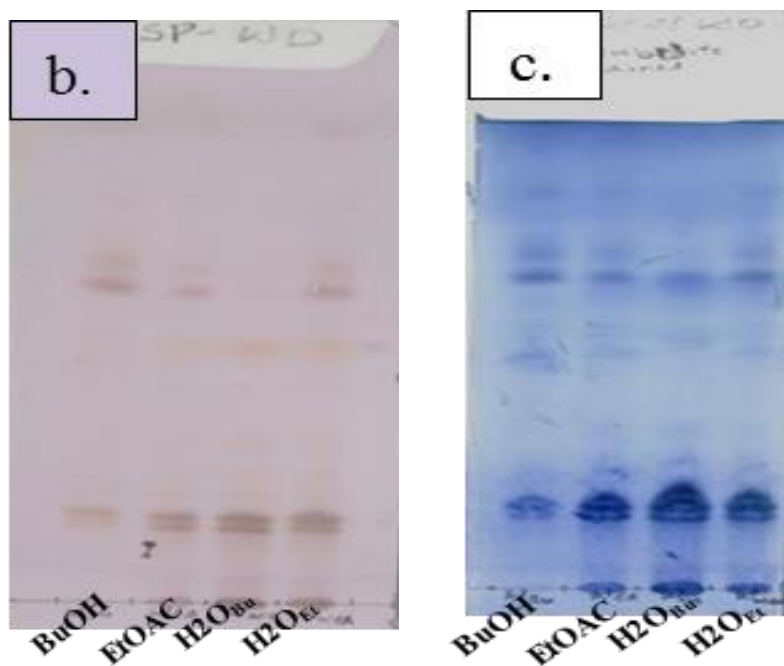
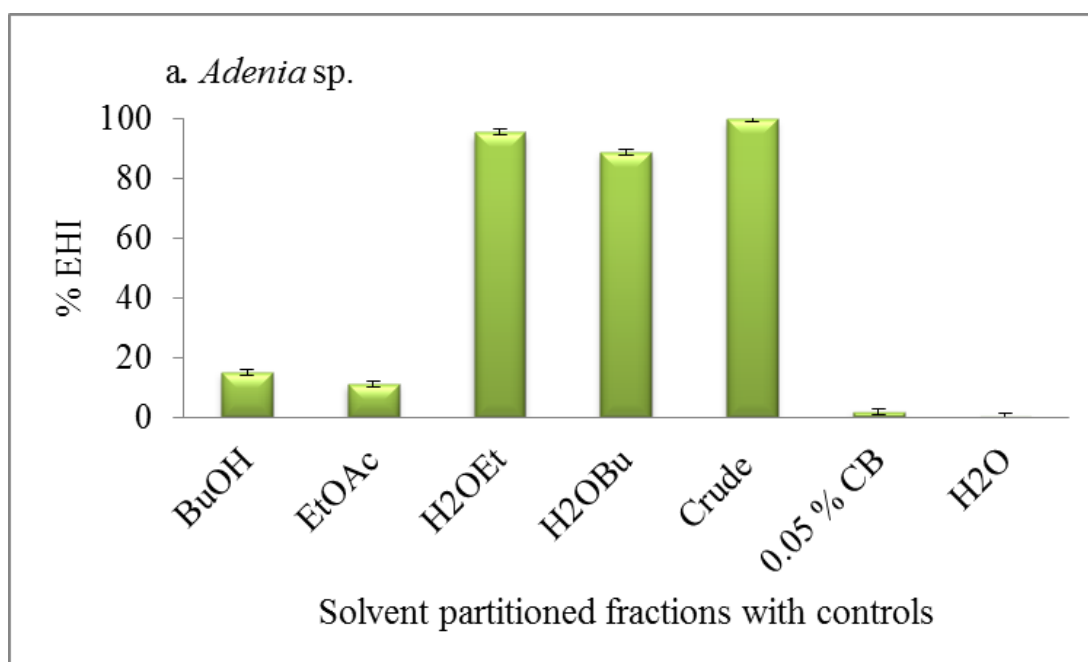


Figure 4.4. Egg hatch inhibition (EHI) and chromatograms of solvent partitioned fractions of *Adenia* sp. water extract. Butanol (BuOH), ethylacetate (EtOAc), H₂O_{Bu} (water from BuOH-H₂O solvent system), H₂O_{Et} (water from EtOAc-H₂O solvent system). EHI (a); thymol stained (b) and molybdate (c).

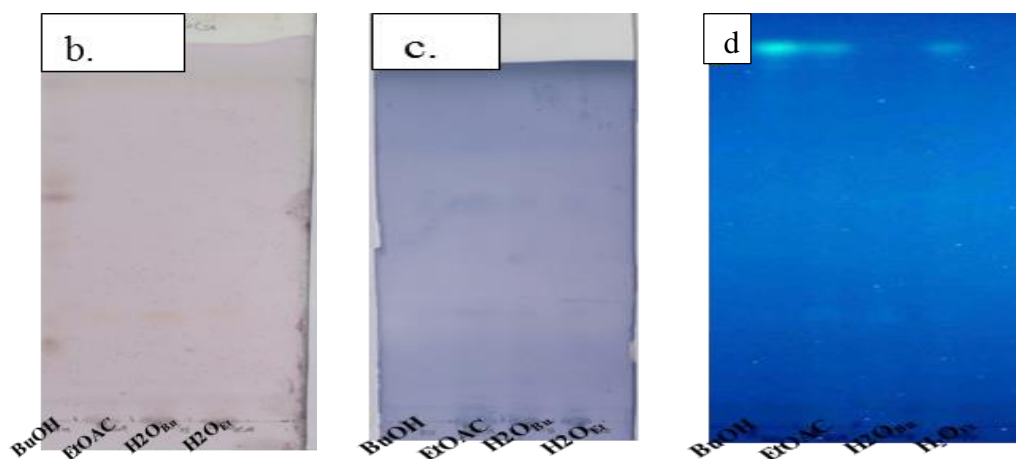
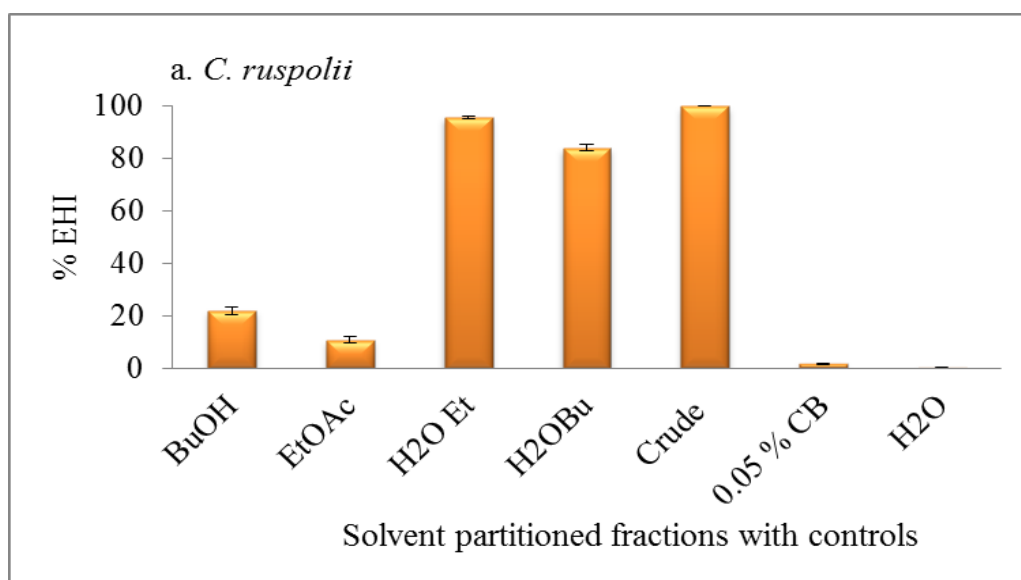


Figure 4.5. Egg hatch inhibition (EHI) and chromatograms of solvent partitioned fractions of *C. ruspolii* water extract. Butanol (BuOH), ethylacetate (EtOAc), H₂O_{Bu} (water from BuOH-H₂O solvent system), H₂O_{Et} (water from EtOAc-H₂O solvent system). EHI (a); thymol stained (b) and molybdate (c) under UV-366nm (d).

The water fractions showed significantly greater EHI activity than their organic counterparts ($P < 0.001$), and this was of similar magnitude between the plants. The butan-1-ol fractions of both plants exhibited slightly greater EHI activities compared to their ethylacetate fraction counterparts. The ethyl acetate fractions of both plants exhibited the lowest EHI activities (Figures 4.4a and 4.5a).

4.4. Discussion

The relatively high amount of low molecular weight molecules recovery for *C. ruspolii* during first dialysis compared to *Adenia* sp. may be due to low adsorption on the membrane surface and low interaction with high molecular weight molecules that allowed constituents to diffuse out of the membrane to the external water. Similarly, the relatively high amount loss of low molecular weight molecules from *Adenia* sp. during further dialysis compared to *C. ruspolii* might be due to increased volume of external deionized water and dialysis time that allowed its low molecular weight constituents to diffuse out completely into the discarded external deionized water. The loss of 19-30% of small molecule during further dialysis revealed that the membrane technique was not a versatile technique to recover small molecules during further dialysis. It might affect both the yield and the EHI properties of small molecules. The greater EHI properties of external deionized water than sac contents implied that the observed anti-parasitic activity is more likely associated with low molecular weight constituents than with high molecular weight constituents.

The smaller percentage of EHI exhibited by membrane dialysis products of both plants compared to EHI observed for the crude extract at comparable tested concentrations could have arisen from at least three reasons. Firstly, some low molecular weight active constituents may be lost during further dialysis. Secondly, the activity observed for the crude extract could be due the cumulative effect of both low and high molecular weight active constituents in the extract whereas the membrane dialysis process was separated these molecules and hence they tested independently and showed smaller EHI activity compared to the crude extract they derived from. Bioactivity is dependent on both dose and structure of the active

compounds. Thirdly, the solubility in deionized water during reconstitution of recovered samples for bioassay might have been compromised. Thus, even though the concentrations used for assay were comparable, their EHI activity could be different due to the difference in the amount of active constituents in the respective assayed samples or due to solubility difference in deionized water.

The modest EHI activities exhibited by high molecular weight fractions could be due to incomplete removal of active low molecular weight material or interaction with other high molecular weight molecules; alternatively, some high molecular weight fractions might have EHI properties. The ability of molecules to diffuse through a dialysis membrane to the external solution is influenced by many factors such as concentration, interactions, hydrophobicity of molecules, temperature, volume of external solution and stirring rate (Picot *et al.*, 2014).

The decrease in EHI properties of extracts with increased heating time indicates at least partial thermal degradation of some active constituents. The fluorescent spots under UV-light at 366 nm or well stained concentrated spots of heat treated samples might be among the likely active but slightly thermo-labile constituents that survived the thermal degradation or partially degraded in the heat treated extracts. Cheng *et al.* (2014) reported that phenolic compounds in water solution such as protocatechuic acid partially degraded at 200°C and completely decomposed at 300°C upon heating for 20-60 minutes. Thus, the blue fluorescing constituents of *C. ruspolii* at 366 nm could be flavonoids that survived prolonged heating at 100°C for an hour. Önning *et al.* (1994) also reported that oat saponins (avenacosides) were stable when heated at 100°C for 3 h at pH 4-7. However, heating at 140°C at pH 4 led to partial degradation of the saponins. *Adenia* sp. water extract was highly foamy, suggesting

that it might be rich in saponins. Hence, the two close and slow migrating spots on TLC that stained well with thymol and molybdate could be saponins that either stable or partially degraded at 100°C upon heating for 1 h.

In solvent partition, the higher proportion of constituents of both extracts was partitioned into the water solvent system as seen in their respective EHI and TLC profiles. This indicates that most active constituents of crude extracts were preferentially water soluble polar compounds. However, the butan-1-ol phase also showed some EHI properties. The higher in EHI properties of butan-1-ol phase compared to ethylacetate might be associated with its higher polarity that allowed constituents with medium polarity and amphiphilic properties to be partitioned into butan-1-ol than ethylacetate, as the dielectric constant of butan-1-ol at 20°C is three times higher ($\epsilon=17.9$) than that of ethylacetate ($\epsilon=6.02$).

The constituents of *Adenia* sp. water extract were partitioned into both butan-1-ol and ethylacetate. This implied that the extract contained constituents with range of polarities. The thymol and molybdate stained chromatograms of solvent partition products revealed that *Adenia* sp. extract contained amphiphilic constituents that could partition into both water and organic phases although the majority was found in water phase. For instance, *Adenia* sp. extract was highly foamy and hence could contain saponins. Saponins are amphiphilic that contain both hydrophobic part (non-sugar moiety) and hydrophilic part (sugar moiety) in the same molecule. Hence, they can partition into both organic and water phases. The partitioning products of the three solvent phases also showed EHI properties although the activity was dependent on the polarity of solvent system used. Therefore, there were good correlations between the EHI and TLC profiles (Figures 4.4 and 4.5) of both plants. McPartland

et al. (2013) reported that the partitioning of the anti-cancer agent, paclitaxel and its structural analogue but major unwanted by-product, cephalomannine from plant cell culture broth into ethylacetate ($\epsilon=6.02$) or dichloromethane ($\epsilon=8.93$) revealed that the highest proportion of paclitaxil partitioned into ethylacetate compared to dichloromethane. This implies that potential solvent mixtures show varying affinity and selectivity to discriminate structurally related compounds during partitioning process. This finding also revealed that the partitioning efficiency of a solvent in the mixture is not only dependent on its dielectric constant but also affected by other factors. Similarly, Enejoh *et al.* (2012) also reported that for a methanol crude extract of *Citrus aurantifolia* partitioned between ethyl acetate, hexane, or water solvent system and assayed against *H. bakeri* eggs and larvae, the highest EHI activity was observed for methanol crude extract followed by ethylacetate fraction whereas the highest larvicidal property exhibited again by crude methanol followed by water fraction. This indicates that different solvent system with different affinity and selectivity captures different phytochemical groups with diverse structures and polarity that can go either to organic or water phase.

These findings are similar with our findings where the crude extracts of both plants partitioned between butan-1-ol and ethylacetate. In our study, the constituents of crude extracts having similar TLC profile partitioned between the organic and water solvents. Thus, the active principles of both extracts partitioned only slightly into lower-polarity solvents (ethyl acetate or butan-1-ol); the majority was found in the water phase.

In conclusion, the physico-chemical treatments employed on the crude extracts of *Adenia* sp. and *C. ruspolii* strongly suggest that the major constituents of both plant

extracts responsible for the EHI activities observed are highly polar, water-soluble, small and moderately heat-labile molecules.

However, separation of low and high molecular weight constituents of plant crude extracts using membrane dialysis is not a versatile technique due to loss of low molecular weight constituents during further dialysis. It is better to use column chromatographs such as Bio-Gel P-2 and Sephadex LH-20 columns where almost 100% sample recovery is possible. Heat stability testing followed by bioassay may be assessed by boiling the water crude extract at temperature greater than 100°C at different time of incubation. Solvent partition may also be further assessed using various organic solvents other than butanol and ethylacetate.

Chapter Five: Bioassay-guided fractionation and chromatographic profiling of *C. ruspolii* water extract

5.1. Abstract

Clarified crude water extract of *C. ruspolii* was separated into discrete fractions based on their molecular sizes on gel-permeation chromatography (GPC) by use of water as isocratic eluent. The resulting discrete fractions were bioassayed for their EHI properties against *T. circumcincta* eggs. In this study, bioassay and TLC profiling of Bio-Gel P-2 fractions of *C. ruspolii* were done to (i) identify active and inactive fractions, (ii) study the effect of change in sample and column bed volumes on the elution positions of active fractions, (iii) develop chromatograms and detect separated spots in day light, under UV-light and after staining with various chromogenic or fluorogenic reagents, and (iv) pool active fractions based on their TLC profiles for subsequent quantitative bioassay-guided isolation and purification. The EHI test results showed that discrete fractions differed remarkably in EHI activities, suggesting that *C. ruspolii* active constituents were partitioned between a small numbers of fractions based on their molecular sizes. Chromatogram profiles of separated spots of *C. ruspolii* showed that fractions containing void volume (V_0) and included volume (V_i) eluates were influenced by sample size loaded, column bed volume, volume of fraction collected, and flow rate. Moreover, there was a strong correlation between EHI properties exhibited and TLC profiles of these active fractions. Thus, combining Bio-Gel P-2 fractions of *C. ruspolii* into three distinct pools was done based on fractions similarity in EHI and TLC profiles of separated spots examined under UV-light and after staining with molybdate.

5.2. Introduction

A medicinal plant extract is a mixture of compounds and require different separation techniques to isolate individual active compounds from this initial mixture. Hence, the extract must initially be separated into discrete fractions and then bioassayed to identify fractions containing target compounds (Atawodi *et al.*, 2009). Chromatography is one of the most powerful methods of separation, isolation, purification and analysis of natural products (Sharma and Paliwal, 2013; Gogoi *et al.*, 2016). Chromatographic methods are classified based on the separation mechanisms and nature of stationary and mobile phases employed. Gel-permeation chromatography (GPC) is one of those techniques that exploit the ability of molecules to move through a column of gel that has pores of clearly defined sizes (Siqueira *et al.*, 2010). Following sample application, molecules larger than pores of the stationary phase matrix are excluded from the internal volume within the beads. They, therefore, migrate quite rapidly through the column and emerging at void volume (V_0), whilst molecules smaller than or equal to the matrix pores (as well as those intermediate in size) equilibrate with both the external and internal liquid volumes, causing them to migrate much more slowly and emerge at elution volumes (V_e or V_i) greater than V_0 . It is a form of partition chromatography used to separate molecules of different sizes. However, various factors should be considered when designing a GPC fractionation experiment. These include matrix choice, sample size and concentration, column parameters, choice of eluent and effect of flow rate. The commonly used GPC matrices consist of porous beads composed of cross-linked polyacrylamide, agarose, dextran or combinations of these, and is usually supplied

either in suspended form or as dried powders. The sequence of separation of molecules based on molecular sizes on GPC is illustrated in Figure 5.1.

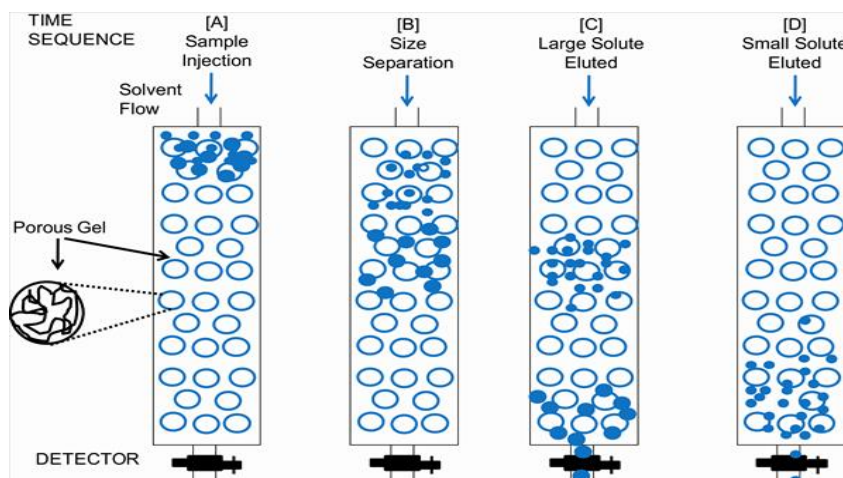


Figure 5.1. The gel permeation chromatography (GPC) separation set up (SEC image search: <https://www.medicinescomplete.com>).

GPC fractions usually contain a mixture of compounds with similar molecular sizes but different physico-chemical properties, and therefore, they will not be isolated and purified on single analytical technique (Gibbons, 2012). Thus, chromatogram profiling of such fractions assists to determine the number and nature of constituents and to choose appropriate bioassay-guided isolation and purification techniques (Jayashre, 2013; Mfotie *et al.*, 2014). TLC is a planar chromatographic method that separates constituents of fractions on thin layers of adsorbents that are in most cases coated on glass, plastic or aluminium sheets. The basic principles of separation on TLC and profiling of natural product constituents are achieved by application of a mixture (extract or its fraction) as a spot or band on to a sorbent, development of TLC chromatogram in sufficient and suitable solvent (Figure 5.2) followed by examining of separated spots in daylight, under UV (at 254 and 366 nm) or after staining with appropriate chromogenic or fluorogenic reagents (Sharma, 2013). A

factor in quantifying migration of a compound on a particular sorbent and in a particular solvent system is retention factor (R_F -value). This is defined as:

$$R_F = \frac{\text{Compound distance from the origin (midpoint)}}{\text{Solvent distance from origin}}$$

Thus, R_F values are always ratios, never greater than 1, and vary depending on sorbent and/or solvent system.

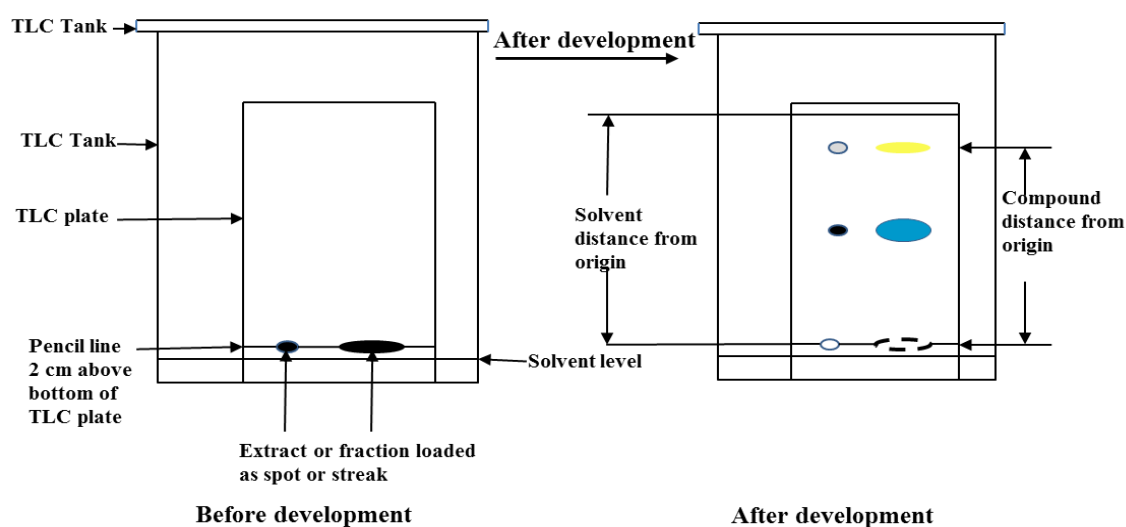


Figure 5.2. TLC equipment and development set up.

The objectives of this work were to (i) separate crude extract of *C. ruspolii* into discrete fractions based on their molecular sizes and carry out EHI tests to identify active fraction(s) for detailed studies, (ii) study how chromatographic factors such as sample size, column bed volume and flow rate affect the degree of separation of extract on GPC, (iii) establish chemical fingerprints of constituents of GPC fractions through TLC analyses, and (iv) pool active fractions based on their EHI and TLC profiles for further bioassay guided isolation and purification studies (Chapter Seven).

5.3. Materials and methods

5.3.1. Crude extract preparation

Powdered root sample (50 g) of *C. ruspolii* were macerated in 1 L of de-ionized water containing 0.05% (w/v) chlorobutanol (CB) to inhibit microbial growth. Macerated sample was stirred continuously at room temperature for 72 h. The supernatant was filtered through mira cloth, specifically designed for quick filtration of gelatinous materials. *C. ruspolii* filtrate was centrifuged at $41837 \times g$ for 30 min. (DuPont SA-600 centrifuge, Thermo Fisher Scientific, Waltham, USA). Clear supernatants were pooled and stored at -20°C in 50 ml aliquots (See section 2.7.1).

5.3.2. Gel-permeation chromatography

In this study, GPC with Bio-Gel P-2 matrix (Bio-Rad, Poole, UK) was used to prepare discrete fractions containing constituents of similar molecular sizes from water extracts of *C. ruspolii*. 3.5 ml (run-1) and 6.6 ml (run-2) clarified extracts were loaded onto GPC with 70 ml and 132 ml bed volumes respectively and then isocratically eluted with de-ionized water. Fifty five (run-1) and sixty (run-2) fractions were collected respectively.

The void volume (V_0) of the column is the volume of fraction collected from the time the sample loaded onto the column until non-retained constituent is eluted from the column. The included volume (V_i) of the column is the volume of solvent inside the gel which is available to small analyte (target compound).

The partition coefficient of Bio-Gel P-2 column, is defined as, $K_{av} = \frac{V_e - V_0}{V_t - V_0}$.

Where V_e or V_i is the volume required to elute a target component, V_t is the total liquid volume of the column and V_0 is the volume of liquid outside the beads.

Figure 5.3 shows the flow diagram of Bio-Gel P-2 fractionation of *C. ruspolii* (run-4) that was used for further bioassay guided isolation and purification of compounds (Chapter Seven). Similar Bio-Gel P-2 fractionations were used for other runs.

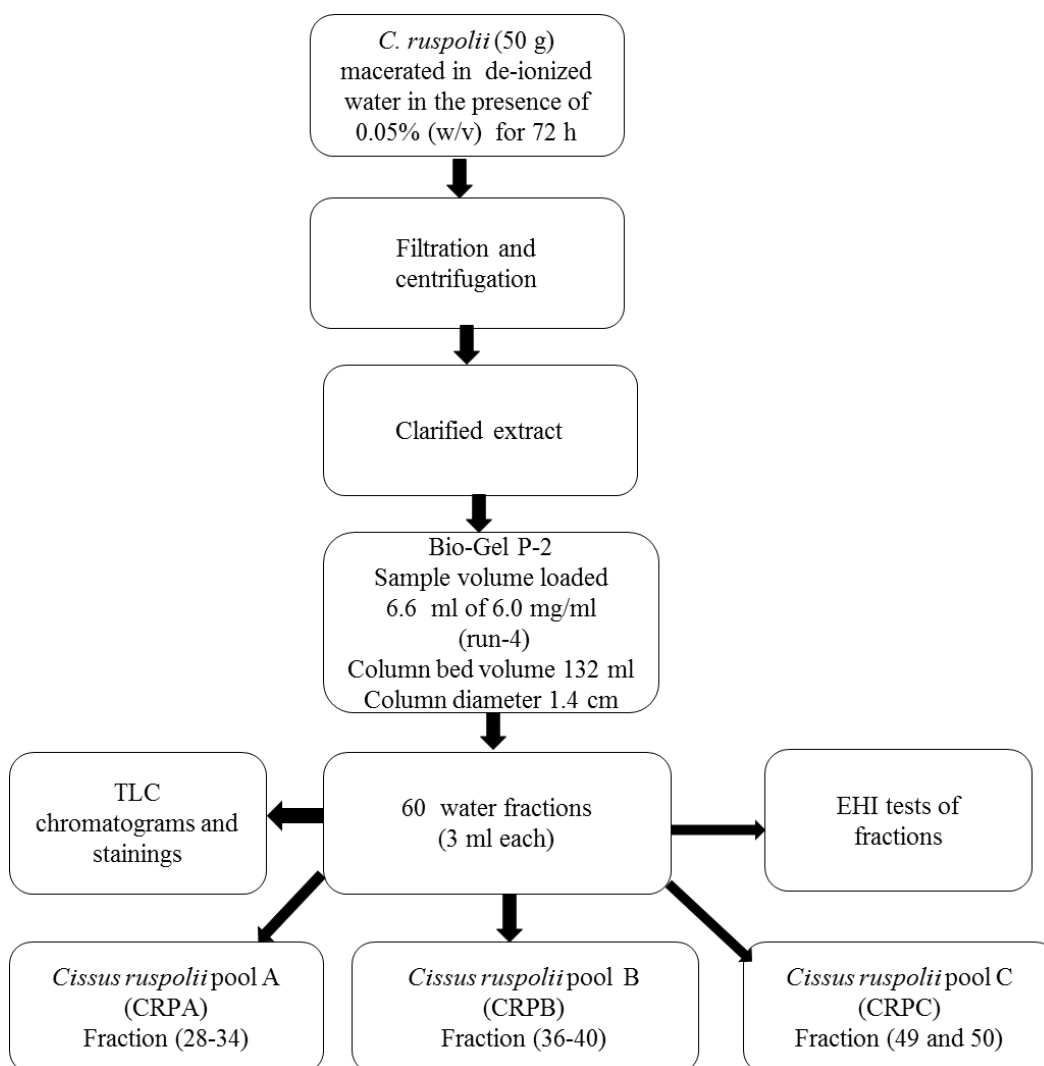


Figure 5.3. Flow diagram of Bio-Gel P-2 fractionation of *C. ruspolii* (run-4).

Bio-Gel P-2 fractions (runs 1 and 2) were used for bio-assay and for detailed TLC analyses of fractions. Fractions (run-3) were used to study the effect of high sample volume loaded on elution positions of void volume (V_0), included volume (V_i) and active pooled fractions (see Table 5.1 below) and TLC analysis of major constituents of active Bio-Gel P-2 fractions using crude extract as marker (see Figure 5.9 below).

5.3.3. Egg hatch inhibition

Each fraction of runs 1 and 2 was bioassayed in triplicates for their EHI properties using *T. circumcincta* eggs as detailed before (see section 2.5.1.3). The EHI bioassay used was as similar as before, and included not only de-ionized water but also the latter enriched with 0.05% (w/v) chlorobutanol as negative controls. This was to ascertain that chlorobutanol, used to inhibit microbial growth in the extracts, did not have significant EHI activity.

5.3.4. Thin-layer chromatography

During each run, small portions (200 µl) of Bio-Gel P-2 fractions were analysed by TLC in butanol-acetic acid-water (4:1:1 by volume) and separated spots were examined in daylight, under UV-light and after staining with various staining reagents (see section 2.9 for more details).

5.3.5. Calculations and statistics

The EHI data were expressed as a percentage, i.e. the number of eggs counted as a percentage of the total of the number of eggs and larvae counted. These data were arcsine transformed prior to analysis of variance (ANOVA), using fraction as factors.

5.4. Results

5.4.1. EHI of *C. ruspolii* Bio-Gel P-2 fractions

In the first GPC run, clarified extract (3.5 ml, 6 mg/ml) of *C. ruspolii* was fractionated on Bio-Gel P-2 and bioassayed for their EHI properties at full strength to identify fractions containing active constituents that inhibit nematode egg hatching. Of the fifty-five fractions bioassayed for their EHI properties in triplicate (run-1), only five fractions exhibited EHI activity > 20% (Figure 5.4). At full strength, fractions 10 to 12 showed 100% EHI while 14 and 15 exhibited modest EHI activities compared to the controls ($P < 0.001$; Figure 5.4). The remaining fractions either did not show any activity at all or showed very low activity.

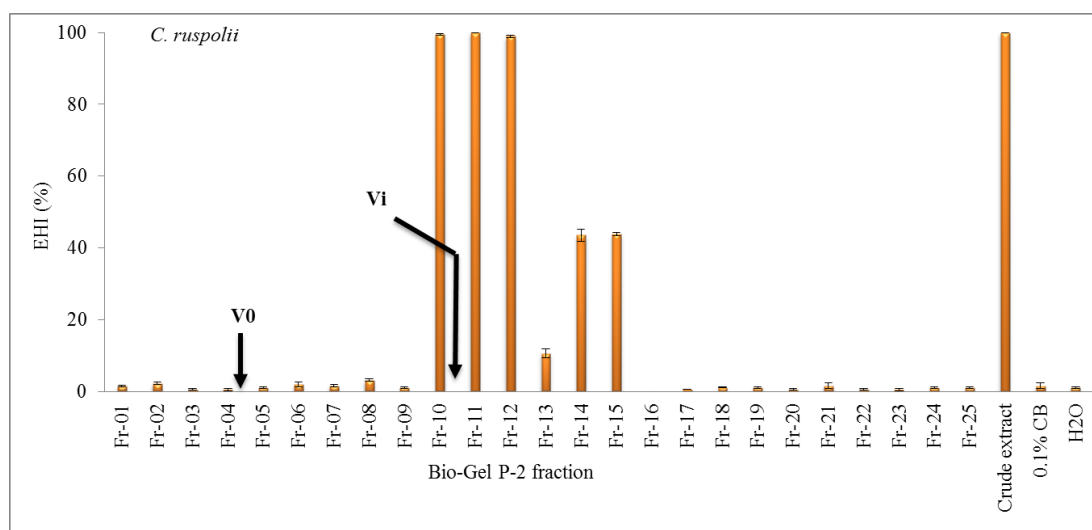


Figure 5.4. EHI of Bio-Gel P-2 water fractions of *C. ruspolii* (run-1). Void volume (V_0), included volume (V_i); 0.05% w/v chlorobutanol and deionized water (negative controls), *C. ruspolii* crude extract (positive control).

Once the active fractions had been identified from EHI tests, TLCs were developed for fractions 1-18 and marker mixture containing D-glucose, sucrose, leucine and ferulic acid on plates with “F₂₅₄” fluorescent indicator to visualize spots in daylight,

under UV-light, and as stainable spots. The chromatograms documented under UV-366 nm and/or after stained with chromogenic reagents are shown in Figure 5.5.

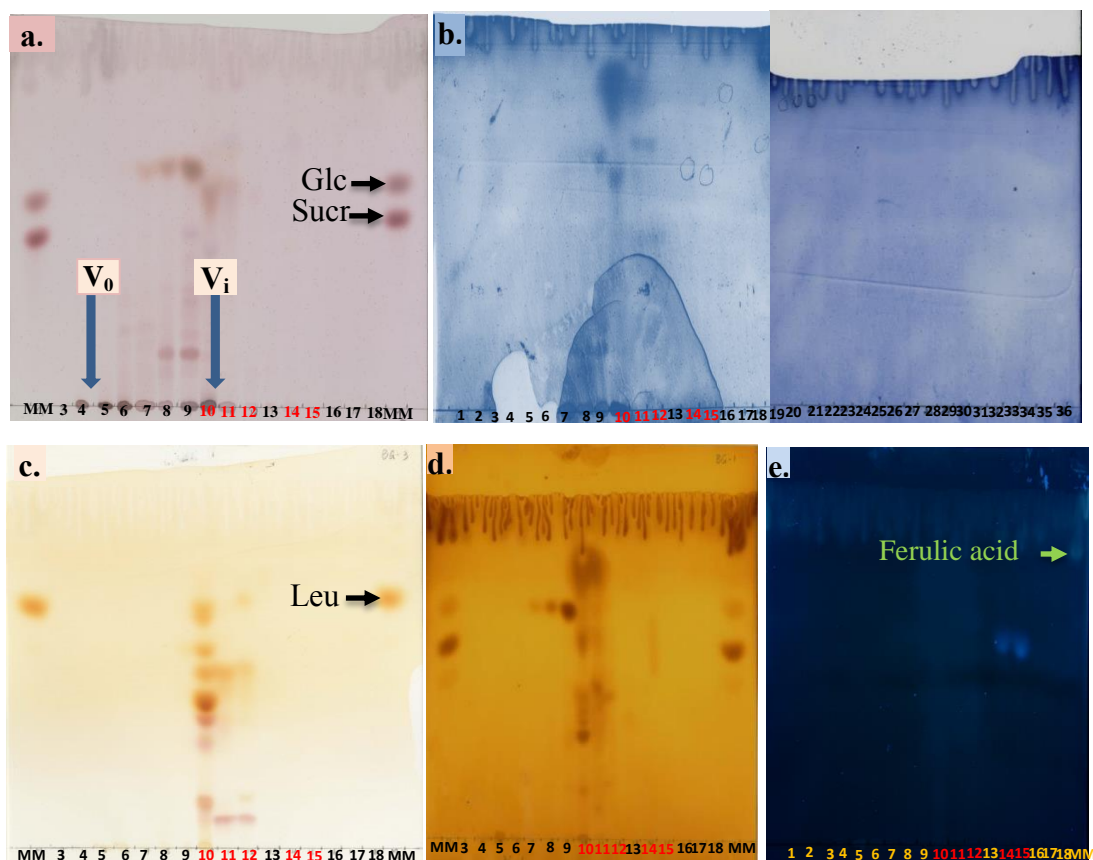


Figure 5.5. Chromatograms of Bio- Gel P-2 fractions (1-18) of *C. ruspolii* (run-1). Thymol stained (a), molybdate (b), ninhydrin (c), iodine (d) and before staining under UV-light at 366 nm (e). Marker mixture: D-glucose (Glc), sucrose (Sucr), leucine (Leu) and ferulic acid. Fractions with EHI activity are labelled red.

Of the eighteen fractions analysed, only fractions 14 and 15 showed blue fluorescent spots under UV-light at 366 nm. However, these blue fluorescent spots could neither be seen under UV-light at 254 nm as dark spots nor stained with any of the chromogenic reagents used. Furthermore, none of the separated spots of any fraction was seen in daylight. However, many of the separated spots and immobile constituents at the origins of fractions 4 to 12 were visualized after staining with chromogenic reagents (Figure 5.5). For instance, several separated spots of fractions

6 to 11 were stained well with thymol (Figure 5.5a). Constituents in fractions 9 to 12 also heavily stained either with molybdate, ninhydrin, iodine or all three of them (Figures 5.5b, 5.5c and 5.5d). Fraction 4 to 5 were identified as V_0 (evidenced from chromatograms stained by thymol and iodine); fraction 10 is V_i (evidenced by ninhydrin staining of the major spots in the fraction that could be amino acids or other primary and secondary amine functional groups containing compounds including non-protein amino acids and alkaloids; Figures 5.5a and 5.5c). Similarly, of the fifteen fractions bioassayed for their EHI properties against *T. circumcincta* eggs in run-2, only seven fractions exhibited significant EHI properties (Figure 5.6). As expected, their EHI activities were dependent on the dilution. Fractions 25, 26, 29 and 30 showed 100% EHI properties at full strengths. Fractions 24, 31 and 36 also showed greater than 70% EHI properties at full strength compared to the controls ($P < 0.001$). The remaining fractions showed either very low activity (such as 27 and 28) to almost no activity (Figure 5.6).

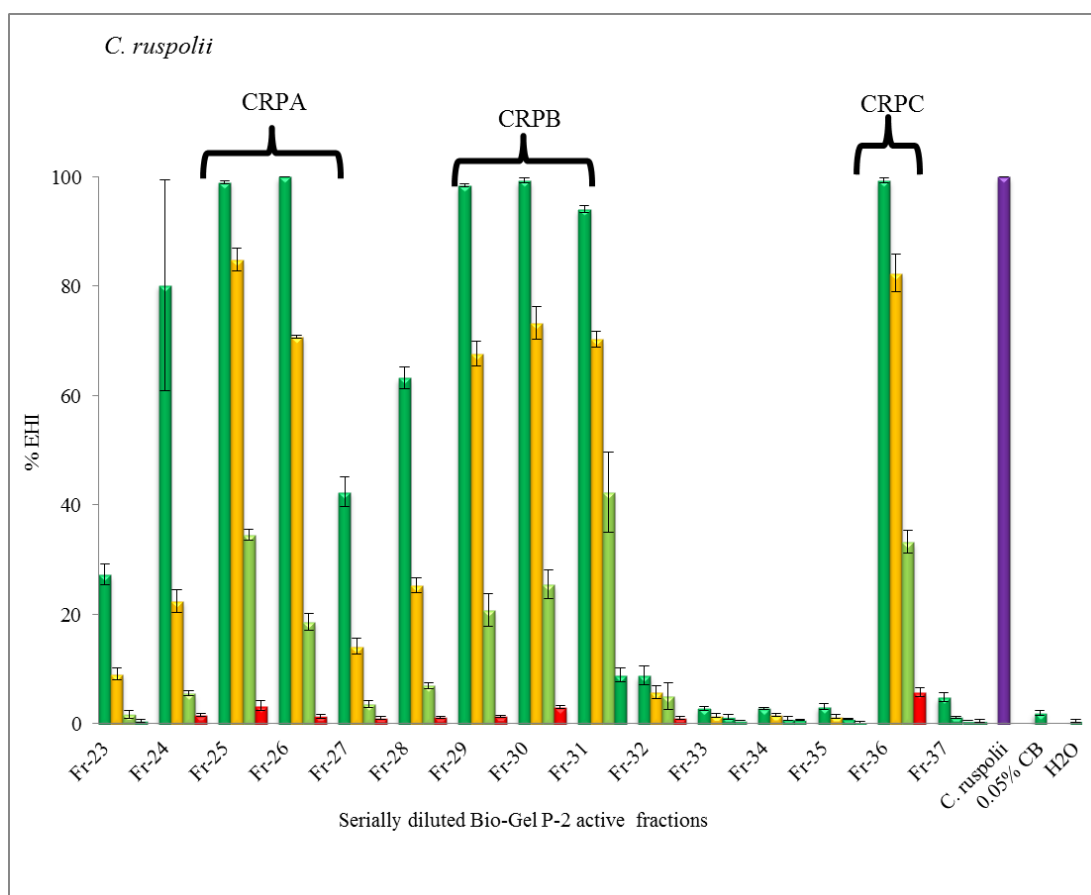


Figure 5.6. EHI of *C. ruspolii* Bio-Gel P-2 fractions (run-2). At full (■), 0.2 (■), 0.04 (■), 0.008 (■) strengths. *C. ruspolii* crude extract (positive control); chlorobutanol (0.05% w/v) and deionized water (H₂O) as negative controls. CRPA, CRPB, CRPC are *C. ruspolii* active pooled fractions.

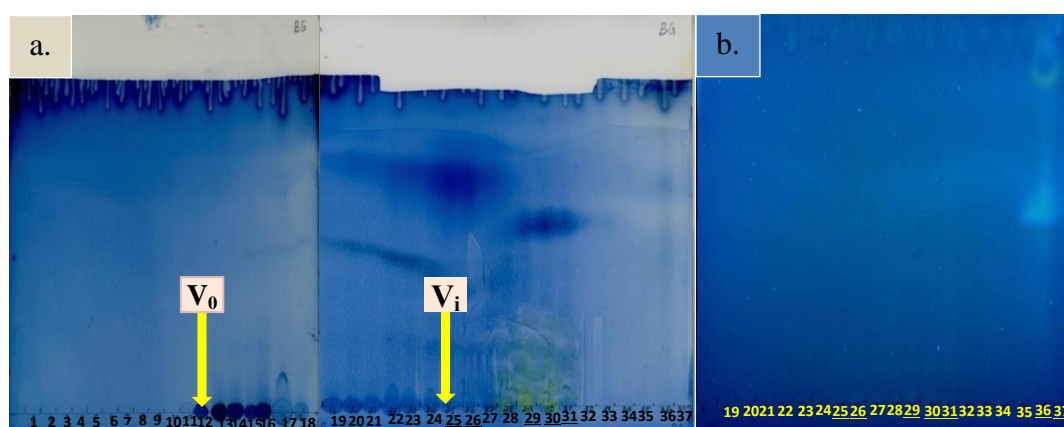


Figure 5.7. Chromatograms of Bio-Gel P-2 fractions (1-37) of *C. ruspolii* (run-2). Molybdate stained fractions 1-37 (a) and fractions 19-37 examined before staining under UV-light at 366 nm (b). Void volume (V_0) and included volume (V_i). Fractions with EHI activity are underlined.

Chromatograms of Bio-Gel P-2 fractions (run-2) also revealed that the active fractions 25 and 26 and 29 to 31 did contain spots that well stained with molybdate (Figure 5.7a). A late-eluted active fraction (Fr-36) also contained two blue- and one yellow-fluorescing spots. In this run, Bio-Gel P-2 fraction 12 is V_0 , because the non-retained constituent (major polymers) that stains with molybdate eluted into this fraction. In comparison to the patterns of separated spots of molybdate stained TLC in Figure 5.5b, the V_i could be approximately fraction 25.

5.4.2. Chromatographic profiling of *C. ruspolii* Bio-Gel P-2 active fractions

The migration profiles (R_F -values) of constituents of active fractions of *C. ruspolii* separated on TLC developed in BAW (4:1:1 v/v/v), examined under UV-light at 366 nm, stained with molybdate and their corresponding elution behaviour on Bio-Gel P-2 (K_{av} -values) of runs 1 and 2 are mapped as shown in the Figure 5.8.

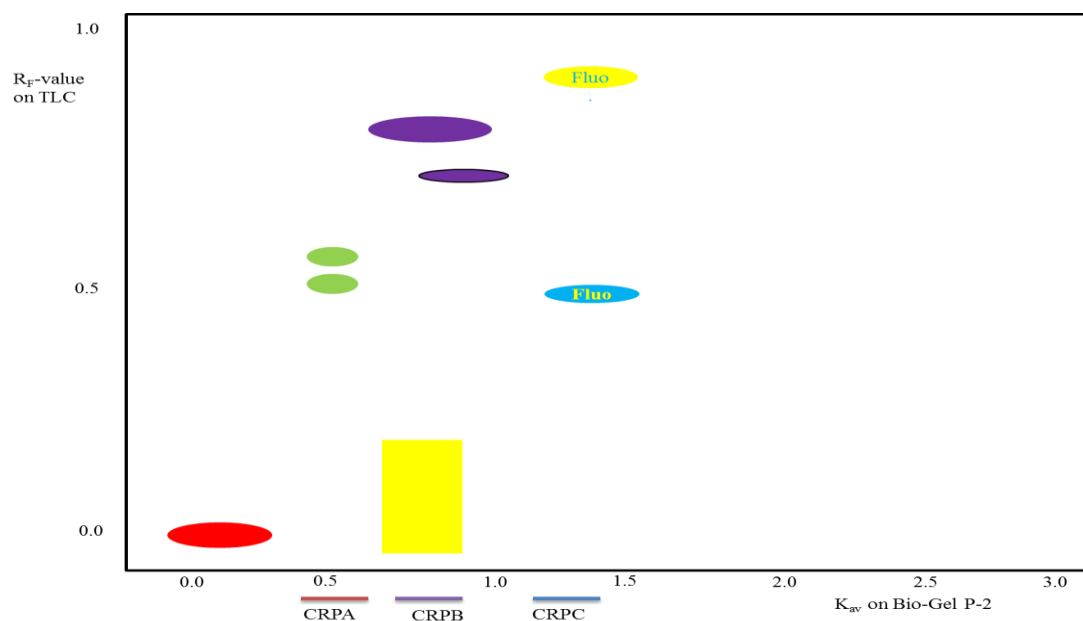


Figure 5.8. R_F -values of separated spots on TLC vs elution behaviour (K_{av} – values) on Bio-Gel P-2 column of *C. ruspolii* active pooled fractions. CRPA (—), CRPB (—), CRPC (—) are active pooled fractions. TLC was developed in BAW (4:1:1 v/v/v). This simple mapping done based on merging of chromatograms of runs 1 and 2. Fluo indicates fluorescent spots at 366 nm.

In run-2, increasing the sample loaded and column height by two-fold simultaneously, shifted the fractions containing V_0 and V_i from fractions 4 and 10 in run-1 (Figure 5.5) to fractions 12 and 25 in run-2 (Figure 5.7), respectively. Moreover, these increased in loaded sample and column bed volumes also resulted in partitioning of active fractions into many neighbouring fractions. These partitioning were revealed by examining of chromatograms under UV-light and after staining with molybdate. For instance, active fractions partitioned into fractions 25 and 26 (CRPA) and 28 to 31 (CRPB) contained well separated and molybdate stained spots with similar R_F -values (Figure 5.7a).

Similarly, the blue and yellow fluorescing constituents under UV-light at 366 nm of the extract also partitioned into fractions 36 and 37 (CRPC; Figure 5.7b). Although fraction numbers to which active constituents partitioned into differed from those in run-1, which is due to change in sample size and column bed volume, patterns of the separated spots on chromatograms remained similar in both runs.

During the third fractionation (run-3), a larger volume of clarified extract (20 ml) was fractionated on Bio-Gel P-2 column previously used in run-2 and reconditioned with de-ionized water for 48 h. The same number and volume of fractions were collected as in run-2. Chromatograms were developed using crude extract as a marker under the same chromatographic development conditions as in run-1 and run-2. The chromatograms were examined under UV-light and after staining with molybdate, as shown in Figure 5.9.

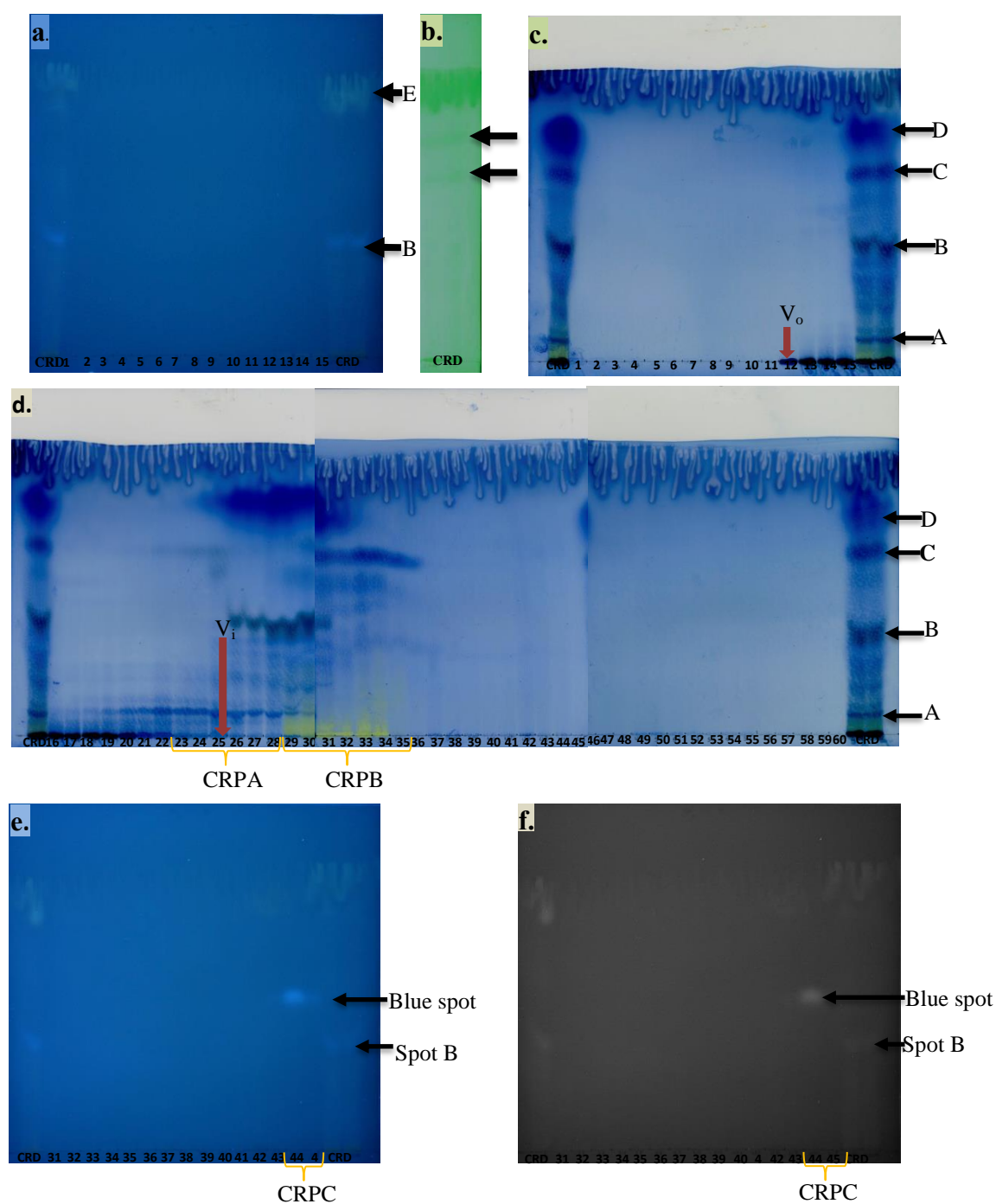


Figure 5.9. Chromatograms of Bio-GelP-2 fractions of *C. ruspolii* (run-3). Developed in BAW (4:1:1 v/v/v) examined under UV-light at 366 nm (a, e and f) and 254 nm (b) and molybdate stained and heated at 105°C for 30 minutes (c and d); void volume (V_0) and included volume (V_i); CRPA, CRPB and CRPC are *C. ruspolii* pooled fractions; A, B, C and D are separated spots of crude (CRD) extract.

Keeping other GPC fractionation parameters constant, increasing the volume loaded by three fold relative to run-2 did not change the position of fractions containing either voided or included volume. However, fractions pooled as CRPA and CRPB were partitioned over many more fractions compared to the previous runs (runs 1 and 2). In run-3, the blue fluorescent compound containing fractions (36 and 37) in run-2 that pooled into CRPC now eluted into fractions 44 and 45. The chromatograms developments were carried out for the same duration (9.5 h) and under the same chromatographic conditions, the R_F -values of major separated spots from the crude extract remained the same. These separated major spots of the crude extract were numbered from bottom to top as spots A, B, C and D with R_F -values of 0.07, 0.39, 0.68 and 0.82 respectively (Figures 5.9c and 5.9d). Spots C and D were dark spots on a green background under UV-light at 254 nm and heavily stained with molybdate but were not fluorescent at 366 nm (Figure 5.9b). Spot B was seen as bright blue fluorescent under UV-light at 366 nm and also stained well with molybdate reagent. However, the blue fluorescent compound partitioned into fractions 14 and 15 (run-1), 36 and 37 (run-2), and 44 and 45 (run-3), and also for fractions 49 and 50 of run-4 (see below) did not stain with molybdate reagent.

During run-4, *C. ruspolii* extract (6.6 ml) was fractionated on the same column which had previously been used for runs 2 and 3 upon reconditioning with deionized water for 48 h. For this round of fractionation, sixty 3-ml fractions were collected. Chromatograms developed using crude extract as marker under the same conditions as previously. The chromatograms examined under UV-light and after stained with molybdate are shown in Figure 5.10.

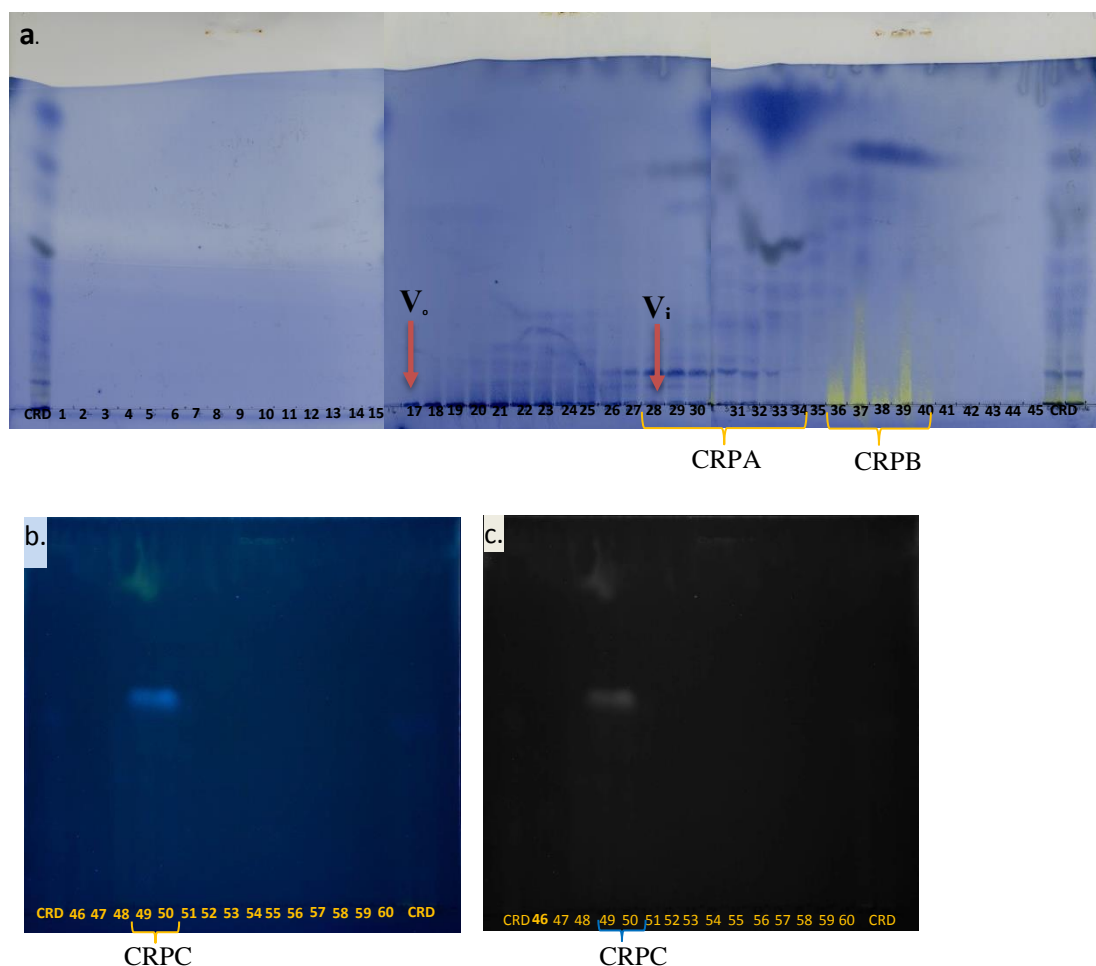


Figure 5.10. Chromatograms of Bio-Gel P-2 fractions of *C. ruspolii* (run-4). Developed in BAW (4:1:1 v/v/v) and molybdate stained and heated at 105°C for 30 minutes (a); examined under UV-light before molybdate staining at 366 nm (b) and 366 nm BW (c). Void volume (V_o) and included volume (V_i). CRPA, CRPB and CRPC are *C. ruspolii* pooled fractions; crude extract (CRD).

The V_o and V_i in fractions 12 and 25 on molybdate stained chromatograms of runs 2 and 3 (Figures 5.7a, 5.9c and 5.9d) now shifted to fractions 17 and 28 in run-4 (Figure 5.10a) respectively. The summary of effects of sample volumes loaded and column parameters on elution position of V_o and V_i and partitioning of active pooled fractions of *C. ruspolii* runs 1-4 into many neighbouring fractions are shown in Table 5.1.

Table 5.1. The summary of effects of sample volumes loaded and column parameters on elution position of V_0 and V_i and active pooled fractions of *C. ruspolii* runs 1-4.

Bio-Gel P-2 column	Bed volume (ml)	Sample loaded (ml)	No. fractions collected	Volume collected (ml)	V_0	V_i	CRPA	CRPB	CRPC
Run 1	70	3.5	55	4	5	10	10 and 11	12	14 and 15
Run 2	132	6.6	60	4	12	25	25 and 26	28-31	36 and 37
Run 3	132	20	60	4	12	25	23-28	29-35	44 and 45
Run 4	132	6.6	60	3	17	28	28-34	36-40	49 and 50

♦Void volume (V_0), included volume (V_i), *Cissus ruspolii* pool A (CRPA), *Cissus ruspolii* pool B (CRPB), *Cissus ruspolii* pool C (CRPC).

5.5. Discussion

In this work, the EHI test results of GPC fractions of *C. ruspolii* (runs 1 and 2) revealed that active constituents of this extract were partitioned into a small number of fractions based on their molecular sizes as seen by TLC. The TLC profiles of fractions examined under UV-light at 254 nm and 366 nm and after staining with various staining reagents (run-1) and molybdate stained (run-2) reaffirmed the distinctive difference between TLC spot profiles of active and inactive fractions, hence there is a strong correlation between the EHI activity and patterns of separated spots of the active versus inactive fractions. The thymol stained constituents could be sugars and/or glycosylated organic compounds. The iodine-stained spots might be an indication of the presence of constituents with unsaturated double bonds whose π -bonds break and add iodine to the carbon-carbon double bonds or form a complex with iodine. Those constituents that stained with molybdate might form organic complex with the central metal (Mo) or donating hydrogen or electrons to reduce molybdate from Mo (VI) to the Mo (IV) oxidation state. Almost all constituents of the active fraction (fraction-10; run-1) of *C. ruspolii* were heavily stained with ninhydrin indicating that this fraction could be rich in nitrogen-containing organic compounds including alkaloids with free primary and/or secondary amine functional groups. The molybdate-stained chromatograms of runs 1 and 2 had similar profiles in terms of migration patterns of separated spots. Similarly, chromatograms examined under UV-light at both shorter and longer wavelengths revealed that *C. ruspolii* extract did contain constituents that fluoresced blue and yellow under UV-light at 366 nm. Spots C and D of crude extract in run-3 seen as dark spots at 254 nm on green back ground but did not seen for runs 1, 2 and 4. This indicates that the

detection of constituents of crude extract under UV-light at 254 nm is dependent on concentration of constituent(s) that fluoresced dark at this wavelength.

Glucose and sucrose were components of the marker mixture used for TLC development of Bio-Gel P-2 fractions in run-1. The two common plant sugars are expected in most of plant crude extracts. Surprisingly, none of the separated bands in the fractions of *C. ruspolii* match with either of the bands. Hence, both sugars are absent in *C. ruspolii* water extracts as free monosaccharide. In general, in a comparison of run 1 with run 2 of *C. ruspolii*, there was a strong correlation between discrete fractions with significant EHI activities and their chromatographic profiles. None of the TLC staining reagents used so far stained the blue fluorescent spots in *C. ruspolii* extract and fractions containing them. This could be either because the amount was not sufficient to react with the chromogenic reagents to form coloured spots or because the compound was not stainable with the reagents used. For instance, even though spot B in run-3 was seen as a blue spot under UV-light at 366 nm, the colour formation reaction with molybdate reagent might not be due to the blue fluorescent compound, but instead it could be due to other component(s) in the mixture having the same R_F -value as the blue compound. This speculation may be supported from two perspectives. Firstly, the blue fluorescent component in Bio-Gel P-2 fractions 44 and 45 (run-3) migrated further (higher R_F -value, Figure 5.9e, f) than the blue fluorescent spot (spot B) of the crude extract. Secondly, the molybdate-stained components in spot B of crude extract were partitioned into those fractions pooled as CRPA and CRPB whereas the blue fluorescent component of spot B was partitioned into CRPC and still blue fluorescent at UV-366 nm but not stainable with the molybdate reagent.

The significant shifts in V_o , V_i and ranges of pooled fractions in *C. ruspolii* run-4 could be due to decrease in both flow rate and volume collected per fraction. The flow rate was slowed down by lowering the solvent reservoir. Moreover, the volume collected per fraction was decreased from 4 ml in runs 1, 2 and 3 to 3 ml in run-4. However, the general trends of separated spots of active fractions and their chromatogram profiles remained similar for all runs. Therefore, pooling of Bio-Gel P-2 fractions of *C. ruspolii* into CRPA, CRPB and CRPC was done based on their EHI tests and TLC profiles of separated spots when examined under UV-light and after stained with molybdate. Bio-Gel P-2 fractions of any run pooled into CRPA are those fractions containing spots A, B and D that stain dark blue with molybdate. For CRPB, these are those fractions containing a spot that stained yellow with molybdate and rich in spot C. Lastly, for CRPC, these are those fractions containing relatively slow migrating and blue fluorescing (major) and fast migrating yellow fluorescing (minor) spots (Figure 5.9) when visualized under UV-light at 366 nm. For further bioassay-guided isolation and purification of active compounds, the main active Bio-Gel P-2 fractions were categorized and merged into pools based on their TLC profiles. Merging of these partially purified active fractions into a small number of pools has many advantages. It enriches pools in active constituents, makes further bioassay-guided isolation and purification more quantitative (i.e. reasonable amount of target compound(s) recovered that is sufficient for physical, chemical and biological assays) than on single fractions, and to minimize time and cost of purification.

There are a number of reports on compounds isolated and purified by bioassay-guided isolation and purification from pooled fractions using different

chromatographic methods in various solvent systems. For instance, anthelmintic lignans (arctigenin and arctiin) active against *Dactylogyrus intermedius* from *Fructus arctii* fruits (Wang *et al.*, 2009), an antifungal anthraquinone, roseanone, active against *Candida albicans* and yeasts from *Cassia fistula* seeds (Jothy *et al.*, 2011), anticancer agents (the long-chain alkane hentriacontane and the diterpene (+)-13S, 14R, 15-trihydroxy-ent-labd-7-ene) active against lymphoma cell lines from *Gymnosperma glutinosum* (Quintanilla-Licea *et al.*, 2012), and anti-osteoporotic triterpenoids and steroids isolated from stem of *Cissus quadrangularis* (Pathomwichaiwat *et al.*, 2015). The cinnamic acid and cinnamic acid derivative with anticoagulant activity were also isolated from traditional perennial medicinal herb *Melastoma malabathricum* by bioassay guided fractionation of hot water leaf crude extract (Khoo *et al.*, 2015). Furthermore, epicatechin, oligomeric proanthocyanidins, procyanidins and flavonoids from 50% EtOH leaf extract of *Combretum mucronatum*, a plant claimed for wound healing and treatment of helminth infections (Spiegler *et al.* 2015), phloroglucinol derivatives such as aspidinol with anthelmintic and antimicrobial properties from petroleum ether leaf extract of *Leucosidea sericea* that traditionally used by indigenous South African people as a vermifuge and astringent (Bosman *et al.*, 2004), and motiol and β -sitosterol with promising antinociceptive from methanolic root extract of *Scorzonera latifolia* (Acikara *et al.*, 2014) were isolated by bioassay-guided fractionation. Two glycosylated flavonoids (quercetin-3-O-rutinoside and kaempferol-3-O-rutinoside) with anti-inflammatory properties in wound healing process from n-butanol extracts of *Morus nigra* fruit (Akkol *et al.*, 2015), and bioactive anthraquinone (1,8-dihydroxy-anthraquinone-3-carboxylic acid) with antimicrobial properties against

aerobic and anaerobic oral bacteria from dichloromethane bark extracts of *Cassia bakeriana* were also isolated by bioassay-guided fractionation (Cunha *et al.*, 2017).

In conclusion, the chromatogram profiling of Bio-Gel P-2 fractions revealed that fractions containing V_0 and V_i eluates were influenced by sample size, column bed volume, volume of fraction collected and flow rate. EHI tests followed by TLC profiling of Bio-Gel P-2 also revealed the distinctive difference between active and inactive fractions. These profiling also assisted to pool active fractions with similar spot patterns on TLC for further bioassay guided isolation and purification studies (Chapter Seven).

Chapter Six: Bioassay-guided fractionations of *Adenia* sp. extract and chromatographic characterisation of resultant fractions

6.1. Abstract

Crude water extract of the second candidate plant (*Adenia* sp.) was separated into discrete fractions on the same column using the same eluent used in fractionations of *C. ruspolii* water extract. The resultant discrete fractions were also bio-assayed against the same nematode eggs to identify active fractions. Chromatographic characterizations of resultant fractions were done using the same TLC analyses methods and staining reagents used in section 5.3.4. The EHI test results showed that discrete fractions containing active constituents were eluted in a small numbers of fractions. The main active Bio-Gel P-2 discrete fractions were merged into pools ASPA, ASPB and ASPC based on their similar in EHI efficacy and spot patterns on chromatogram to enrich these pooled fractions with targeted compounds for further bioassay-guided isolation and purification (Chapter Seven).

6.2. Introduction

Bioassay-guided fractionation is a procedure whereby a crude extract is fractionated either by solvent partition based on polarity or chromatographically due to difference in molecular size or polarity until a pure biologically active compound is isolated (Dauda and Mudi, 2013). Discrete fractions containing compounds with similar properties (such as polarity or molecular size) are bio-assayed to quickly home in on those fractions containing target compounds. These discrete fractions usually contain mixtures of neutral, acidic, basic, lipophilic, hydrophilic, or amphiphilic compounds of similar molecular sizes (Gibbons, 2012). Thus, TLC analysis of Bio-Gel P-2 discrete fractions are very important to know the nature, number and separated spot patterns of active fractions (Sharma, 2013; Jayashre, 2013). This experiment was designed to address similar objectives as stated for *C. ruspolii* in section 5.2, here summarised as (i) EHI to identify active fraction(s) based on molecular size, (ii) sensitivity of GPC separation to sample size, column bed volume (iii) establish TLC-based chemical fingerprints of GPC fractions, and (iv) pool bio-active fractions for bioassay guided isolation and purification (Chapter Seven).

6.3. Materials and methods

6.3.1. Crude extract preparation

Crude extract of *Adenia* sp. was similarly prepared by maceration as detailed in section 2.7.1. The filtrate was centrifuged using Eppendorf 5810R centrifuge (Fisher Scientific Ltd, Loughborough, UK) at $2057 \times g$ for 10 min. The clarified supernatants were used for bioassay-guided fractionations.

6.3.2. Gel-permeation chromatography

The same volumes of *Adenia* sp. water extract and GPC with Bio-Gel P-2 matrix were used under similar conditions as detailed in section 5.3.2 except at different extract concentration (8.45 mg/ml). Figure 6.1 shows the flow diagram of Bio-Gel P-2 fractionation of *Adenia* sp. (run-2) that was used for further bioassay guided isolation and purification of compounds (Chapter Seven). Similar Bio-Gel P-2 fractionation approach was used for other runs. Bio-Gel P-2 fractions (run-1) were used for bio-assay against target nematode eggs to identify active fractions and for detailed TLC analyses of discrete fractions. Run-2 fractions were used to repeat the bioassay, TLC analyses and for bioassay-guided isolation and purification (Chapter Seven). Run-3 fractions were used to study the effect of high sample volume loaded on elution positions of void volume (V_0), included volume (V_i) and active pooled fractions (see Table 6.1 below) and TLC analysis of major constituents of active Bio-Gel P-2 fractions using crude extract as marker (see Figure 6.7 below).

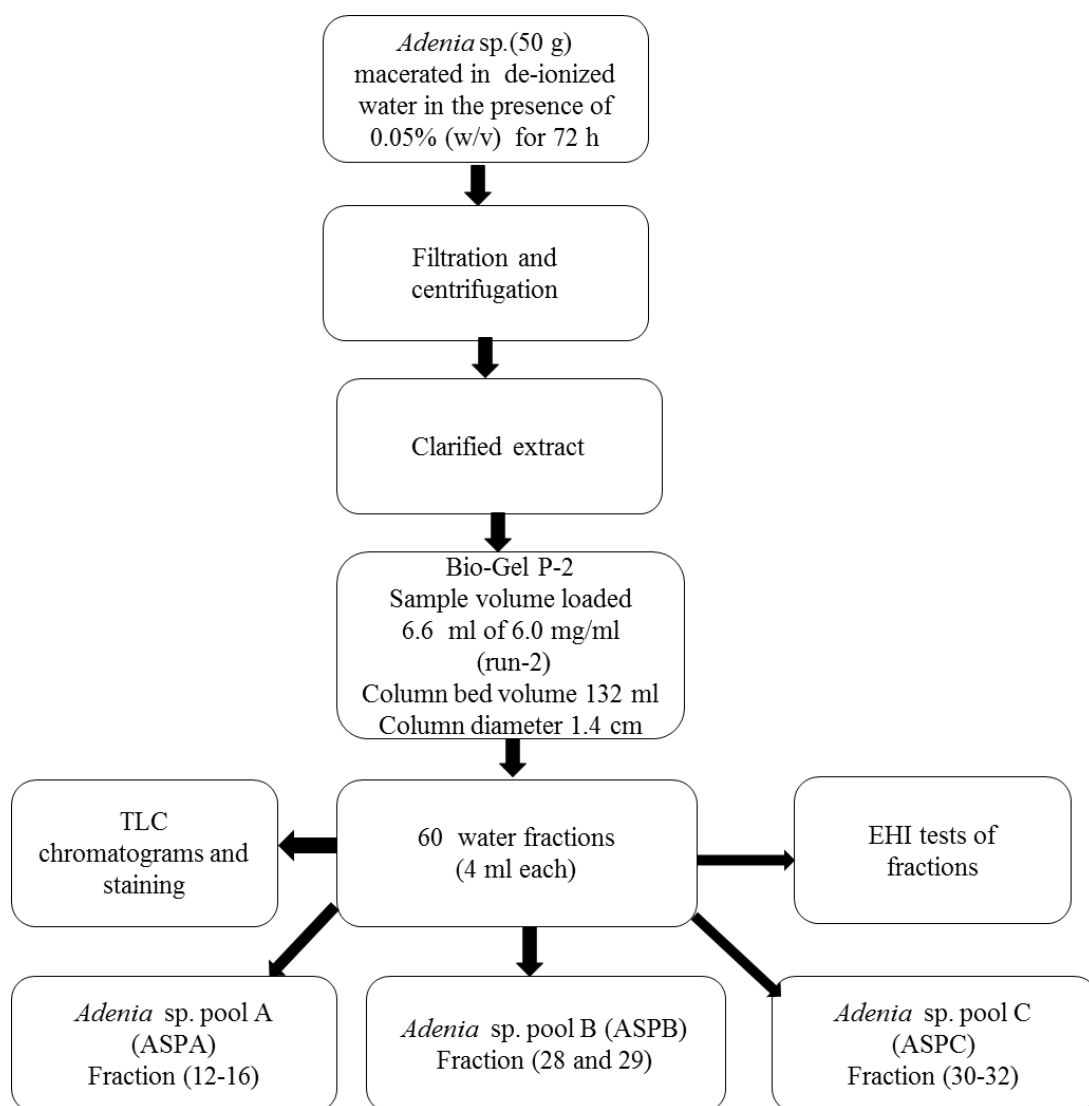


Figure 6.1. Flow diagram of Bio-Gel P-2 fractionation of *Adenia* sp. (run-2).

6.3.3. Egg hatch inhibition

The EHI test for Bio-Gel P-2 fractions was done in triplicate as indicated in section 5.3.3 (see section 2.5.1.3 for more details).

6.3.4. Thin-layer chromatography

The same sample volume, solvent system and staining reagents as used in section 5.3.4 were also used for TLC analyses of *Adenia* sp. Bio-Gel P-2 fractions (see section 2.9 for more details).

6.3.5. Calculations and statistics

The EHI data were expressed as a percentage. The same statistical method and significance level for biological relevance of observed activity detailed in section 5.3.5 were used here.

6.4. Results

6.4.1. Bio-Gel P-2 fractions of *Adenia* sp.

Clarified extract of *Adenia* sp. (3.5 ml of 8.45 mg/ml) was loaded onto Bio-Gel P-2 with 70 ml bed volume and eluted with deionized water. Fifty-five fractions were collected and bioassayed at full strength for their EHI properties to identify fractions containing active constituents that inhibit nematode egg hatching (Figure 6.2).

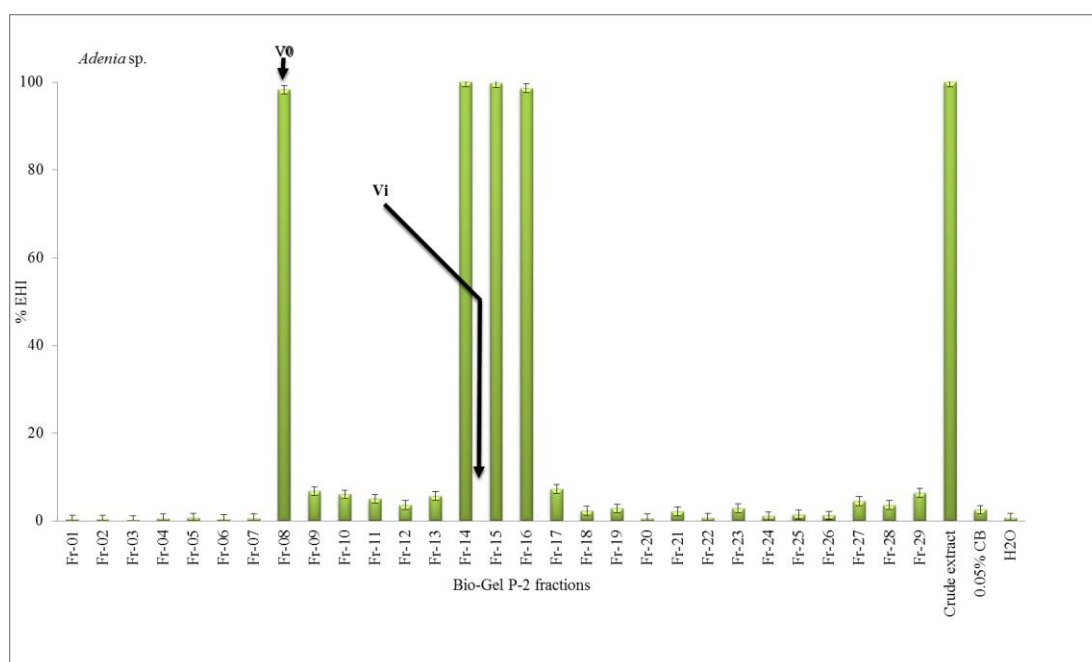


Figure 6.2. EHI of Bio-Gel P-2 fractions of *Adenia* sp. (run-1). Void volume (V_0) and included volume (V_i). Crude extract was used as positive control, and chlorobutanol (0.05% w/v) and deionized water (H_2O) as negative controls.

Fractions 8, 14, 15 and 16 showed 100% EHI activity at full strength compared to controls ($P < 0.001$). The remaining fractions either exhibited very low activity or no activity at all (Figure 6.2). Chromatograms were developed only for fractions 1-18 (Figure 6.3).

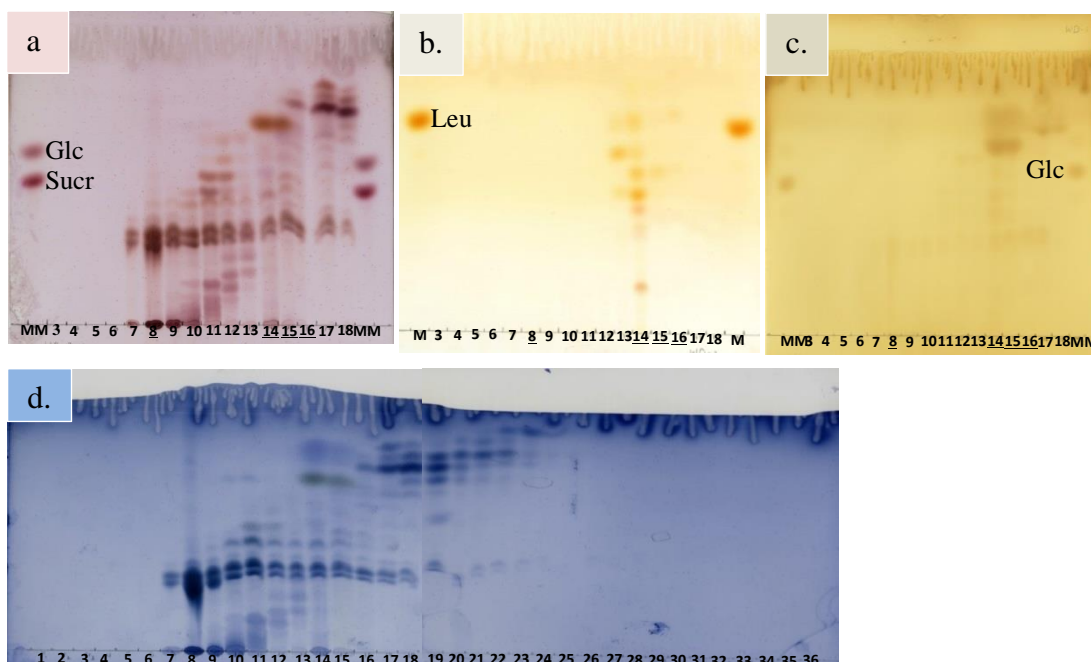


Figure 6.3. Chromatograms of Bio-Gel P-2 fractions (1-18) of *Adenia* sp. Stained with thymol (a), ninhydrin (b) iodine vapour (c). molybdate (d). Marker mixture (MM): D-glucose (Glc), sucrose (Sucr), leucine (Leu) and ferulic acid. Fractions with EHI activity are underlined.

The deductions of V_0 and V_i for *Adenia* sp. Bio-Gel P-2 (run-1) were done based on both thymol and ninhydrin stained chromatograms. The non-retained constituents were largely eluted into fraction-8 although it started to elute in late drops of fraction-7. Hence, fraction-8 was identified as V_0 (fraction containing the non-retained constituents evidenced by thymol staining); fraction 14 was identified as V_i (fraction that contained major amino acids or other nitrogen containing compounds with free amine functional groups as evidenced by ninhydrin staining). For *Adenia* sp. the molybdate stained TLC was also used to deduce both V_0 and V_i , which were similar to the thymol stained chromatogram.

Fractions (7-18) contained constituents that heavily stained with thymol and molybdate reagents. However, only fractions 13-16 and 14-18 did contain constituents that stained well with ninhydrin and iodine vapour, respectively. Based

on the correlation between the EHI and TLC profiles of *Adenia* sp. Bio-Gel P-2 fractions, it was noted that the active fraction (fraction-8) that was rich in two slow and close migrating major spots that heavily stained with thymol and molybdate corresponded to the void volume (V_0) and therefore its constituents might behave like a polymer or micelle in water solution. It was observed that the next neighbouring active fractions (14, 15 and 16) did contain two slow and close migrating spots having similar R_F -values to those major spots of fraction-8 and fast migrating spots that heavily stained brown and dark green with thymol and molybdate respectively. Moreover, these three neighbouring fractions contained approximately equal amounts of the dark green stained spot with molybdate (Figure 6.3d).

After the second Bio-Gel P-2 fractionation (run-2), all molybdate-stained fractions having similar TLC chromatograms to those active fractions of run-1 were also bioassayed for their EHI activities against *T. circumcincta* eggs (Figure 6.4).

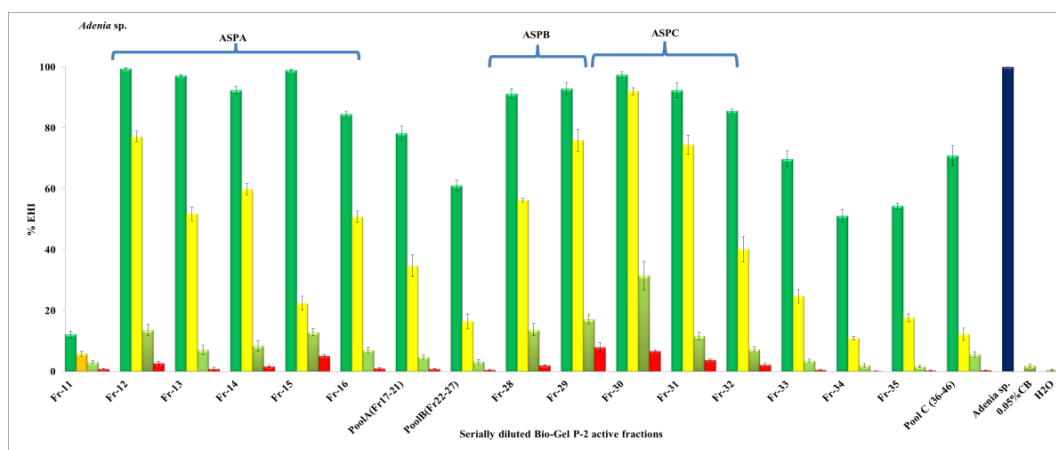


Figure 6.4. EHI tests of *Adenia* sp. Bio-Gel P-2 fractions (run-2). At full (■), 0.2 (■), 0.04 (■), 0.008 (■) strengths. *Adenia* sp. crude extract (positive control), chlorobutanol (0.05% w/v) and deionized water (H_2O) as negative control. ASPA, ASPB, ASPC are *Adenia* sp. pooled fractions.

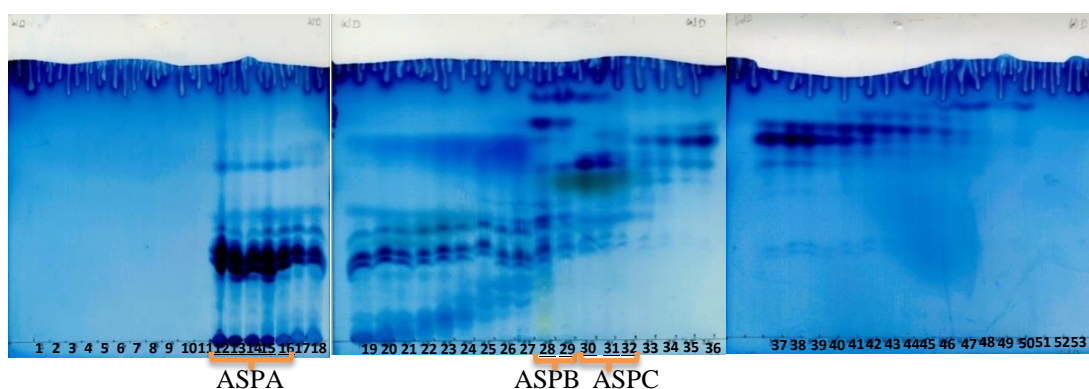


Figure 6.5. Molybdate stained chromatogram of Bio-Gel P-2 fractions of *Adenia* sp. (run-2). ASPA, ASPB, ASPC are *Adenia* sp. active pooled fractions.

Of the fourteen single and three pooled fractions bioassayed for their EHI properties against *T. circumcincta* eggs, 11 fractions exhibited significant ($P < 0.001$) EHI activities at full strength (Figure 6.4). Fractions 12-16 and 28-32 showed greater than 85% EHI activity compared to controls. The active fractions 12-16 that labelled as ASPA were identified by containing two slow and close migrating major spots with R_F -values of 0.23 and 0.27 that stained blue with molybdate. The second active fractions (28 and 29) that labelled as ASPB were identified by their slow-migrating yellow-stained spot in fraction 28 and two fast migrating spots (close to the solvent front) that stained blue with molybdate. Lastly, the active fractions labelled as ASPC (30 to 32) were identified by their two major spots that migrate close to each other that stain dark green (R_F -value of 0.69) and blue (R_F -value of 0.71) with molybdate. One or more of the separated and heavily stained spot(s) with molybdate in these active fractions could be the one(s) that responsible for the observed EHI activity. In runs 1 and 2, the void volumes (V_0) correspond to fraction 8 and 12 respectively. These fractions were among those active fractions pooled as ASPA and thus presumably small molecules. Bio-Gel P-2 is “supposed” to retard small molecules,

however, some active constituents of *Adenia* sp. (most likely small molecules with anomalous behaviour possibly detergent-like molecules such as saponins that form big micelles in water solution might be eluted in V_0 (Figures 6.2, 6.3 and 6.4).

Moreover, in wells incubated with fractions 12-16 at full strengths, all the hatched first stage larvae were observed stretched and non-motile after 24 h of incubation time. Fractions 33-35 and the pooled fraction (36-46) showed moderate EHI activities at full strengths. The EHI test and molybdate stained TLC profiles of GPC fractions also revealed that active constituents of *Adenia* sp. extract (run-2) were partitioned into a wide range of discrete fractions (Figures 6.4 and 6.5).

6.4.2. Chromatographic profiling of *Adenia* sp. Bio-Gel P-2 active fractions

The migration profiles (R_F -values) of constituents of active pooled fractions of *Adenia* sp. separated on TLC developed in BAW (4:1:1 v/v/v) and stained with molybdate and their corresponding elution behaviour on Bio-Gel P-2 (K_{av} -values) of runs 1 and 2 are mapped as shown in Figure 6.6.

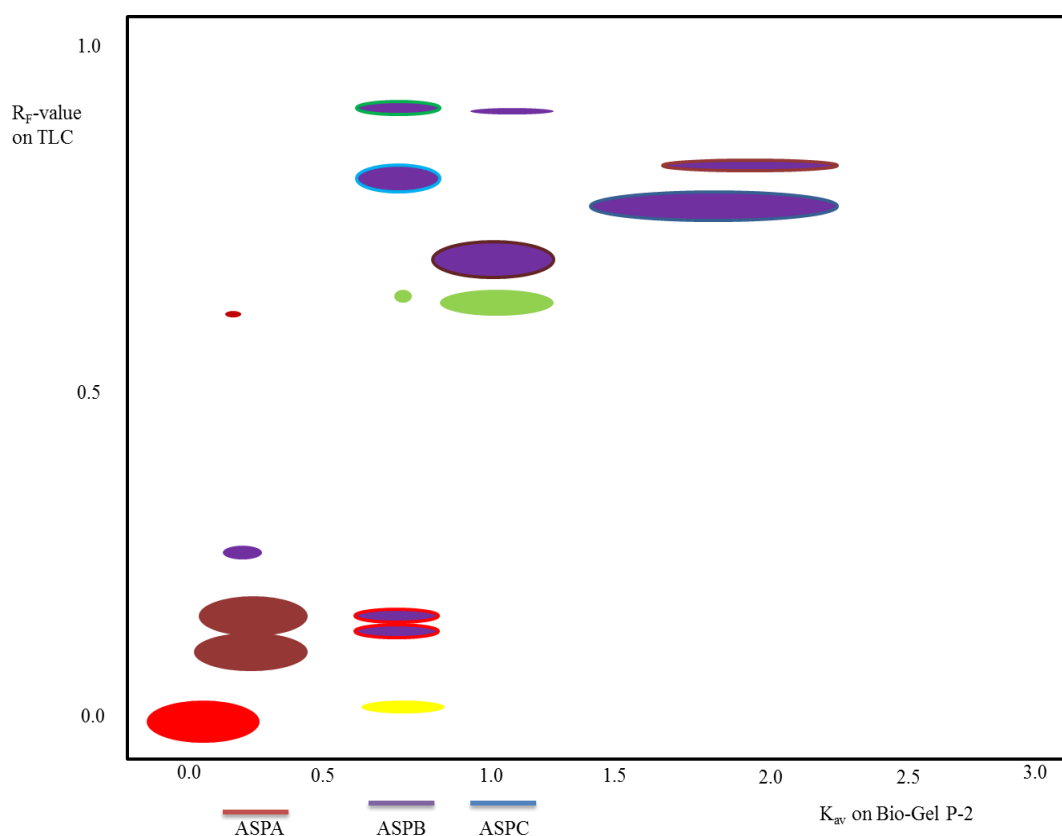


Figure 6.6. R_F -values of separated spots on TLC vs elution behaviour (K_{av} – values) on Bio-Gel P-2 column of *Adenia* sp. active pooled fractions. ASPA (—), ASPB (—), ASPC (—) are active pooled fractions. TLC was developed in BAW (4:1:1 v/v/v). This simple mapping done based on merging of molybdate stained chromatograms of runs 1 and 2.

During the third fractionation (run-3), a three-fold greater volume of clarified extract (20 ml) was used compared with run-2. The same number of fractions and volumes per fraction were collected as in run-2. TLC chromatograms were developed using crude extract as marker under the same chromatographic development conditions as in run-2. The chromatograms were examined under UV-light and after stained with molybdate (Figure 6.7). An increase in volume sample loaded by three fold relative to the second run did not change either V_0 or V_i . However, fractions pooled into ASPA, ASPB and ASPC were partitioned over many more fractions compared to runs 1 and 2. This plant extract contains many minor and major separated spots. The

R_F values of major separated spots in crude extract remained the same on all plates. These separated major spots in crude extract were indicated as spots A, B, C, D, E, F and G with R_F -values of 0.23, 0.27, 0.33, 0.60, 0.63, 0.70, and 0.80 respectively (Figure 6.7)

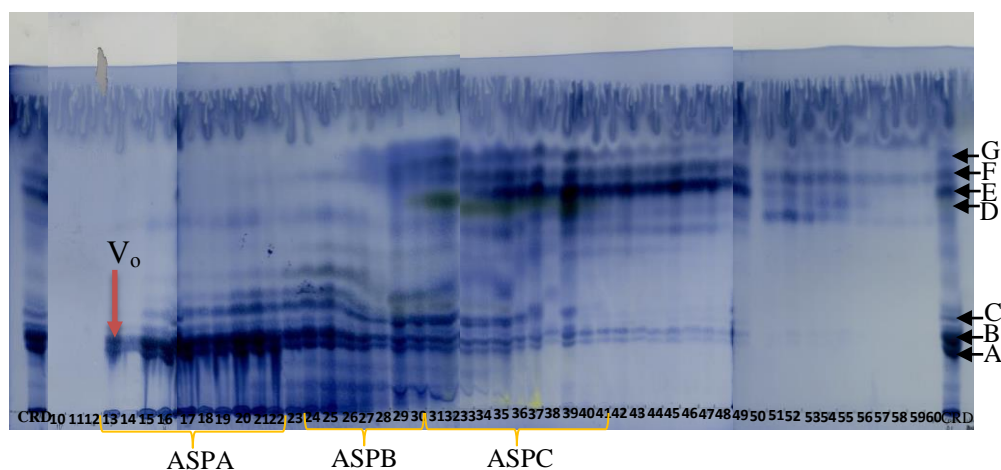


Figure 6.7. TLC profiles of Bio-GelP-2 fractions of *Adenia* sp. (run-3). Developed in BAW (4:1:1 v/v/v) stained with molybdate and heated at 105°C for 30 min.; ASPA, ASPB and ASPC stand for *Adenia* sp. pooled fractions; A-G are separated spots of crude (CRD) extract.

The summary of effects of sample volumes loaded and column parameters on elution position of V_o and V_i and partitioning of active pooled fractions of *Adenia* sp. runs 1-3 into many neighbouring fractions are shown in Table 6.1.

Table 6.1. The summary of effects of sample volumes loaded and column parameters on elution position of V_o and V_i and active pooled fractions of *Adenia* sp. runs 1-3.

Bio-Gel P-2 column	Bed volume (ml)	Sample loaded (ml)	No. of Fractions collected	Volume collected (ml)	V_o	V_i	ASPA	ASPB	ASPC
Run 1	70	3.5	55	4	8	8	7 and 8	14 and 15	16
Run 2	132	6.6	60	4	12	12	12-16	28 and 29	30-32
Run 3	132	20	60	4	13	13	13-22	24-30	31-40

♦Void volume (V_o), included volume (V_i), *Adenia* sp. pool A (ASPA), *Adenia* sp. pool B (ASPB), *Adenia* sp. pool C (ASPC).

6.5. Discussion

The bioassay-guided fractionations of *Adenia* sp. water crude extract and TLC characterisation of Bio-Gel P-2 fractions revealed that active constituents were partitioned into a small number of fractions based on their molecular sizes. As such, outcomes on *Adenia* sp. obtained here are in agreement with many reports on compounds isolated and purified by bioassay-guided isolation and purification as discussed in Chapter five (see section 5.5). Chromatograms examined under UV-light shown that *Adenia* sp. water extract did not contain any fluorescent spot. Such a result could indicate the absence of metabolites with UV-active chromophore functional groups in the extract. From Bio-Gel P-2 fractionations of *Adenia* sp. (runs 1 and 2), it was noted that the void volumes (V_0) correspond to fraction 8 and 12, respectively. These fractions were among those active fractions pooled as *Adenia* sp. pool A (ASPA). Thus, the $V_0=V_i$ observed in *Adenia* sp. implies that the general principle of separation of constituents of medicinal plant crude extracts on GPC based only on molecular size may not necessarily be effective. This is because separation of constituents of a mixture based only on molecular size may work for biomolecules (primary metabolites) but may not work for plant secondary metabolites which are known for their diverse physicochemical properties. These diverse physicochemical properties could be related to the diverse phytochemical classes they belong to and the functional groups in their structures that influence their elution behaviour on GPC.

The early eluted, yellowish and foamy fractions of *Adenia* sp. (run-2) that pooled into ASPA were frothy as long as in water solution. The foamy nature of these fractions or their pool (ASPA) may be due to the presence of phytochemicals known

as saponins (Bernhoft, 2010) with detergent properties due to the presence of both lipophilic (non-sugar) and hydrophilic (sugar) moieties in the same molecule.

In conclusion, chromatogram profiling of Bio-Gel P-2 fractions of *Adenia* sp. revealed that fractions containing V_0 and V_i eluates were less influenced by both sample size and column bed volume compared to *C. ruspolii* extract. In contrast to the latter, *Adenia* sp. water extract is highly foamy; therefore, positive for saponins. Saponins are small molecules with detergent-like properties that form big micelles (i.e. behave like large molecules) in water solution and would be expected to elute early during GPC fractionation using water as eluent. Thus, elution positions of V_0 and V_i in *Adenia* sp. were largely influenced by the physico-chemical properties of its constituents, and as such influences of sample size and column bed volume would be less pronounced. EHI test results and chromatographic characterisation of Bio-Gel P-2 fractions were used to group active fractions into three pools for further bioassay-guided isolation and purification studies (Chapter Seven).

Chapter Seven: Isolation and purification of compounds from pooled active fractions of *C. ruspolii* and *Adenia* sp.

7.1. Abstract

Medicinal plant extracts and fractions are complex mixture of various types of bioactive compounds with a range of polarities. In this study, various chromatographic techniques, marker compounds, staining reagents and solvent systems were employed for profiling of crude extracts, pooled active fractions and purified compounds from these active pools. Paper chromatography, high voltage paper electrophoresis (HVPE), preparative thin layer chromatography (PTLC) and thin layer chromatography (TLC) were used for profiling of constituents of crude extracts, pooled fractions and/or purified compounds. Sephadex LH-20 and reversed phase C₁₈ columns followed by PTLC were sequentially used with the objective of isolation, purification and profiling of constituents from active pooled fractions of *C. ruspolii* and *Adenia* sp. These sequential applications of column chromatography followed by preparative TLC developed in BAW (4:1:1 v/v/v) solvent system resulted in the isolation and purification of three compounds with R_F-values of 0.13, 0.58, and 0.68 from CRPA; one from CRPB, with an R_F-value of 0.73; one from CRPC (a blue fluorescent compound under UV-light at 366 nm with an R_F-value of 0.53) and two compounds from ASPA, with R_F-values of 0.23 and 0.27. The purities of these compounds were examined by TLC as they appeared as single spot. Some of these compounds also showed significant EHI properties (P<0.05) at tested strengths. The level of yellow-stained constituent in the *C. ruspolii* crude extract with molybdate reagent was semi-quantitatively estimated to be ~48 mM. The compound is negatively charged substance with similar ionic mobility as inorganic phosphate under the same condition in HVPE.

7.2. Introduction

Chromatography is the method of choice in handling the problem of isolation and purification of a compound of interest from a complex natural mixture (Józwiak *et al.*, 2007). Chromatographic profiling of bioactive constituents of medicinal plant extracts and fractions is also an integral part of isolation and purification steps. Advances in separation technology have opened up numerous possibilities for the purification and scaling up of bioactive phytochemicals. Plant extracts and fractions usually occur as complex mixture of various types of bioactive compounds with a range of polarities (Jamil *et al.*, 2012). Therefore, various chromatographic techniques and solvent polarities are employed for isolation, purification and profiling of constituents of active fractions and purified compounds (Guiochon, 2001).

Chromatographic isolation and purification on Sephadex LH-20 involve surface adsorption, partition, and size limit modes of purification mechanisms (Praman *et al.*, 2013; Karthika *et al.*, 2014). The surface adsorption purification mechanism depends on differences in polarity between constituents of a sample to be separated. During this process, there is a competition between the constituents of a sample to be purified and the mobile phase (eluent) for adsorption sites of stationary phase. For instance, on polar stationary phase, constituents with low polarity proportionally spend more time in the mobile phase and eluted first than those that are highly polar (i.e. the one that retained longer). As the components move through the sorbent, their relative rates of migration are affected by their individual affinities for the sorbent. Isolation and purification occur when one compound is more strongly adsorbed by the sorbent than the other components. When the sorbent is silica or alumina, polar

natural products move slowly compared to nonpolar ones. Adsorption takes place as a result of the interaction between the compound and groups associated with the sorbent. In the case of silica, which has silanol groups (Figure 7.1.) binding occurs between the compound and free hydroxyls on the sorbent.

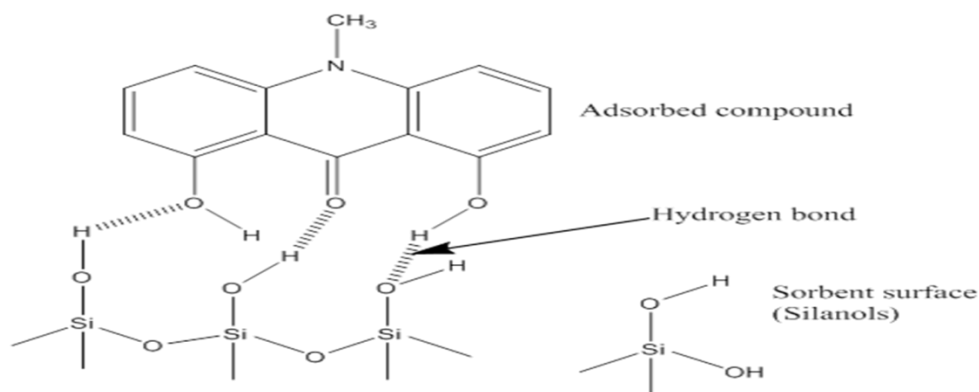


Figure 7.1. Adsorption and hydrogen bonding between compound and silica gel sorbent surface.

In this particular illustration, adsorption involves hydrogen bonding between compound functional groups and adsorbent surface hydroxyl groups. Silica gel is less polar than alumina and is an acidic adsorbent, thus preferentially retaining basic compounds (Tang *et al.*, 2011) whereas alumina is a basic adsorbent, thus preferentially retaining acidic compounds. The choice of mobile phase is equally important because the optimum isolation and purification of targeted constituents are not only dependent on the chosen stationary phase but also dependent on the polarity and order of eluents used.

In partition mode of isolation and purification, constituents of a sample are separated based on their relative solubility in the stationary and mobile phases. In molecular sizing mode, constituents of plant samples are separated according to their size or molecular weight (Choche *et al.*, 2014). The stationary phase consists of a porous

cross-linked polymeric gel with varying size and shape such that large molecules tend to be excluded by the smaller pores and move preferentially with the mobile phase. The degree of cross-linking can be varied to produce beads with a range of pore sizes to fractionate samples over different molecular weight ranges. The stationary phase gels can either be hydrophilic for separations in water or polar solvents, or hydrophobic for use with non-polar or weakly-polar solvents. The smaller molecules are able to diffuse into and out of the smaller pores and will thus be retained longer in the system. The components of a mixture therefore elute in order of decreasing size or molecular weight.

Reversed phase column (such as C₁₈ column) is a non-polar (apolar) stationary phase (Figure 7.2) with the highest affinity for non-polar constituents.

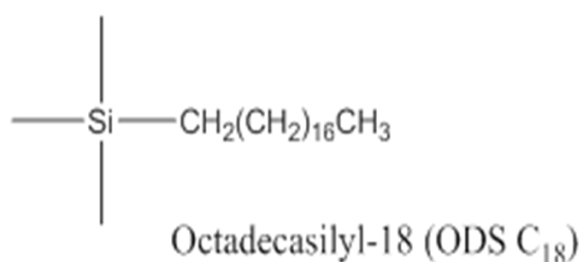


Figure 7.2. Reversed phase C₁₈ (modified silica stationary phase).

Isolation and purification of constituents from target samples on such columns are facilitated by differences in the relative strength of interaction between targeted compounds and a matrix substituted with suitably hydrophobic groups (Çitoğlu and Acıkara, 2012). In this study, therefore, various chromatographic techniques were employed with the objective of separation, isolation, purification and profiling of active constituents from water extracts of both plants, and testing purified components for their EHI activity.

7.3. Materials and methods

In this study, various chromatographic techniques, marker compounds, staining reagents and solvent systems were employed for profiling of crude extracts, pooled active fractions and purified compounds from the active pools. Paper chromatography, high voltage paper electrophoresis, preparative thin layer chromatography (20 cm × 20 cm coated with silica gel 60G with 0.5 and 1 mm thickness with glass backings Merck, Darmstadt, Germany) and TLC were utilized for profiling of constituents of crude extracts, pooled fractions and/or purified compounds. Sephadex LH-20, reversed phase C₁₈ columns followed by PTLC were sequentially utilized with the objective of isolation, purification and profiling of constituents of active compounds from these active pooled fractions of *C. ruspolii* and *Adenia* sp. (See section 2.10). The anthelmintic properties of the resultant ever increasingly purified fractions were tested using the EHI test as detailed before (section 2.5.1.3), during which observations on larval motility were also taken. Resulting EHI data were compared with positive and negative controls, where a synthetic anthelmintic (Zolvix®) was used as positive control.

Paper chromatograms were done using Whatmann No. 1 (57 × 46 cm, Merck, Darmstadt, Germany) for active pooled fractions of both plants using an arbitrary phenolic marker mixture containing ferulic and caffeic acids to assess the presence or absence and nature of fluorescent compound(s) in the active pooled fractions (Chapters Five and Six). The chromatogram was examined under UV-light at UV-366 nm before and after exposure to ammonia vapour.

The ASPC was also loaded onto PC, developed in BAW (4:1:1 v/v/v). The sample loaded region of PC chromatogram was cut into 6 cm × 4 cm bands, washed, and supernatants recovered and then bioassayed for their EHI properties as detailed in 2.5.1.3. This is to assess the suitability of PC for isolation and purification of active pooled fractions.

C. ruspolii crude water extract, and Bio-Gel P-2 active pooled fractions of *C. ruspolii* and *Adenia* species were also separated into bands on preparative TLC plates (20 × 20 cm, coated with silica gel 60G, 0.5 and/or 1 mm thicknesses with glass backings (Merck, Darmstadt, Germany) in n-butanol-acetic acid-water (4:1:1 v/v/v). The fluorescent bands were marked with pencil under UV-light at 366 nm and the remaining non-fluorescent region divided into bands (with 1 cm band width each) and collected separately. The bands were numbered from origin to top. The band recovered from the region above the solvent front was used as negative control. All recovered bands from all pools were bio-assayed for their EHI properties as detailed in section 2.5.1.3.

7.4. Results

7.4.1. Paper chromatographic profiling of pooled active fractions

The paper chromatogram of active pooled fractions of *C. ruspolii* and *Adenia* sp. and an arbitrary phenolic marker mixture containing ferulic and caffeic acids is shown in Figure 7.3. This experiment was conducted to assess the presence or absence of fluorescent compound(s) in active pooled fractions of both plants.

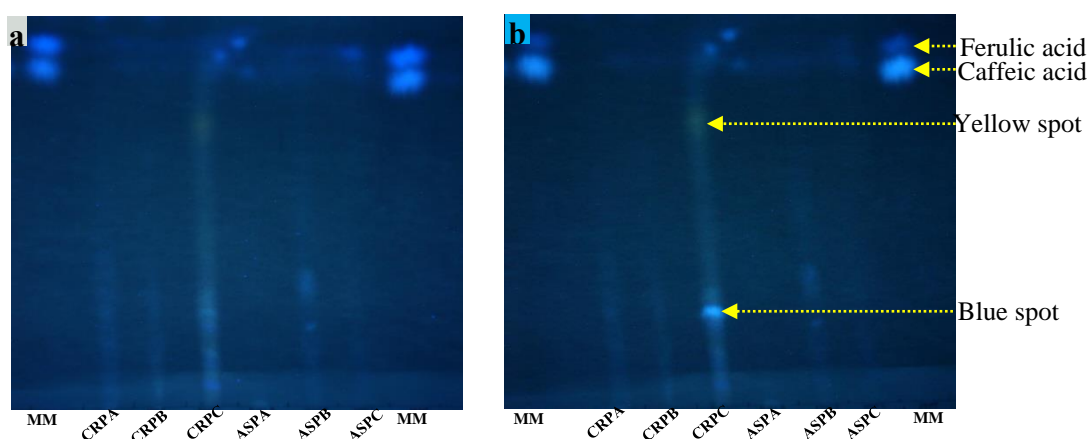


Figure 7.3. Paper chromatogram of active pooled fractions of *C. ruspolii* and *Adenia* sp. Marker mixture contained caffeic and ferulic acids. Chromatogram under UV-light at 366 nm before exposed to ammonia vapour (a) and after being exposed to ammonia vapour (b). Blue and yellow spots are fluorescent compounds in CRPC.

Figure 7.3 showed that only CRPC contained fluorescent compounds under UV-light at 366 nm. This pool contained two major fluorescent compounds, fluorescing blue and yellow with R_F -values of 0.24 and 0.71 respectively. The blue fluorescing spot migrates much slower than marker mixtures, as ferulic and caffeic acids had R_F -values of 0.88 and 0.82, respectively. Moreover, this blue fluorescent spot in CRPC became bright blue and had similar colour and colour intensity to caffeic acid upon fumigating with ammonia vapour.

PC chromatogram was also developed for ASPC. This experiment was designed to assess PC as a suitable preparative chromatographic technique to separate constituents of the active pooled fractions. The EHI properties of bands recovered from paper chromatograms of ASPC are shown in Figure 7.4.

Of the eleven supernatants (run-1) tested for their EHI properties, only two of them showed EHI activities compared to controls (Figure 7.4a). Fraction-0 (the fraction recovered from the first band that included 2 cm above and below the origin) showed greater than 90% EHI while fraction-1 (band-2) also showed less than 20% EHI activity as shown in Figure 7.4a. In the repeated experiment of ASPC isolation on PC followed by EHI tests of recovered supernatants, only the first two bands showed similar EHI properties as in the first run (Figure 7.4b).

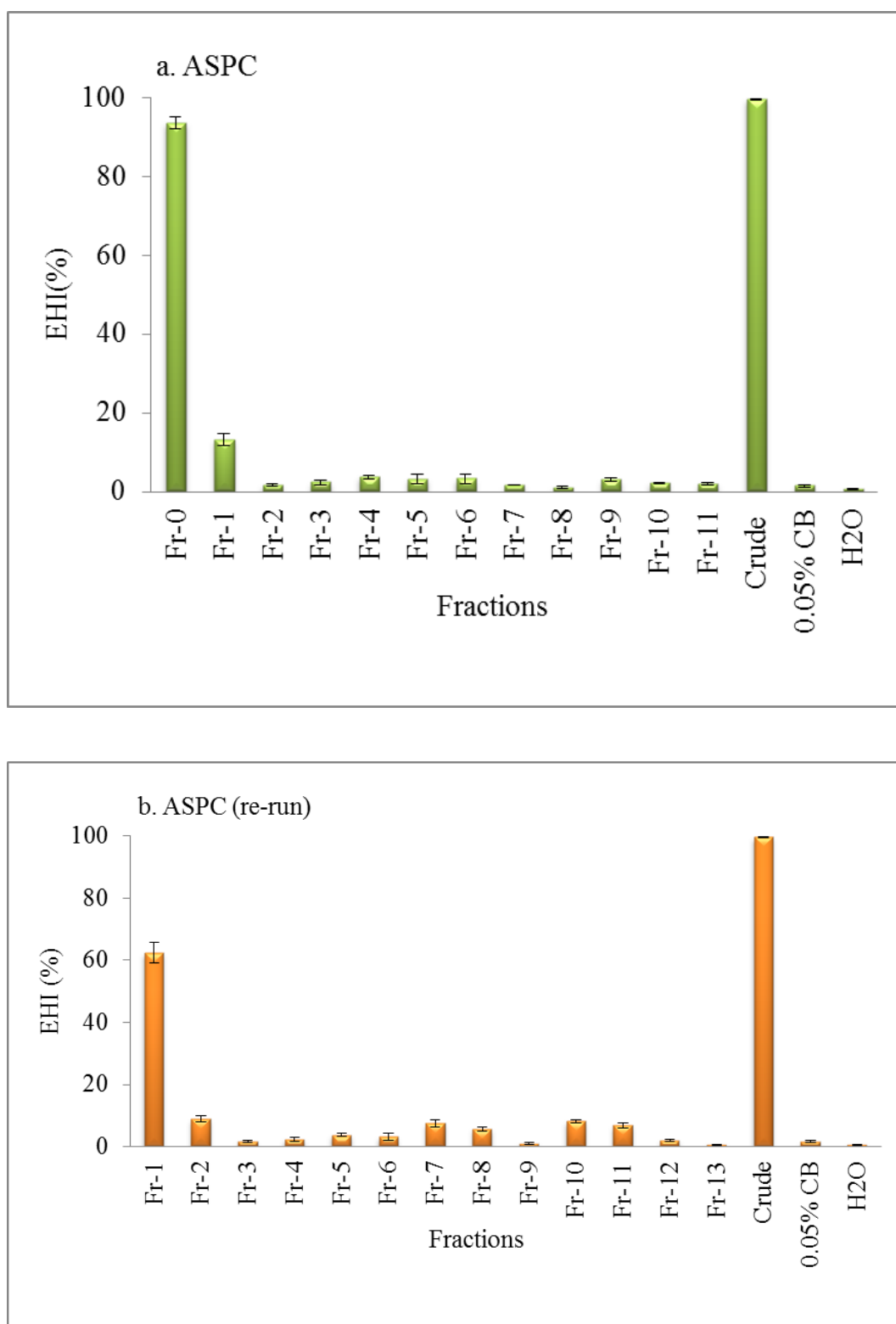


Figure 7.4. EHI of ASPC fractions eluted from paper chromatogram. First run (a) and repeated experiment (b).

7.4.2. PTLC isolation and TLC profiling of *C. ruspolii* extract

The PTLC separated bands of *C. ruspolii* water crude extract examined under UV-light and TLC chromatograms of recovered bands examined under UV-light and after stained with molybdate are shown in Figure 7.5.

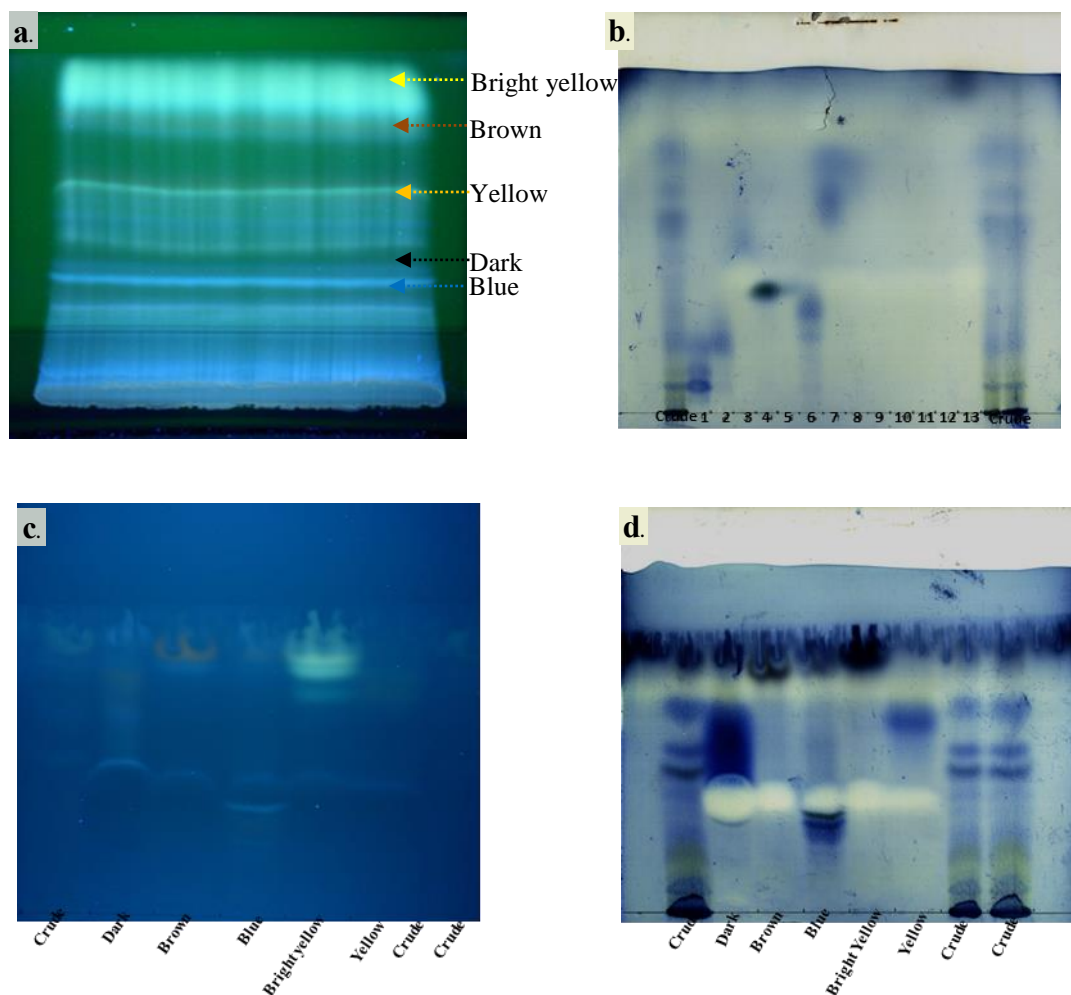


Figure 7.5. PTLC and TLC chromatograms of *C. ruspolii* extract and recovered bands. PTLC of crude extract at 366 nm (a) molybdate stained recovered bands (b) recovered fluorescent bands at 366 nm (c) molybdate stained fluorescent bands (d).

An attempt to isolate constituents of *C. ruspolii* water extract on PTLC resulted in the recovery of five UV-active major compounds at 366 nm (Figure 7.5a). These partially purified fluorescent bands were labelled from bottom to top as blue, dark,

yellow, brown and bright yellow with R_F -values of 0.33, 0.4, 0.6, 0.8 and 0.93, respectively. The chromatogram of fluorescent and non-fluorescent bands of partially purified fractions of *C. ruspolii* extract that stained with molybdate are shown in Figure 7.5b. The molybdate stained chromatogram of these fractions showed that fractions 1-7 and 13 contained constituents that stained blue with molybdate. However, the major blue fluorescent (band-6) stained deep blue green with molybdate reagent as shown in Figure 7.5b. During TLC re-run, the blue fluorescent compound at 366 nm (Figure 7.5c) was again stained blue green with molybdate (Figure 7.5d).

7.4.3. *C. ruspolii* extract purification on C_{18} column

The chromatograms examined under UV-light at 254 nm and 366 nm and then stained with molybdate reagent are shown in Figure 7.6. In this isolation and purification trial experiment, two blue fluorescent compounds were detected on TLC chromatogram at UV-366 nm (Figure 7.6). The first blue fluorescent with R_F -value of 0.47 was eluted in deionized water whereas the second blue fluorescent with R_F -value of 0.73 was eluted in 60% MeOH eluent (Figure 7.6a). The blue fluorescent that eluted in deionized water was stained blue green with molybdate while the second blue fluorescent that eluted in 60% MeOH did not stain. Moreover, the slowest migrating and dark blue stained spot with molybdate with R_F -value of 0.13 was eluted in 20% MeOH. Constituents of *C. ruspolii* water extract were largely eluted in deionized water except the two compounds that eluted in 20% and 60% MeOH (Figure 7.6). However, the constituent of the extract that stains yellow with molybdate did not elute into any fraction collected (Figure 7.6d).

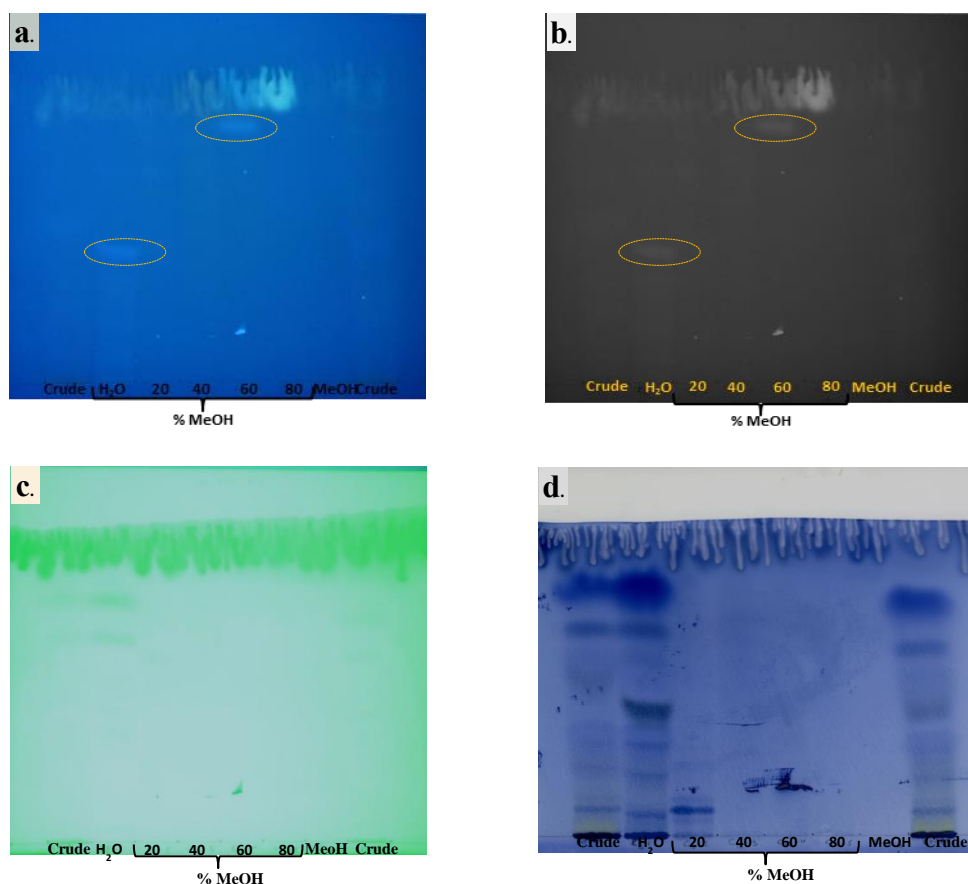


Figure 7.6. Chromatograms of C₁₈ fractions of *C. ruspolii* crude extract. Under UV-light at 366 nm (a) 366 nm BW (b) 254 nm (c) after molybdate stained (d). The 20, 40, 60 and 80 show percentages of methanol in the gradient eluents used.

7.4.4. PTLC profiling of CRPC

PTLC isolation and profiling of blue and yellow fluorescent constituents of CRPC under UV-light at 366 nm was done on PTLC plates with glass backings under similar conditions but different in sample size loaded and PTLC thickness used. The first purification was done by loading 2 ml on to PTLC plate with 1 mm thickness (Figure 7.7a) and the second run done by loading 1 ml onto PTLC plate with 0.5 mm thickness (Figure 7.7b). The band labelled as fraction-6 on the first preparative chromatogram (Figure 7.7a) and the blue band on the second preparative chromatogram (Figure 7.7b) are the same compound. Similarly, the band labelled as

fraction-10 on first preparative chromatogram is also corresponding to the yellow fluorescent spot on the second preparative chromatogram.

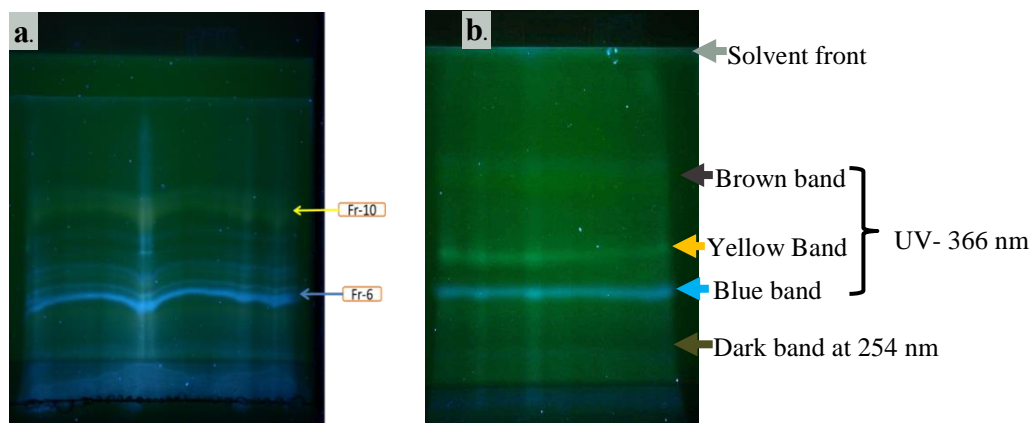
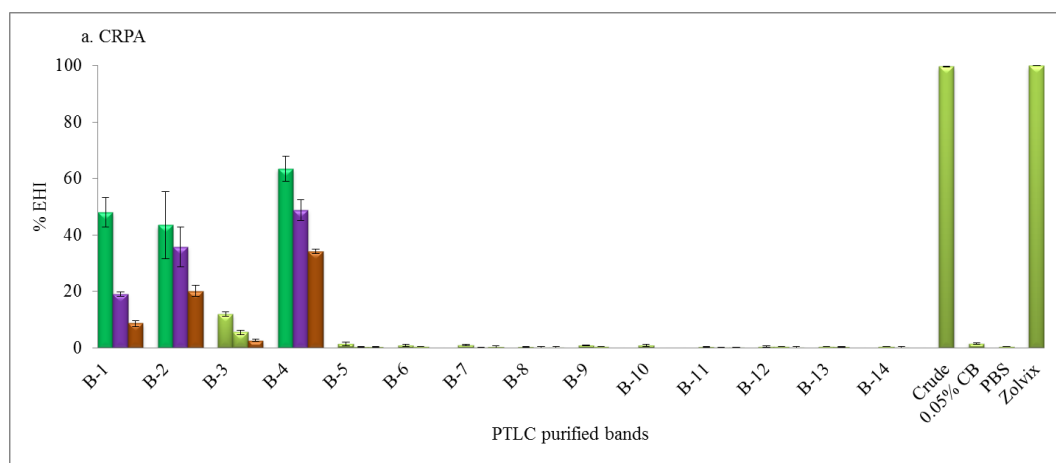
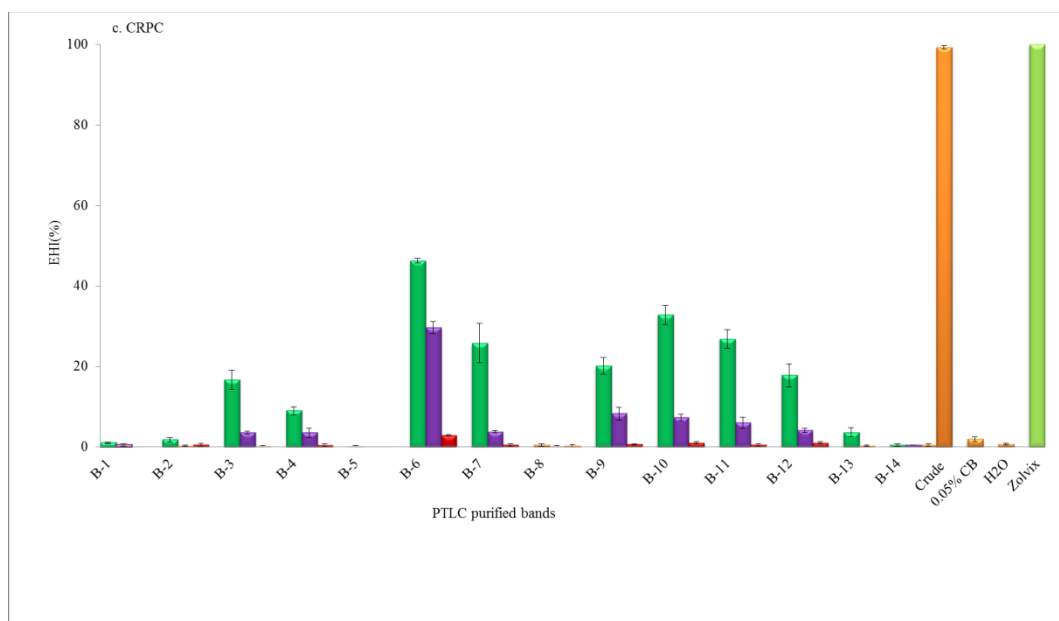
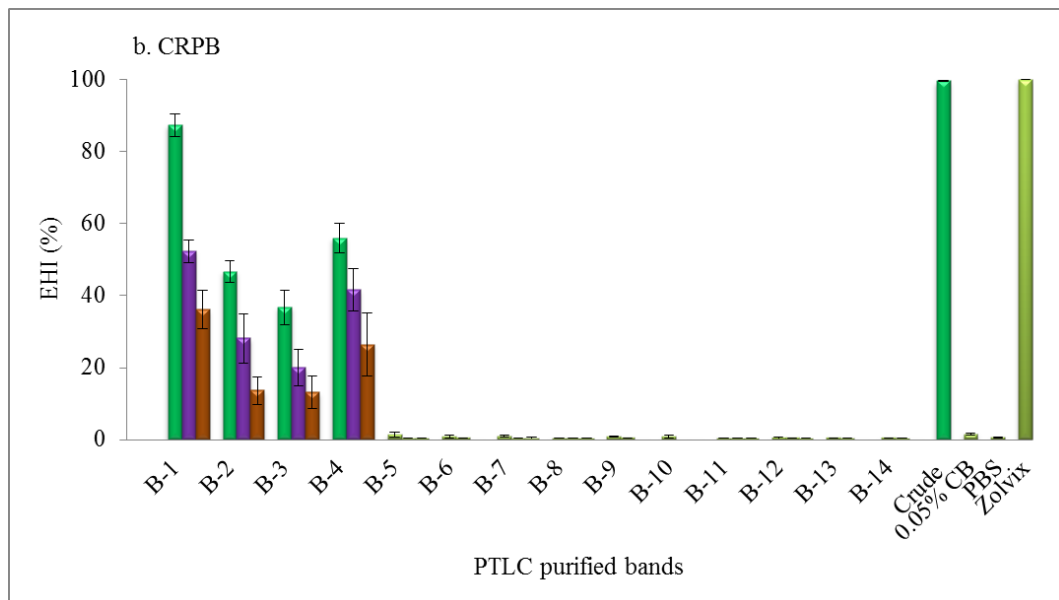


Figure 7.7. PTLCs of CRPC examined under UV-light at 366 nm. PTLC thickness 1 mm (a) and 0.5 mm (b). Fr-6 (a) corresponds to blue band (b) and Fr-10 (a) corresponds to yellow band (b).

7.4.5. EHI tests of partially purified bands on PTLC from active pooled fractions of *C. ruspolii*

Bio-Gel P-2 pooled active fractions of *C. ruspolii* were attempted to be purified on PTLCs (1 mm thick) with glass backings. The EHI tests and pH of CRPC water fractions are shown in Figure 7.8.





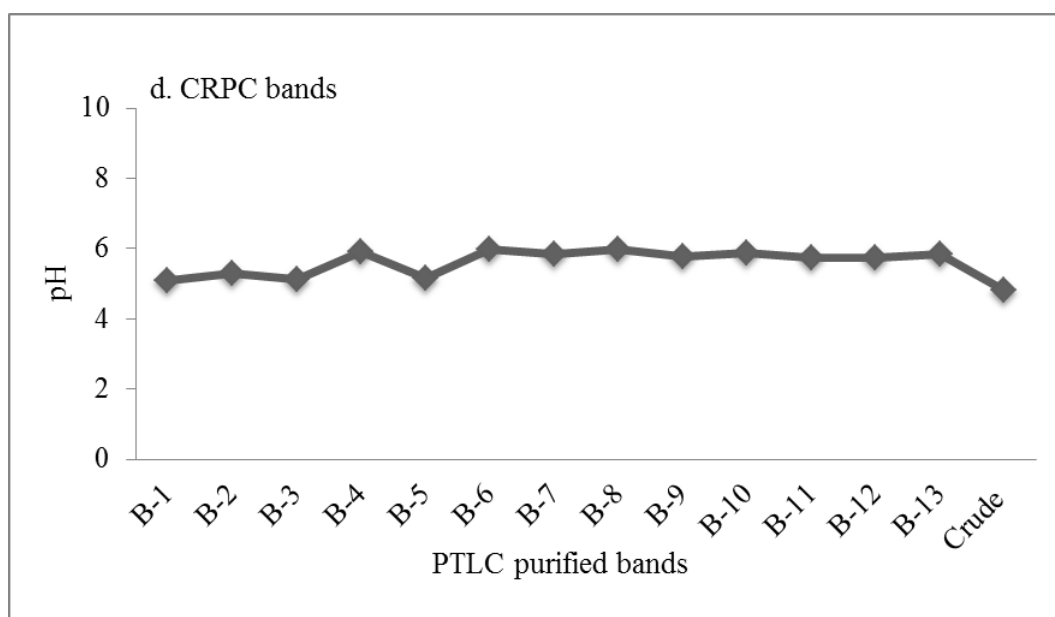


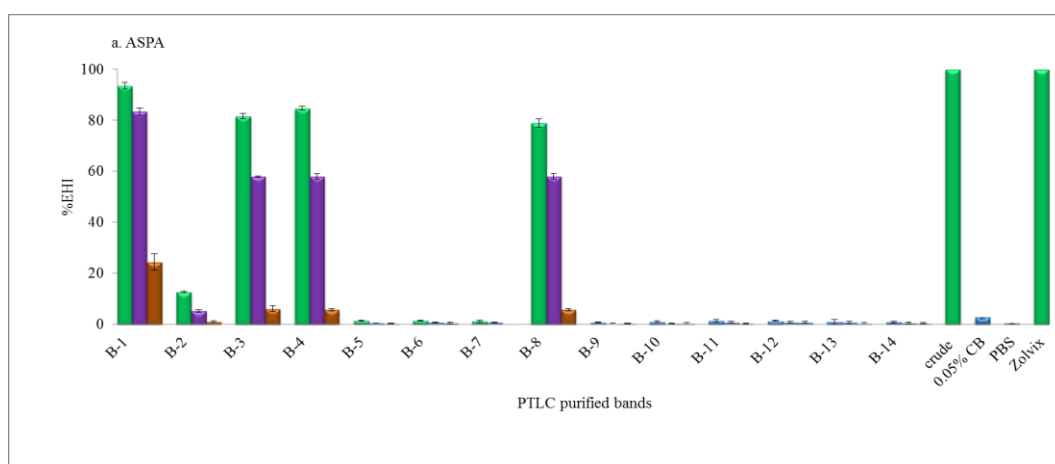
Figure 7.8. EHI of PTLC purified bands from active pooled fractions of *C. ruspolii*: CRPA (a), CRPB (b), CRPC (c) and pH of the recovered bands from CRPC (d). The band above the solvent front (Band-14) was used as negative control and crude extract as positive control. EHI tests of *C. ruspolii* (run-2) supernatants. At full (■), 0.5 (■), 0.25 (■), 0.125 (■) strengths. *C. ruspolii* crude and zolvix (positive control); chlorobutanol (0.05% w/v) and PBS as negative control.

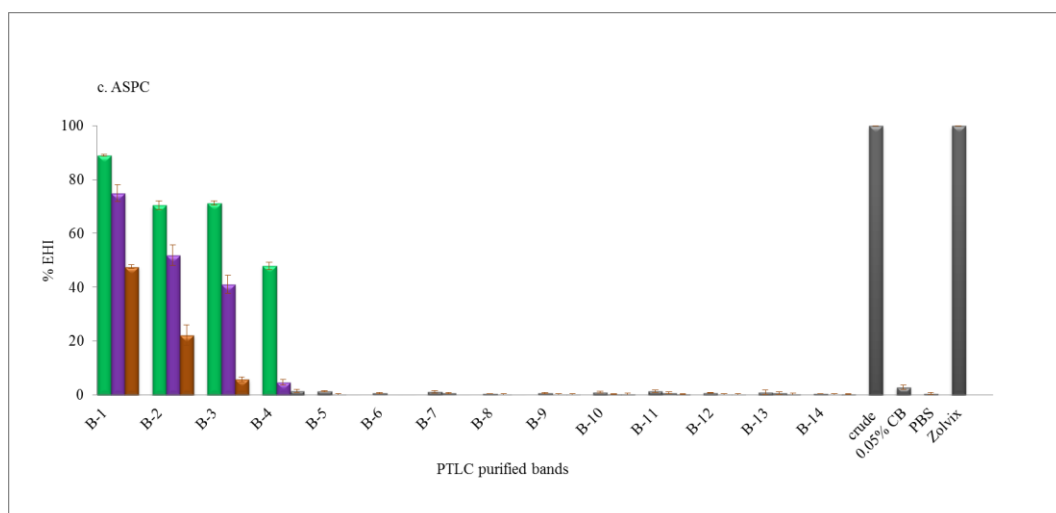
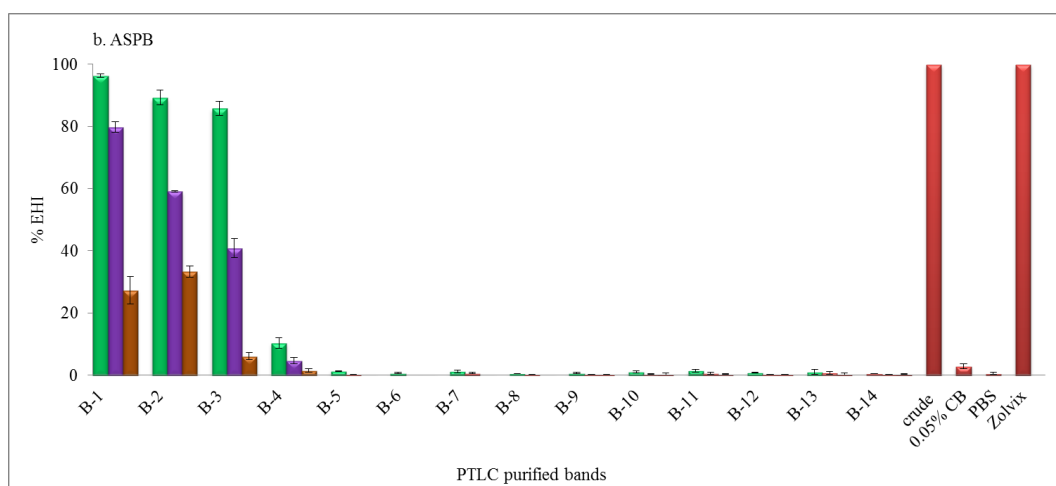
Supernatants of bands 1, 2 and 4 from CRPA (Figure 7.8a) and 1-4 from CRPB (Figure 7.8b) showed significant ($P < 0.05$) EHI as well as larval paralysis or death at full strength compared to controls. For CRPC, supernatants of bands 6, 7, 10 and 11 were also showed modest EHI activities (Figure 7.8c). In particular, the blue (fraction-6) and yellow (fraction-10) fluorescent components of this pool showed both EHI and subjectively observed LMI properties. In those fractions with LMI properties, the first stage larvae were stretched and did not move. This effect was seen after 24 h incubation with plant extracts. Upon further incubation for another 24 h, no larvae showed any motility and remained stretched. The pH of water crude extract and supernatants of bands recovered from CRPC on PTLC was determined to see the effect of constituents of these supernatants on the pH of the incubation

medium that might cause parasite egg hatch inhibition (Figure 7.8d). All supernatants and *C. ruspolii* water crude extract had pH greater than 4.

7.4.6. EHI tests of partially purified bands from active fractions of *Adenia* sp.

In this experiment, thirteen sample bands and one blank band per pool were tested for their anti-parasitic properties *in vitro*. As seen in *C. ruspolii*, some PTLC purified bands from active pooled fractions of *Adenia* sp. also showed dose dependent EHI and LMI properties (Figure 7.9). Of the PTLC purified bands of ASPA, fractions 1, 3, 4 and 8 showed greater than 70% EHI at full strengths (Figure 7.9a). Their serially diluted lower strengths also exhibited low to moderate egg hatch inhibition activities. For ASPB and ASPC, PTLC purified bands 1-3 exhibited greater than 70% EHI activities at full strengths compared to controls (Figure 7.9b, c). The serially diluted lower strengths also showed dose dependent EHI activity.





d. Eggs incubated with purified bands

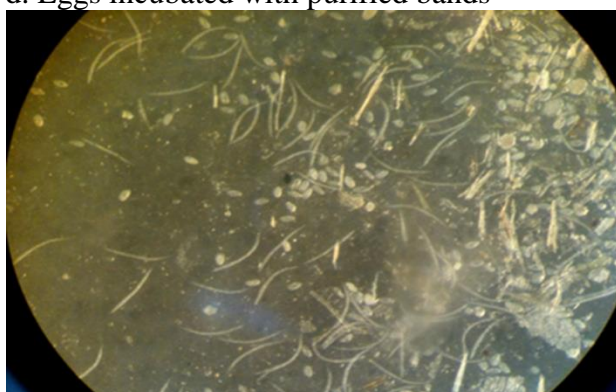


Figure 7.9. EHI tests of PTLC purified bands of active pooled fractions of *Adenia* sp. ASPA (a), ASPB (b), ASPC (c) and egg suspension incubated with recovered supernatant (d). At full (■), 0.5 (■), 0.25 (■), 0.125 (■) strengths. *Adenia* sp. crude and zolvix (positive control); chlorobutanol (0.05% w/v) and PBS as negative control.

7.4.7. Isolation of constituents of *C. ruspolii* active fractions and their EHI tests

7.4.7.1. Isolation and purification of CRPA constituents on Sephadex LH-20 column chromatography

In this experiment, the first Bio-Gel P-2 pooled fraction of *C. ruspolii* (CRPA) was fractionated on Sephadex LH-20 to isolate and purify its constituents by step-wise elution method as described in section 2.10.1. Of the eighty fractions collected, the first 30 fractions were water fractions, as switching of eluent from de-ionized water to 20% MeOH was done after 30 fractions had been collected. The vanillin stained TLC chromatogram showed that all constituents of this pool eluted in water fractions 13-22 (Figure 7.10). The relatively fast migrating constituent that stained green with vanillin reagent having R_F -value of 0.60 (spot C) was predominantly partitioned into fractions 13 and 14 although very small amount of that also partitioned into fraction-15. In similar manner, the relatively slow migrating constituent that stained green with vanillin reagent having R_F -value of 0.47 (spot B) was largely partitioned into fraction-16 although a small amount partitioned into fraction-17. Fractions 19 and 20 were mainly rich in pure and the slowest migrating constituent that stained brown with vanillin having R_F -value of 0.13 (spot A). The fastest migrating constituent (spot D) that stained pink with vanillin reagent having R_F -value of 0.80 was partitioned into fraction-22. Neither of constituents of this pool partitioned into MeOH gradient eluents (20, 40, 60 and 80%) nor into absolute MeOH. The isolation and purification of CRPA on Sephadex LH-20 resulted in the purification of at least three compounds; (1) the fastest migrating compound that stained pink with vanillin reagent having R_F -value of 0.80 and partitioned into fraction 22; (2) the second fastest migrating compound that stained green with vanillin reagent with R_F -value of

0.60 and partitioned into fractions 13 and 14; and (3) the slowest migrating compound that stained brown with R_F -value of 0.13 and predominantly partitioned into fractions 19 and 20 (Figure 7.10).

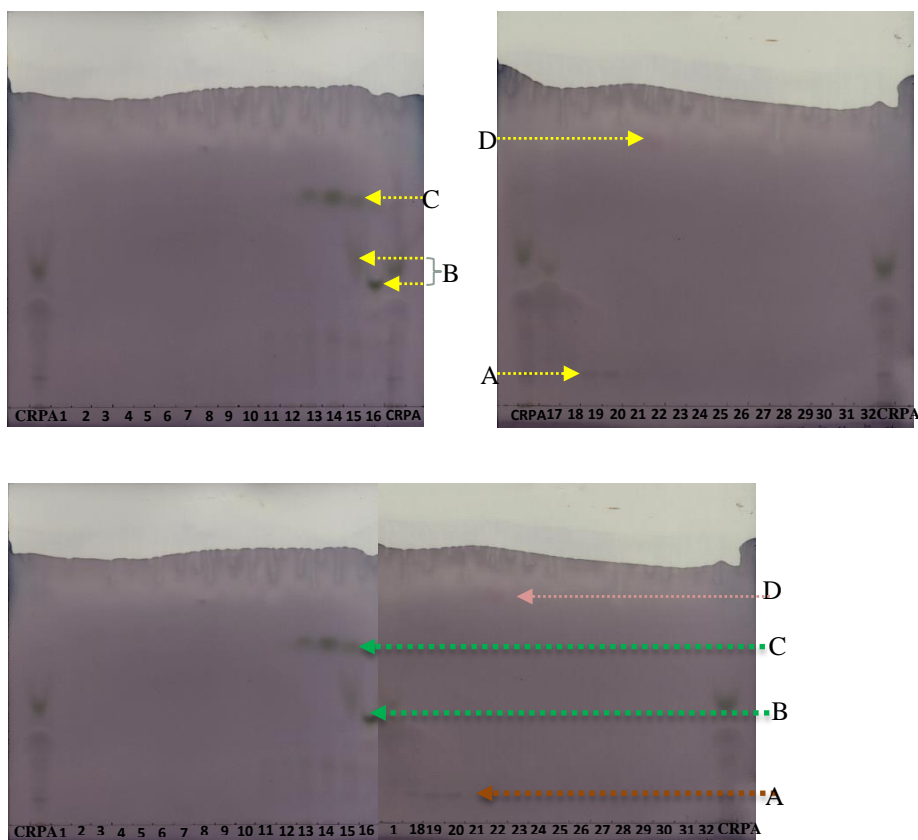


Figure 7.10. Vanillin stained chromatograms of Sephadex LH-20 water fractions from CRPA. A, B, C and D are separated spots.

To re-check the purity of the aforementioned compounds, TLC re-run was done for Sephadex LH-20 fractions (13-20) using CRPA (as marker) at full and their serially diluted lower strengths under the same chromatographic conditions as shown in Figure 7.11.

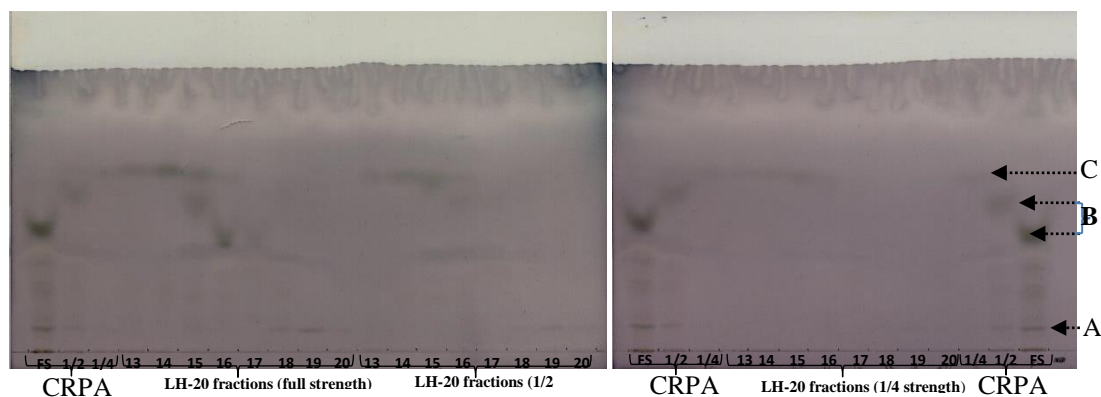


Figure 7.11. Vanillin stained chromatogram of Sephadex LH-20 fractions from CRPA. CRPA used as marker at full and diluted lower strengths. A, B and C are separated spots.

The TLC re-run for Sephadex LH-20 purified fractions and CRPA at full and their serially diluted lower strengths under the same chromatographic conditions resulted in almost the same chromatogram profiles and R_F -values for isolated and purified compound(s) in each fraction. However, the R_F -values of separated constituents of the marker were dependent on the strength of the CRPA loaded (i.e. R_F -values of separated spots decreased with increased strengths of CRPA loaded). The very close migrating constituents of CRPA that stained green with vanillin reagent (spot B and C) were seen as one compound on TLC at full strength. On the other hand, these compounds had different R_F -values in Sephadex LH-20 fractions 15 and 16 as seen in Figure 7.11.

7.4.7.2. Further purification of fractions 13-20 from CRPA on RP C_{18} column

Sephadex LH-20 purified fractions 13-20 from CRPA were loaded separately onto C_{18} columns that were primed with absolute methanol followed by deionized water. The same eluents and elution order used in Sephadex LH-20 were also used in this experiment as described in section 2.10.2 including 10% MeOH. For deionized water

and 10 and 20% MeOH eluents, five sub-fractions (1 ml each) and for the remaining eluents (5 ml each) were collected. However, chromatogram was developed only for the first three eluents fractions, i.e. deionized water, 10 and 20% MeOH. The chromatogram profiles of the three solvent systems are shown in the Figure 7.12.

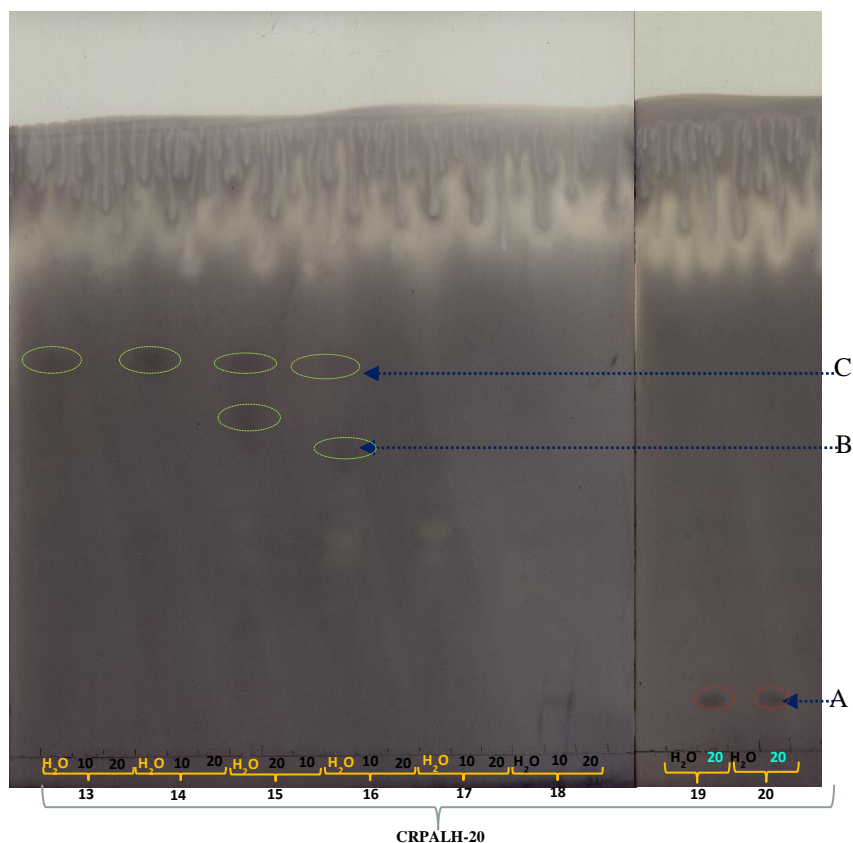


Figure 7.12. Vanillin stained chromatogram of C_{18} purified fractions from CRPA. Chromatogram heated at 120°C for 3 h. 10 and 20 show 10% and 20% MeOH fractions. H_2O stands for water fractions. A, B, C are separated spots. The numbers 13-20 are Sephadex LH-20 water fractions of CRPA.

In an attempt to further purify the Sephadex LH-20 fractions on C_{18} column, constituents of fractions 13-18 were again eluted in deionized water. However, the Sephadex LH-20 water fractions 19 and 20 (Figure 7.11) now eluted in 20% MeOH upon further purification on C_{18} column (Figure 7.12). To double check the purity of the aforementioned fractions, a TLC re-run was done for all five water sub-fractions and pooled fractions of 10 and 20% MeOH under the same chromatographic

conditions. The re-run and vanillin reagent stained chromatogram of C₁₈ fractions 13-17 revealed that fractions 13 and 14 had contained the same compound with R_F-value of 0.68 that stained green with vanillin reagent (Figure 7.13). Fractions 15 and 16 did contain two very close migrating compounds that stained green with vanillin reagent with R_F-values of 0.58 and 0.68 respectively. Fraction 17 also contained only a small amount of the relatively slow migrating compound with R_F-value of 0.58.

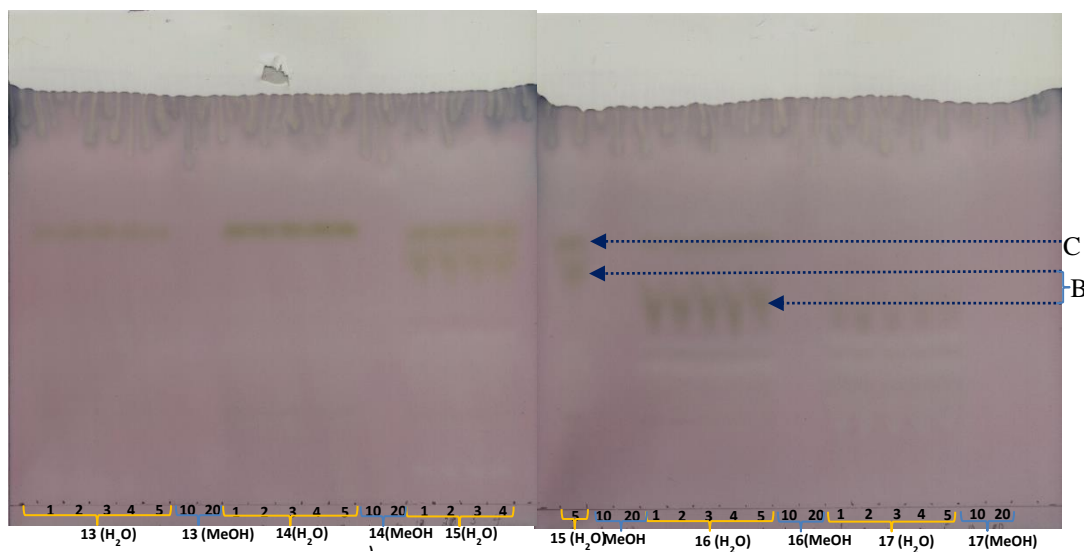


Figure 7.13. Vanillin stained chromatogram of C₁₈ water sub-fractions (1-5) and 10 and 20% MeOH gradient pooled fractions from CRPA. A, B, C are separated spots.

7.4.7.3. Further purification of C₁₈ water fractions of CRPA on PTLC

PTLC purifications of C₁₈ water fractions 14, 16 and 17 were done using washed and dried non-fluorescent chromatograms as described in section 2.10.3.2. The PTLC developments were done twice under the same chromatographic conditions to achieve maximum band separations. Strips (2 cm) of dried PTLC plates were cut-off from one side, stained with vanillin reagent and heat activated in oven to enhance reaction(s) between staining reagent used and purified bands. These vanillin stained spots detected on the PTLC strips were used to locate (mark) the position(s) of

separated bands and to number them from bottom to top. As seen in Figure 7.14, one band from fraction-14, five bands from fraction-16, and three bands from fraction-17 were detected and numbered on PTLC using their respective vanillin reagent stained PTLC strips. The bands were scraped off the PTLC plates separately and mixed with deionized water to completely wash the compounds off the silica gel. Then, the mixture was centrifuged at $2057 \times g$ for 35 min. to completely sediment any insoluble particulates from the coating material and to recover pure and water soluble compound as supernatant from each band. The PTLC strips also revealed that fraction 14 (B-1) and fraction 16 (B-5) had the same R_F -value. This was the fast migrating compound that stains green with vanillin reagent with R_F -value of 0.68 (in one run only) during C_{18} purification. Similarly, vanillin stained PTLC strips of fractions 16 and 17 shown that B-4 from fraction 16 and B-3 from fraction 17 are slightly slow migrating that also stains green with vanillin reagent with R_F -value of 0.58 and hence bands (B-4 and B-3) from fractions 16 and 17 respectively could also be the same compound (Figure 7.14).

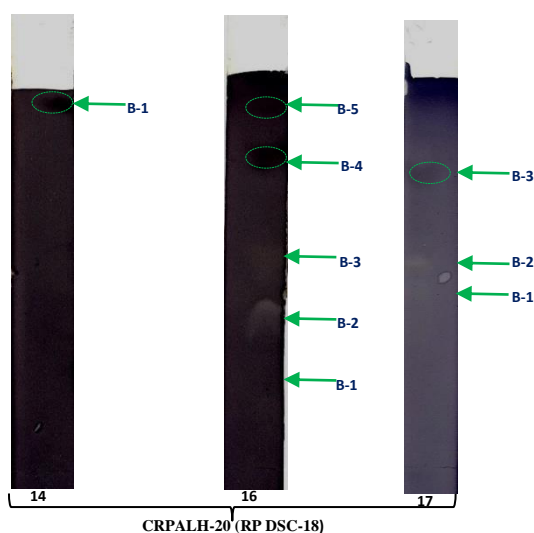


Figure 7.14. PTLC strips of C_{18} water fractions of CRPA. B-1 to B-5 show separated bands of fractions. The numbers 14, 16, and 17 are Sephadex LH-20 fractions.

Chromatograms were also developed for recovered water supernatants after centrifugation (Figure 7.15) to check the recovery of purified compounds from bands and their degree of purity. These chromatograms were also used to confirm whether all the marked bands on plates using strips were real compounds or artefacts.

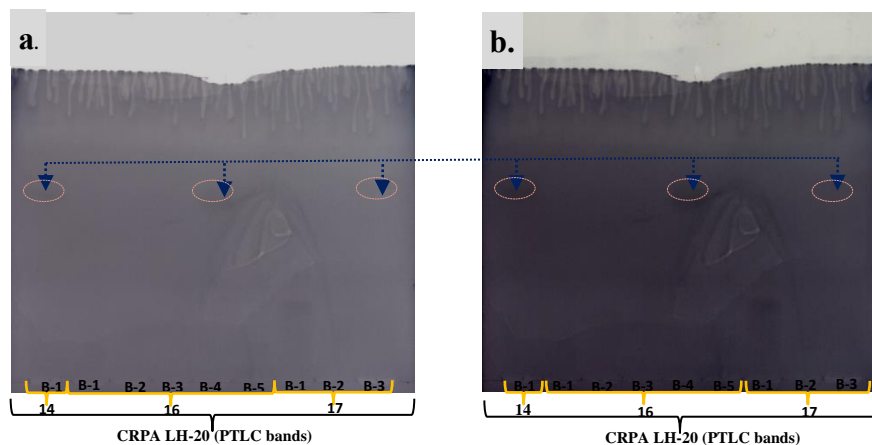


Figure 7.15. Vanillin stained chromatograms of supernatants recovered from PTLC purified bands from ASPA Sephadex LH-20 water fractions 14, 16 and 17. Arrows show spots of purified compounds. Chromatogram heated in oven at 120°C for 30 min. (a) and 3 h (b). Arrows and circles show purified compounds.

The final TLC run for supernatants of recovered compounds from PTLC purified bands showed that only B-1 from 14, B-4 and B-5 from 16 and B-1 and B-3 from 17 were found to be well stained with vanillin reagent (Figure 7.15). These PTLC purified bands (B-1 and B-5) from C₁₈ fractions 14 and 16 respectively had the same colour and R_F value. Similarly, those purified bands (B-4 and B-3) from C₁₈ water fractions 16 and 17 respectively also had the same colour and R_F-value (Figure 7.15).

7.4.7.4. The EHI tests of purified compounds from CRPA

The EHI tests for crude extract, CRPA, C₁₈ fraction and PTLC purified compounds from C₁₈ water fractions 14, 16 and 17 were tested as indicated in section 2.5.1.3 using both negative and positive controls. The EHI results showed that all tested samples exhibited some EHI properties compared to controls (Figure 7.16).

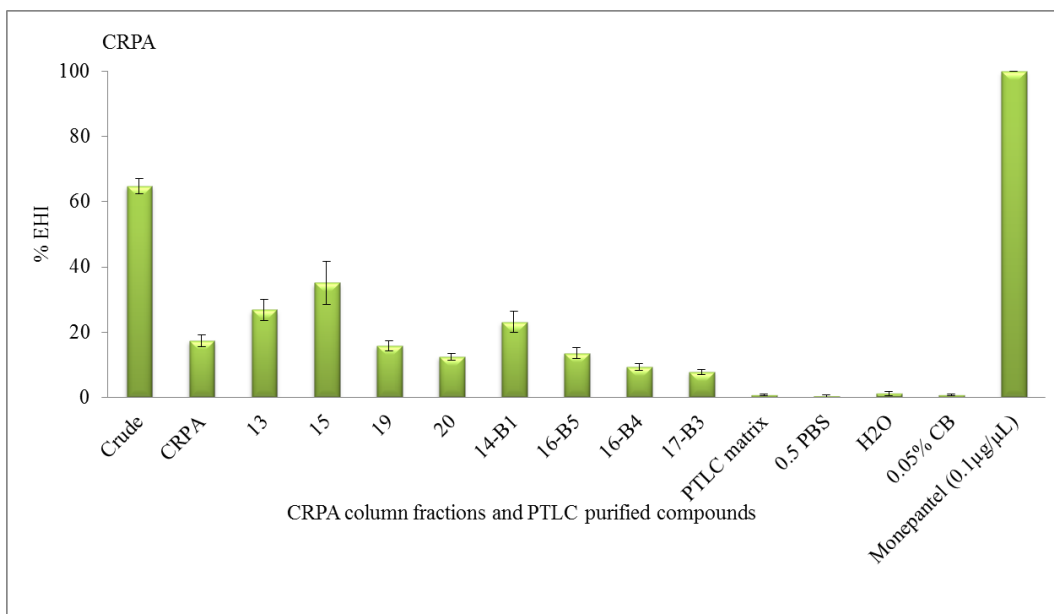


Figure 7.16. EHI of PTLC purified compounds from CRPA and controls. PTLC matrix (band above the solvent front), 0.5PBS, H₂O and 0.05% chlorobutanol are negative controls; monepantel, crude, CRPA and water fractions of LH-20 and C₁₈ fractions are positive controls. B₁, B₃, B₄ and B₅ are purified bands from LH-20 water fractions 14, 16 and 17.

7.4.8. Isolation of constituents from CRPB and their EHI tests

7.4.8.1. Isolation and purification of CRPB (Run-4) on Sephadex LH-20

As described in section 2.10.1, water pooled fraction of CRPB was also isolated on Sephadex LH-20 based on their physicochemical properties. Of the eighty fractions collected, the first 30 fractions were water fractions. The molybdate stained chromatogram of Sephadex LH-20 fractions of this pool revealed that most of its constituents were partitioned into water fractions (15-22) except the one that eluted lately in methanol gradient eluent (Figure 7.17). Of the constituents eluted in deionized water, three major constituents were detected on molybdate stained chromatogram. These are the most polar, slow migrating, tailed yellow spot with R_F-value of 0.07 (spot A); moderately polar, slightly concentrated blue stained spot with

R_F -value of 0.60 (spot B); relatively less polar, fast migrating and concentrated blue spot with R_F -value of 0.67 (spot C). This pool also contained other minor constituents that stained blue with molybdate reagent. The relatively fast migrating and concentrated blue stained spot with R_F -value of 0.67 was predominantly partitioned into fractions 17 and 18, however, very little of it also partitioned into fraction-16. In similar manner, slow migrating, tailed and yellow stained spot with R_F -value of 0.07 was also largely partitioned into fractions 16 and 17 with a small amount of it partitioning into fraction-15. Fractions 19-21 were predominantly rich in the second major constituent in the pool with moderately polar, slightly concentrated blue stained spot.

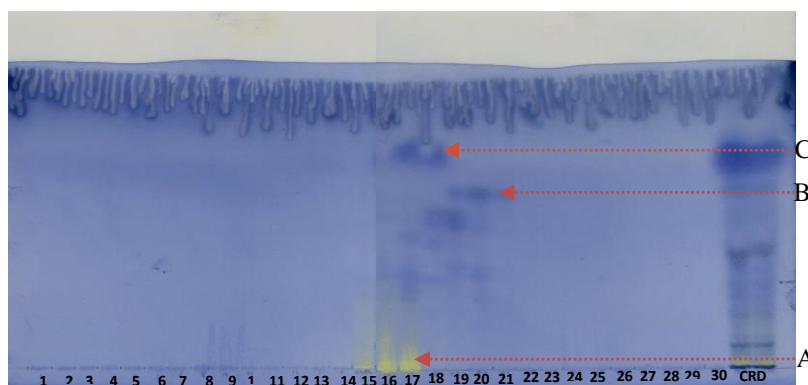


Figure 7.17. Molybdate stained chromatogram of Sephadex LH-20 water fractions from CRPB and crude extract (CRD) as marker. A, B, C show major separated spots of CRPB.

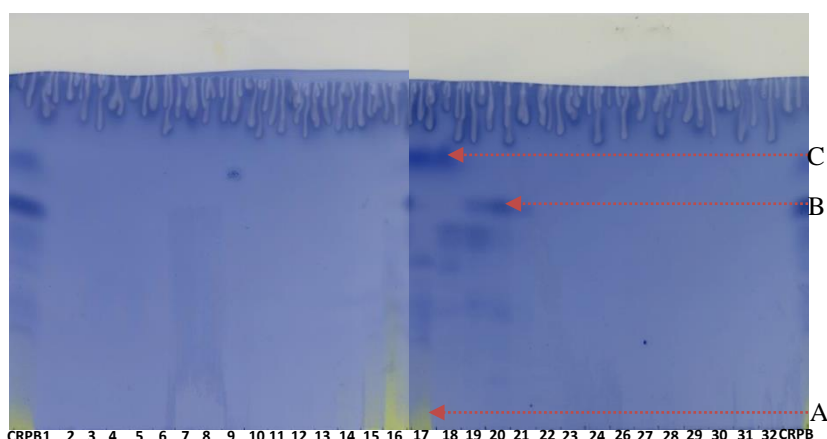


Figure 7.18. Molybdate stained chromatogram of Sephadex LH-20 water fractions from CRPB (re-run) and CRPB as marker. A, B, C are major separated spots.

The pH of Sephadex LH-20 water fractions of CRPB was also determined to check the acidity or alkalinity properties of constituents. In this experiment, the pH of both Sephadex LH-20 water fractions and crude extract was greater than 4 as shown in Figure 7.19.

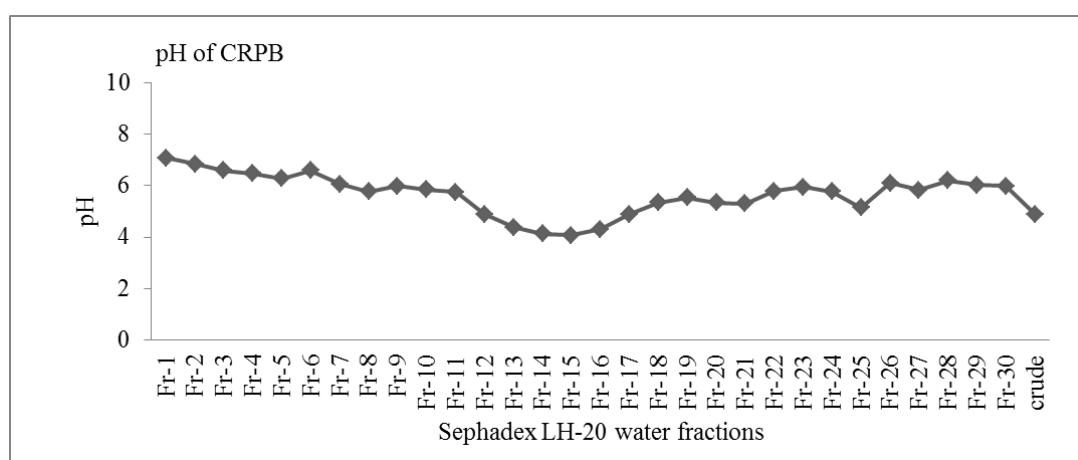


Figure 7.19. The pH of Sephadex LH-20 water fractions of CRPB.

The highest pH value 7.01 and the lowest pH value 4.07 were determined for fractions 1 and 15 respectively. The lowest pH value region was determined for fractions 13 to 16.

Fractions containing analytes were identified from the molybdate stained chromatograms. The EHI tests were done for Sephadex LH-20 fractions 15 to 22 separately and 56 to 58 as a pool with both negative and positive controls (Figure 7.20). The Sephadex LH-20 fractions (15-22) contained constituents that stain with molybdate and fractions 56-58 appeared as smear in the region very close to the origin (run-1) as shown in Figure 7.21a.

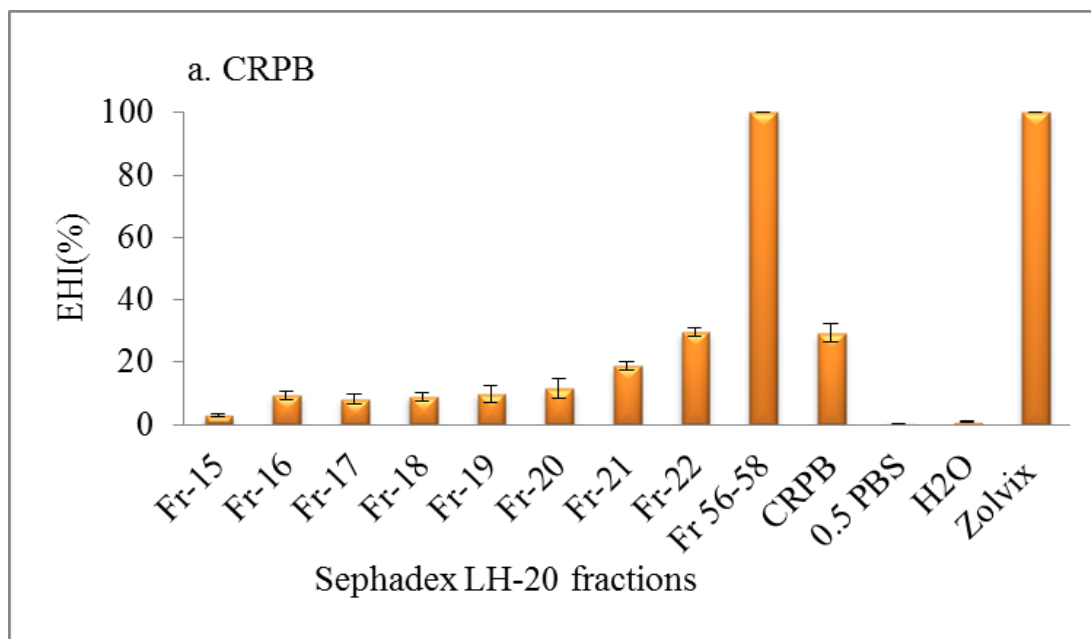


Figure 7.20. EHI of Sephadex LH-20 fractions of CRPB and controls. De-ionized water and 0.5PBS (negative controls) and CRPB and Zolvix (positive controls).

Sephadex LH-20 pooled fraction (56-58) at 100 μ l showed 100% EHI activity. CRPB and Sephadex LH-20 water fractions 21 and 22 showed only about 20% EHI activities at the same sample strength. However, the remaining fractions also showed very low EHI activities (Figure 7.20). The EHI test of smeared fractions (Figure 7.21a.) was found to be very significant, chromatogram re-run was done under the same chromatographic conditions and stained with molybdate reagent again (Figure 7.21b).

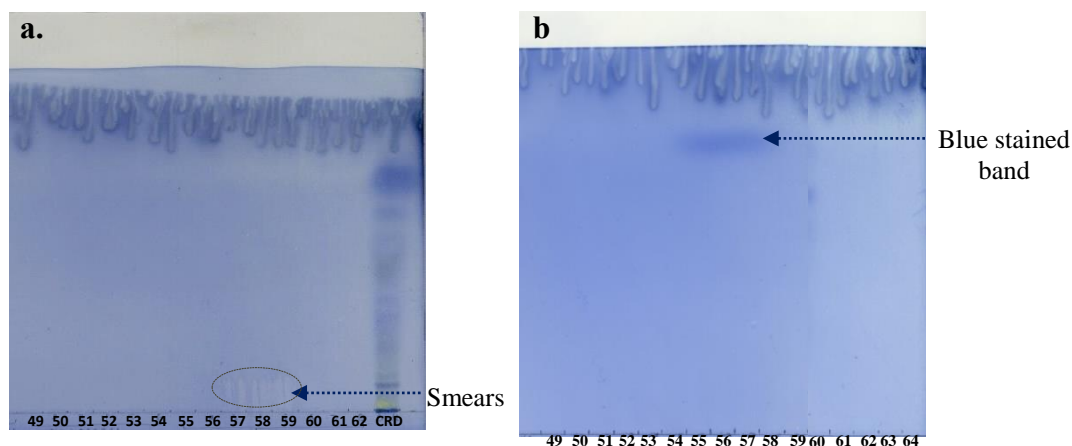


Figure 7.21. Molybdate stained chromatograms of Sephadex LH-20 fractions (49-64) from CRPB. First run (a), re-run (b). Arrows show smears (a) and blue stained (b) in fractions (56-58).

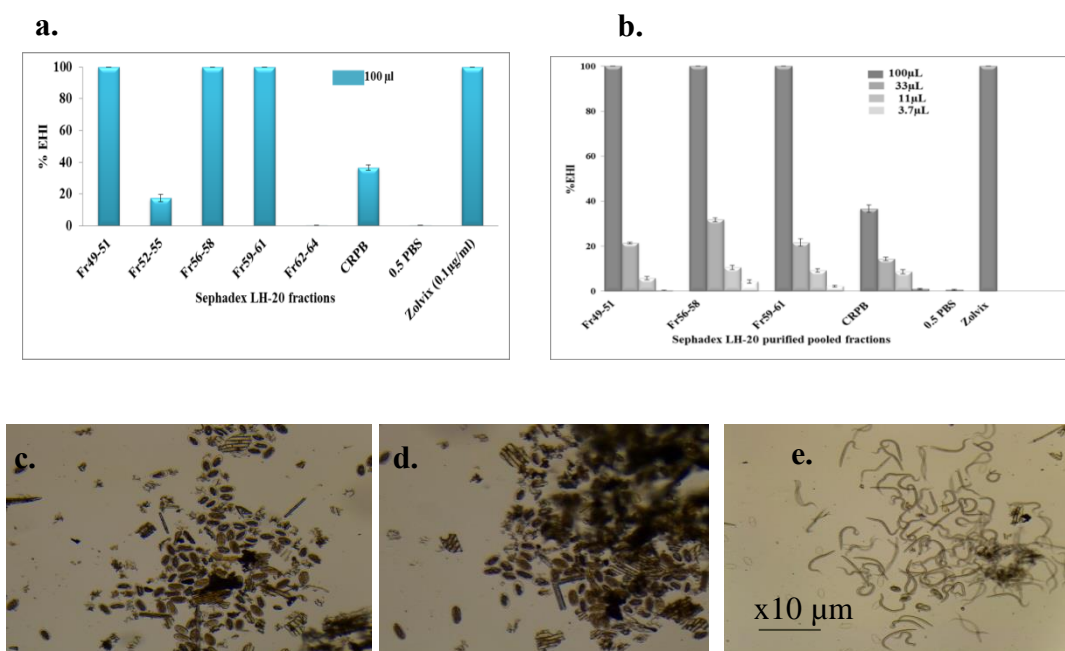


Figure 7.22. Mean percentage EHI of Sephadex LH-20 pooled fractions of CRPB. First run EHI (a) and repeated EHI (b). Eggs incubated with pooled fractions at full strengths (c and d) and eggs incubated with 0.5 PBS (e, negative control). Zolvix and CRPB were used as positive controls.

The spots of fractions 56-58 that appeared as smears very close to the origin in the first run (Figure 7.21a) now migrated very close to the solvent front during TLC re-run and appeared as blue band on molybdate stained chromatogram (Figure 7.21b). To further assess the likelihood of the same constituent being partitioned into

neighbouring fractions, two pooled fractions (from each side) were assessed for their EHI activities at full and their serially diluted lower strengths. During first and second EHI runs, it was observed that these pooled fractions showed highly significant ($P < 0.05$) and dose dependent EHI activities. At the highest strength (100 μ l), the purified pooled fractions 49 to 51, 56 to 58 and 59 to 61 showed 100% EHI properties (Figure 7.22a, c, d) compared to the mother Bio-Gel P-2 pooled fraction (CRPB) and controls. The serially diluted lower strengths also showed dose dependent EHI properties (Figure 7.22b). Although the fractions on both sides of the targeted pooled fraction (56 to 58) showed significant EHI, they were not stained with molybdate to confirm the presence of a compound responsible for the observed activity (Figure 7.21b). Therefore, re-run of TLC chromatograms for these pooled fractions and staining them with various staining reagents was deemed needed to confirm the presence of compound(s) in these active pooled fractions.

7.4.8.2. Chromatographic characterization of Sephadex LH-20 purified active pooled fractions of CRPB

This experiment was basically designed to fully characterize the chemical nature and stainability of Sephadex LH-20 purified active compound(s) from CRPB using various staining reagents. To achieve this objective, chromatograms of Sephadex LH-20 purified active pooled fractions were developed using CRPB, quercetin dihydrate, oleic acid and β -sitosterol as markers as shown in section 2.10. The chromatograms were examined in daylight, under UV-light and after stained with various staining reagents to confirm the presence, nature and R_F -value of the active compound in various solvent systems.

7.4.8.2.1. Visualization in day light and under UV-light

The scanned chromatograms using Doc-It (digital TLC chromatogram imaging system) and examined in daylight are shown in Figure 7.23.

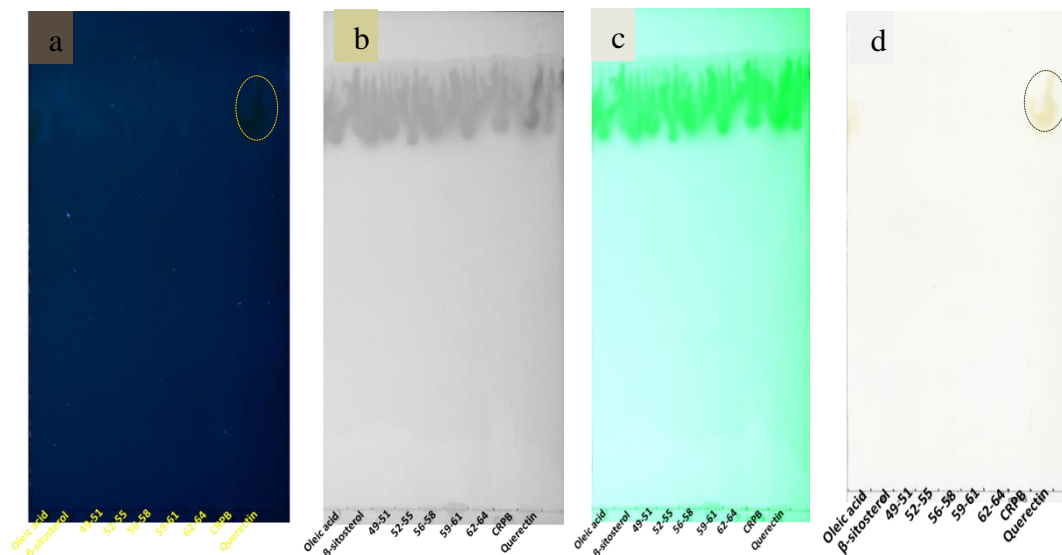


Figure 7.23. Chromatogram of Sephadex LH-20 purified pooled fractions from CRPB and markers. Under UV-light at 366 nm (a), 254 nm (b), 254 BW (c) and in day light (d). Oleic acid, β -sitosterol, quercetin are markers. CRPB as control. The circled spot shows quercetin dihydrate. BW is black and white background.

Only the marker quercetin dihydrate was seen as dark green spot under UV light at 366 nm (Figure 7.23a) and as yellow spot in day light (Figure 7.23d). However, neither Sephadex LH-20 purified compounds nor other remaining constituents of CRPB detected under UV-light at both 254 nm and 366 nm and/or in day light (Figure 7.23).

7.4.8.2.2. Iodine vapours staining

The iodine vapour stained chromatogram of Sephadex LH-20 purified active pooled fractions from CRPB and markers are shown in Figure 7.24.

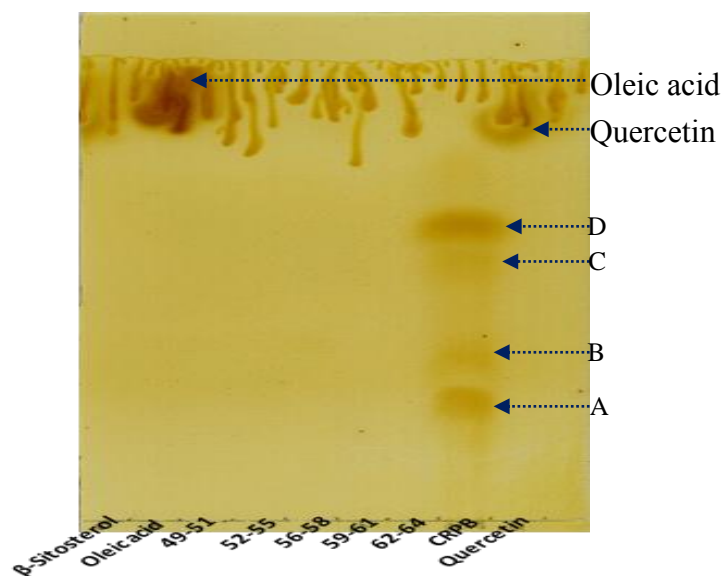


Figure 7.24. Iodine stained chromatogram of Sephadex LH-20 purified pooled fractions from CRPB and markers. β -sitosterol, oleic acid, quercetin and CRPB are markers. A, B, C and D are separated spots of CRPB.

In this study, oleic acid and quercetin dihydrate were stained brown and yellow with iodine vapours respectively. Similarly, the four major separated spots of CRPB (spots A to D) also gave intense yellow coloured spots with iodine.

7.4.8.2.3. Re-staining of iodine stained chromatogram with vanillin reagent

The chromatogram first stained with iodine vapour and then re-stained with vanillin-conc. H_2SO_4 after evaporation of iodine in fume hood is shown in Figure 7.25. The purified compounds that were not stained with iodine vapour now stained pink colour with vanillin-conc. H_2SO_4 . The colour of the marker (oleic acid) also changed from brown to blue. Moreover, the different separated spots of CRPB were also stained with vanillin reagent differently (Figure 7.25).

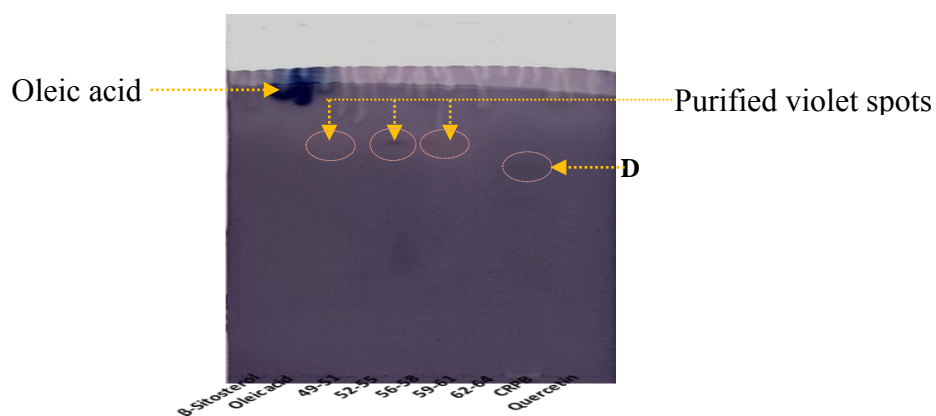


Figure 7.25. Vanillin re-stained chromatogram of Sephadex LH-20 purified pooled fractions from CRPB and markers. β -sitosterol, oleic acid, quercetin and CRPB are markers. Chromatogram heated at 120°C for 30 min. Arrows show purified spots.

7.4.8.2.4. Molybdate staining

The molybdate stained chromatogram of Sephadex LH-20 purified pooled fractions from CRPB and markers are shown in Figure 7.26.

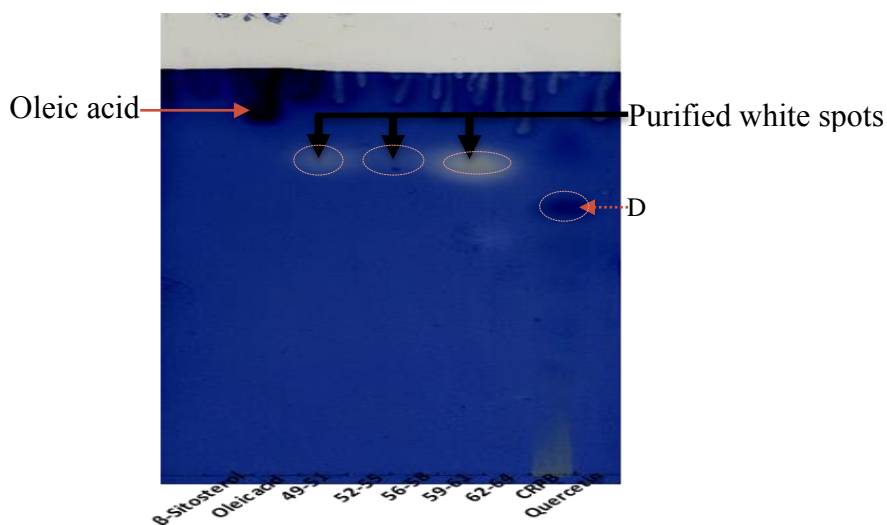


Figure 7.26. Molybdate stained chromatogram of Sephadex LH-20 purified pooled fractions from CRPB and markers. β -sitosterol, oleic acid, quercetin and CRPB are markers. Chromatogram was heated at 105°C for 3 h. Arrows show spots of purified compound.

The purified active pooled fractions of CRPB were stained negatively (white spots) with molybdate reagent upon prolonged heating whereas the major constituent of

CRPB (spot D) and oleic acid stained deep blue with the same reagent. The most polar and slow migrating constituent of CRPB also stained yellow.

7.4.8.2.5. Antimony (III) chloride staining

The chromatogram of Sephadex LH-20 purified pooled fractions from CRPB and markers that first stained with Carr-Price reagent and then re-stained with antimony (III) chloride- acetic acid in chloroform is shown in Figure 7.27.

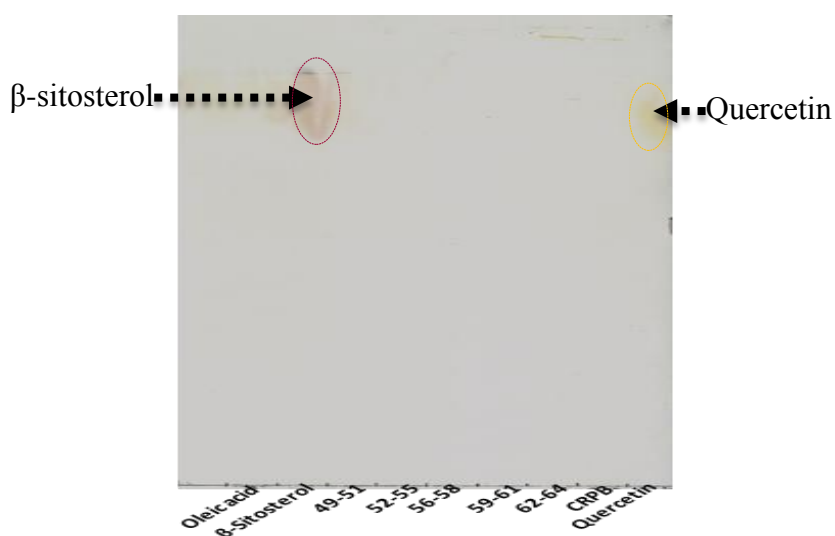


Figure 7.27. Antimony (III) chloride stained chromatogram of Sephadex LH-20 purified pooled fractions from CRPB and markers. Chromatogram heated at 100°C for 5 min. β -sitosterol, oleic acid, quercetin and CRPB are markers.

When the chromatogram was first stained with Carr-Price reagent, there was no fluorescent spot visualised at 366 nm both for Sephadex LH-20 purified pooled fractions and separated spots of CRPB. The only fluorescent spot observed under UV-light at 366 nm was the marker, quercetin (data not shown). The chromatogram used for flavonoids detection was re-stained with antimony(III)chloride-acetic acid in chloroform to detect the presence of steroids and diterpenes in both CRPB and its purified fractions. After heat treatment at 100°C for 5 min., only the marker (β -

sitosterol) was stained with the reagent and visualized as brown-red in daylight (Figure 7.27), intense red colour under UV lamp at 366 nm in the dark and as grey fluorescent spot under Doc-It at longer wavelength (366nm BW).

7.4.8.2.6. Vanillin in conc. H₂SO₄ staining

The vanillin stained chromatograms of Sephadex LH-20 purified active pooled fractions from CRPB with markers that developed in two solvent systems are shown in Figures 7.28 and 7.29. In these runs, samples were loaded on to full TLC plate as circular spot with 2 cm in diameter.

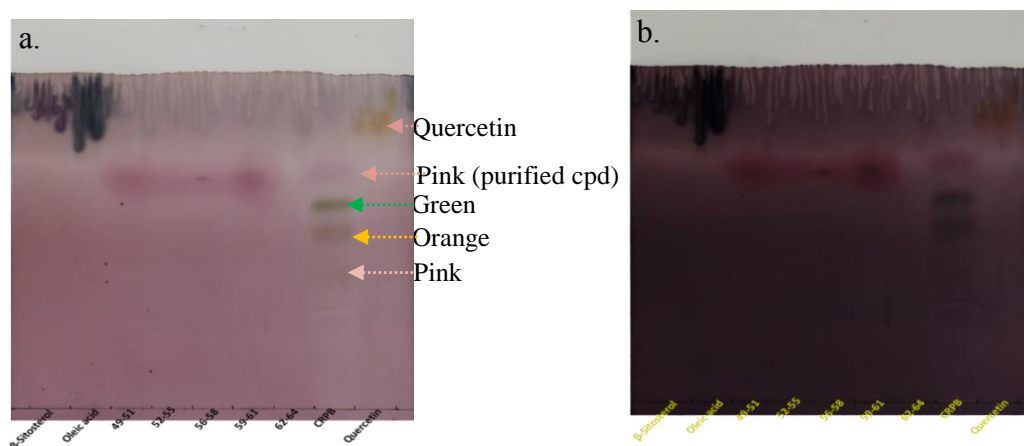


Figure 7.28. Vanillin stained chromatograms of Sephadex LH-20 pooled fractions from CRPB and markers. β -sitosterol, oleic acid, quercetin and CRPB are markers. Chromatogram was developed in BuOH-HOAc-H₂O (4:1:1 v/v/v), dried and heated at 120°C for 30 min. (a) and 3 h (b).

The chromatogram developed in BAW and stained with vanillin revealed that constituents of the four Sephadex LH-20 purified pooled fractions were relatively less polar, stained pink with vanillin and migrated the same distance on TLC with R_F-value of 0.73 (Figures 7.28a and 7.28b). The CRPB also contained three other distinctly vanillin stained major constituents (pink, orange and dark green spots) with R_F-value of 0.4, 0.53, and 0.60 respectively (Figure 7.28b). All the reference markers

are less polar compared to any constituents of CRPB that distinctly stained with vanillin reagent and migrated with the solvent front: quercetin dihydrate (orange), oleic acid (blue green) and β -sitosterol (dark pink) as seen in Figure 7.28. The spot of pool (56-58) that developed in chloroform-methanol-acetic acid (10:2:1 v/v/v) solvent system and stained pink with vanillin reagent revealed the presence of dark violet at the centre of the spot upon prolonged heating.

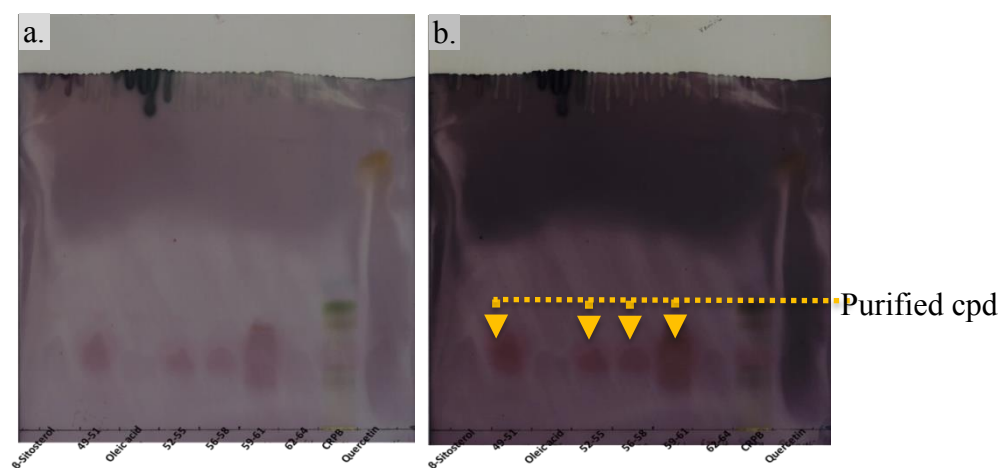


Figure 7.29. Vanillin stained chromatograms of Sephadex LH-20 purified compound(s) from CRPB and markers. Chromatogram was developed in CHCl_3 -MeOH-HOAc (10:2:1 v/v/v), dried and heated at 120°C for 30 min. (a) and 3 h (b). Arrows show purified compound.

The chromatogram developed in chloroform-methanol-acetic acid (CMA) also showed that the constituents of the four Sephadex LH-20 purified pools were stained pink with vanillin and migrated the same distance on TLC with R_F -value of 0.20 (Figure 7.29).

Table 7.1. Summary of chromatographic characterization and EHI tests of Sephadex LH-20 purified pooled fractions from CRPB.

LH-20 Purified Pooled fractions from CRPB	Spot colour with staining reagents (colour intensity due to charring upon heating)								
	Presence/absence at origin	Under UV- light	Iodine reagent	Vanillin reagent	Molybdate reagent	R _F -value		EHI (%) of at full and one-third strength	
						BAW (4:1:1)	CMA (10:2:1)	100 µl	33.3 µl
49-51	-	-	-	Pink	White (+)	0.73	0.2	100	21
52-55	-	-	-	Pink	White (±)	0.73	0.2	< 20	NT
56-58	±	-	-	Pink	White (±)	0.73	0.2	100	32
59-61	±	Dark cap in CMA	-	Pink	White (±)	0.73	0.2	100	22
62-64	-	-	-	Pink	White (++)	0.73	0.2	0	NT

Data summary Key: The ranking of colour intensities formed by staining reagents upon heating (charring) in oven as: high intensity (+++), medium intensity (++), low intensity/ presence (+), undecided (±), non-staining /absent (-), not tested (NT). Butanol-acetic acid-water (BAW) and chloroform-methanol acetic acid (CMA) solvent systems.

7.4.8.3. Further purification of C₁₈ purified compound(s) on PTLC

Further purifications of C₁₈ purified water pooled fractions of 49-51 and 56-58 on PTLC were done as described in section 2.10.2. PTLC strips (2 cm) and TLC chromatograms of purified compounds stained with vanillin reagent and heated in oven to activate and enhance reactions for detection of the separated bands are shown in Figure 7.30. The vanillin stained strips were used to locate and mark the position of the separated bands. The vanillin stained PTLC strips and the corresponding chromatograms of supernatants of purified bands revealed that both pooled fractions contained only one compound per pool. They also showed that the purified bands on the PTLC strips and their corresponding chromatograms had the same R_F-value of 0.73 (Figure 7.30).

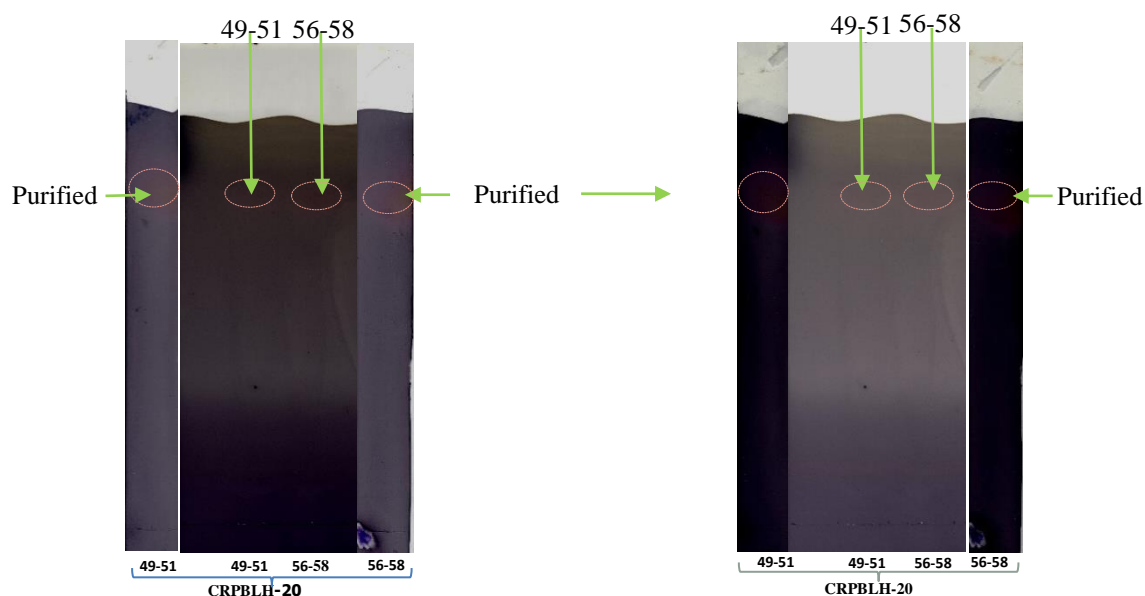


Figure 7.30. Vanillin stained chromatograms and PTLC strips of purified compound(s) from CRPB. Both chromatograms were heated at 120°C for 3 h. Arrows and circles show purified compounds.

7.4.8.4. The EHI tests of PTLC purified compound (s) from CRPB

The EHI of PTLC purified active pooled fractions from CRPB and controls is shown in Figure 7.31. The EHI result revealed that crude extract, CRPB and supernatants from PTLC purified bands of pooled fractions of 49-51 and 56-58 showed significant EHI properties ($P < 0.05$) compared to negative controls.

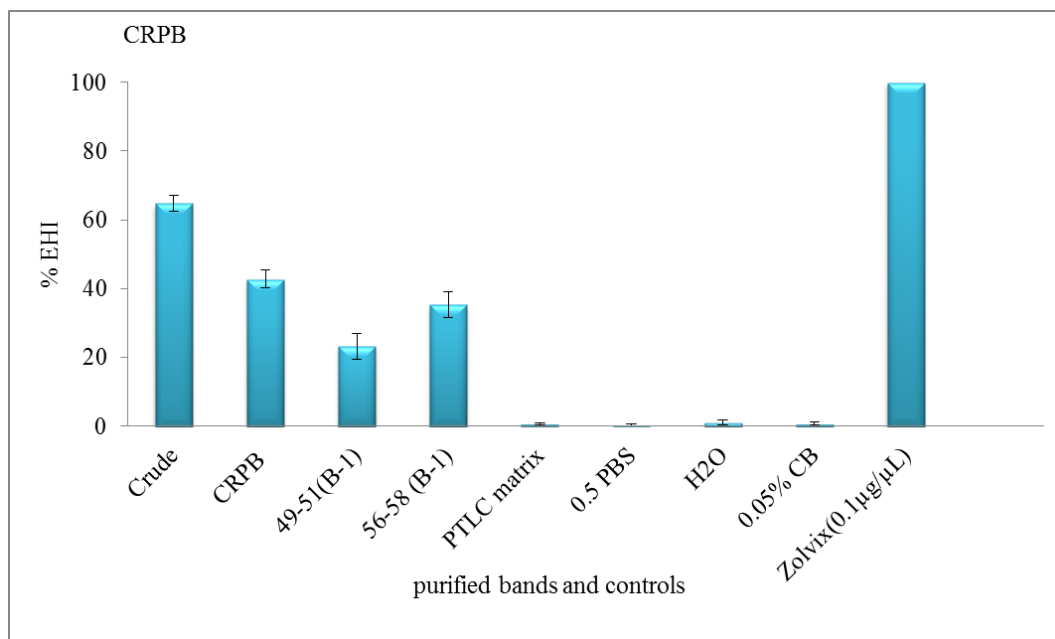


Figure 7.31. Mean percentage EHI tests of PTLC purified compounds from CRPB and controls. PBS, H₂O, 0.05% CB (negative controls) and Zolvix (positive control).

7.4.9. Isolation of active constituents from CRPC and their EHI tests.

7.4.9.1. Isolation and purification of CRPC on Sephadex LH-20 column chromatography

In this purification process, the same procedure employed for purification of constituents of other pooled fractions of *C. ruspolii* was also applied to isolate and purify the major blue fluorescent constituent of this pool. The chromatograms of Sephadex LH-20 water fractions from CRPC and marker examined under UV-366 nm and then stained with vanillin reagent are shown in Figure 7.32. The chromatogram examined under UV-light at 366 nm revealed that the major and blue fluorescent constituent of this pool was partitioned into water fractions 12-14.

The blue fluorescent compound under UV-light at 366 nm, but not stained with vanillin in conc. H₂SO₄, was predominantly partitioned into fraction-13 (Figure

7.32). The CRPC did contain not only the blue fluorescent compound but also other constituents that partitioned into less polar methanol gradient solvent systems such as the one that partitioned into fraction-69 and the yellow fluorescing spot at UV-366 nm that migrated with the solvent front and stained pink with vanillin reagent (Figure 7.33).

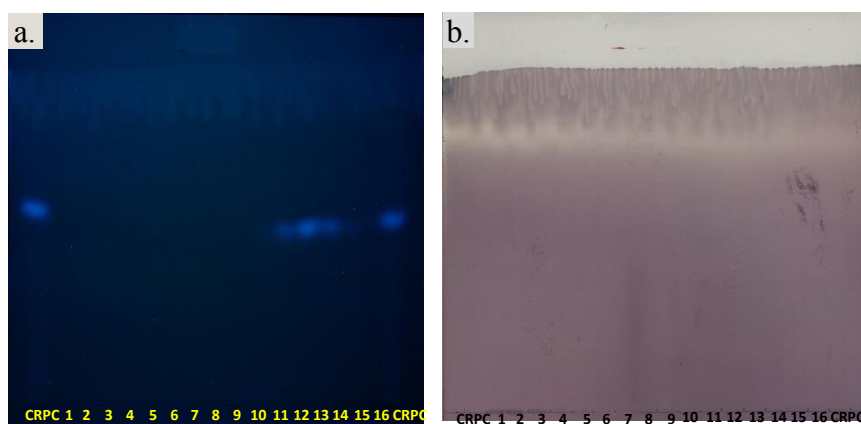


Figure 7.32. Chromatograms of Sephadex LH-20 water fractions from CRPC and marker: Under UV-light 366 nm (a); vanillin stained and heated at 120°C for 30 min. (b). CRPC used as marker.

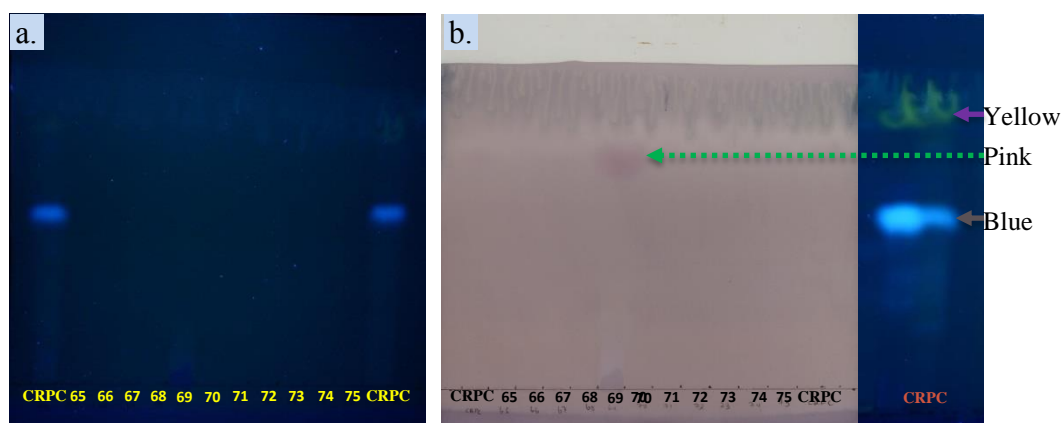


Figure 7.33. Chromatograms of Sephadex LH-20 water fractions from CRPC: at UV-366 nm (a) vanillin stained and heated at 120°C for 30 min. (b).

7.4.9.2. Further purification of blue fluorescent compound on C₁₈ column

The chromatogram of purified fractions from Sephadex LH-20 water fraction-13 from CRPC further purified on C₁₈ column that examined at UV-366 nm and then stained with vanillin reagent is shown in Figure 7.34. In this purification step, the partially purified fraction-13 on Sephadex LH-20 was loaded onto a reversed phase C₁₈ column to further purify the blue fluorescent compound. The same eluents and elution order used in Sephadex LH-20 were also employed here. However, in contrast to Sephadex LH-20, five sub-fractions (1 ml each) per eluent were collected for the water and 20% MeOH solvent systems to maximize the probability of blue fluorescent compound recovery that is pure enough for NMR and MS analyses (Chapter 8). TLC was developed for all water sub-fractions (separately) and 20% MeOH (as pool) to see whether the blue fluorescent compound completely partitioned into the water sub-fractions again or also partitioned into the next eluent (20% MeOH).

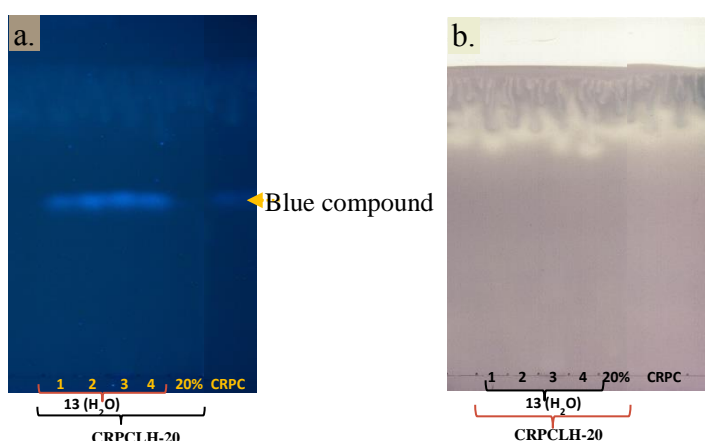


Figure 7.34. Chromatograms of Sephadex LH-20 water fraction-13 from CRPC further purified on C₁₈ column. The 20% stands for 20% MeOH. Chromatogram examined at 366 nm (a) vanillin stained and heated at 120°C for 30 min. (b).

The chromatogram examined at UV-366 nm revealed that the blue fluorescent constituent in Sephadex LH-20 water fraction-13 with R_F value of 0.53 again

partitioned into water sub-fractions during further purification on C₁₈ column chromatography (Figure 7.34a). Moreover, neither the blue fluorescent compound nor other constituents in both water and 20% MeOH fractions stained with vanillin reagent (Figure 7.34b). These chromatographic screenings of the C₁₈ purified fractions confirmed that the blue fluorescent compound is qualitatively pure enough for MS and NMR analyses (Figure 7.34). The 20% MeOH sub-fractions were pooled together to enrich the pool with target constituent(s) that also subsequently enrich the aliquot used for TLC development. Enrichment of the aliquot for TLC development is used to confirm the presence or absence of the blue fluorescent and others constituents (if any) that stained with vanillin in this pooled fraction.

To further characterize the blue fluorescent compound using various staining reagents, the Bio-Gel P-2 pooled fraction (CRPC) was loaded on to TLC plate with fluorescent indicator at “F_{254 nm}” as a 2 cm band in six replicates. The chromatogram examined under UV-366 nm is shown in Figure 7.35.

The chromatogram (Figure 7.35) was cut into six strips (2 cm each). These strips were stained with various staining reagents to examine the chemical nature and its ability to stain with various staining reagents. Here, we also utilized all staining reagents used to characterize the purified pooled fractions from CRPB. But, none of them stained the blue spot differently (data not shown).

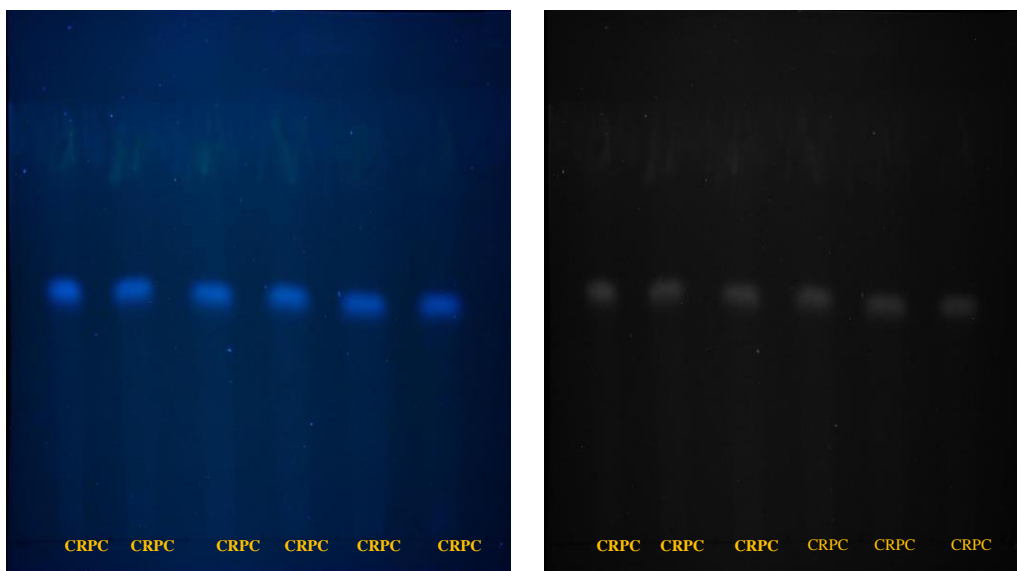


Figure 7.35. Chromatogram of CRPC replicates at UV-366 nm (a) at 366 nm BW (b). BW stands for black and white background at 366 nm.

7.4.9.3. Further purification of blue fluorescent compound on PTLC

The PTLC and TLC chromatograms of Sephadex LH-20 purified water pooled fractions of 12 and 14 visualized at UV-366 nm are shown in Figure 7.36.

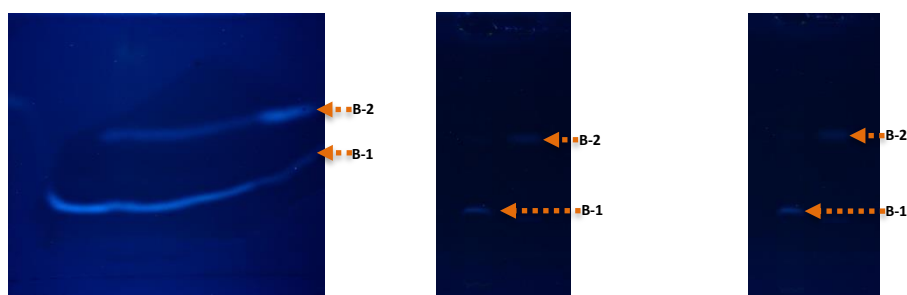


Figure 7.36. PTLC and TLC chromatograms of Sephadex LH-20 pooled fractions 12 and 14 from CRPC. Chromatograms were examined at UV-366 nm. B-1 and B-2 are separated bands.

PTLC and its corresponding TLC chromatograms of purified bands (Figure 7.36) indicated that the pooled fraction contained two blue compounds. The first compound is the bright blue, polar, water soluble and slow migrating compound with

R_F-value of 0.25. The second compound is slightly dark blue, polar, water soluble, fast migrating with R_F-value of 0.50.

7.4.9.4. The EHI tests of PTLC purified compounds from CRPC

The EHI tests were also conducted for crude extract, CRPC, and PTLC purified bands as indicated in section 2.5.1.3. The EHI result revealed that crude extract, CRPC, and PTLC purified bands showed significant ($P < 0.05$) EHI properties compared to negative controls (Figure 7.37) though activity of CRPC, B-1 and B2 was very low.

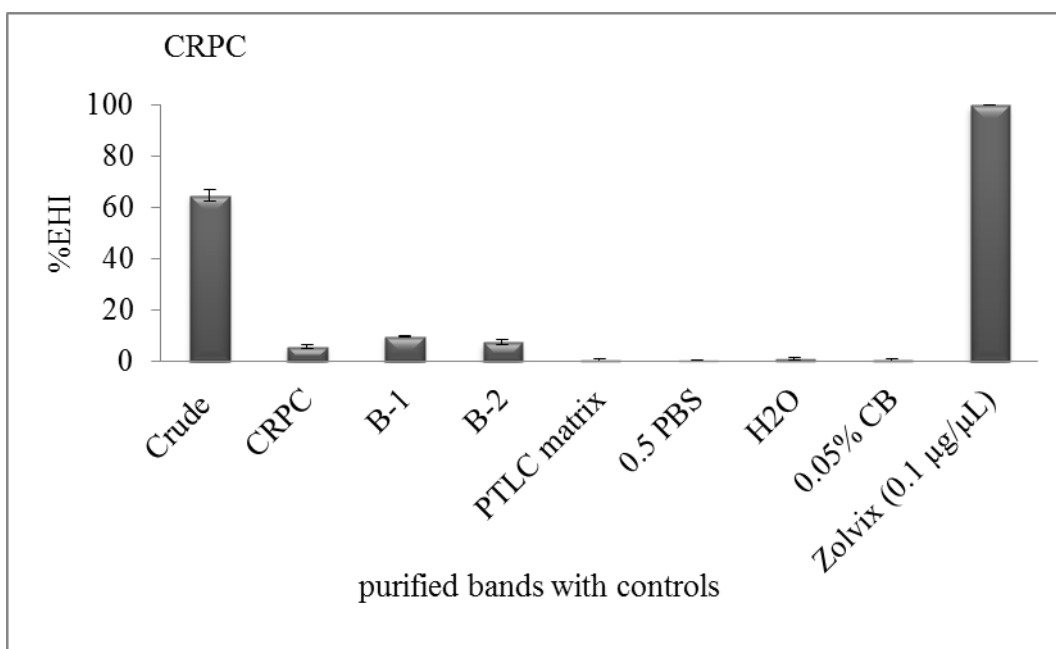


Figure 7.37. The EHI tests of PTLC purified compound(s) from CRPC. Crude extract, CRPC and Zolvix (positive controls); PBS, H₂O and 0.05% CB (negative controls). B-1 and B-2 are purified bands.

7.4.10. Isolation of active compounds from *Adenia* sp. active pooled fractions

7.4.10.1. Isolation of constituents of ASPA on Sephadex LH-20 column

The first Bio-Gel P-2 pooled fraction of *Adenia* sp. (ASPA) was loaded onto previously used but washed and reconditioned Sephadex LH-20 column to isolate and purify the major constituents of this pool by solvent gradient elution method as detailed in section 2.10.1. The first Bio-Gel P-2 pooled fraction of *Adenia* sp. (ASPA) is known for its two slow migrating major constituents that heavily stained with various staining reagents, including thymol, molybdate and vanillin. These two major constituents stained pink, blue and dark green that turn to dark brown upon prolonged heating with thymol, molybdate and vanillin reagents, respectively.

As for *C. ruspolii* pooled fractions, eighty fractions (4 ml each) were collected, TLC developed, stained with vanillin reagent, heated in oven at 120°C for 30 min. and 3 h. The vanillin stained chromatograms are shown in Figure 7.38.

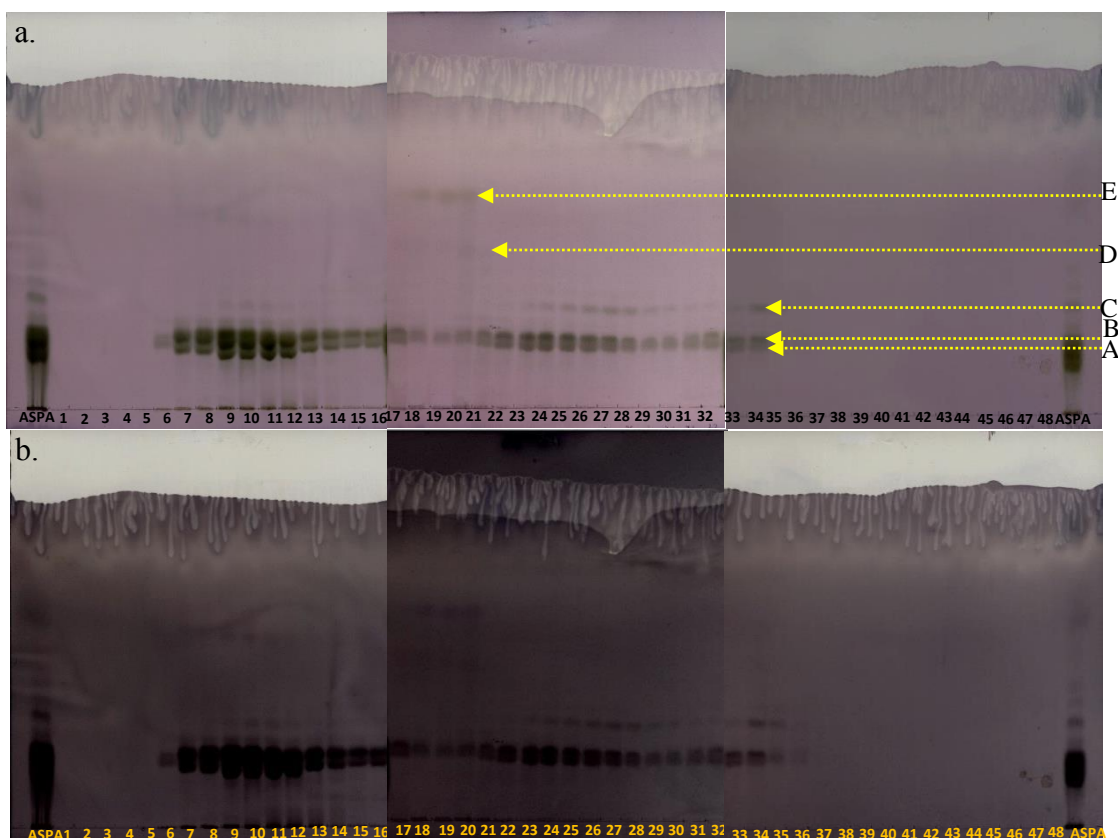


Figure 7.38. Vanillin stained chromatograms of Sephadex LH-20 fractions from ASPA. Chromatogram heated at 120°C for 30 minutes (a) 3 h (b). A to E are separated spots.

The vanillin stained chromatogram revealed that all constituents of this pool eluted in deionized water (the first eluent) and partitioned into fractions (6-35). These fractions had various physical characteristics and could be categorized into four groups: (1) yellowish and foamy (7-12); (2) light turbid and foamy (13-16); (3) light turbid but not foamy (17-20); and (4) highly turbid but not foamy (21-28). The two major constituents of these categorized fractions also had distinct chromatographic profiles as dark green spots (7-12), light green spots (13-17) and light brown spots (18-35) as seen in Figure 7.38a. In general, the vanillin stained chromatogram revealed that ASPA had contained five constituents labelled as A, B, C, D and E with

R_F -values of 0.20, 0.23, 0.27, 0.40, and 0.67 respectively (Figure 7.38a). The yellow and foamy fractions (7-12) remained frothy as long as in water solution.

7.4.10.2. Further purification of water fraction from ASPA on C_{18} column

In this further isolation and purification step, the partially purified Sephadex LH-20 fraction-9 (ASPALH-20-9) from the yellowish and foamy groups was loaded onto C_{18} column and eluted by solvent gradient. In addition to eluents and elution order used in Sephadex LH-20, 10% MeOH was also included in this isolation and purification step. To maximize the probability of getting major active constituents in pure form, five sub-fractions (1 ml each) were collected for the first three eluents: de-ionized water, 10 and 20% MeOH eluents and 5 ml (each) for the remaining less polar MeOH gradient eluents. The vanillin stained TLC chromatogram of the first three eluents are shown in Figure 7.39.

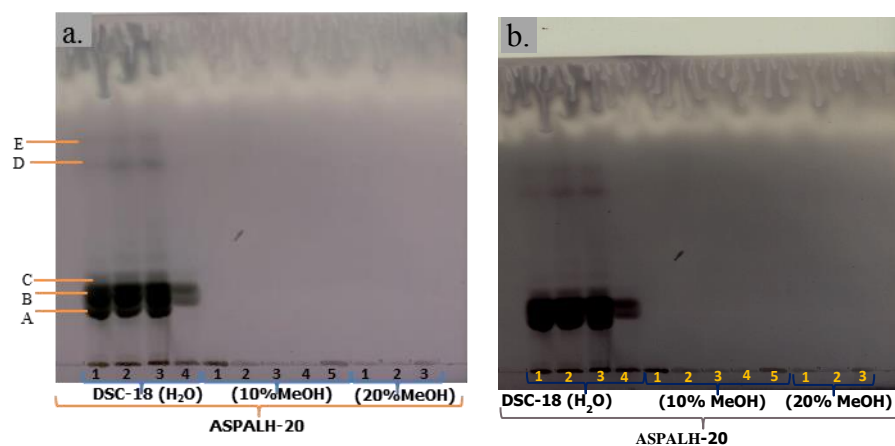


Figure 7.39. Vanillin stained chromatograms of C_{18} water and methanol gradient fractions of ASPA. Chromatogram heated at 120°C for 30 min. (a) 3 h (b). A to E are separated spots.

The chromatogram (Figure 7.39) showed that all the constituents of ASPALH-20-9 were also eluted in deionized water on C_{18} column. For instance, the five vanillin stained spots (A, B, C, D and E) with R_F -values of 0.20, 0.23, 0.27, 0.40, and 0.67

which were eluted in water on Sephadex LH-20 also eluted in the same eluent during further purification on C₁₈ column.

7.4.10.3. Further purification of C₁₈ water fraction on PTLC

Reversed phase C₁₈ water fraction-2 from ASPALH-20-9 was loaded on to half (8 cm) of non-fluorescent TLC as a band/streak (4 µl/cm) to further isolate and purify the two major and active compounds of this fraction. The PTLC was developed twice to distinctly isolate and purify the two closely eluted major compounds responsible for the observed anti-parasitic properties of this pool. The other half of the PTLC was also loaded with the same volume of de-ionized water to recover parallel bands to the target purified compounds as control. The bands recovered from the deionized water region were used as blank control for both EHI tests and NMR analysis of purified compounds. The blank control used in NMR analysis was to differentiate NMR spectra of purified compounds from those due to the co-eluted contaminants (binders) from the coating materials during sample recovery from the silica gel. As used in the purification of compounds from C₁₈ fractions of *C. ruspolii* pools, the vanillin stained strip was also used to locate and mark the position of separated bands on PTLC. The 3 cm marked band was sub-divided into six smaller bands (0.5 cm each) to maximize the pure compound recovery per band for NMR and MS analysis. The silica gel with sample per band was divided into two and separately mixed with de-ionized water, centrifuged and supernatants collected in separate vials to recover pure compounds from these bands. For the two supernatants per band, TLC was developed and stained with vanillin reagent to confirm the degree of purity of recovered compounds from sub-bands. This confirmed that the slow migrating (B_{1/1}) with R_F-value of 0.23 and the relatively fast migrating with R_F-value of 0.27 (B_{3/1})

and B_{4/1}) fractions were pure compounds and labelled as compound A and B respectively (Figure 7.40). Both purified compounds were submitted for NMR analysis with corresponding blanks from the de-ionized water zone as negative controls (Chapter Eight).

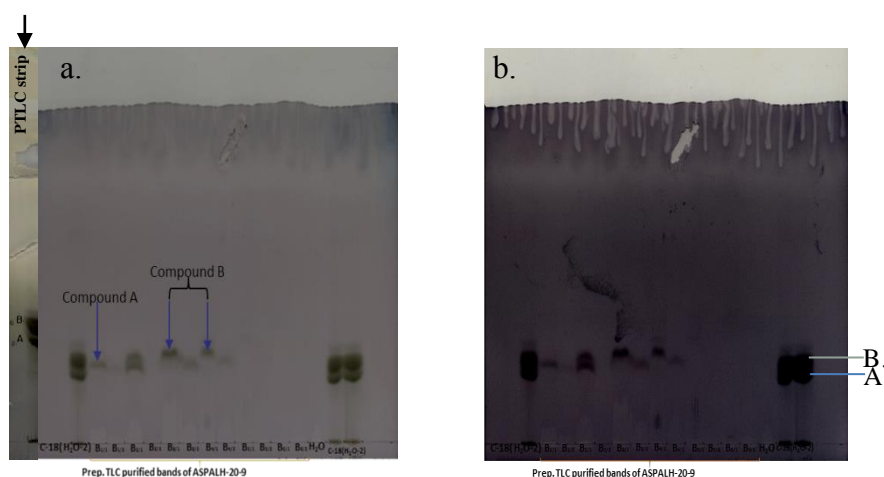


Figure 7.40. Vanillin stained chromatograms and PTLC strip of C₁₈ fraction-2 from ASPA Sephadex LH-20 fraction-9. Chromatogram heated at 120°C for 30 min. (a) and 3 h (b). A and B are purified compounds

The two closely migrating bands of the pellet recovered from ASPALH-20 pooled fractions 21-28 also had similar R_F-values as compound A and B (Figure 7.41).

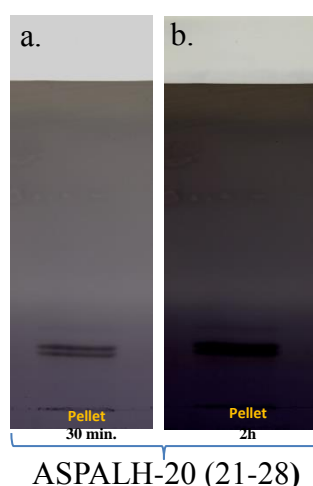


Figure 7.41. Vanillin stained chromatograms of white pellet recovered from ASPA Sephadex LH-20 pooled fraction (21-28). Chromatogram heated at 120°C for 30 min. (a) and 2 h (b).

This pellet was recovered from highly turbid but not foamy Sephadex LH-20 pooled fraction (21-28) upon cooling in freezer at -20°C. They were from the late eluted Sephadex LH-20 water fractions. They may have high affinity to the stationary phase of Sephadex LH-20 or less polar than other components of ASPA.

7.4.10.4. EHI tests of isolated and purified compounds from ASPA

The EHI test was conducted for crude extract, ASPA, Sephadex LH-20, C₁₈ and PTLC purified compounds (A and B) as indicated in section 2.5.1.3 using both negative and positive controls. The EHI test result revealed that crude extract, Sephadex LH-20 pooled fractions 7-12 and 13-20, recovered pellet from pooled fraction 21-28, C₁₈ water fraction from ASPALH-20-9 and PTLC purified compound B from C₁₈ water fraction-2 showed greater than 50% EHI properties (Figure 7.42).

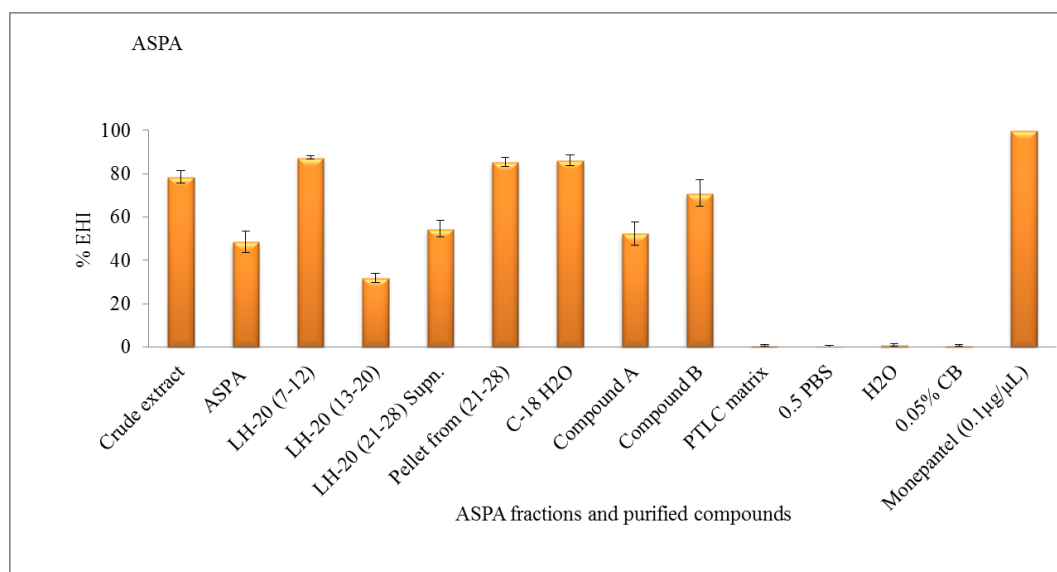


Figure 7.42. The EHI tests of PTLC purified compounds A and B from ASPA with both positive and negative controls.

Moreover, the first stage larvae from hatched eggs in culture well plates containing crude extract, Sephadex LH-20 pooled fraction (7-12), C₁₈ water fraction-2 and compound B were observed as stretched and non-motile after 24 h. This observation was further monitored for another 24 h, however, there was no motility (i.e. the larvae remained stretched and non-motile).

Table 7.2. Summary of spot colour and R_F-values of major constituents of Bio-Gel P-2 active pooled fractions of *C. ruspolii* and *Adenia* sp. examined under UV-light and after stained with universal reagents.

Plant	Bio-Gel P-2 active pooled fraction	Major compounds isolated	Spot colour			
			UV-366 nm	Molybdate	Vanillin	R _F - value
<i>C. ruspolii</i>	CRPA	Spot A	-	Dark blue	Brown	0.13
		Spot B	-	Dark green	Green	0.47
		Spot C	-	Dark green	Green	0.60
		Spot D	-	Blue	Pink	0.80
	CRPB	Spot A	-	Tailed yellow	-	0.07
		Spot B	-	Blue	-	0.60
		Spot C	-	Blue	-	0.67
	CRPC	CRPC LH-20-13	Blue	-	-	0.53
	<i>Adenia</i> sp.	Compound A	-	Dark blue	Green	0.23
		Compound B	-	Dark blue	Green	0.27

7.4.11. Qualitative characterization and semi-quantitative determination of yellow stained component of *C. ruspolii* extract

7.4.11.1. Chromatogram profiling of yellow stained constituent of *C. ruspolii* extract

A chromatogram was developed for *C. ruspolii* water crude extract and authentic markers sodium dihydrogen phosphate dihydrate (NaH₂PO₄ · 2H₂O), sodium pyrophosphate (Na₄P₂O₇), ATP, 3-phosphoglyceric acid (3-PGA), D-Glucose-6-phosphate (Glc6P) and then stained with molybdate to test for the presence of

inorganic phosphate and/or phosphorylated metabolites in this water crude extract (CRD).

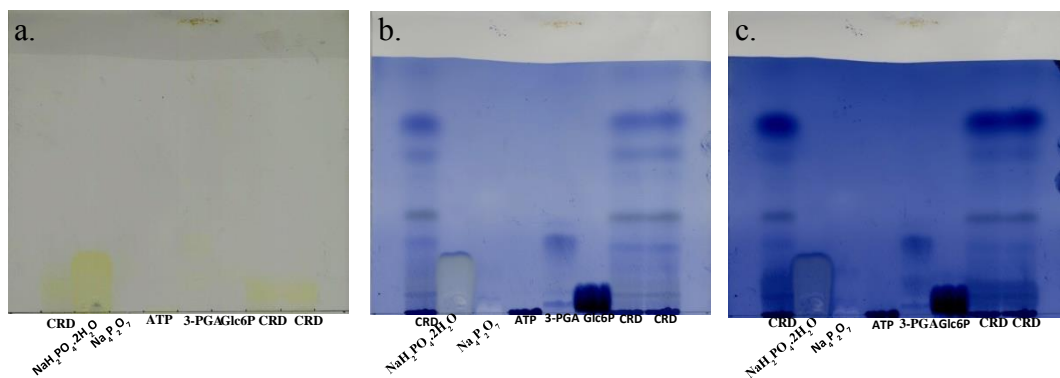


Figure 7.43. Molybdate stained chromatograms of *C. ruspolii* water crude extract and phosphates. Chromatogram in day light (a) after heating in oven at 120°C for 30 min (b) 3 h (c).

The water crude extracts of *C. ruspolii* and sodium dihydrogen phosphate dihydrate stained yellow with molybdate at similar position on TLC before heating in an oven. Moreover, the other phosphorylated authentic markers also stained faint yellow with molybdate at similar positions under the same conditions (Figure 7.43).

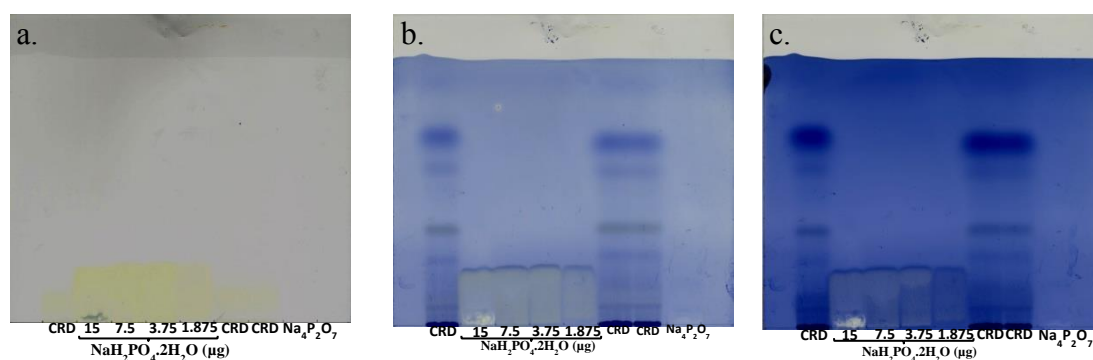


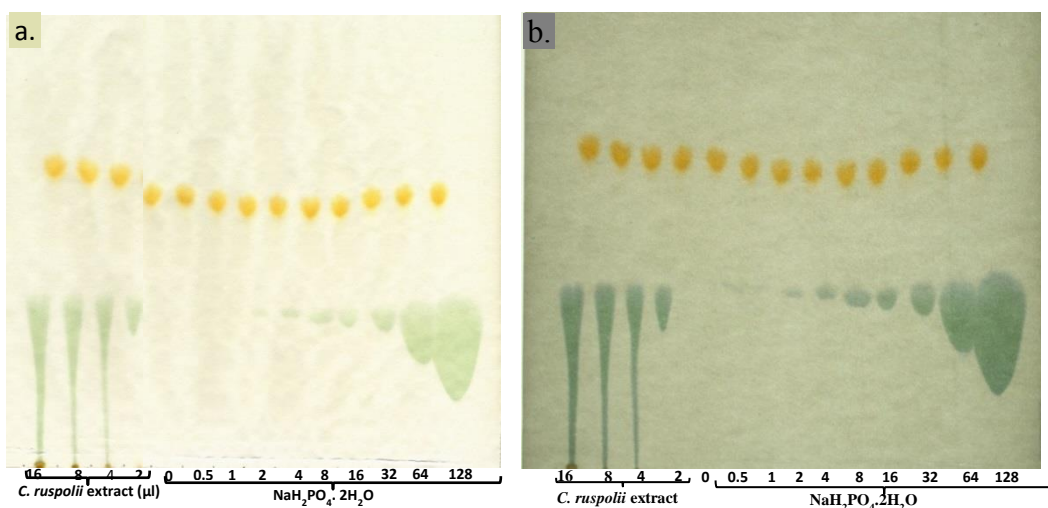
Figure 7.44. Molybdate stained chromatograms of *C. ruspolii* water extract with markers. Sodium dihydrogen phosphate dihydrate and sodium pyrophosphate are markers: in day light (a) heated at 120°C for 30 min. (b) and 3 h (c).

To further generate evidence, TLC was developed for the crude extract with serially diluted sodium dihydrogen phosphate dihydrate and then stained with molybdate to

re-confirm and qualitatively estimate the level of the yellow stained compound (may be P_i) in the crude extract visually by comparing with the colour intensity formed by serially diluted standard sodium dihydrogen phosphate dihydrate after molybdate staining.

7.4.11.2. HVPE analysis for P_i in *C. ruspolii* water extract

The HVPE experiments were carried out in two buffer systems: in acidic buffer (at pH 2.0) and in nearly neutral buffer (at pH 6.5) to qualitatively identify the yellow stained compound with molybdate in the crude extract based on its electrophoretic mobility in comparison to serially diluted standard sodium dihydrogen phosphate dihydrate using paper electrophoresis. Both water crude extract (at all volumes loaded) and sodium dihydrogen phosphate dihydrate and its serially diluted lower concentrations migrated to anode in HVPE under both acidic and nearly neutral conditions as shown in Figures 7.45 and 7.46.



the organic dye (Orange G) that is used as guide marker to monitor uniform migration of loaded samples.

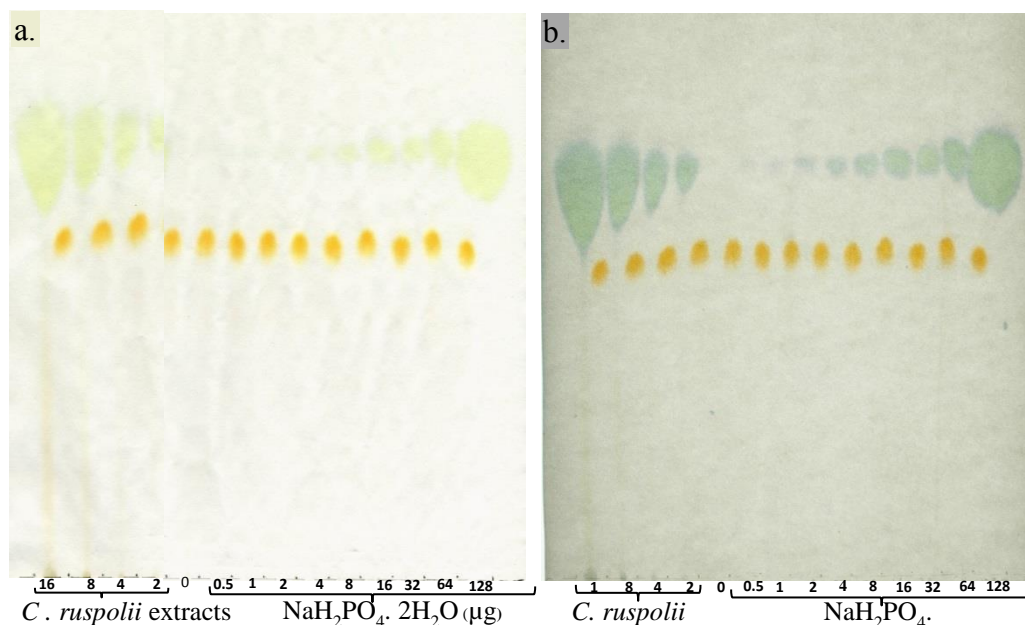


Figure 7.46. Molybdate stained electrophoretograms of *C. ruspolii* water crude extract and sodium dihydrogen phosphate dihydrate at pH 6.5. Electrophoretograms before exposure to sun light (a) after exposure to sunlight (b).

Both samples had average ionic mobility (M_{OG}) of 0.53 at pH 2.0 (Figure 7.45) and 1.27 at pH 6.5 (Figure 7.46) respectively. Moreover, both samples migrated only a little slower under acidic condition (pH 2.0) than nearly neutral at pH 6.5. The rate of colour change from yellow to blue was enhanced by prolonged exposure to sun light.

7.4.11.3. Semi-quantitative determination of the level of yellow stained constituent of *C. ruspolii* crude extract by colorimetric method

The mean intensities of molybdate stained spots on paper electrophoretogram before exposure to sunlight were determined by scanning and using Photo shop tool. The mean of each spot was adjusted by taking the mean intensity difference of the target

spot and background (de-ionized water loaded region). Sigma Plot software was used to plot the mean intensity readings versus the concentration of the standard sodium dihydrogen phosphate dihydrate that best fit for determination of the inorganic phosphate level in various volumes of crude extract loaded as shown in Figure 7.47.

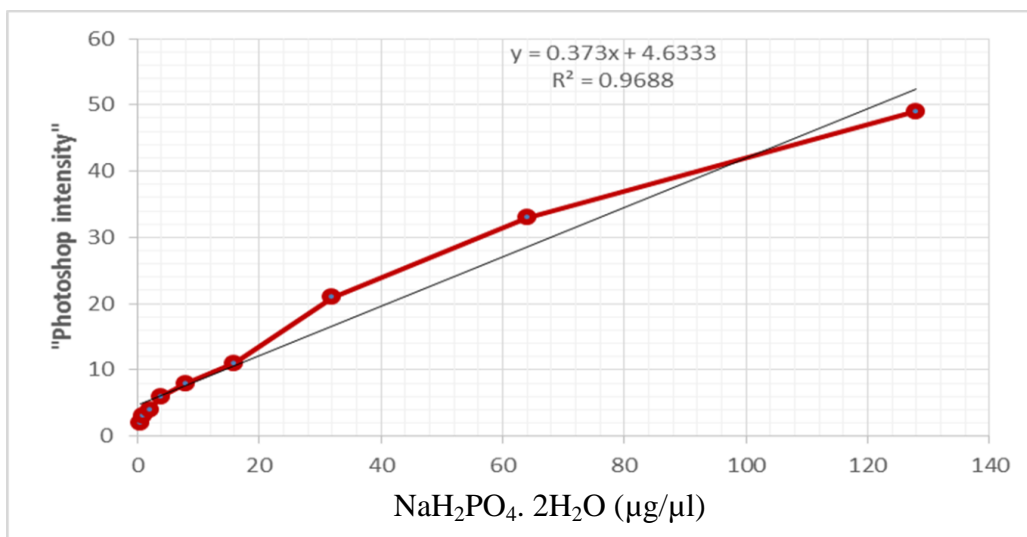


Figure 7.47. Mean intensity of molybdate stained spots of standard sodium dihydrogen phosphate dihydrate versus their concentration.

The mean intensities of molybdate stained spots of the standard were linear at lower concentration between 0.5 and 16 µg/µl and chosen as the region of best fit for determination of the inorganic phosphate level in various volumes of crude extract loaded.

The amount of inorganic phosphate per µl of crude extract loaded was determined semi-quantitatively by inserting the adjusted mean intensity into the equation generated by Sigma Plot for standard sodium dihydrogen phosphate dihydrate used. Then the graph of inorganic phosphate vs volume of crude extract loaded was plotted as shown in Figure 7.48 to see the accuracy and precision of determination of the yellow stained constituent of crude extract.

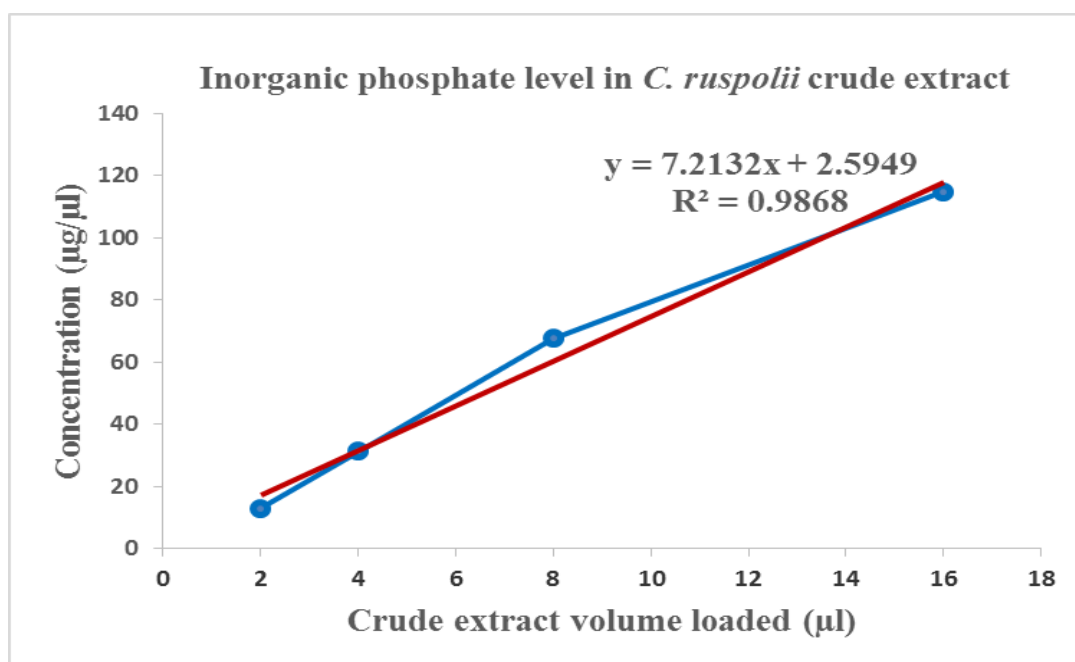


Figure 7.48. The plot of [Pi] vs volume of crude extract loaded onto PC.

The result showed that the amount of constituent of *C. ruspolii* crude extract that stains yellow with molybdate reagent was 7.5 µg/µl.

7.5. Discussion

7.5.1. PC isolation and profiling of active pooled fractions of *C. ruspolii* and *Adenia* sp.

Of the six active pooled fractions (three pools per plant) assessed for the presence or absence of UV-active constituents, only CRPC had contained two major fluorescent compounds at 366 nm, i.e. a blue and a yellow fluorescing constituents. The slow migration of the blue fluorescent spot in CRPC compared to the markers ferulic and caffeic acids indicates that it might be a water soluble and bulky phenolic compound. The similarities in fluorescence colour and colour intensity of a compound in CRPC and caffeic acid might be related to similarities in electronic structures around fluorescing functional groups in both compounds. Moreover, the fluorescence intensities of both the blue and the yellow spots in CRPC were enhanced after exposure to ammonia vapour indicating that deprotonation by ammonia resulted in extended π -electron system that increases fluorescence intensities of both spots. Esmaili *et al.* (2011) reported that the detection of phenolic compounds and their colour intensities on TLC under UV-light was enhanced on fumigation with ammonia vapour. As such, it might be speculated that both the blue and the yellow fluorescent constituents of CRPC could be phenolic compounds.

When the experiment was done to isolate and purify constituents of ASPC on PC, only the water supernatants recovered from lower bands (i.e. bands from 2 cm above and below the origin and the next band to it) exhibited EHI activities during both runs. This indicated that constituents of ASPC responsible for the observed EHI activities did not migrate far on PC (i.e. they might strongly bind to cellulosic fibres at and/or near the origin as shown in Figure 7.4). The chromatographic papers are made up of cellulose, which has numerous hydroxyl (-OH) functional groups (Jensen

1956) that could form strong covalent bond with active constituents of ASPC containing various electron withdrawing functional groups in their structures. Hence, these EHI results (Figure 7.4) strongly support the view that PC is not a suitable chromatographic technique for quantitative isolation and purification of potential bioactive plant secondary metabolites in the samples analysed.

7.5.2. PTLC isolation and TLC profiling of *C. ruspolii* water crude extract

This experiment was designed to assess the suitability of preparative planar chromatography (20 cm x 20 cm size, coated with silica gel 60G, 0.5 mm thickness with glass backings) to isolate and purify constituents of Bio-Gel P-2 active pooled fractions. This isolation and purification of constituents of *C. ruspolii* water crude extract on PTLC resulted in the recovery of eight partially purified bands: five UV-active and three non-fluorescent but molybdate stained constituents (Figures 7.5a and 7.5b). Supernatants recovered from bands 1-7 and 13 had contained constituents that stained with molybdate. The chromatogram re-run of the fluorescent bands revealed that the blue fluorescent compound (Figure 7.5c) had other non-fluorescent but co-migrating compound(s) that stained blue green with molybdate (Figure 7.5d). This assessment revealed that PTLC developed in BAW (4:1:1 v/v/v) solvent system alone may not be a suitable technique that lead to isolation and purification of compounds from active pooled fractions although it can be used in combination with other chromatographic techniques. This finding also revealed that solvent systems other than BAW may be explored for preparative chromatogram development to achieve optimum isolation and purification of constituents of active pooled fractions on PTLC.

7.5.3. *C. ruspolii* water crude extract purification on C₁₈ column

C. ruspolii water extract purification on a reversed phase C₁₈ column was also done to assess its suitability for further isolation and purification of Bio-Gel P-2 active pooled fractions. There were two blue fluorescent compounds detected on chromatogram, i.e. the one eluted in deionized water and stained blue green with molybdate and the second blue spot that eluted in 60% MeOH but did not stain with molybdate (see section 7.4.3). These two blue spots are either two different compounds or the second blue compound could be the hydrolytic degradation product of the first blue compound. This is because glycosylated flavonoids and those having ester, amide, and anhydride linkages in their structures might undergo hydrolytic degradation upon storage in water solution for long time even at -20 °C (Loftsson, 2014).

The constituent of *C. ruspolii* water extract that stains yellow with molybdate did not elute into any fraction. This could indicate that either it was below the detection limit of molybdate reagent or strongly adsorbed to the column packing material and not eluted into any fractions collected (Figure 7.6d). Thus, C₁₈ column was selected as a suitable technique to be used in combination with other column and planar chromatographic techniques for isolation and purification of active pooled fractions of *C. ruspolii* and *Adenia* sp.

7.5.4. PTLC profiling of CRPC and EHI test

The PTLC purified major fluorescent constituents of CRPC that fluoresce blue and yellow could be flavonoids (Figure 7.7). This is because detection of flavonoids on TLC or PTLC with fluorescent indicator at F_{254 nm} is usually performed under UV-

light at 254 nm (for those flavonoids that cause fluorescence quenching) or at 366 nm; depending on the type of structure, flavonoids show yellow, green or blue fluorescence) (Waksmundzka-Hajnos *et al.*, 2008). These blue and yellow fluorescent compounds of CRPC exhibited strong EHI properties. The first stage larvae were stretched and non-motile in those wells incubated with supernatants from these bands. Being stretched and lack of larval motility could be due to the effect of partially purified blue and yellow fluorescent constituents that might inhibit egg hatch as well as cause permanent paralysis or death of larvae.

7.5.5. EHI tests of partially purified bands from active fractions of *C. ruspolii*

Supernatants from bands 1, 2 and 4 of CRPA (Figure 7.8a), 1-4 of CRPB (Figure 7.8b) and 6, 7, 10 and 11 of CRPC (Figure 7.8c) were exhibited significant anti-parasitic properties compared to controls. Some supernatants such as the lower bands from CRPA and CRPB and the blue and the yellow bands from CRPC exhibited both EHI and LMI properties. In those fractions with observed LMI properties, the first stage larvae were stretched and did not move. This effect was seen after 24 h incubation with plant extracts. Upon further incubation for another 24 h, no larvae showed any motility and remained stretched. This effect indicates that those partially purified supernatants from active bands did contain PSMs with anti-parasitic properties.

The pH of crude extract and PTLC fractions of CRPC determined using pH meter was greater than 4 (Figure 7.8d). Hatching of nematode eggs does not occur if the pH of the medium is less than 2 during the incubation period (Moinuddin *et al.*, 2011). This is because lower pH (high acidic medium) causes coagulation of germinal mass

of the parasite eggs during incubation. Thus, the anti-parasitic properties of partially purified bands from Bio-Gel P-2 active pooled fractions on PTLC are unlikely due to pH change to incubation medium. However, the activity exhibited might be due to other mechanisms such as interaction of active constituents with cell membrane structure of the parasite eggs or larvae. For instance, the active constituents of these fractions could bind to lipids or hydrolyse chitin, a polymer of β -1, 4-linked N-acetylglucosamine that is an essential structural component of shells of nematode eggs (Rao *et al.*, 2005). The eggs shell of nematodes consists of up to five layers depending on the species (Stein and Golden, 2015), but the most common form has three layers (Smyth, 1994). The outer vitelline layer is derived from oolemma and has a membrane-like structure. The middle chitinous layer is (the thickest layer that provides structural strength to the egg shell due to the presence of chitin micro fibril core (providing tensile strength) with collagen-like protein coat (providing rigidity). It also acts as a sieve and preventing larger molecules reaching the lipid layer (Smyth, 1994). The innermost lipid layer is rich in lipoproteins and represents the main permeability barrier of the eggs shell. Therefore, the nematode parasite egg inhibition properties of fractions could also be due to induced alterations to the egg shell that subsequently changes in the perivitelline fluid surrounding the larvae (D'Angelo *et al.*, 2014). Moreover, the constituents of partially purified bands and crude extract could also cause permeability changes to the eggshell and interfere with larval development.

7.5.6. EHI tests of partially purified bands from active fractions of *Adenia* sp.

The EHI efficacy of the partially purified bands on PTLC from active pools of *Adenia* sp. indicated that active constituents responsible for the observed anti-parasitic activity are slow migrating, hydrophilic and highly polar compounds.

The supernatants of partially purified bands 1, 3, 4 and 8 from ASPA (Figure 7.9a); 1-3 and 4 from ASPB (Figure 7.9b) and 1-3 from ASPC (Figure 7.9c) showed greater than 70% EHI at full strengths. The serially diluted lower strengths also showed dose dependent EHI activity. In particular, supernatants of bands 1, 3 and 4 from ASPA showed strong EHI and first stage larvae inhibition properties (Figure 7.9a, d) as all first stage larvae were observed stretched and non-motile before stopping the hatching process with Lugol's reagent. The Bio-Gel P-2 active pooled fraction of *Adenia* sp. (ASPA) is highly foamy in water solution and it could be rich in saponins. Saponins are glycosides with detergent properties due to the presence of both lipid-soluble (the steroid or triterpene) and water-soluble (the sugar) moieties in the same molecule (Bernhoft, 2010). The strong larval paralysis/ larvicidal properties of saponins might be due to their ability to form complexes with sterols such as cholesterol and lophenol (Runners, 2004) in larval membrane and then disrupt cell membranes (Doligalska *et al.*, 2011). Many studies have revealed that saponins are among the most active compounds in terms of nematotoxic activity because of their specific interactions with cell membranes and collagen proteins present on the cuticles of the parasite larvae, causing changes in cell membrane permeability and cellular death (Argentieri *et al.*, 2008; Eguale *et al.*, 2011).

7.5.7. Isolation of compounds from active pooled fractions of *C. ruspolii*

7.5.7.1. Isolation and purification of compounds from *C. ruspolii* pool A (CRPA)

All constituents of CRPA were eluted in water fractions on Sephadex LH-20 indicating that they are preferentially water soluble and polar compounds. The isolation and purification of CRPA on Sephadex LH-20 resulted in the purification of three compounds based on vanillin stained chromatogram: the pink spot with R_F -value of 0.80 that partitioned into fraction 22; the green spot with R_F -value of 0.60 that partitioned into fractions 13 and 14 and the brown spot with R_F -value of 0.13 and exclusively partitioned into fractions 19 and 20 (Figure 7.10). The very close migrating constituents of CRPA that stained green with vanillin reagent (spots B and C; Figure 7.10) were seen as one compound on TLC at full strength. This might be due to the interactions between constituents in the pool that did not assist complete separation of the two compounds and hence seen as single green spot on chromatogram. On the other hand, these compounds had different R_F -values in Sephadex LH-20 fractions 15 and 16 as seen in Figure 7.11. Therefore, they could be different compounds with different R_F -values or the same compound partitioned into neighbouring fractions but differ in amount that affected their migration rates as exhibited in their R_F -values. The vanillin stained TLC chromatogram also reaffirmed the degree of purity of the Sephadex LH-20 isolated and purified water fractions from CRPA (Figure 7.11).

In experiments conducted to further purify Sephadex LH-20 fractions 13-20 on C_{18} column, constituents of fractions 13-18 were again eluted in deionized water. Therefore, moving from Sephadex LH-20 to C_{18} column did not bring any

improvement in further purification of constituents of Sephadex LH-20 fractions 13-18. However, the Sephadex LH-20 water fractions 19 and 20 (Figure 7.11) were now eluted in 20% MeOH on C₁₈ column (Figure 7.12). This result is in agreement with the finding in section 7.4.3 where the same constituent from *C. ruspolii* crude extract was eluted in 20% MeOH on C₁₈ column. Furthermore, this result supports the view that Sephadex LH-20 fractions 13, 14, 19 and 20 were pure compounds.

The slight difference in R_F-value of the slow migrating and green stained spot in fractions 16 and 17 (spot B) could be due to difference in amount of this constituent partitioned into these fractions, interaction between constituents or difference in solvent equilibration of the respective chromatographic tank during chromatogram development (Figure 7.13).

The final purifications for fractions 14, 16 and 17 were carried out on washed, non-fluorescent preparative TLC plates with plastic backings. The aim of washing was to avoid any potential contaminants from the PTLC matrix during purified sample recovery from PTLC plates that would interfere with NMR and MS analysis. The final TLC run for supernatants recovered from PTLC purified bands showed that only one compound from 14, two compounds from 16 and two compounds from 17 were well stained with vanillin reagent and therefore these compounds are more likely pure and real compounds (Figure 7.15). Moreover, PTLC purified bands (B-1 and B-5) from C₁₈ fractions 14 and 16 respectively had the same colour and R_F-value. Thus, they are assumed to be the same compound. Similarly, those purified bands (B-4 and B-3) from C₁₈ water fractions 16 and 17 respectively had the same colour and R_F-value, therefore; they are also assumed to be the same compound (Figure 7.15). The remaining supernatants (those recovered from other bands marked

on PTLC strips) could be artefacts. The artefact formation could occur either due to prolonged heating of TLC strips stained with vanillin reagent or the staining reagent interacted with residual acidic solvent (BAW) used for PTLC development. This is because the standard heating temperature and duration (time) for TLC stained with vanillin in conc. H_2SO_4 is 120°C for 5 min. Prolong heating at this temperature (as used in this study) results in charring of polymeric binders used to bind coating materials to plates. Acidic and/or basic residual solvents from solvent system used for TLC development also affect the visualization reactions of the staining reagents (Dykes and Rooney, 2006).

7.5.7.2. Isolation and purification of compounds from CRPB

The isolation and purification of CRPB on Sephadex LH-20 did not result in the purification of any compound eluted in water fractions (Figure 7.17 and 7.18). This unsuccessful purification on Sephadex LH-20 might be because of one of four reasons. Firstly, the crude extract was prepared by maceration using deionized water and only polar, water soluble components were extracted. Secondly, CRPB itself was the Bio-Gel P-2 water pooled fraction and its constituents are also polar and water soluble. Therefore, it is less likely to elute such compounds in less polar solvents. Thirdly, the sample was loaded on to the column in water solution (water sample) rather than in slurry form thus there was no time for loaded sample to be adsorbed to the packing material before the first eluent used. Fourthly, the first 30 fractions (4 ml each) collected were water fractions. The Sephadex LH-20 fractions 56-58 appeared as smears near the origin on chromatogram in the first run (Figure 7.21a). They also appeared as blue band very close to the solvent front (re-run) after molybdate staining (7.21b). The smears near the origin might be due to solubility problem of

samples in n-butanol-acetic acid-water (2:1:1 v/v/v) that used to reconstitute them for sample loading on TLC. The appearance of the spots of these fractions as a band during re-run could be due to sideways diffusion and overlap of spots in BAW (4:1:1 v/v/v: the solvent used for TLC development).

Chromatographic characterization of CRPB and its Sephadex LH-20 purified pooled fractions were also done by examining the chromatograms in daylight, under UV-light and after staining with various staining reagents. The chromatogram examined in daylight and under UV-light revealed that neither CRPB nor its purified pooled fractions had contained constituents seen in daylight or under UV-light (Figure 7.23). This result indicates that CRPB and its Sephadex LH-20 purified pooled fractions do not contain compounds that absorb and reflect light with characteristic wavelength in daylight or UV-active compounds such as flavonoids. TLC profiling of UV-active phytochemicals are usually assessed under UV-light at 254 nm (shorter wavelength) and 366 nm (longer wavelength) to be seen as dark or fluorescent spot(s) respectively (Lalrinzuali *et al.*, 2015).

Iodine is a very useful universal reagent and the use of iodine vapour enables detection of separated substances rapidly and economically before final characterization is done with a group specific reagent. Iodine molecules stain spots of many organic molecules and give brown chromatographic zones on a yellow background (Joshi, 2012; De *et al.*, 2010). In this experiment, none of the Sephadex LH-20 purified pooled fractions from CRPB was stained with iodine. However, the separated spots of CRPB were stained brown on yellow background with iodine vapour. This indicates that CRPB did contain organic constituents such as

unsaturated compounds with free C-C double bond(s) that add or form complex with iodine.

Vanillin in sulphuric acid is also a universal reagent that stains a range of organic compounds such as plant secondary metabolites containing nucleophile that react with the aldehyde functional group in vanillin (Dykes and Rooney, 2006). All the purified pooled fractions of CRPB (Figure 7.28) were stained pink with vanillin and had the same R_F -value. This indicates that they are the same compound: the relatively least polar and fast migrating constituent of CRPB. Moreover, the three other constituents of CRPB were also distinctly stained with vanillin as pink, orange and dark green spots (Figure 7.28b). These colour differences of separated spots of CRPB might be related to their chemical and electronic structures.

The spot of purified pool fraction (56-58) that developed in chloroform-methanol-acetic acid (10:2:1 v/v/v) and stained pink with vanillin reagent revealed the presence of dark violet at the centre of the spot upon prolonged heating. This dark spot could be an impurity having the same R_F -value as the target compound or an artefact formed due to the acidic residual solvent used for TLC development or the target compound might be degraded and charred upon prolonged heating.

In general, chromatogram analyses of Sephadex LH-20 purified pooled fractions from CRPB revealed that the purified compound is polar, partitioned into neighbouring fractions, stained pink with vanillin, having R_F -values of 0.73 and 0.2 in BAW and CAM solvent systems respectively (Figures 7.28 and 7.29).

During further purification, the vanillin stained PTLC strips and the corresponding TLC profile of supernatants of PTLC purified bands also shown that pooled fractions

(49-51 and 56-58) contained only one compound per pool: one of the constituents of CRPB that migrated very fast on TLC and stained pink with vanillin reagent (Figure 7.30) in BAW solvent system. The TLC chromatogram of recovered supernatants from purified bands showed that the spots were well stained with vanillin reagent and appeared as single pink spot with the same R_F -value. This re-affirmed that the compound partitioned into both pooled fractions is real and assumed to be the same compound.

7.5.3.3. Isolation and purification of compounds from CRPC

The blue fluorescent compound isolated on Sephadex LH-20, from CRPC and further purified on C_{18} column chromatography followed by PTLC is polar, completely eluted in water fraction with R_F -value of 0.53. Moreover, it is a compound that does not stain with any reagents used in this study including vanillin in conc. H_2SO_4 reagent (Figure 7.34b). However, it remained blue fluorescent spot under UV-light at 366 nm after being stained with antimony (III) chloride in chloroform reagent that is used for detection of flavonoids (data not shown). Therefore, the blue fluorescent constituent of CRPC could be a flavonoid. For instance, the non-stainable nature of the blue fluorescent spot with staining reagents such as vanillin in concentrated sulphuric acid (universal reagent) could be due to lack of functional group in its structure that reacts with the aldehyde functional group of vanillin in acidic medium or the reactive functional group of a compound may be inaccessible due to steric effects. The blue fluorescent compound that further purified on PTLC resulted in two blue fluorescent bands. This indicates that the blue fluorescent compound could be unstable and undergo degradation due to hydrolytic reaction in water solution upon storage for long time (Loftsson, 2014).

7.5.8. Isolation and purification of compounds from *Adenia* sp. pool A (ASPA)

The *Adenia* sp. Bio-Gel P-2 pool A (ASPA) fractionated on Sephadex LH-20 had resulted in four groups of fractions (see section 7.4.10.1): yellowish and foamy (7-12), light turbid and foamy (13-16), light turbid but not foamy (17-20), highly turbid but not foamy (21-28).

The foamy nature of ASPA LH-20 fractions 7-12 remained frothy as long as in water solution and hence could contain saponins which are glycosides composed of a hydrophobic aglycone and hydrophilic sugar residues that foam in water solution. Foam formation or being frothy in water solution that persists for more than 10 minutes is the standard chemical test method for the presence of saponins (Tiwari *et al.*, 2011). The Sephadex LH-20 fractions (7-12) have also shown two major, slow and close migrating and donut shaped spots on chromatogram that stain green with vanillin and then turn brown upon prolonged heating. The ASPALH-20 fraction-9 was selected as a representative sample of Sephadex LH-20 fractions (7-12) for further isolation and purification of the two major compounds on C₁₈ column. The vanillin stained chromatogram of C₁₈ fractions (Figure 7.39) revealed that all constituents of ASPALH-20-9 were also eluted in deionized water on C₁₈ column. This implies that changing the polarity of the column packing material from Sephadex LH-20 with both lipophilic and hydrophilic nature to relatively apolar modified reversed phase C₁₈ did not improve the isolation and purification of the early eluted active constituents of ASPA (spots A and B). However, those constituents of ASPA with similar molecular sizes and R_F-values but possibly differ in polarity that were eluted in water fraction-9 on Sephadex LH-20 now eluted into different water fractions on C₁₈ column. There are two main reasons for this

unsuccessful isolation and purification of ASPA major constituents on C₁₈ column. Firstly, ASPALH-20-9 was loaded on to C₁₈ in a relatively large volume of de-ionized water compared to the column bed volume; therefore, the sample did not get sufficient time to be adsorbed to the stationary phase before the first eluent was used. Secondly, the constituents of this sample were originally from the water crude extract, hence, it is less likely to partition into any less polar MeOH gradient eluents used. Thus, one of the water fractions from C₁₈ column was deemed to be isolated and purified on preparative planar chromatography.

The C₁₈ water fraction-2 loaded onto PTLC and developed in BAW (4:1:1 v/v/v) resulted in the isolation of the two major constituents of ASPA: spots A and B. Based on the degree of purity confirmed from vanillin stained chromatogram, the slow migrating (B_{1/1}) with R_F-value of 0.23 and the relatively fast migrating with R_F-value of 0.27 (B_{3/1} and B_{4/1}) were identified as pure compounds and labelled as compound A and B respectively (Figure 7.40). These purified compounds were used for EHI tests and NMR analysis (Chapter Eight).

7.5.9. The EHI tests of isolated compounds from *C. ruspolii* pooled fractions

The sequential application of Sephadex LH-20 and reversed phase C₁₈ columns followed by preparative TLC had resulted in isolation and purification of three compounds from CRPA, one compound (each) from CRPB and CRPC respectively. Isolated compounds from all active pooled fractions of *C. ruspolii* were tested for their anti-parasitic properties and exhibited significant ($P < 0.05$) EHI against *T. circumcincta* eggs compared to negative controls although the activities vary with concentration of purified compounds. For isolated compounds, only 20% (v/v) of

supernatant of each sample was used for the test. This likely explains why observed EHI activity of purified compounds was generally lower than the crude extract but it was significantly greater than the negative controls. In the previous tests for crude extract and Bio-Gel P-2 fractions, it was observed that their activities were dependent on the dose (concentration/strength). Some of the purified compounds from active pooled fractions exhibited strong biological activity (such as nematode EHI) at very low concentration. The observed anti-parasitic properties might be related to a strong relationship between the structure and pharmacological properties of bioactive compounds (Tiwari *et al.*, 2014). In general, bioactivity of any bioactive compound is not only dependent on concentration (dose) and structure but also on combination of both dose-effect and structure-function relationship (Engström, 2016).

7.5.10. EHI tests of isolated and purified compounds from ASPA

Sequential application of column chromatography followed by PTLC also resulted in purification of two major compounds from ASPA. The ASPA, its partially purified fractions and isolated compounds A and B also showed strong anti-parasitic properties very few live larvae were recorded (Figure 7.42). The crude extract, ASPA, Sephadex LH-20 and C₁₈ water fractions and PTLC purified compounds A and B could contain active compound(s) that inhibit egg hatching or cause permanent first stage larvae paralysis or death. The purified compound B also showed higher EHI activity compared to compound A. This could be related to higher concentration (dose) or the structure of compound B might better interact with target receptor in the membrane structure of egg shell or first stage larvae.

The *Adenia* sp. water crude extract, ASPA, its various water fractions and purified compounds A and B from ASPA are known for their being frothy or foam formation properties in water solution which is an indicator for the presence of saponin. Doligalska *et al.* (2011) reported that glycosylated saponins at both C-3 and C-28 induce a permeability change in cuticle and cell membranes of nematodes and results in cell death. Thus, the first stage larvae motility inhibition properties of *Adenia* sp. water crude extract, its various water fractions and purified compounds A and B might be due to the presence of glycosylated saponins.

7.5.11. Qualitative characterization and semi-quantitative determination of yellow-stained component of *C. ruspolii* extract

A constituent of water crude extract of *C. ruspolii*, phosphorylated metabolites and serially diluted authentic $\text{NaH}_2\text{PO}_4 \cdot 2\text{H}_2\text{O}$ (at all concentrations) were all stained yellow with molybdate at similar position on TLC (Figures 7.43 and 7.44). Similarly, the molybdate stained electrophoretogram of *C. ruspolii* crude extract revealed that a constituent that stains yellow with molybdate and turns blue upon exposure to natural sunlight is a negatively charged substance with similar charge-to-mass as $\text{NaH}_2\text{PO}_4 \cdot 2\text{H}_2\text{O}$ under the same condition in HVPE. Both samples migrated to anode and had average ionic mobility of 0.53 at pH 2.0 (Figure 7.45) and 1.27 at pH 6.5 (Figure 7.46) respectively. Moreover, both samples migrated only a little slower under acidic condition (pH 2.0) than nearly neutral at pH 6.5. The rate of colour change from yellow to blue was enhanced by prolonged exposure to natural sun light. The level of the yellow stained constituent in the *C. ruspolii* crude extract was semi-quantitatively estimated by colorimetric method and found to be about 7.5 $\mu\text{g}/\mu\text{l}$ of crude extract (48 mM). Furthermore, the estimated level of yellow stained constituent in this sample was in the range of the amount of inorganic phosphate reported for various plant tissues in distinctly different plant species. For instance, Delhaize and Randall (1995) reported that phosphate concentration in the fresh tissue of mutant *Arabidopsis thaliana* was in the range of 20-60 mM. Both chromatogram and electrophoretogram experiments were supported the speculated inorganic phosphate in the *C. ruspolii* water crude extract

However, this yellow stained constituent did not elute in any solvent during fractionation of *C. ruspolii* crude extract on C_{18} column (see section 7.4.3). Thus, the

possibility of organic compounds such as flavonoids having the same charge-to-mass ratio as inorganic phosphate and stain yellow with molybdate need to be investigated (Ortutu and Aremu, 2016; Rebiai and Lanez, 2012; Ibrahim *et al.*, 2013; Shabbir *et al.*, 2013).

In general, the current research interest on medicinal plants exhibits the demand for plant drugs throughout the world because of its valuable phytochemicals (Veeresham, 2012). Phytochemical investigations are carried out to discover pharmacologically active substances that can be formulated as new drugs or used as blue print to synthesise new bioactive compounds with pharmaceutical and biomedical importance (Atanasov *et al.*, 2015; Bajpai *et al.* 2016). Nowadays, various chromatographic techniques lead to exploration of new bioactive compounds of plant origin that can also be used directly in pharmaceutical and agrochemical industries (Ingle *et al.*, 2017). The chromatographic and spectral fingerprints also play an important role in the isolation, purification and identification of bioactive compounds of natural product origin (Bonikowski *et al.*, 2016). There are a number of chromatographic techniques employed for isolation, purification and profiling of constituents of a mixture in medicinal plants. For instance, bioassay-guided purification of 60% EtOH crude extract of *Desmodium adscendens* on Sephadex LH-20 resulted in the isolation of two isomeric glycosylated flavonoids with antioxidant properties (Zielińska-Pisklak *et al.*, 2015). Masoko and Nemudzivhadi (2015) reported that two structurally related phytosterols with antibacterial properties were isolated and purified by sequential application of column and preparative TLC from *Ricinus communis* that traditionally used in South Africa for the treatment of wounds, sores and boils.

In conclusion, the preliminary experiments conducted to assess the suitability of both open column and planar chromatographic techniques were informed us to use both techniques sequentially during further isolation and purification of active pooled fractions. The chromatographic profiling that carried out using UV-light and various staining reagents at each stage of isolation and purification helped us to assess the number and nature of constituents, spot colour, R_F -value and degree of purity of fractions and purified compounds. The sequential applications of column chromatography followed by PTLC resulted in the isolation and purification of three compounds from CRPA; one compound (each) from CRPB and CRPC and two compounds from ASPA. The purities of these compounds were confirmed as they appeared as single spot on chromatogram under UV-light or after stained with various reagents in particular with vanillin reagent. The EHI and for some subjectively observed LMI properties of purified compounds have supported the view that the two medicinal plants have anti-parasitic properties that interfere the different stages of the parasite life cycle.

Chapter Eight: Analytical and spectroscopic characterization of some anthelmintic compounds isolated from *Adenia* sp. and *C. ruspolii*

8.1. Abstract

Analytical and spectroscopic characterization of anthelmintic compounds isolated from two Ethiopian medicinal plants was carried out to propose and/or elucidate their structures. The structures of two triterpenoid saponins (A and B) isolated from *Adenia* sp. were successfully proposed based on the nature of the compounds, tandem mass (MS/MS) data, sugars detected on TLC after TFA hydrolysis and supportive information from their one dimensional proton nuclear magnetic resonance (1D- ^1H -NMR) and two dimensional proton nuclear magnetic resonance (2D- ^1H -NMR), bioassay data and the literature. However, similar structure proposal/elucidation for compounds from *C. ruspolii* was not achieved due to lack of sufficient sample size to run carbon-13 nuclear magnetic resonance (^{13}C -NMR) and distortionless enhancement by polarization transfer (DEPT-135), contamination of some purified compounds with ill-characterised substances from the preparative thin layer chromatography (PTLC) matrix, and in some cases NMR and MS data did not support each other. The triterpenoids isolated from *Adenia* sp. pool A (ASPA) may have closely similar oleanane type core structures and the same trisaccharide attached to the hydroxyl group at C-3 although compound A was found to also contain a galactose unit attached to its C-28 carboxyl functional group. A trisaccharide consisting of rhamnose, xylose and unknown sugar may have been common to both A and B. The fourth sugar monomer, galactose, may have been attached to the carboxyl functional group of compound A. The unknown sugar may

have an unusual double bond in the pyran ring and the formula of $C_5H_8O_4$. Alternatively, the trisaccharide consisting of rhamnose, xylose and the third sugar that migrated very closely to rhamnose on TLC chromatogram of TFA hydrolysate may be quinovose (6-deoxy-D-glucose and an epimer of rhamnose with chemical formula of $C_6H_{12}O_5$). In conclusion, the anthelmintic properties exhibited *in vitro* by *Adenia* sp. water extracts could have arisen from saponins.

8.2. Introduction

Spectroscopy is the study of the interaction of electromagnetic radiation (EMR) with matter. Several spectroscopic and analytical techniques are used in the identification and characterization of compounds from natural products, including nuclear magnetic resonance (NMR), ultraviolet spectroscopy, infrared spectroscopy, mass spectrometry (MS) and X-ray crystallography (Kwan and Huang, 2008). NMR is a technique used to determine a compound's unique structure through identification of its carbon-hydrogen framework (Fukushi, 2006). Mass spectrometry (MS) is based on the production of gaseous, positively or negatively charged ions from chemical species that are subsequently separated according to their mass-to-charge (m/z) ratio and detected (Glish and Vachet, 2003). Combined with collision-induced dissociation (CID), a second MS can be used to provide tandem mass spectrometry (MS/MS). Using both NMR and MS methods, structures of organic molecules may be elucidated, ideally by using all of the different NMR experiments (Fuloria *et al.*, 2013), i.e. proton nuclear magnetic resonance (^1H -NMR), carbon-13 nuclear magnetic resonance (^{13}C -NMR), distortionless enhancement by polarization transfer (DEPT), heteronuclear spin quantum correlation (HSQC), heteronuclear multiple bond correlation (HMBC), ^1H - ^1H correlation spectroscopy (COSY) and nuclear overhauser enhancement spectroscopy (NOESY). The objective of this chapter was to characterize and propose/elucidate structures of compounds isolated from active fractions of both plants responsible for the observed activities using such chromatographic, analytical and spectroscopic methods. Due to lack of sufficient amount of purified sample needed for analysis, only a restricted number of NMR experiments were conducted. Here, only proton NMR combined with MS (where

possible) were used; the other types of NMR techniques particularly ^{13}C -NMR and DEPT-135 could not be employed.

8.3. Materials and methods

Briefly, for *Adenia* sp., compounds A and B from the C₁₈ water fraction-2 of ASPA were purified on PTLC in 4:1:1 v/v/v BAW (see section 7.4). For *Cissus ruspolii*, compounds *C. ruspolii* pool A Sephadex LH-20 fraction-13 (CRPALH-20-13 or compound C) and *C. ruspolii* pool A Sephadex LH-20 fraction-20 (CRPALH-20-20 or compound A) were obtained from C₁₈ water and 20% MeOH fractions of CRPA, respectively. The proton NMR spectra were generated as detailed in section 2.11. The proton NMR data alone was not sufficient to propose/elucidate structures of these compounds and therefore MS analysis was also undertaken. Thus, a water sample containing compounds A and B obtained from C₁₈ water fraction-1 originally from ASPA and CRPALH-20-20 (compound A) from CRPA were submitted for MS analysis. Deuterium oxide (D₂O) and acetonitrile-water (1:1) solvents were used for NMR and MS analyses, respectively (see section 2.11 for details).

8.4. Results and Discussion

8.4.1. 1D-¹H-NMR spectra of compounds from *Adenia* sp. pool A (ASPA)

The 1D-¹H-NMR spectra of compound A and B are shown in Figures 8.1 and 8.2, respectively.

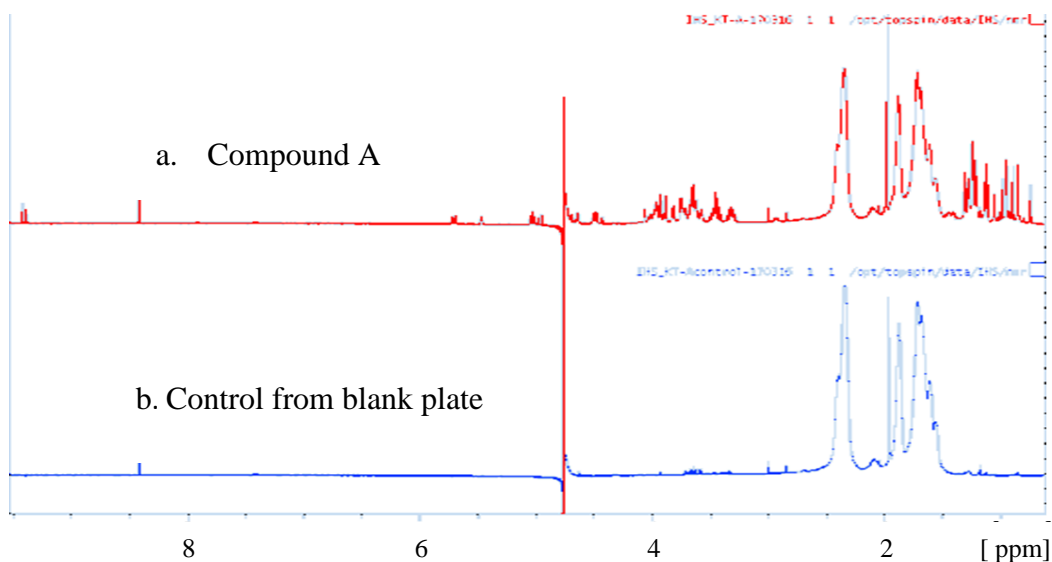


Figure 8.1. 1D-¹H-NMR spectra of compound A (*Adenia* sp.) and blank. Spectrum of compound A (a) and of a control from a blank plate (b) (sample source is detailed in section 2.10 and Figure 2.5).

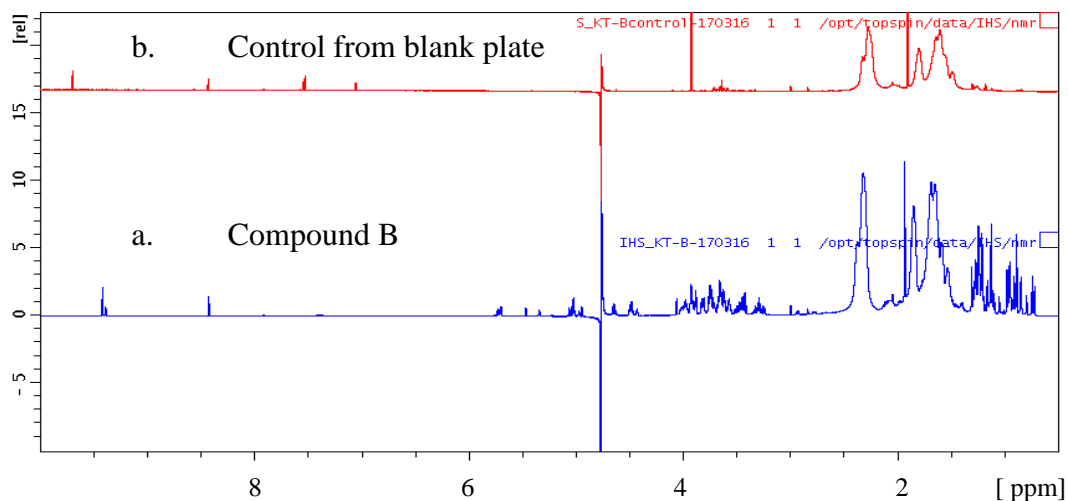


Figure 8.2. 1D-¹H-NMR spectra of compound B (*Adenia* sp.) and control. Spectrum of compound B (a), spectrum of control from blank plate (b) (sample source is detailed in section 2.10 and Figure 2.5).

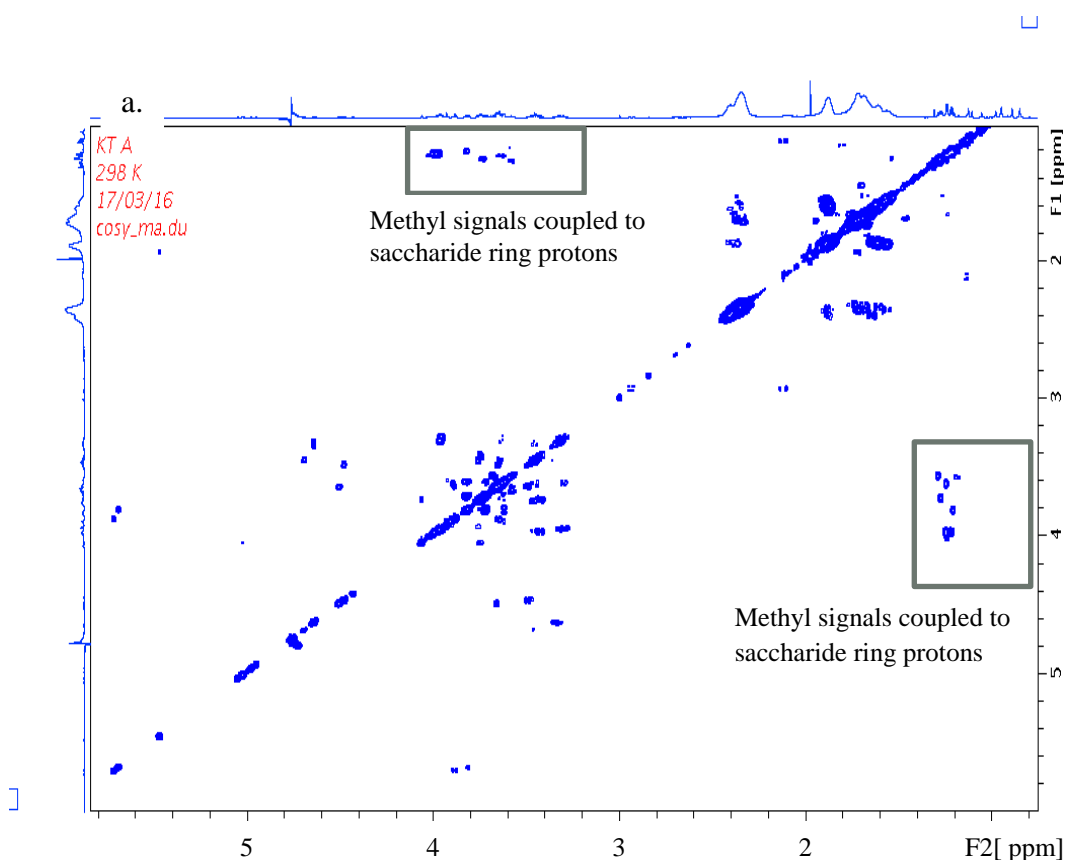
In these spectra, the most intense peaks occurred around 1.4-2.2 ppm arising from probable methyl groups (Figures 8.1a and 8.2a). The less intense peaks around 2.4-4.2 ppm arise from both the methylene ($-\text{CH}_2-$) as well as the methine groups. In the compound A spectrum, signals of protons between 1.4-2.4 ppm could be due to methyl ($-\text{CH}_3$) protons attached to saturated carbon atoms and the methylene protons of carbon atoms with no hydroxyl group on neighbouring carbon atoms. The signals between 3.8-4.0 ppm could also be due to proton-proton couplings of aglycone and sugar moieties. The signals of protons between 4.5-6.0 ppm may be due to proton signals of residual hydroxyl functional group(s) of the target compound or its minor impurities. This is possible because hydrogen-deuterium exchange is a reversible process and thus small signals of hydroxyl functional group protons are observed in a ^1H -NMR spectrum of a highly deuterated sample. These types of proton signals are referred to as residual signals (https://en.wikipedia.org/wiki/Hydrogen-deuterium_exchange dated December 2016). Furthermore, the signals between 4.2-5.4 ppm may be due to the olefinic methine ($-\text{CH}=\text{CH}-$) groups. The signal greater than 8.0 ppm may be due to the residual carboxylic acid protons in the target compound, other minor constituent(s) in the mixture with the free carboxylic functional groups or due to the NMR solvent (as signal around 8.5 ppm is appearing in almost all 1D- ^1H -NMR runs including the controls).

Similarly, in the compound B spectrum, signals of protons between 1.4-2.2 ppm are due to methyl ($-\text{CH}_3$) protons attached to saturated carbon atoms and methylene protons in the target compound. The signals between 4.2-5.4 ppm may be due to the presence of olefinic methine group(s) in compound B. The signals of protons

between 5.5-6.0 ppm could also be due to residual hydroxyl functional group protons of sugar moieties or other minor impurities in compound B.

8.4.2. 2D-COSY NMR spectra of compounds from *Adenia* sp. pool A (ASPA)

The 2D-COSY spectra of the two compounds (A and B) were generated through NMR. Although the 1D- ^1H -NMR spectra were not strong enough to assign the coupling between neighbouring (vicinal) protons, it was suggested that the two compounds contained the same oligosaccharide with methyl proton signals coupled to saccharide ring protons as seen between 3.8-4.0 ppm (Figure 8.3). There are also many off-diagonal vicinal proton couplings other than those due to sugar moieties, thus possibly due to couplings between neighbouring protons in the aglycone moieties.



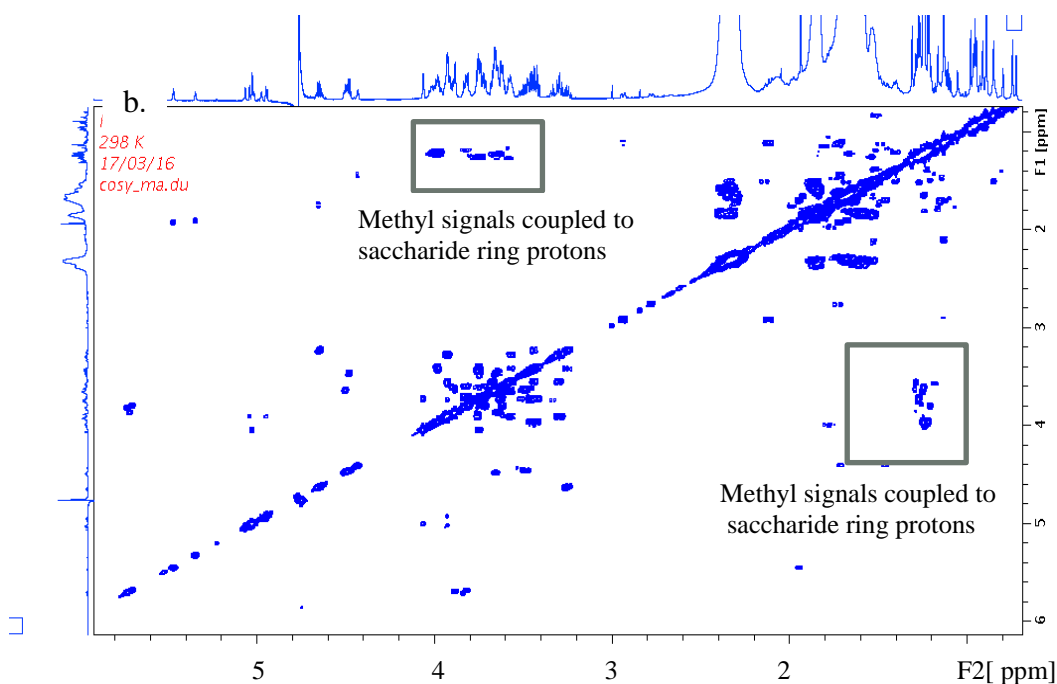


Figure 8.3. 2D-COSY spectra of compound A (a) and compound B (b) from ASPA.

8.4.3. MS spectra of compounds from *Adenia* sp. pool A (ASPA)

The MS spectra of the two compounds A and B isolated from *Adenia* sp. pool A (ASPA) are shown in Figures 8.4 and 8.5. Figure 8.4 shows the mass spectrum of the mixture that contains peaks for each compound present in the mixture with characteristic ionic species and has its unique molecular weight produced during soft ionization methods. The two major compounds of ASPA that migrate very closely on TLC and purified on PTLC for NMR analysis were selected based on their molecular ion mass as shown in Figure 8.4.

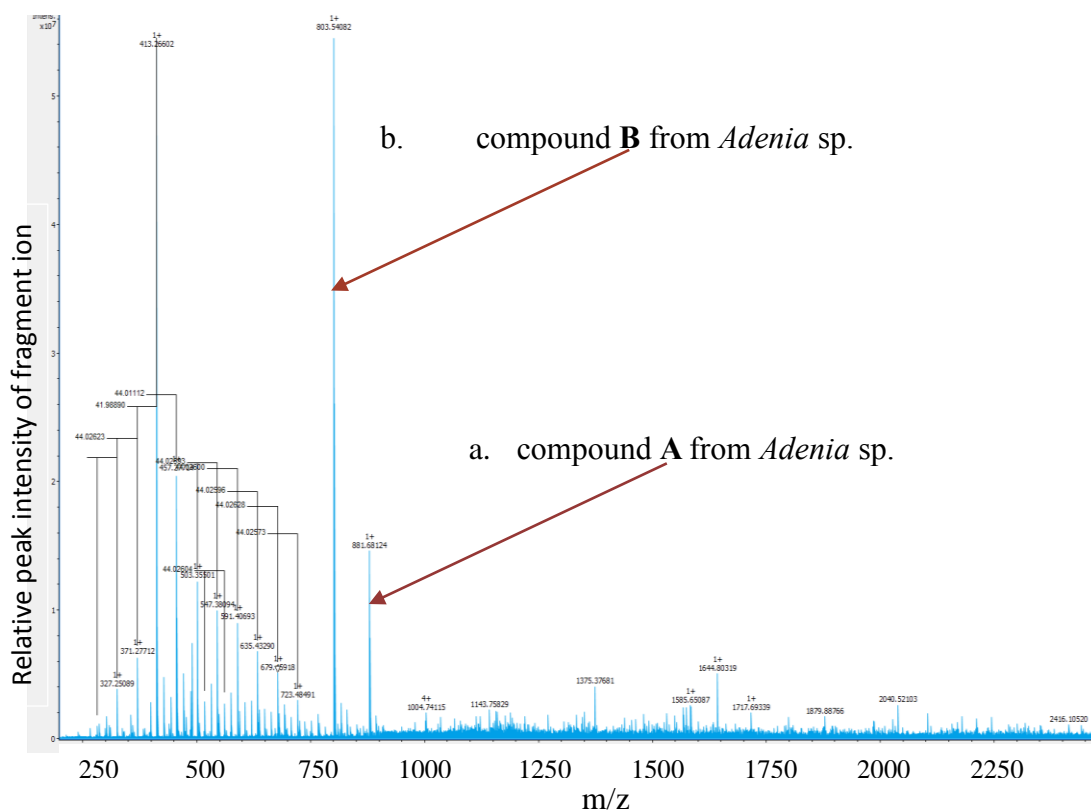


Figure 8.4. MS spectrum of a mixture containing A and B of *Adenia* sp. (C_{18} water fraction-1) with characteristic ionic species and their unique molecular weight. The two major and closely migrating constituents of ASPA: Arrows show compound A (a) and compound B (b) to be selected by the first MS as precursor ions for CID mode of fragmentation in MS/MS spectrometry.

At this stage, the only information derived from the mass spectrum is the molecular weight of components in the mixture, though one would like to see fragment ions that provide structural information for the components of interest. In Figure 8.5, the first mass spectrometer was used to select a single (precursor) mass that was characteristic of a given compound (A or B) in a mixture. The mass selected ions (in this case compounds of interest A and B that represent the major constituents of target sample) passed through a region one by one where they were activated to fall apart to produce fragment (product) ions by CID.

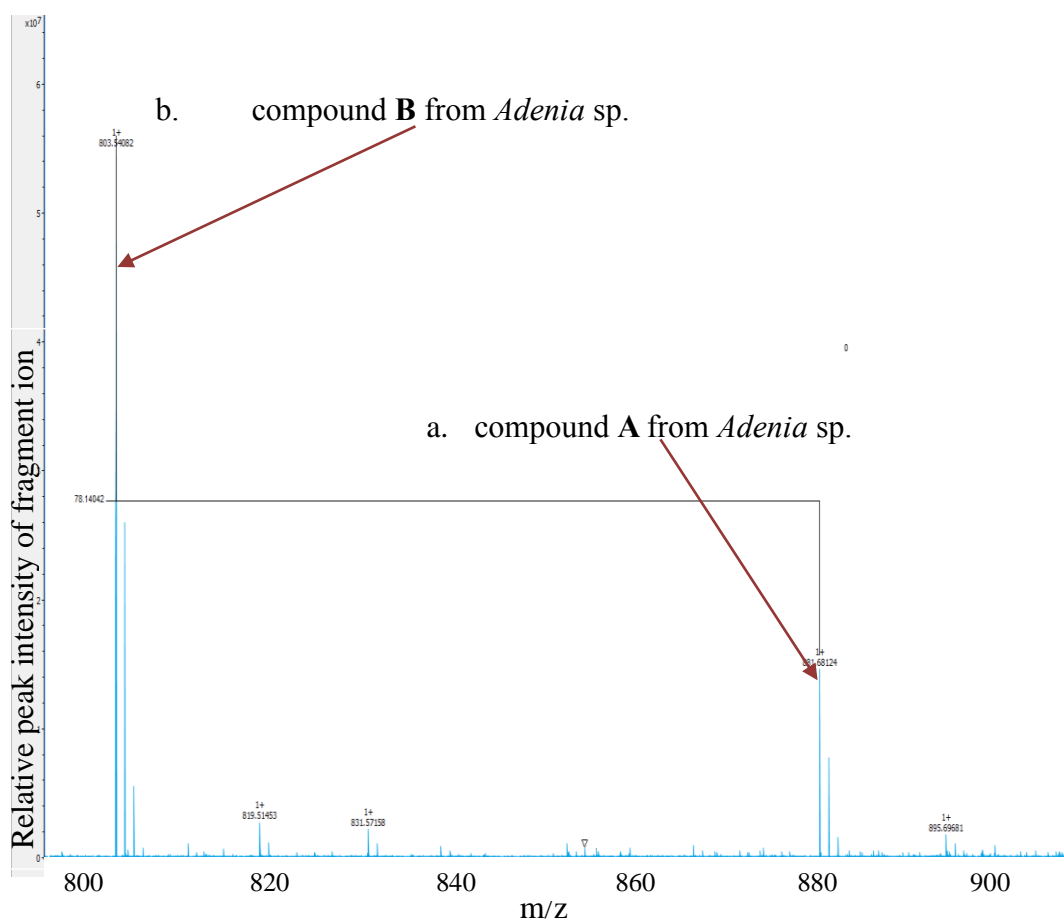


Figure 8.5. MS spectrum of mass selected ions. Compound A (a) and compound B (b) from *Adenia* sp. selected by the first MS as precursor ions for CID mode of fragmentation in MS/MS spectrometry. The mass difference between A and B is 78.140 g/mole. Arrows show the mass selected ions.

The second mass spectrometer was used to separate the fragment ions of compounds A or B separately according to mass-to-charge ratio. The resulting “MS/MS” spectrum (Figures 8.6 and 8.7 for compound A and B, respectively) consists only of product (fragment) ions from selected precursor, i.e. A or B.

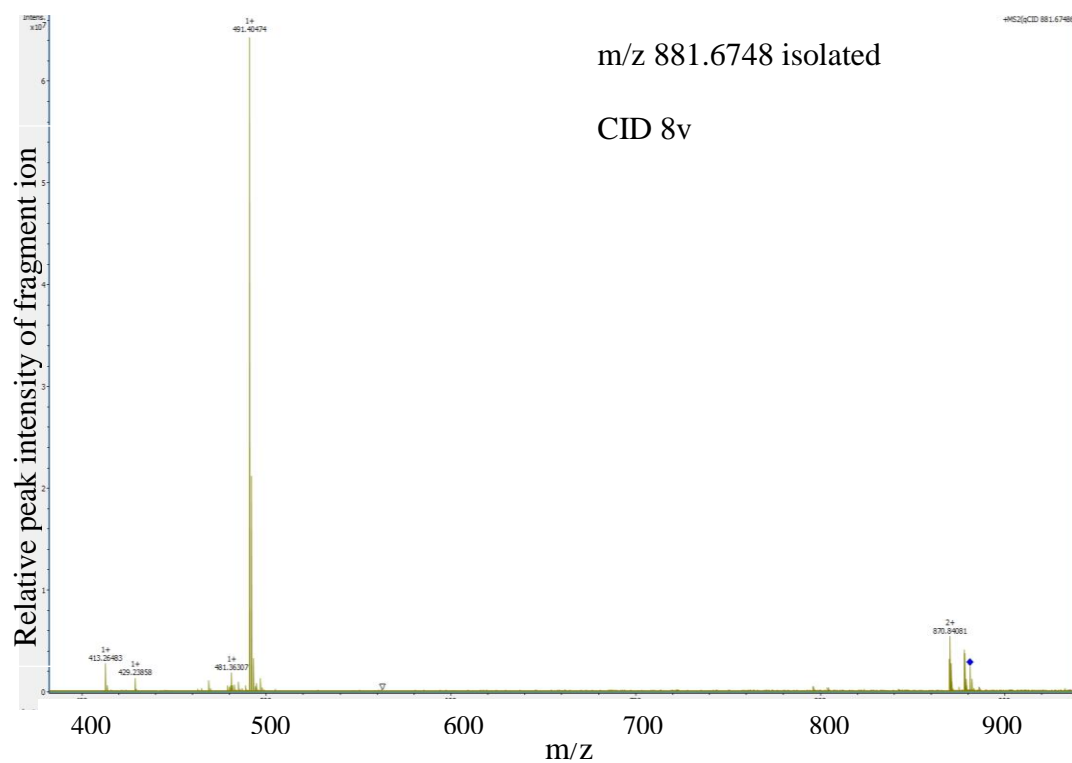


Figure 8.6. MS/MS spectrum of compound A (*Adenia* sp.) based on a selected parent ion mass. The diamond (♦) shows the mass of the presumed molecular ion (M^+) of compound A with $m/z = 881.6748$ g/mole; the most intense fragment peak derived from this, with $[M+1]^+$ at m/z 491.4047, is the base peak.

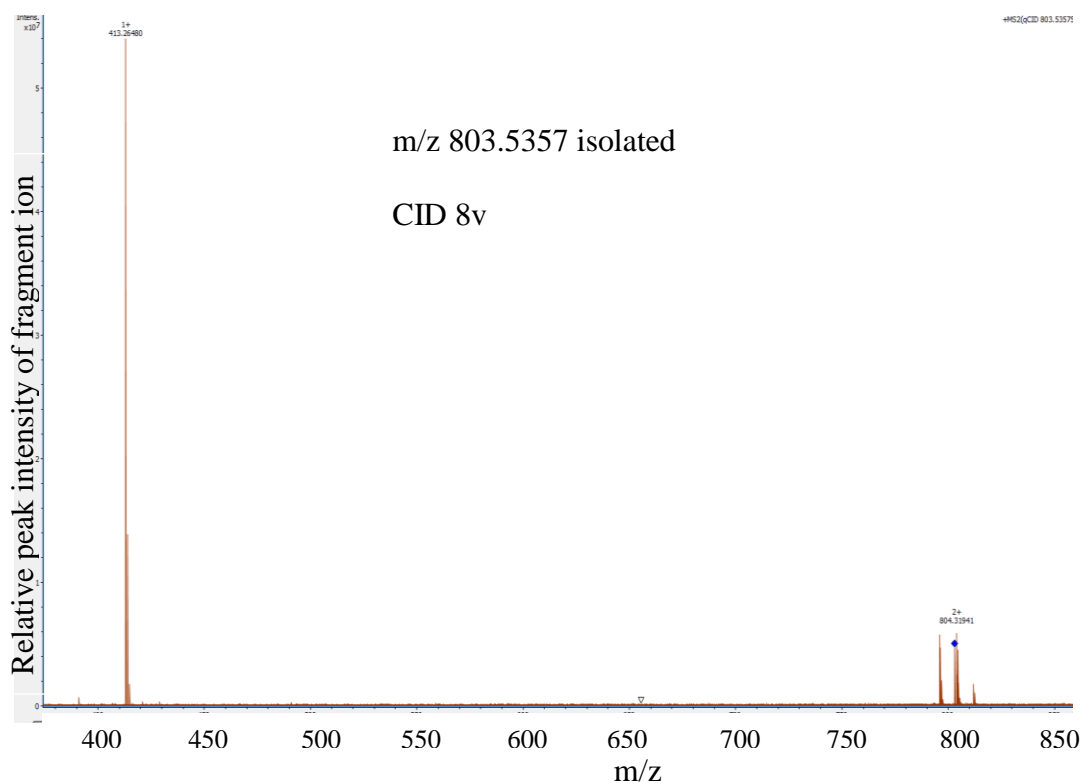


Figure 8.7. MS/MS spectrum of compound B (*Adenia* sp.) based on the selected parent ion mass. The diamond (♦) shows the mass of molecular ion (M^+) of compound B with $m/z = 803.5357$ g/mole; the most intense fragment peak derived from this, with $[M+1]^+$ at $m/z 413.2648$, is the base peak.

The m/z values of the presumed parent ions of compounds A and B were observed as 881.6748 (Figure 8.6) and 803.5357 (Figure 8.7) respectively. Thus, the mass of the parent ions A and B would be approximately 882 and 804 g/mole. To convert the masses into chemical formulae based on their chemical nature and most probable elemental composition, the conventional atomic masses used by chemists and others for any chemical calculations including structure elucidation were used. Thus, here, ^1H , ^{12}C and ^{16}O were used for mass calculations. However, mass spectroscopists are interested in the actual mass of the most abundant isotope of a given element. This is due to the fact that MS is basically designed to measure the mass of a given compound based on the actual masses of the most abundant isotopes of the elements in that compound. Structure elucidation is not only based on mass of a compound but

also correct application of the octet rule. Both lead to the same structure as far as the nature and elemental composition of the target compound is known. Moreover, structure elucidation is not only dependent on the data from MS but also uses data from IR, NMR and UV. Thus, the information from these spectroscopic techniques results in adjustment of number of a given elemental composition such as hydrogen atom that results in the adjustment of the determined molecular mass to elucidate the most probable structure of the target compound.

Honouring the above data, and atomic mass and octet rules used, and assuming that the ~881.6784 and ~803.5357 peaks observed in the spectra represent molecular mass of the (parent) ion, the formulae may be $C_{46}H_{74}O_{16}$ and $C_{45}H_{72}O_{12}$, respectively. Similarly, the formulae of the fragment base peaks of A and B with $[M+1]^+$ at m/z approximately 491.40474 and 413.26480 g/mole could be $C_{30}H_{50}O_5$ and $C_{29}H_{48}O$, respectively.

8.4.4. Interpretation of MS spectra to propose structures of compounds A and B from ASPA

To put forward proposed structures of compounds A and B, two possible scenarios (Scenario I and II) were developed using a series of arguments derived from the work carried out and relevant literature. For Scenario I, the proposed structures of compounds A and B were mainly based on MS spectra with additional supporting information from 1D- 1H -NMR, 2D-COSY NMR data, the physicochemical properties and TLC profiles of compounds A and B, literature and bioassay data. This was done before detection of sugars by TLC from TFA hydrolysates. For Scenario II, the proposed structures were mainly based on the nature of sample

(highly foamy), base peaks of the MS spectra, assuming that the molecular ions of compounds A and B were not detected and should be greater than 882 and 804 g/mole as evidenced by presence of peaks with mass greater than 882 g/mole on MS spectra of A and 804 g/ mole on MS spectra of B and four sugars detected by TLC of TFA hydrolysates of C₁₈ fractions containing A and B. All the other premises for Scenario I are also valid for Scenario II, except the formula masses of parent ions.

8.4.4.1. Scenario I: Proposed structures of compounds A and B based on MS/MS and NMR spectra

The proposed structures of compounds A and B are shown in Figure 8.8.

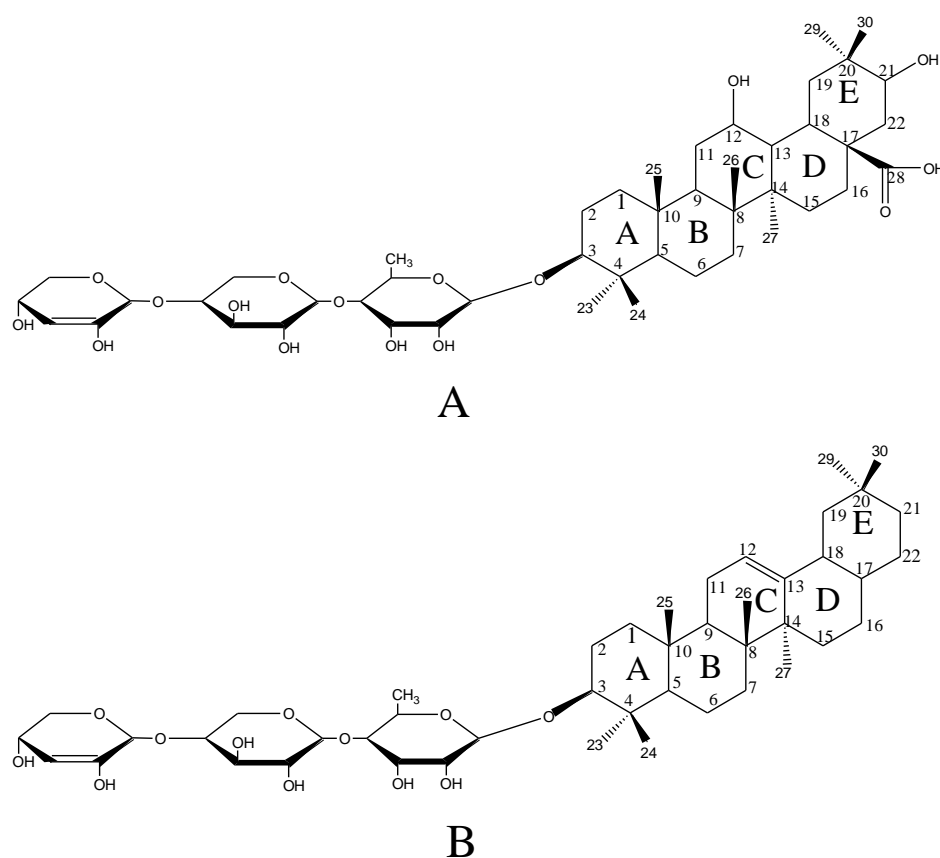


Figure 8.8. Proposed structures of compounds A and B (*Adenia* sp.) based on Scenario I.

Portions of the PTLC-purified compounds A and B were used to generate NMR spectra. From the 2D-COSY NMR data of compounds A and B (Figure 8.3), it was speculated that both compounds A and B contained the same oligosaccharide. The 1D-¹H-NMR spectra revealed that there are different types of protons in the structures of both compounds. In particular, the signals between 1.4-2.4 ppm regions suggest the presence of protons due to methyl (-CH₃) attached to a triterpenoid core ring and the methylene (-CH₂-) protons of carbon atoms of the fused ring with no hydroxyl group on neighbouring carbon atoms.

Although the 1D-¹H-NMR spectra were not strong and sharp enough to assign all the couplings between neighbouring (vicinal) protons, COSY spectra of compounds A and B were signifying that the two compounds contained the same oligosaccharide with methyl signals coupled to saccharide ring protons as seen between 3.8-4.0 ppm (Figure 8.3). Moreover, the blue spots are very close to each other indicating that there are many neighbour proton-proton couplings and was difficult to assign all the couplings. Thus, MS analysis was deemed needed to progress with possible structure elucidation. The MS data of compounds A and B (see Figure 8.6 and 8.7) revealed that the fragment pumped away (i.e. not detected) from both A and B had very similar masses (measured 390.27012 and 391.05460, respectively), and that the difference in mass between A and B is 78.14042 g/mole. The mass difference of ~78 g/mole may reflect the difference between the base peaks, i.e. probably the mass difference between the aglycone parts of compounds A and B. Thus, the aglycone of compound A may possibly differ from the aglycone of compound B by one carbon, two hydrogen and four oxygen atoms (totalling 78 g/mole and close to the measured mass 78.14042 g/mole). Compounds A and B were derived from *Adenia* sp. water

extracts thus they could be water soluble PSMs, which include certain alkaloids, saponins and phenolic compounds (Bernhoft, 2010) as candidate compound classes for the identity of A and B. It was observed that water crude extracts of *Adenia* sp. are highly foamy (Chapter Six). Being foamy or frothy (to form 1 cm foam) in water solution that persists for 15 minutes or longer is indicative of saponins (Ladan *et al.*, 2014). The foamy constituents of *Adenia* sp. were eluted from a Bio-Gel P-2 column as ‘pool A’ (ASPA; Figure 6.1). Both the crude extract and ASPA showed strong EHI and LMI activities *in vitro* (Chapter Six). PTLC-purified foamy compounds (A and B) from the foamy C₁₈ water fraction also showed significant EHI (P<0.05) and LMI (subjective observation) at the tested concentrations (section 7.4). The genus *Adenia* belongs to the family *Passifloraceae*. Oleanane type triterpene glycosides have been isolated from various parts of plants belonging to this family, e.g. *Passiflora quadrangularis* (Voutquenne *et al.*, 2003). Oleanolic acid (3 β -hydroxy-olea-12-en-28-oic acid) and its isomer, ursolic acid are triterpenoid compounds that widely exist in nature in the free acid form, or as aglycones for oleanane- and ursane-type triterpenoid saponins (Sun *et al.*, 2006). The chemical structures of oleanolic acid and ursolic acids are shown in Figure 8.9.

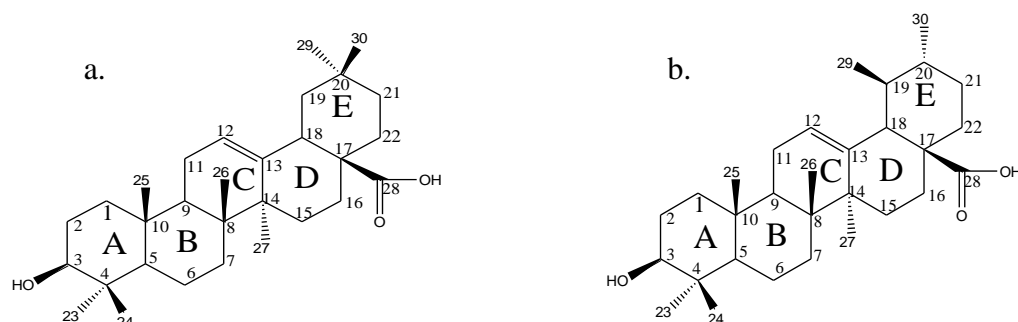


Figure 8.9. Chemical structures of oleanolic acid (a) and ursolic acid (b).

Moreover, since compounds A and B co-eluted on Bio-Gel P-2, Sephadex LH-20 and C₁₈ columns and migrated very close to each other on TLC with R_F-values of 0.23 and 0.27 respectively, their structures may likewise be closely related. The mass difference between A and B is again supportive of the idea that they have closely related core structures.

Most saponins occur as glycosides, consisting of a hydrophilic (glycone) moiety and a hydrophobic (aglycone) moiety, which give saponins emulsifying properties as detergents (Bernhoft, 2010). The aglycone core structures consist of either pentacyclic triterpenoids (30 carbon atoms), or tetracyclic steroids (27 carbon atoms). Both compounds A and B contain greater than 27 carbon atoms in their respective aglycones as derived from their chemical formulae and hence triterpenoid is the best candidate core structure. Triterpenoids are compounds initially containing thirty carbon atoms made from six isoprene units (C₅H₈), though some subsequently lose a small number of C atoms during their metabolic modifications. They could have been derived from squalene (C₃₀H₅₀), which in turn is formed upon head to head coupling of two sesquiterpenoid units, which are again formed by biochemical modifications such as oxidation or rearrangement of sesquiterpene, C₁₅H₂₄ units (Trojanowska and Osbourn, 2002). Farnesyl pyrophosphate is also used as intermediate precursor of squalene in both the mevalonate and non-mevalonate pathways that leads to the biosynthesis of sterols, triterpenoids and other terpenes (see Figure 1.3 for details). The oleanane skeleton is the most common in triterpenoids. The triterpenoid backbone then undergoes various modifications such as oxidation, decarboxylation, substitution and glycosylation (Haralampidis *et al.*, 2002). In saponins, the hydrophilic part is the sugar moiety glycosidically attached to

the hydroxyl functional group at C-3 in both steroids and triterpenes, or both at the –OH group on C-3 (as a glycoside) and at the C-28–COOH group (as a glycosylester) in oleanane type triterpenes. Moreover, glycosylation on other hydroxylated carbons is also possible (Sun *et al.*, 2006).

Tandem mass spectrometry (MS/MS) analysis that uses the CID fragmentation primarily targets “soft” bonds, such as ether and ester linkages between sugar moieties and aglycones. These bonds are formed during condensation reactions, and are broken easily (Bahrami *et al.*, 2014). The most intense peak (base peak) with definite m/z ratio in the MS spectrum is a reliable peak to consider during structure elucidation of organic compounds. As a general principle, the stability of the base peak is due to the presence of double bonds, cyclic structures or aromatic rings in the target base peak ion that stabilize the molecular ion and increase the probability of its detection in MS spectra (McLafferty and Turecek, 1993). This is because the carbocation in the base peak fragment ion is stabilised by delocalisation over the conjugated double bonds, cyclic structures and/or aromatic rings. Therefore, the core structures of compounds A and B should contain conjugated double bonds, cyclic structures and/or aromatic rings to be stable and seen as base peak.

Since compounds to be proposed are saponin glycosides, the core skeletons (aglycones) of compounds A and B are mainly based on carbon and hydrogen atoms as they derived from the precursor isoprene (C₅H₈) units. Hence, it is assumed that the maximum possible carbons and hydrogens followed by oxygen atoms were used to write a chemical formula to match the m/z of the parent ions (M⁺ or M⁺). The molecular formulae of compounds A (~882 g/mole) and B (~804 g/mole) could be

$C_{46}H_{74}O_{16}$ and $C_{45}H_{72}O_{12}$ respectively. Here, the conventional masses of 12, 1 and 16 g/mole for C, H and O respectively were used to convert the molecular ion mass to chemical formula. The fragment lost (sugar moiety) during CID fragmentation in MS was determined by mass difference between the parent ion mass and the base (aglycone) peak. Then, the allocation of carbon, hydrogen and oxygen atoms in the formulae to their respective aglycones and sugar moieties per compound was done by converting the masses (m/z) of the base peaks into chemical formulae then to plausible chemical structures. Thus, from $[M+1]^+$ of base peaks of A and B, the molecular masses of the A and B aglycones should be ~490 g/mole and ~412 g/mole respectively. The corresponding chemical formulae for these aglycones could be $C_{30}H_{50}O_5$ and $C_{29}H_{48}O$. The 30 and 29 carbon atoms in aglycones of A and B respectively can best be explained as triterpenoids as shown in Figure 8.10.

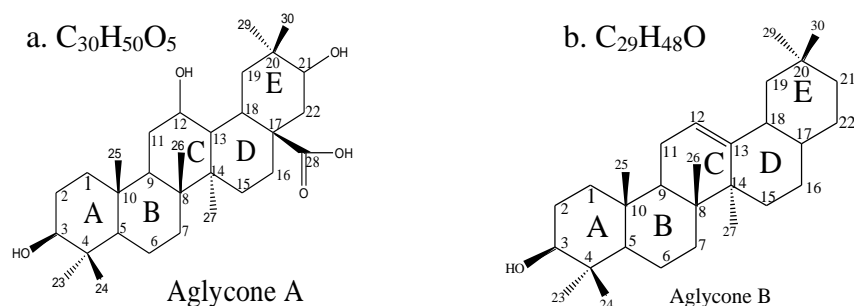


Figure 8.10. The chemical formulae and proposed structures of triterpenoid aglycones, with (a) the aglycone of compound A and (b) the aglycone of compound B (*Adenia* sp.).

The sugar moiety ($\Delta m/z$ between parent ion and CID-generated aglycone = 390.27) is the same for both A and B and is suggested to have the formula of $C_{16}H_{26}O_{12}$, possibly representing a trisaccharide. However, fitting a structure to $C_{16}H_{26}O_{12}$ requires a double bond to be proposed in one of its monomer residues, although double bonds are unusual in sugar molecules. The chemical formula and proposed

structure of trisaccharide sugar moiety common to both compounds A and B (Scenario I) is shown in Figure 8.11.

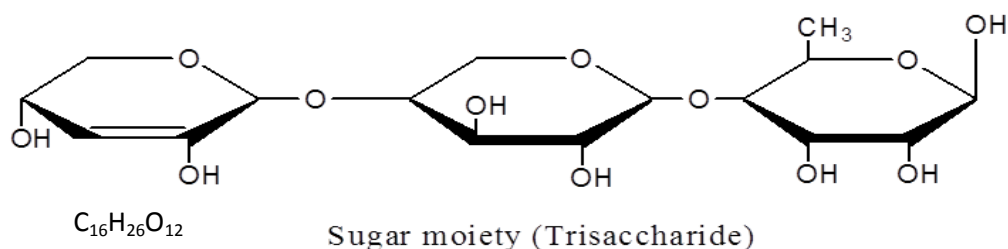


Figure 8.11. Scenario I: Chemical formula and proposed structure of trisaccharide sugar moiety common to both compounds A and B (*Adenia* sp.).

Fractions containing these compounds did not stain with ninhydrin, indicating the absence of primary and secondary amino groups (Chapter Six), so the masses marked on the MS/MS spectra (Figures 8.6 and 8.7) are probably derived exclusively from C, H and O atoms. The sugar moieties common in saponins are glucose, galactose, glucuronic acid, xylose, and rhamnose (Francis, 2002). However, rhamnose and xylose are the most common sugars in saponin glycosides. During condensation reactions between the aglycones and sugar moieties, water is lost.

Thus, based on (1) the number of oxygen atoms in the aglycone part for compound A, (2) TLC profiles, (3) base peak intensities, (4) mass and aglycones mass differences of A and B from MS/MS spectra, (5) abundance of oleanane type triterpenoids in the family *Passifloraceae*, (6) the foamy nature of the solutions containing these compounds and (7) the foamy nature of compounds A and B recovered from PTLC, it can be proposed that the core structures of both compounds A and B are oleanane type triterpenoids and then the proposed structures (Figure 8.10) were generated to be consistent with the experimental and literature findings.

The linkage between sugar monomers in a trisaccharide could be (1,2-, 1,3- or 1,4- or mixture of them). In the proposed structures of A and B (Figure 8.8), arbitrarily show 1,4-linkages.

8.4.4.2. Scenario II: Proposed structures of compounds A and B based on MS/MS spectra and sugar analysis by TLC

The proposed structures of compounds A and B (Figure 8.12) were done based on the assumption that the molecular ions of compound A and B were not detected and should be greater than 882 and 804 g/mole, as evidenced by presence of peaks with mass greater than 882 and 804 g/mole on MS spectra of A and B respectively. The thymol stained chromatogram of TFA hydrolysates of samples containing compounds A and B also revealed the presence of four major sugars detected by TLC (Figure 8.13).

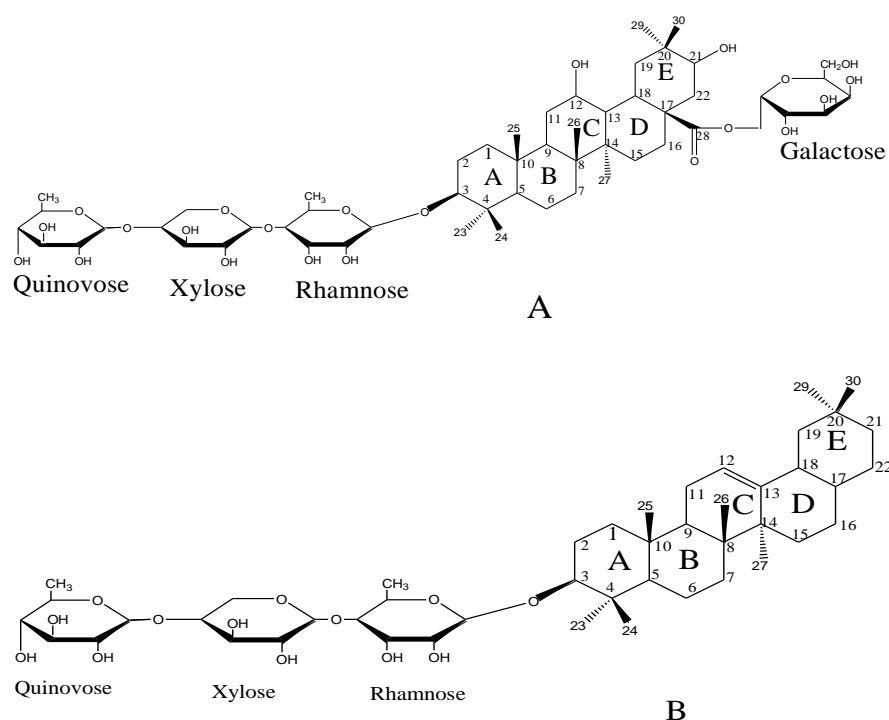


Figure 8.12. Proposed structures of compounds A and B (*Adenia* sp.) based on MS spectral data and chromatograms of TFA hydrolysates.

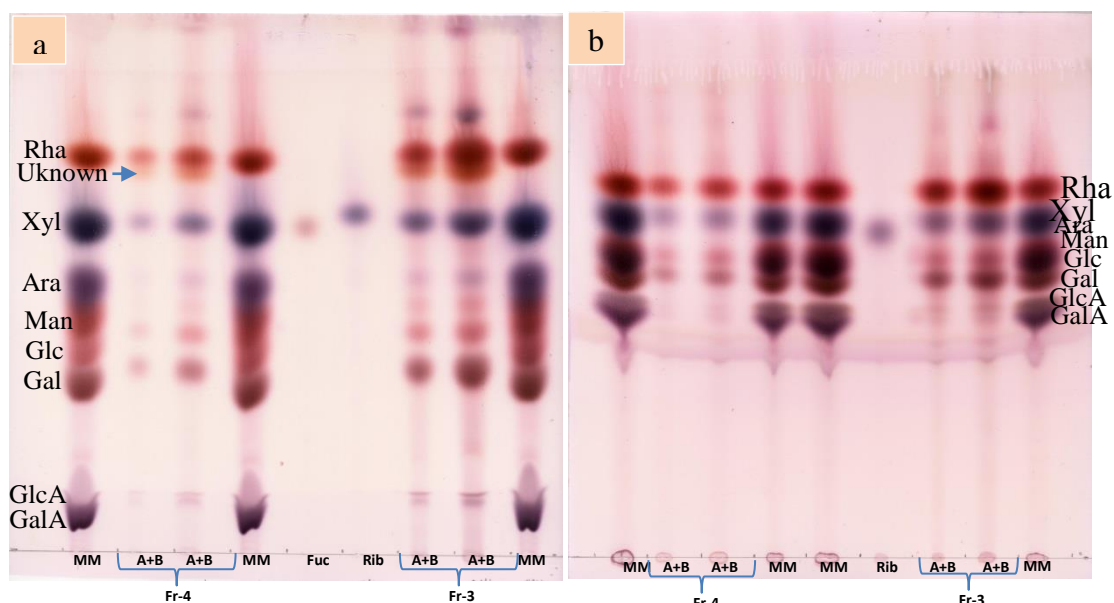


Figure 8.13. Thymol stained chromatograms of TFA hydrolysed C_{18} water fractions 3 and 4 of ASPA. (a) developed in EPAW (6:3:1:1); (b) developed in BAW (2:1:1). Marker mixture: galacturonic acid (GalA), glucuronic acid (GlcA), galactose (Gal), glucose (Glc), mannose (Man), arabinose (Ara), xylose (Xyl), unknown sugar (may be quinovose) and rhamnose (Rha).

Assignment of a molecular ion for a given compound from an MS spectrum is not always possible due to instability of the parent ion. Thus, interpretation of MS spectra is mainly dependent on the most stable (intense) peak commonly known as the base peak. Therefore, the interpretation of the core structures of compounds A and B was done on the basis of the base peaks $[M+1]^+$ at m/z 491.407 and 413.265, respectively. Scenario I, above, is also valid here as far as the interpretation of the core structures was not dependent on parent ion mass. The number of monosaccharide residues detected by TLC in TFA hydrolysates is greater than the trisaccharide sugar moieties speculated from the parent ions marked on the MS spectra. From the chromatogram profiles of TFA hydrolysed C_{18} water fraction mixtures containing A and B (Figure 8.13), four major monosaccharides were

detected using marker mixtures. These are rhamnose (Rha), xylose (Xyl), galactose (Gal) and an unknown sugar (more likely the isomer of rhamnose, quinovose).

The oleanane-type triterpenoid compound (compound A) contains both hydroxyl and carboxylic acid functional groups. The trisaccharide moiety (containing Rha, Xyl and an unknown sugar but may be quinovose) would usually be glycosidically attached to the hydroxyl functional group on C-3, and galactose is more likely to be glycosyl-esterified with the carboxylic acid group (C-28). So, it is possible to accommodate the four TLC-detected (three known and one unknown which may be quinovose) sugars in the structures of compounds A and B. Moreover, compound A has two additional hydroxyl functional groups other than the one common to both A and B at C-3. However, compound B can only form the O-glycosidic linkage with the same trisaccharide through its hydroxyl functional group at C-3 as in A. This has already been confirmed from the MS spectral data. Therefore, the four major sugars detected could be accommodated between compounds A and B as shown in Figure 8.12. Moreover, there are still positions to accommodate all sugars supposed to be parts of compounds A and B (Sun *et al.*, 2006). This is done by assuming that parent ion mass of compound A was not detected on the MS spectrum and the true mass of A should be higher than the previously marked mass (molecular ion mass used in scenario I), albeit undetectable due to instability. Figure 8.5 provides support to this argument as there are signals on MS spectrum with m/z values greater than the marked molecular ion including the 895.69. Thus, compound A, which is proposed to contain both hydroxyl and carboxylic acid functional groups in its aglycone can accommodate up to eight sugar monomers (Sun *et al.*, 2006) between hydroxyl group at C-3 and its C-28 (carboxylic acid) as shown in Figure 8.14

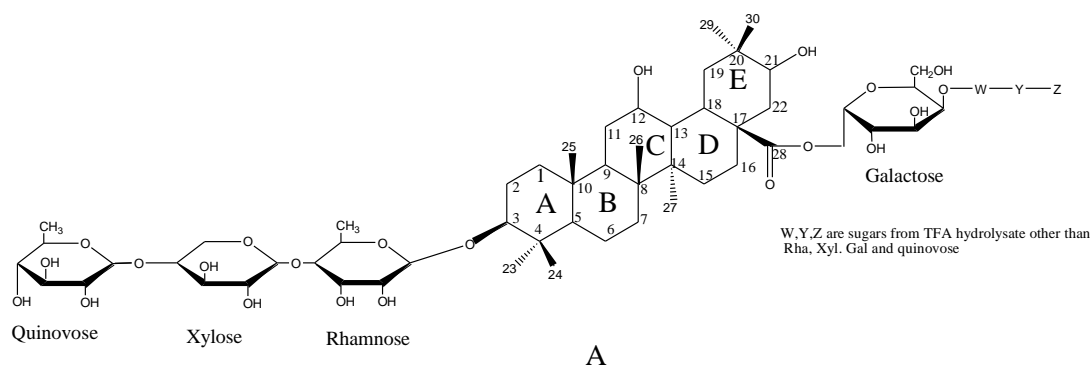


Figure 8.14. Proposed structure for compound A (*Adenia* sp.) and possible positions to accommodate more sugars.

In addition, one could envisage possible glycosylation of the two additional hydroxyl groups in the core structure. If it is assumed that the three monomeric residues in the hydrophilic part of compounds A and B are commonly occurring sugars, then no double bond should exist in it. Consequently, the parent (molecular) ions marked on MS spectra is also invalid unless we assume the trisaccharide moiety contains other unknown non-sugar molecule (e.g. a derivative of xylose) attached to the other two sugars or one of the sugars may have unusual double bond in the structure.

As a general principle, the success of interpretation of MS spectra is dependent on the accuracy and precision of the edited MS spectra generated, careful conversion of mass to elemental composition based on the chemical nature of the target compound(s) and construction of the probable target compound(s) based on the octet rule. The most stable fragment (usually the base peak) is the most important fragment to be dealt with for successful interpretation of the MS spectra, as in scenario I. Thus, all the information about the base peaks in scenario I such as the nature of the sample (saponin), the core structure of compounds A and B (oleanane type triterpenoids base peaks) and factors that affect the stability of the base peak are assumed to be still valid.

In general, the tandem mass spectrometry (MS/MS) analysis selectively generated MS data only for the major constituents (compounds A and B) of C₁₈ water fraction, i.e. in the absence of chemical background and other components in the fraction mixture. The proposed structures of triterpenoid saponins A and B have oleanane type core structure and are therefore stable due to the fused ring structures that stabilize the carbocations formed during soft ionization process such as CID fragmentations. In such mode of fragmentation, only weak bonds such as ether and ester linkages in compounds A and B are easily broken and sugar moieties could be released as neutral molecule or free radicals.

The chromatograms of TFA hydrolysates revealed the presence of four sugar residues as glycone moiety and confirmed the presence of rhamnose and xylose which were proposed in scenario I. All sugars detected on TLC after TFA hydrolysis can fully be accommodated between compounds A and B.

The EHI properties exhibited both by compounds A and B is likely due to the aglycone parts of the saponins. This is because sugars in glycosylated drugs or bioactive PSM are mainly used as protective groups in prodrugs, to increase water solubility and/or for recognition by the receptors during targeted drug delivery (Filice and Palomo, 2012; Li *et al.*, 2014) rather than known for having direct anthelmintic properties. Although steroidal and triterpenoid saponins are structurally distinct, they have main functional properties in common such as the ability to form complex with sterols in membrane structure (Francis, 2002; Jawale, 2014). Therefore, the anthelmintic properties of compounds A and B and fractions containing them might be due to the triterpenoid core structures that form complex with sterols in the membrane structure of nematodes.

8.4.5. General information on compounds from *C. ruspolii* and their NMR and MS data

Many compounds from the active pooled fractions of *C. ruspolii* purified on PTLC (Section 7.4) were contaminated with an ill-characterised substance from PTLC plate matrix, and therefore no satisfactory NMR and/or MS data were available except for CRPALH-20-13 (compound C) and CRPALH-20-20 (compound A) which had not been loaded onto PTLC. CRPALH-20-13 was eluted from a RP C₁₈ column in water whereas CRPALH-20-20 was eluted in 20% MeOH on the same column (Figures 7.12 and 7.13)). Both were from *C. ruspolii* active fractions 28-34 pooled as CRPA in Bio-Gel P-2 (run-4; Figure 5.3) and were thus expected to be compounds with relatively low molecular weight. Many major components of this pool stained well with ninhydrin (Figure 5.5), implying that they contain amine functional group(s) that form “imine (=C=N-) adducts” with ninhydrin. Thus, they are nitrogen containing compounds, possessing primary and/or secondary amino groups, possibly including alkaloids. CRPALH-20-13 contained spot C, which stained green changing to brown upon prolonged heating, whereas CRPALH-20-20 contained spot A which stained brown with vanillin reagent (Figures 7.12 and 7.13).

Both A and C appeared sufficiently pure for NMR and MS analysis as each was clearly seen on TLC as a single spot. However, to avoid contamination with PTLC matrix, the C₁₈ fractions were not further purified by PTLC prior to NMR and MS analyses. Both samples were dried in the same Speed Vac at the same time and submitted together for NMR analysis.

8.4.5.1. Attempts to propose/elucidate compound A based on NMR data

The 1D- ^1H -NMR spectrum suggested that the sample was contaminated with formic acid and acetone due to strong singlet peak at 8.4 ppm and multiplets around 2.1 ppm. However, contamination with formic acid and acetone was unlikely as both A and C had been dried in the same Speed Vac and submitted for NMR analysis at the same time. A re-run of the 1D- ^1H -NMR spectrum of compound A after removal of the D_2O , which would also be expected to remove any traces of formic acid and acetone, resulted in virtually the same spectrum as the first run (Figure 8.15).

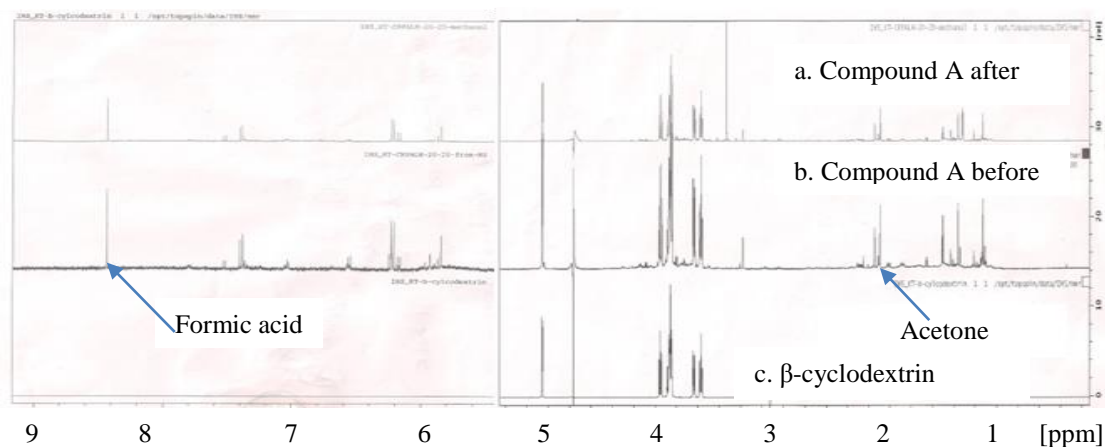


Figure 8.15. 1D- ^1H -NMR of compound A (*C. ruspolii*) and authentic β -cyclodextrin. Proton resonance signals of compound A after MS analysis (a), before MS analysis (b), authentic β -cyclodextrin (c).

Thus, those peaks initially assigned to formic acid and acetone were likely to be real signals from compound A. The absence of formic acid and acetone was further justified by the outcomes of a DEPT-135 experiment (Figure 8.16).

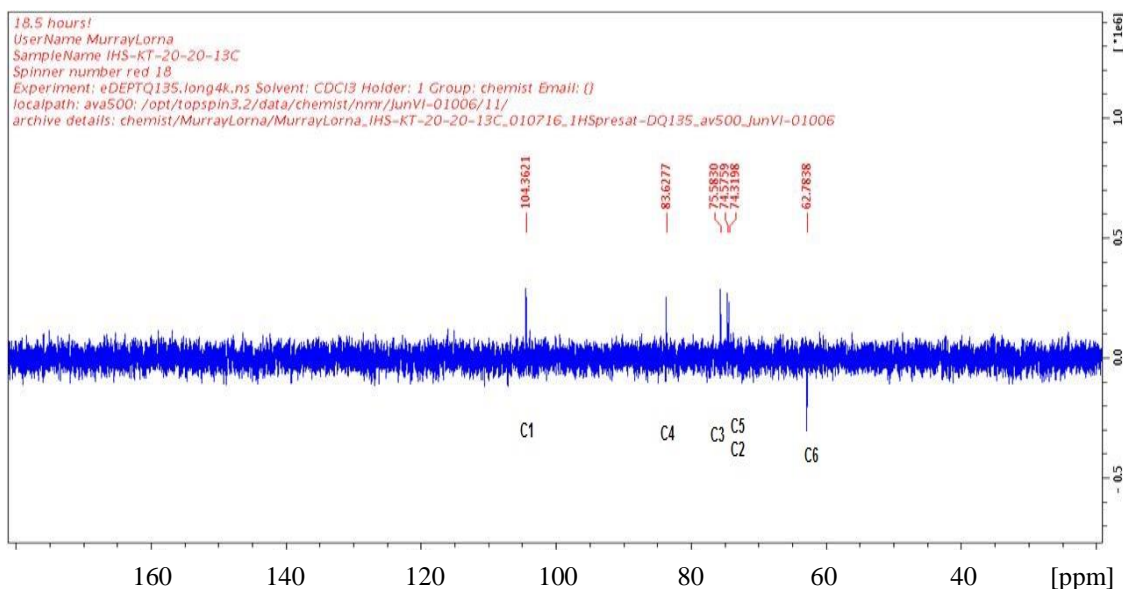


Figure 8.16. The DEPT-135 spectrum of compound A (*C. ruspolii*).

If the strong proton peak at or near 8.4 ppm (Figure 8.16) was due to the contaminant formic acid, it should also have a strong ^{13}C -signal at or near 166 ppm. Similarly, two ^{13}C -signals were expected for acetone near 31 ppm (due to methyl carbons resonance) and 206 ppm (due to carbonyl carbon resonance although the spectrum did not cover this range). However, there were no signals in the 31 ppm region. Thus, the presence of formic acid and acetone are not supported. This DEPT-135 spectrum may also suggest that compound A could be essentially pure β -cyclodextrin, as only six carbons are seen on the DEPT-135 spectrum, though this is not consistent with the proton spectrum which shows β -cyclodextrin (Figure 8.16c) as a component of compound A. There is another 1D- ^1H -NMR spectrum for compound A (CRPALH-20-20) as shown in Figure 8.17 below. This 1D- ^1H -NMR spectrum strongly supports the DEPT-135 spectrum in Figure 8.16 as the principal component proton resonance signals are in the same region as the pure β -cyclodextrin (Figure 8.16) but as above is not consistent with the 1D- ^1H -NMR spectrum of compound A before and after MS analysis as shown in the Figure 8.15.

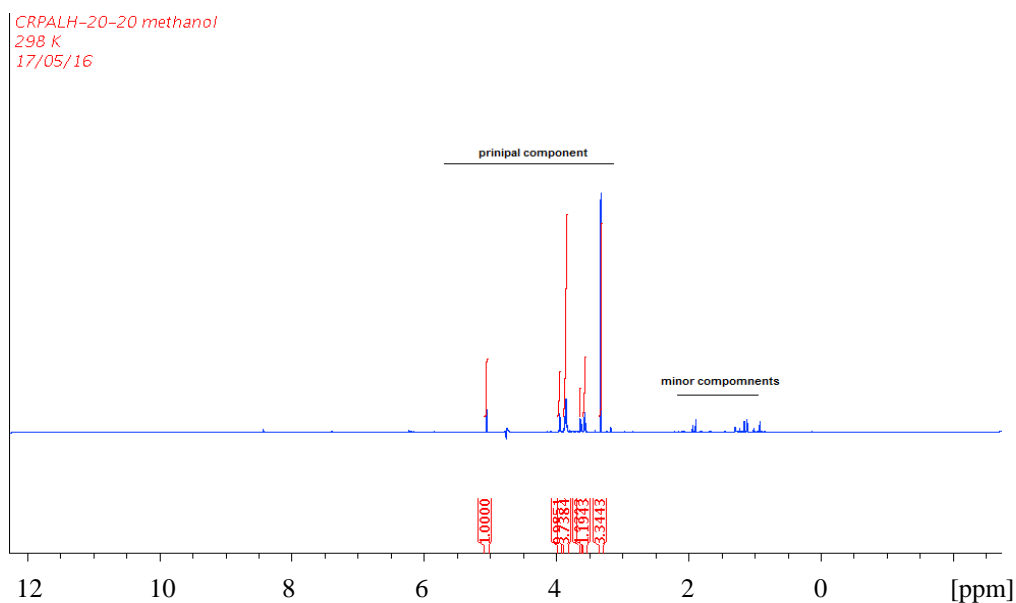


Figure 8.17. 1D- ^1H -NMR of compound A (*C. ruspolii*).

The COSY spectrum also indicates that CRPALH-20-20 contained only six carbons. However, the 1D- ^1H -NMR spectra used in 2D-COSY (Figure 8.18) is different from that shown in Figure 8.15. It should be noted that only one preparation (20% MeOH from C₁₈) was submitted for NMR and MS analysis of compound A (CRPALH-20-20) as mentioned in general information on compounds from *C. ruspolii* (see section 8.4.5).

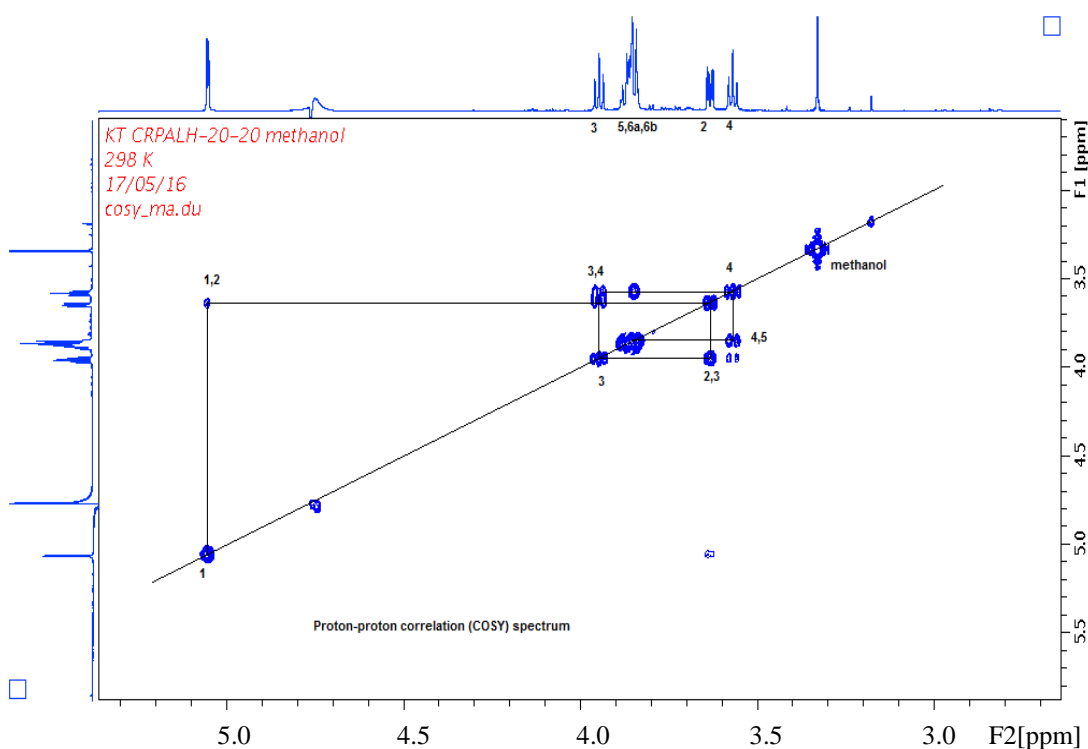


Figure 8.18. The COSY spectrum of compound A (*C. ruspolii*).

The HSQC (Figure 8.19) is based on the 1D- ^1H -NMR spectrum shown in Figure 8.17. This spectrum also supports the DEPT-135 data and contradicts with 1D-proton NMR of the same sample shown in Figure 8.15.

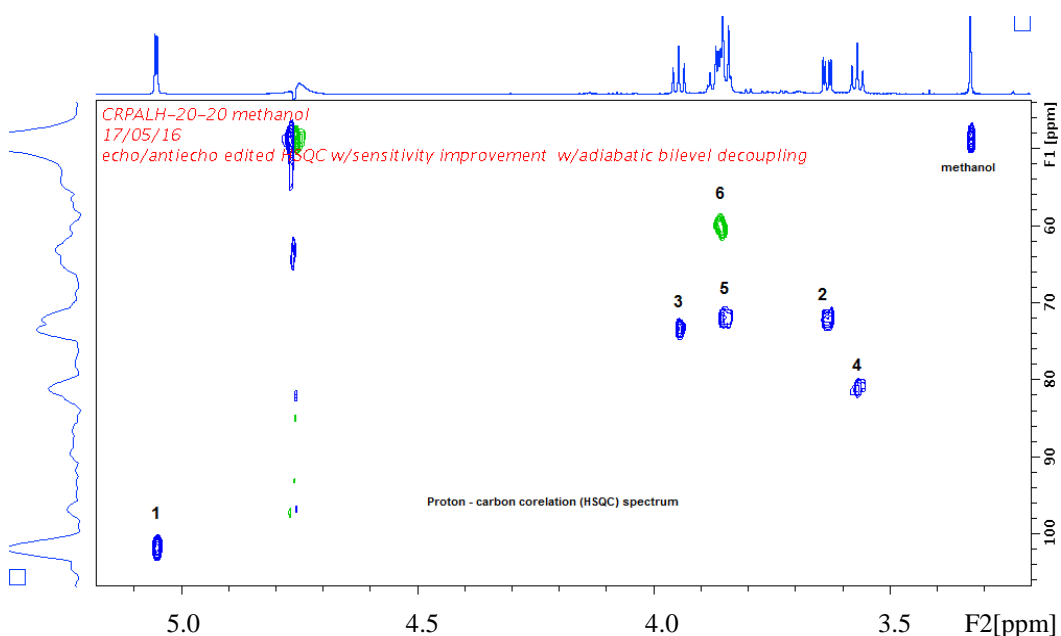


Figure 8.19. The HSQC spectrum of compound A (*C. ruspolii*).

8.4.5.2. The MS data of compound A

The MS data suggested that compound A (CRPALH-20-20) is nitrogen-containing, with molecular mass of about 1280 g/mole (calculated based on the average atomic mass of the elements in the simulated compound as mentioned earlier). The simulated MS spectrum that best matched the MS spectrum of compound A had the chemical formula of $C_{77}H_{100}N_{16}O_2$ as shown in Figure 8.20. The loss of one or two electrons during ionization is possible in MS analysis.

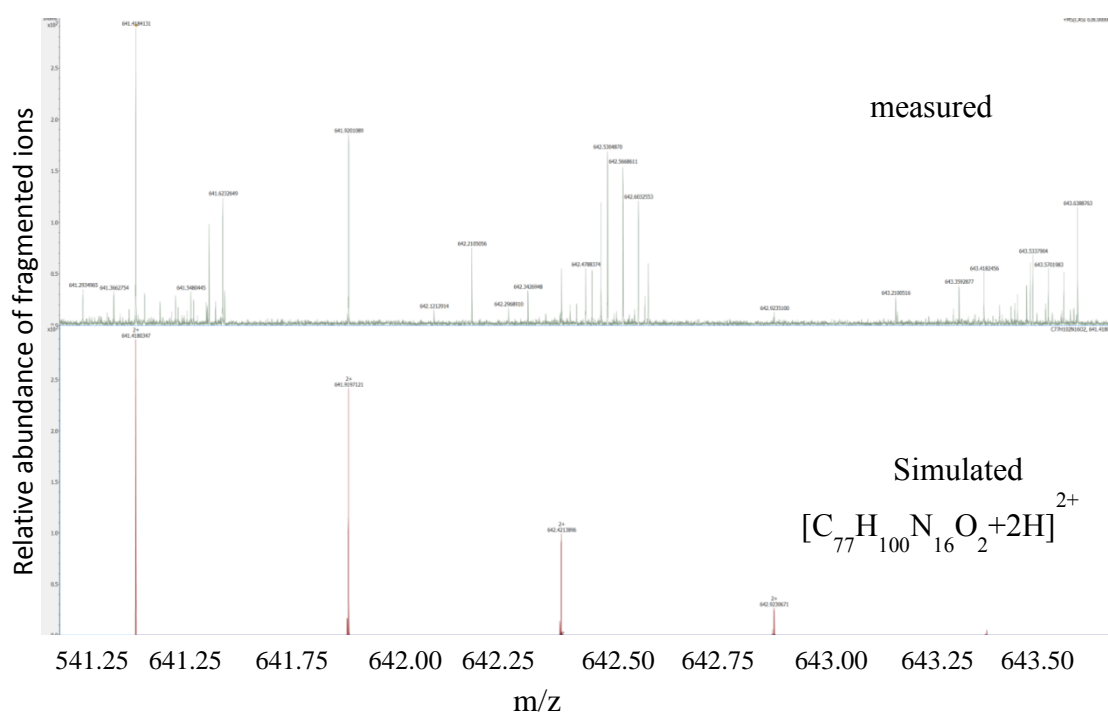


Figure 8.20. The simulated molecular formula suggested for compound A (*C. ruspolii*).

To get the molecular formula of compound A, double bond equivalent (DBE) calculation from MS data suggested was done. The DBE value is used to determine the degree of unsaturation or number of rings to construct the core structure of the target compound. The possible number of rings and/or double bonds for chemical formula $C_{77}H_{100}N_{16}O_2$ is 36. Thus, it is possible to assume the presence of aromatic

rings such as benzene ring as far as DBE is greater than 4 (i.e. 4 DBE represents one benzene or aromatic ring). It can be assumed that all unsaturated bonds are in the form of benzene rings and the target compound should contain a maximum of nine aromatic rings as core structure. There are many secondary metabolites that contain aromatic fused rings such as alkaloids and other nitrogen containing derivatives. Moreover, from the MS spectrum, the mass of the most abundant, stable peak (base peak) is about 641 Da (i.e. half of molecular mass suggested for targeted compound). Thus, the target compound may be a symmetrical molecule that could fragment into two almost identical fragments (Figure 8.21).

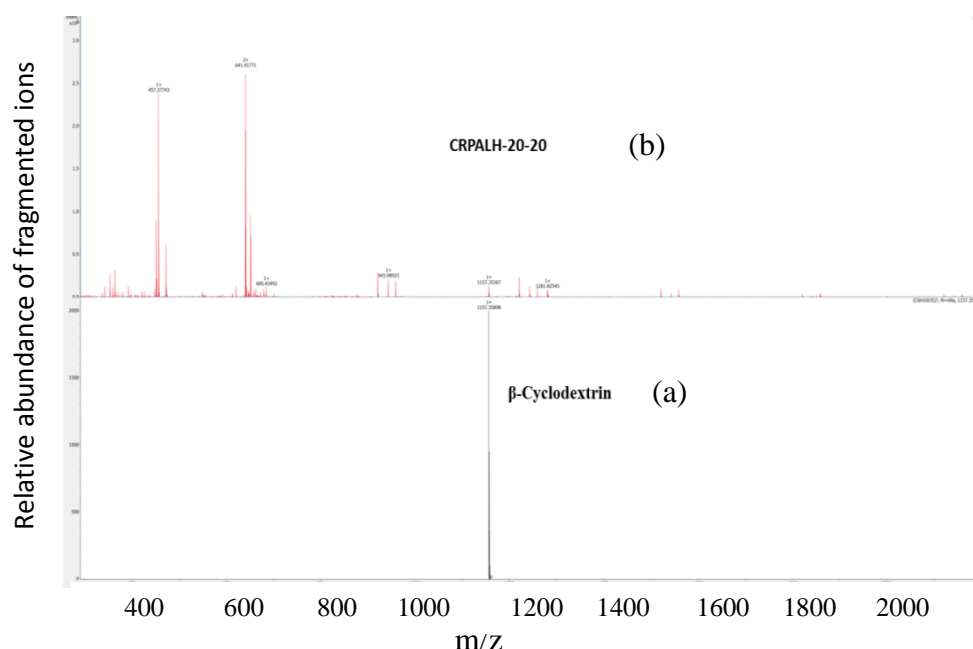


Figure 8.21. MS spectra of β -cyclodextrin (21a) and compound A in *C. ruspolii* (21b).

Based on 1D- ^1H -NMR spectra of compound A, the NMR data suggested the possible presence of β -cyclodextrin (Figure 8.15). However, there is a contradiction between the nitrogen containing with DBE of 36 equivalent to 9 aromatic rings, almost symmetric compound with base peak about 641 g/mole with parent mass of 1280 g/mole suggested from MS data and β -cyclodextrin speculated from NMR data. If β -

cyclodextrin ($C_{42}H_{70}O_{35}$) with 1134.3693 g/mole shares more than 85% of the mass of compound A, the remaining mass 146 g/mole would be contributed by other group attached to it. This implies that the target compound cannot be symmetric with such small mass difference between β -cyclodextrin and mass of parent compound. Moreover, the glycosidic linkages between seven glucose monomers of β -cyclodextrin are equally likely to be fragmented as seen in Figure 8.21 during MS analysis and by default cannot be symmetric. That indicates that there is no stable fragment for β -cyclodextrin as there is no fragment peak seen at m/z greater than 400 except for the parent β -cyclodextrin sodium at about 1157 g/mole.

The small peak at m/z 1157.354 on spectrum of compound A (CRPALH-20-20) is very close to the β -cyclodextrin. Na^+ (with calculated mass 1157.359 and measured mass 1157.359) used for simulation (Figure 8.21b). The presence of β -cyclodextrin. Na^+ in compound A (CRPALH-20-20) may be speculated. However, the β -cyclodextrin sodium used for simulation was from an authentic sample in the laboratory and hence it is very difficult to claim the presence of the β -cyclodextrin sodium in compound A based only on the match between a small peak in compound A with the molecular ion peak of authentic β -cyclodextrin sodium. However, it cannot be excluded that one of the fragment ions of compound A could have the same mass as the molecular ion of β -cyclodextrin sodium. Moreover, stable base peak at about 641 g/mole and the next most abundant fragment at about m/z 457 having almost similar intensity to the base peak are the most abundant and stable peaks of compound A (CRPALH-20-20). If β -cyclodextrin sodium were a major component of compound A, one should see similar fragment ions corresponding to the most intense peaks of compound A. However, there is no corresponding peak or

peaks for β -cyclodextrin. This again reaffirms β -cyclodextrin is not the core structure of CRPALH-20-20. This data tend to support the presence of aromatic rings or double bonds in CRPALH-20-20 as seen from the DBE calculation.

In general, there are contradictions between 1D- ^1H -NMR vs DEPT-135 and DEPT-135 vs MS data. There are also two different 1D- ^1H -NMR spectra for CRPALH-20-20 (Figures 8.15 and 8.17). However, the first 1D- ^1H -NMR (see Figure 8.15) supports the MS data. The first proton spectrum of CRPALH-20-20 strongly supports the mass spectrum because the small peaks between 6.0-8.0 ppm could be due to non-equivalent protons on benzene rings and the strong peak at 8.4 ppm may be due to the equivalent aromatic protons signal attached to anthracene type (fused) aromatic rings. The stability of the base peak and its neighboring in the mass spectrum of this compound may be due to the presence of such aromatic ring structure in CRPALH-20-20. There are also strong aliphatic protons peaks between 0.9-3.2 ppm which are not seen in the β -cyclodextrin spectrum. Thus, because of the aforementioned reasons the structure proposal or elucidation of compound A (CRPALH-20-20) was not successful.

8.4.5.3. Attempt to propose the structure of CRPALH-20-13 (compound C)

To elucidate structure of a compound, it is helpful if one knows the general chemical nature of the target compound from chemical and/or chromatographic screenings. Compound C was among the constituents of *C. ruspolii* Bio-Gel P-2 active pooled fraction (CRPA). The components of this pool were eluted in the included volume (V_i) of Bio-Gel P-2 (Figure 5.5) and probably therefore have relatively small molecular sizes. Compounds that eluted later than the V_i (e.g. as CRPB and CRPC) must have had an affinity for the polyacrylamide gel matrix of Bio-Gel P-2, causing

them to elute later than predicted by their molecular weights. The constituents of CRPA would classically be expected to have similar molecular sizes, less than about 200 Da (the approximate low-Mr cut-off for Bio-Gel P-2); however, larger compounds with an affinity for the gel may also have ended up in pool CRPA. Many constituents of CRPA stain well with ninhydrin and these are likely to be the common amino acids which are usually found in water extracts of plants or other water soluble nitrogen containing compounds including alkaloids and non-protein amino acids. On Sephadex LH-20, compound A eluted in fraction 20 (CRPALH-20-20), i.e. later than compound C, suggesting some degree of hydrophobicity, supported by its low R_F on TLC (see Figure 7.12).

The 1D- ^1H -NMR and ^{13}C -NMR spectra are an initial attempt at structure elucidation from NMR data. However, none of my samples was sufficient in amount to generate ^{13}C -NMR data. This compound was eluted in the V_i of the Bio-Gel P-2 column and pooled as CRPA. Thus, it may contain small molecules, as seen in the tentatively proposed structure from NMR data. The 1D- ^1H -NMR of compound C is complex, not sharp and not integrated. Hence, signal overlapping would be expected. Some proton signals higher than 7 ppm may be cut off (Figure 8.22). Thus, it is impossible to get detailed information on the number of hydrogen atoms of any class of compound from this spectrum.

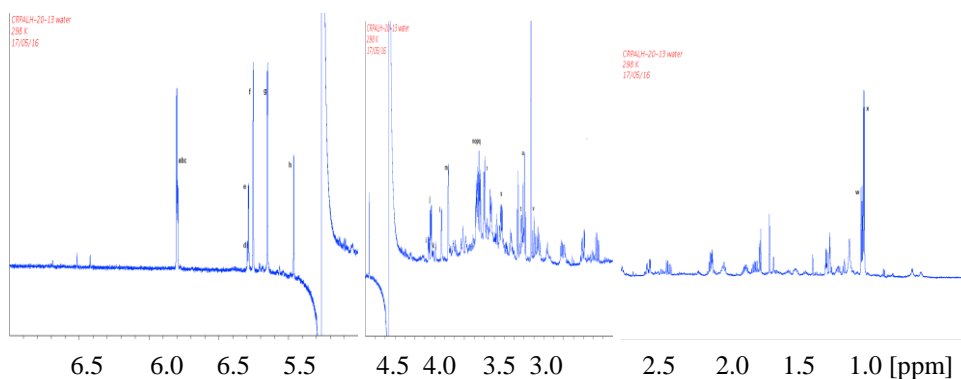


Figure 8.22. ^1H -NMR spectrum of compound C (*C. ruspolii*).

The proton spectrum of compound C has many signals. There are several pairs of signals in approximate intensity ratios 1:2 for example methyl doublets w and x, multiplets i and j, multiplets l and m. The region from 4.5-6.5 ppm contains 8 signals (a-h) from protons attached to carbons bearing oxygen atoms. The spectrum is complex. However, a considerable simplification of the spectrum was obtained from a series of 1D-TOCSY experiments (Figure 8.23) by irradiating signals a, c, d, e, f, h, w and x using a mixing time of 400 ms. 1D-TOCSY is useful for dividing the proton signals (those with very similar chemical shifts) into groups or coupling networks, specially when the multiplets overlap. These showed the separate spectra for the separate spin systems in which these protons are located. 1D-TOCSY and the COSY spectrum of nine separate spin systems were identified.

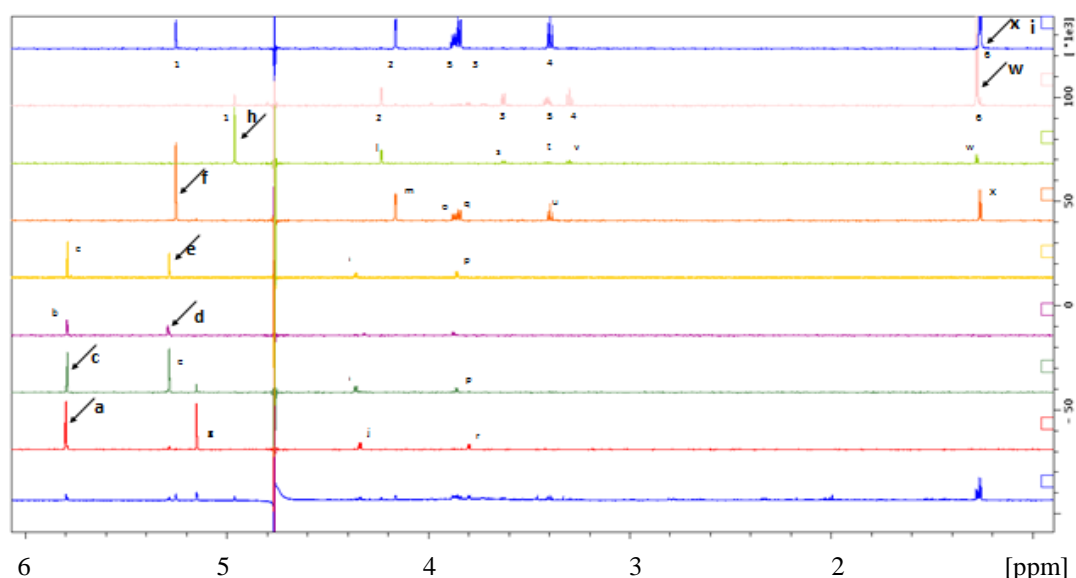


Figure 8.23. TOCSY irradiation of *C. ruspolii* compound C. The arrow shows the irradiation point and a, c, d, e, f, h, w and x are sequentially irradiated signals.

No ^{13}C -NMR and DEPT-135 spectral data could be obtained, which might have indicated the nature, type and exact number of carbon atoms in the compound. The COSY spectrum of *Cissus* compound C (Figure 8.24.) indicates that there are many vicinal proton couplings in the molecule. This also supports the complexity of spectra observed in 1D- ^1H -NMR and also the sample is not a simple molecule. One of the suggested structure is a very small molecule (1,2,3,4-tetrahydroxy-tetrahydrofuran) attached to rhamnose but the COSY spectrum shows many off-diagonal vicinal proton couplings. It also shows the importance of ^{13}C -NMR and DEPT-135 data to verify that these ranges of couplings can only be accommodated in the suggested structure.

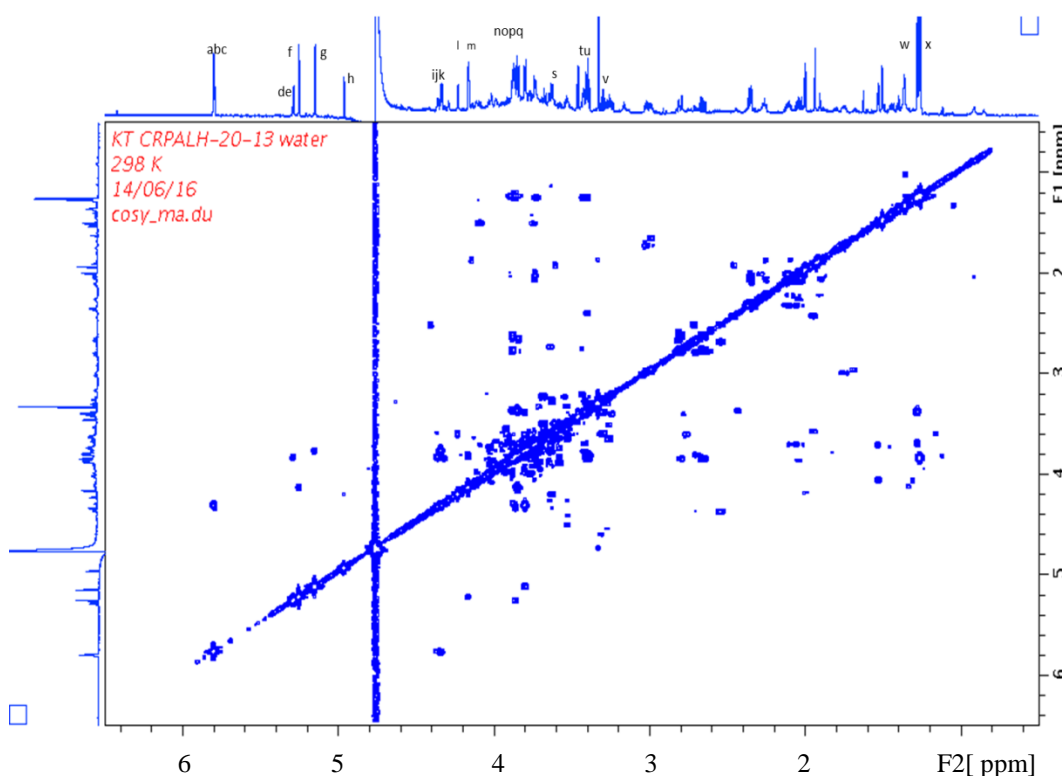
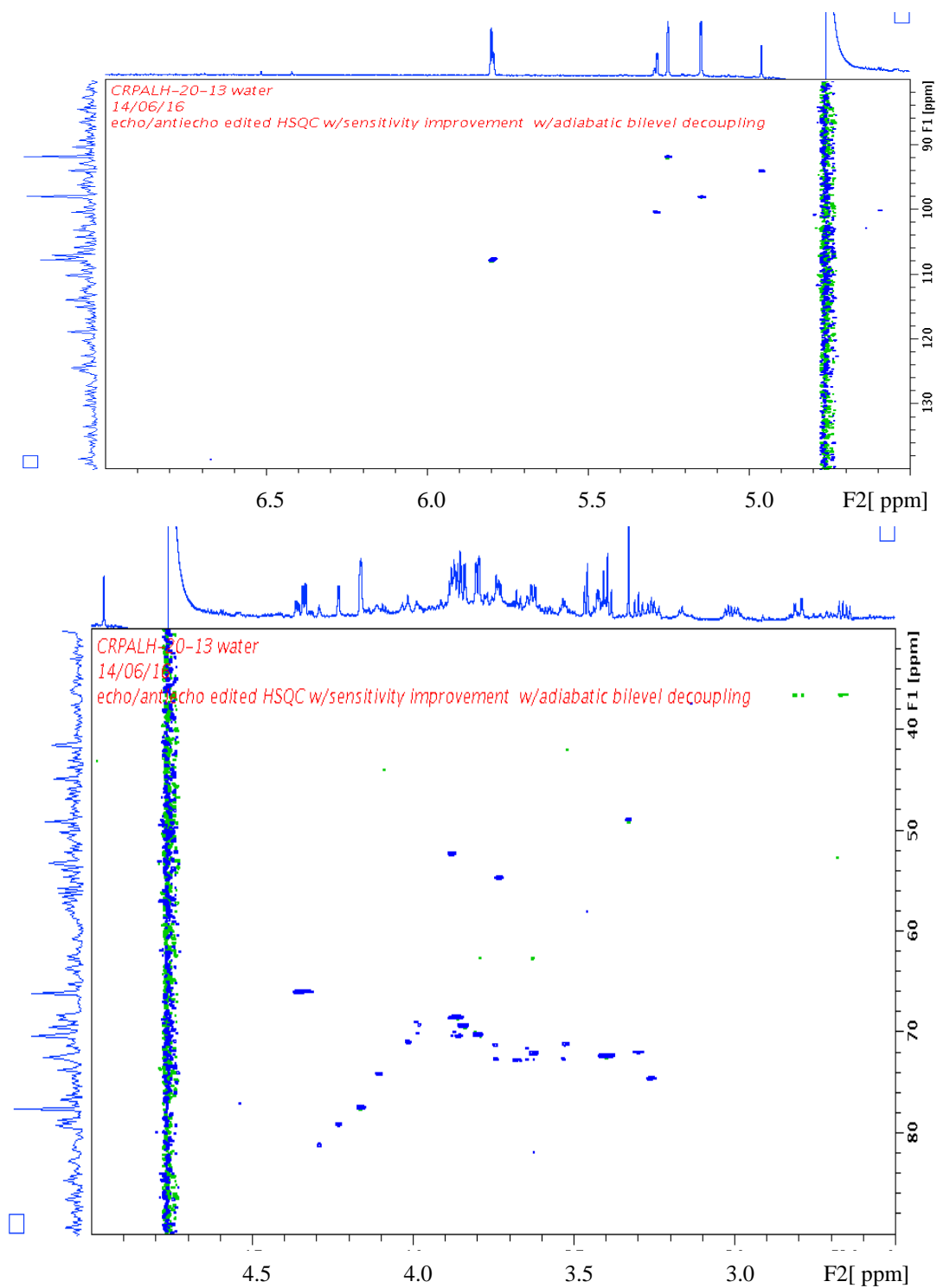


Figure 8.24. 2D-COSY spectra of compound C (*C. ruspolii*).

In HSQC (Figure 8.25), signals between 1.0-1.9 ppm (blue dots) could be due to methyl protons attached to carbon atoms with no other electronegative atoms attached to them. The signals between 2.0-2.9 ppm might be due to methylene protons (green dots). The proton signals between 3.4-4.4 ppm could be due to methylene protons on a carbon atom where the carbon containing the protons is attached to oxygen atom (blue dots). The proton signals between 5.0-6.0 ppm could be due to protons attached to carbons containing carbon-carbon double bonds or methylene protons where the carbon atom is directly attached to oxygen atom. Much of the proton-carbon couplings were observed in the region between 3.4-4.4 ppm for protons and 60-80 ppm for carbons implying that ether or ester linkages are highly likely. There were no proton-carbon couplings in the aromatic region as there is no proton-carbon coupling signal between 6.5-8.0 ppm for protons and greater than 110

ppm for carbons. However, there are proton signals in the aromatic region in $^1\text{D}-^1\text{H}$ -NMR spectrum as seen in Figure 8.22.



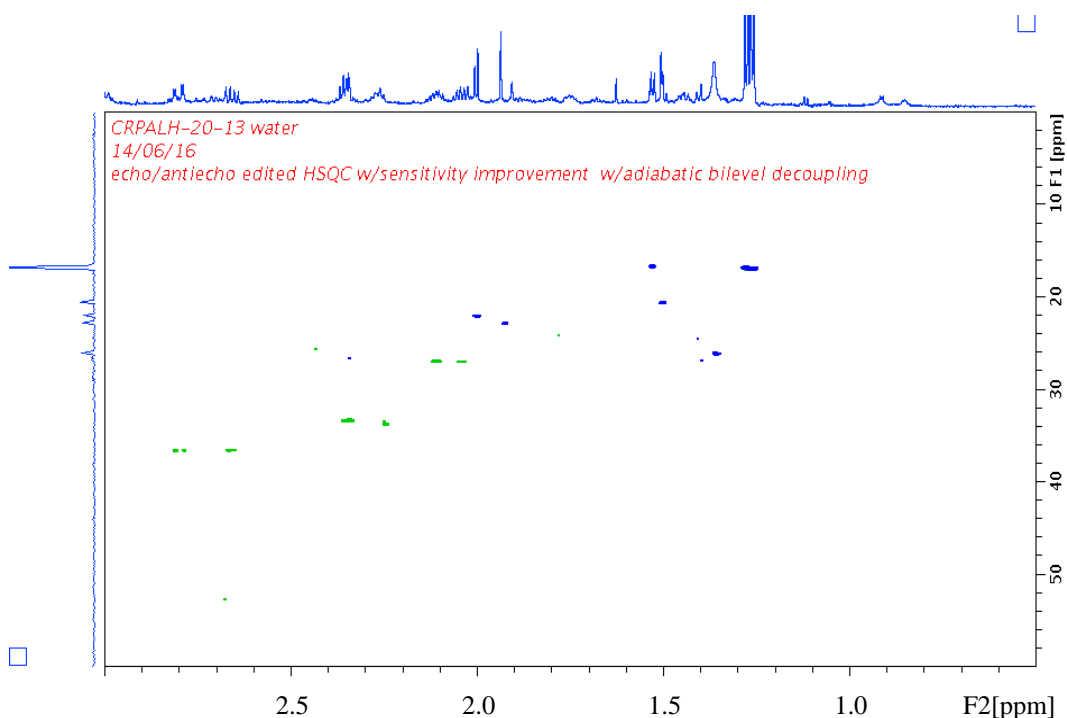


Figure 8.25. HSQC spectrum of *C. ruspolii* compound C.

Based on the aforementioned 1D- ^1H -NMR and 2D- ^1H -NMR and by considerable over-simplification of the complex spectra, CRPALH-20-13 (compound C) structure was tentatively suggested as unknown non-sugar moiety attached to rhamnose or very small molecule (1,2,3,4-terahydroxy-tetrahydrofuran) attached to rhamnose as shown in Figure 8.26.

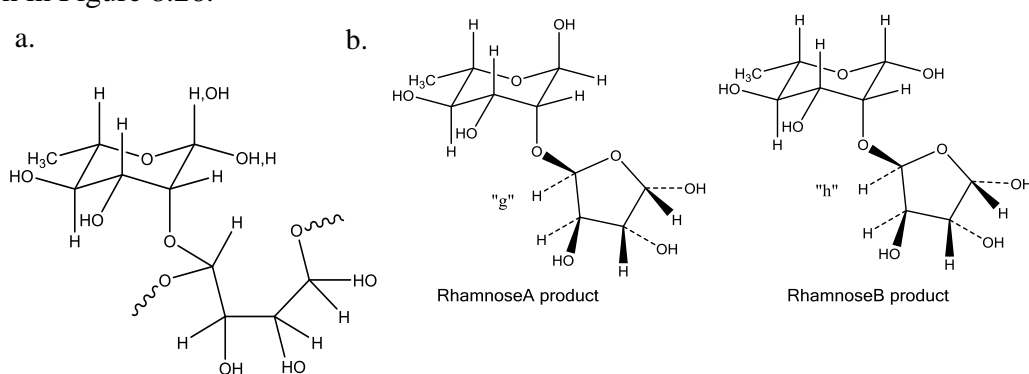


Figure 8.26. Tentatively suggested structures of compound C present in *C. ruspolii*. Rhamnose attached to unknown non-sugar moiety (a), α -rhamnose attached to 1,2,3,4-terahydroxy-tetrahydrofuran (b) or β -rhamnose attached to 1,2,3,4-terahydroxy-tetrahydrofuran (c).

C. ruspolii compound C exhibited modest EHI activity at the tested strength *in vitro*. The suggested structure(s) may not be justified in terms of quantitative structure–activity relationship like those compounds A and B isolated from *Adenia* where compounds having similar core structures like them have been reported (Francis, 2002; Doligalska *et al.*, 2011) for their anti-parasitic activities.

Structure elucidation for compounds with complex proton spectra, as seen for *C. ruspolii* compounds A and C, ^{13}C -NMR, DEPT-135 and MS data are essential. Without knowing the chemical nature and the exact number of carbons in the molecule, attempting structure elucidation of a compound with such complex spectra like this based on proton NMR only may be impossible.

In general, the structural elucidation of compound A (CRPALH-20-20) and C (CRPALH-20-13) from *C. ruspolii* were not successful because of lack of sufficient sample to run ^{13}C -NMR and in some cases NMR and MS data did not support each other.

Chapter Nine: Preliminary evaluation of anthelmintic activities of *C. ruspolii* and *Adenia* sp. water extracts against *Heligmosomoides bakeri* in a mouse model

9.1. Abstract

This study was carried out to evaluate anthelmintic activities of *Adenia* sp. and *C. ruspolii* water extracts *in vivo* against the intestinal nematode *Heligmosomoides bakeri* in a mouse model using distilled water and ivermectin as negative and positive controls, respectively. Thirty two female 8-wk-old mice were divided over 4 groups (I-IV) of 2 cages each, with 4 mice per cage, and fed a standard diet *ad libitum*. All mice were infected with 200 infective *H. bakeri* larvae in 0.2 ml de-ionized water on day 0. Group I received deionized water (negative control), Group II received the *Adenia* extract, Group III received the *C. ruspolii* extract, and Group IV received ivermectin (positive control). Dosing of plant extracts was initially planned at 500 mg/kg BW for five consecutive days from day 26 onwards, whilst the positive control was planned to be drenched only once at 0.2 mg/kg body weight. However, toxicity effects observed for especially the plant extracts led to having to use reduced dose levels and drenching frequencies, resulting in an averaged oral dose of 219 mg/kg body weight for *C. ruspolii* and 250 mg/kg body weight for *Adenia* sp. over two applications one week apart. Blood samples for haematology were collected on day 22 before drenching and on day 36 at dissection. *C. ruspolii* and *Adenia* sp. extracts reduced mice faecal egg counts by 55 and 54% respectively ($P < 0.05$). The *Adenia* sp. and *C. ruspolii* extracts also reduced worm burdens, by 78 and 55%, respectively ($P < 0.05$). Plant extract dosing did not significantly affect BW or liver, kidney and small intestinal weight ($P > 0.05$). However, drenching with *Adenia* sp.

increased spleen weight and red blood cell concentrations, whilst drenching with *C. ruspolii* increased segmented neutrophil and reduced lymphocyte percentages. In addition, both plants numerically increased kidney weight compared to controls. Overall, the data revealed that the plants extracts showed anthelmintic activity *in vivo*, thus supporting the ethno-medicinal use of these plants.

9.2. Introduction

Parasitic diseases are of great medical concern as they can cause severe economic losses to livestock production (Sykes, 1994; Enejoh *et al.*, 2015). Among the parasitic diseases, helminthosis poses a major constraint to livestock production globally specially in the tropics and subtropics (Argaw *et al.*, 2014). In developing countries like Ethiopia, the disease causes direct production losses in livestock (Tesfalem, 2016), arising from both severe morbidity and mortality. Helminthosis is severe in Sub-Saharan Africa, especially in Ethiopia during the wet season when the infection rate is up to 100% in livestock, though the infection persists throughout the year in small ruminants (Gebresilassie and Tadele, 2015).

Heligmosomoides bakeri is a trichostrongylid nematode found in small rodents (Bryant, 1973), including mice (*Mus musculus*). It is an important laboratory model for chronic nematode infections, specially for small intestinal nematodes with a developmental stage in the intestinal wall, due to its persistence; following a single infection, mice can remain positive for *H. bakeri* for many months (Behnke and Harris, 2009). In this respect, *H. bakeri* resembles hookworms of humans (*Ancylostoma duodenale*) and gastrointestinal nematodes of domestic animals such as *H. contortus* and *T. circumcincta* of sheep (Geets and Gryseels, 2000). In addition, the *H. bakeri* mouse model is also used in anthelmintic screening, including plant extracts with purported anti-parasitic properties arising from plant secondary metabolites (Behnke *et al.*, 2009).

It was previously identified that the C57BL/6 strain is a preferred mouse strain to test anti-parasitic properties of plants (Behnke *et al.*, 2009; Athanasiadou *et al.*, 2015).

Relative to other strains tested, these mice are characterised as poor responders as they maintain the infection for many weeks. They also appeared to experience sufficient performance penalties during parasitism, which makes them appropriate model organisms for livestock. The two water plant extracts studied here had been selected based on their strong anthelmintic activity compared to other types of extracts and plants used in this PhD project through an extensive series of *in vitro* screenings for anthelmintic properties (Chapter Three). Therefore, the objective of this study was to evaluate anthelmintic efficacy and possible side effects of *C. ruspolii* and *Adenia* sp. water extracts *in vivo* in C57BL/6 mice experimentally infected with *H. bakeri*.

9.3. Materials and methods

9.3.1. Animals and housing

A total of 32 female C57BL/6 mice were obtained from University of Edinburgh, UK. Their initial body weight (BW) \pm standard error averaged 19.1 ± 0.06 g. Mice were housed in groups of four, in plastic cages containing saw-dust bedding and adapted for one week in the animal house prior to usage. The mouse room was maintained at a temperature of $(21 \pm 2^\circ\text{C})$ with relative humidity of $(45 \pm 5\%)$ under a 12 h light/dark cycle. All animals had *ad libitum* access fresh tap water and a standard pelleted mouse diet (RM3; SDS, Witham, UK), formulated to supply 202 g/kg digestible protein and 12.2 MJ/kg digestible energy. Animals were cared for in accordance with the guideline to the care and use of experimental animals. The experimental protocol was reviewed and approved by SRUC Ethical Review Body

(AE ED 28/2016) and University of Edinburgh Veterinary Services (249-KB-16), and conducted under Home Office authority (PPL 60/4395).

9.3.2. Mice handling during oral gavage

Larval suspension, plant extracts, de-ionized water and anthelmintic (see below) were administered via oral gavage. In this procedure, a bulb-tipped gastric gavage needle mounted to a tuberculin (1-ml) syringe was used to deliver substances directly into the stomach. The mice were gently restrained (grasped by the loose skin of the neck and back) to immobilize the head. Then, the mice were maintained in an upright (vertical) position and the gavage needle was passed along the side of the mouth. Following the roof of the mouth, through gravity, the needle was advanced into the oesophagus and then toward the stomach. After the needle had been passed to the correct length, the samples were injected.

9.3.3. Experimental infection

The larvae propagation and life cycle maintenance of *H. bakeri* before baermannisation are detailed in section 2.12.1. The infective larvae of *H. bakeri* were prepared through baermannisation of stock infective larvae. The final concentration was set at 1000 L₃ per ml. Each mouse was inoculated with 200 *H. bakeri* L₃ by oral gavage with 0.2 ml of this larval suspension (day 0). This infection model has been previously used to establish chronic, sub-clinical parasitic infection in this strain of mice, and is consistent with a minimum possibility of accidental over-challenging (Athanasiadou *et al.*, 2015).

9.3.4. Plant extracts and anthelmintic stock solution preparation

Freeze dried water extracts of *Adenia* sp. and *C. ruspolii* (550 mg each) were separately dissolved in 10 ml of deionized water to prepare stock solution with 55 mg/ml concentration. The required concentrations were prepared by serial dilution of the stock solution. The ivermectin stock was prepared by adjusting the dose (mg/kg BW) based on the 2.5 ml of 0.08% ivermectin (ORAMEC ® Drench, Merial Animal Health Ltd, Harlow, UK) per 10 kg BW recommended for sheep drench. The lower concentrations were also prepared by serial dilution.

9.3.5. Experimental design

The eight cages were randomly assigned to one of four experimental treatments, i.e. each treatment consisted of two boxes and thus eight mice. Group I received deionized water (negative control), Group II received the *Adenia* extract, Group III received the *C. ruspolii* extract, and Group IV received ivermectin (positive control). Dosing of water (0.2 ml) and plant extracts (0.2 ml at 500 mg/ kg BW) was initially planned to be done for five consecutive days from day 26 onwards, whilst the positive control was planned to be done only once at 0.2 mg/kg BW. To manage sampling intensity, dosing was planned to start for one box per treatment on day 26 and one box on day 27. Hereafter, this is referred to as day 26 for both boxes per treatment. Dose volume for plant extract and negative control treatments was standardized at 0.2 ml as used in previous studies (Athanasiadou *et al.*, 2015).

Some mice showed abnormal, near moribund behaviour on day 26, 10 minutes after plant extract and anthelmintic dosing. Those that exceeded the expected mild severity limit were euthanized as per Home Office guidelines. Thus, five mice were

euthanised on day 26 (Group I: 0; Group II: 1; Group III: 3; Group IV: 1). The treatment protocol for day 27 and subsequent dosing was amended; dose level was reduced by half following every time a single dose was given and negative effects on behaviour (such as sitting hunched, not feeding well, not exploring, difficulty of breathing and seizures etc) were observed, and dosing frequency reduced from five consecutive daily events to two events one week apart (day 26 and day 33). Consequently, only two mice required to be euthanised on day 27 (Group I: 0; Group II: 1; group III: 1 and Group IV: 0). Following the protocol readjustment, some mice temporarily exceeded the mild severity limit, which led to a further reduction in dose for *C. ruspolii* though mice sufficiently recovered within one h post treatment so that progression to euthanasia was not needed. The 500 mg/kg BW dose level was chosen based on intensive literature survey of medicinal plants with anthelmintic properties in mice model. It was the lowest dose level used as reported in many research articles with no adverse effect. In this study, the dosage regime re-adjustments of plant extracts and positive control were done due to the adverse effect observed in mice treated with both plant extracts at chosen dose level (500 mg/kg BW). Ivermectin was also administered twice because of the re-adjustment of the initial dose to lower dose level due to its toxicity. The initial and re-adjusted doses during the treatments are summarized in Figure 9.1.

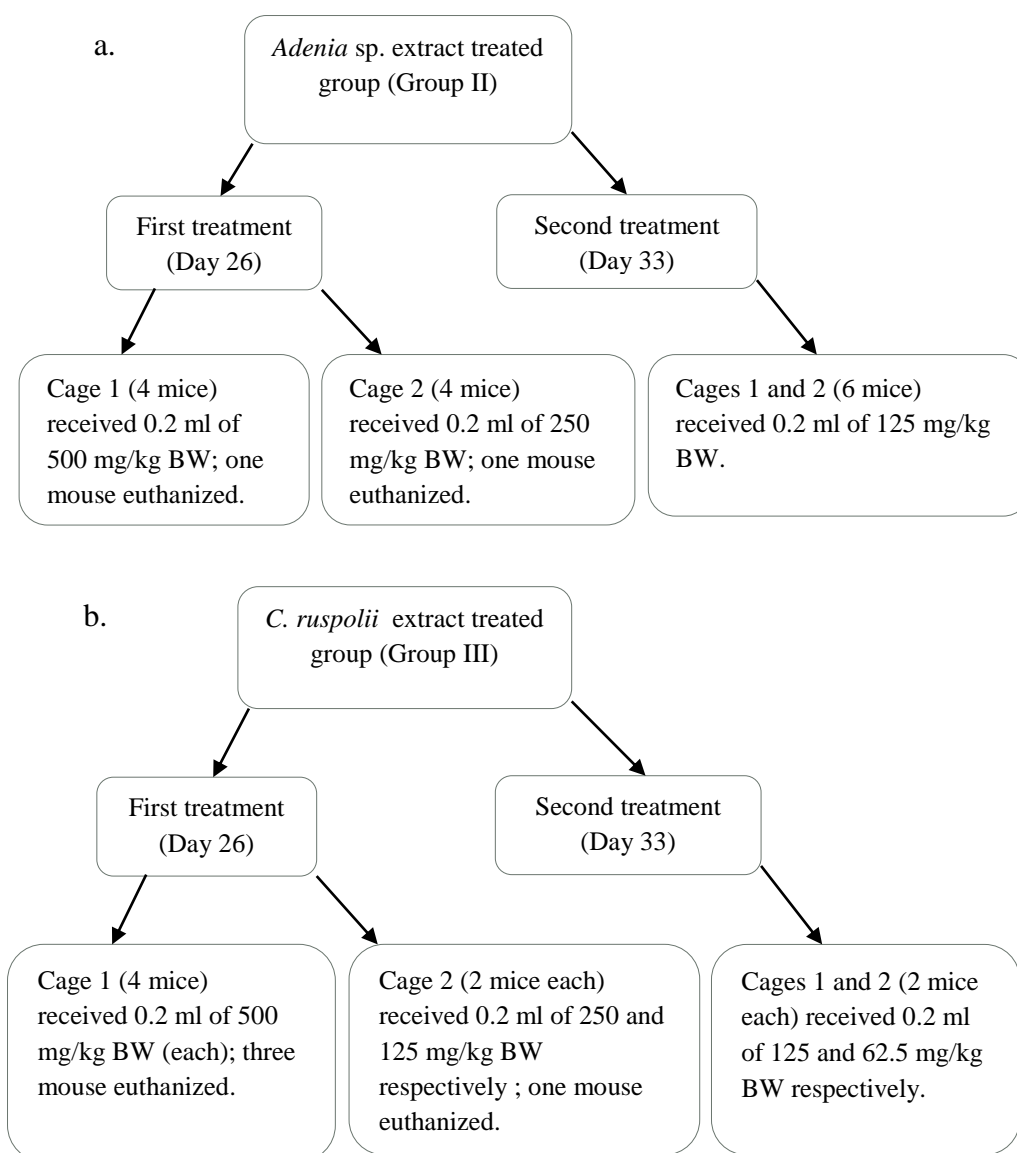


Figure 9.1. Flow diagram of dose levels and dose frequencies of plant extracts. *Adenia* sp. (a) and *C. ruspolii* (b).

9.3.6. Body and organ weights measurements

The BW of each mouse was recorded at the beginning of study during grouping, ear tagging and infection (day 0), post infection prior to treatment (day 22), after first treatment (day 29), and after second treatment (day 36; dissection). On the day of dissection, animals were killed by Schedule one (euthanised by gradual CO₂ overdose) and necropsised. Small intestine, liver, kidneys and spleen were recovered

carefully and weighed separately. The small intestine was processed for worm burden determination (see below). Connective and adipose tissues were removed from the organs before weighing. Digital electronic balance with accuracy of 0.01g was used to determine body and organ weights.

9.3.7. Blood sampling and determination of haematological parameters

Blood samples (0.2 ml per mouse) were collected through mandibular bleeding (day 22, pre-treatment) and from caudal vena cava and cardiac chamber (day 36, at dissection) in sterile heparinized lithium anti-coagulant tubes for haematology. Volumes collected proved insufficient to also analyse for biochemistry. Haematological parameters were assessed for the concentration of total red blood cell (RBC) and differential white blood cell (WBC) counts using ADVIA 2120 haematology system (Bayer, Germany). It is a bench-top automated flow cytometry-based system that uses light scatter and staining reagents such as myeloperoxidase and oxazine 750 to provide a complete blood cell count, a WBC differential (percentages of neutrophils, lymphocytes, monocytes, eosinophils, basophils) and reticulocyte measurements (Harris *et al.*, 2005; Mwale *et al.*, 2014).

9.3.8. Faecal sampling and faecal egg counts (FEC)

Faecal sampling and FEC were done prior to drench on day 22 (to confirm infection establishment and provide individual mouse baseline), after first treatment (day 29) and on morning of dissection (day 36). Briefly, faeces collection was done through moving mice to a clean cage where they stayed individually for about 2 h to collect the faecal pellets produced. Faecal weight collected ranged from 0.06 to 0.73 g. Faecal pellets were collected separately using spatula and placed in plastic bags

labelled with mouse identification. The faecal pellets were placed in 50 ml plastic test tubes, mixed with tap water and mashed into smooth paste with applicator sticks. Egg recovery was done by a saturated salt floatation technique and FEC was done by the method detailed in section 2.5.1.3. The FEC (epg) per mouse was calculated based on the number of eggs counted in faecal sample (g) collected per mouse.

9.3.9. Post-mortem worm count

The method of Athanasiadou *et al.* (2015) was used for worm count. Briefly, the entire small intestine of each mouse was recovered, opened by cutting along its longitudinal axis with a pair of fine scissors, cut into small pieces, suspended in the normal saline and incubated at 37°C for about 3 h to enable the migration of the worms into the solution. Then, 10% (v/v) formalin was added to normal saline solution containing the recovered adult worms to preserve them prior to counting. The mixture was poured into petridish portion by portion and viewed using the magnifying lens where the reddish worms were identified, counted (fished out with pin/needle), sexed and recorded.

9.3.10. Calculations and statistics

Anthelmintic efficacies of the extracts were assessed by counting the eggs and worms in the treated animals and comparing with counts from the untreated control mice. The percentage of deparasitisation (efficacy) in terms of reduction in the egg counts (FEC reduction test, FECR) or worm counts (total worm count reduction test, TWCR) for the various groups was calculated using the following formula (Simon *et al.*, 2012):

$$\% \text{ efficacy} = ((N-n)/N) \times 100$$

Where N is mean egg/worm count in negative control group (Group I) and n is mean egg/worm counts in the test groups (Groups II and III) and positive control group (Group IV). The expression of organ weights per unit BW did not improve detection power over the use of absolute organ weights, and therefore the latter has been used.

Analysis of variance (ANOVA; GenStat 16th edition) and Tukey's Multiple Comparison Test (Graphpad Instat version 5) were used to compare the anthelmintic effects of the plant extracts with those of ivermectin and the non-treated (distilled water) group. The experimental unit for statistical analysis was the mouse, as each mouse was treated individually. Data collected pre-treatment were used as covariates, where applicable (e.g. haematology). The results were summarized as arithmetic means with SEM. Differences were considered significant at $P < 0.05$, and considered a tendency at $0.05 < P < 0.10$.

9.4. Results

9.4.1. Anthelmintic effects of crude water extracts

9.4.1.1. Effect of extracts on FEC

Figure 9.2 shows the effects of plant extracts on FEC. A significant reduction in FEC was observed in mice treated with plant extracts compared to the deionized water treated group. At an averaged dose level of 219 and 250 mg/kg BW, crude water extracts of *C. ruspolii* and *Adenia* sp. resulted in 55% and 54% FECR, respectively, compared to deionized water-treated group ($P<0.05$). Ivermectin at an average dose of 0.15 mg/kg BW showed highly significant FECR of 99.9% ($P<0.0001$) in comparison with the deionized water treated group. There was however, no difference in FEC between *C. ruspolii* and *Adenia* sp. extract treated groups ($P=0.67$; Table 9.1).

Table 9.1. The dose level and effect of extracts on FEC (epg) at dissection.

Treatment	Av. dose level	No. of mice at dissection	FEC(epg) \pm SEM	Range of FEC
Water	0	8	8740 \pm 630	6168-10439
<i>Adenia</i> sp.	250	6	3938 \pm 829	3555-4186
<i>C. ruspolii</i>	219	4	3903 \pm 1426	3047-5246

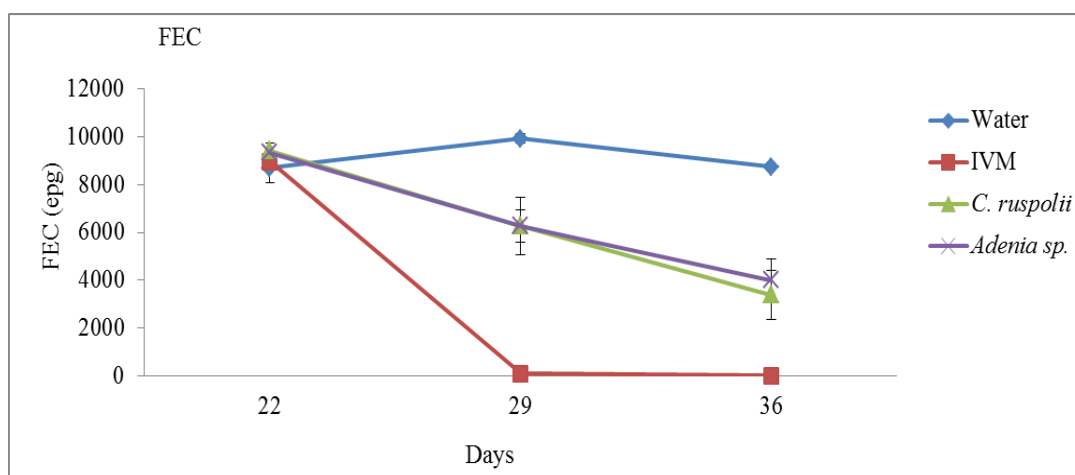


Figure 9.2. The effect of extracts on faecal egg counts (FEC) in mice infected with *H. bakeri*. Orally treated with water (—), *C. ruspolii* (—), *Adenia* sp. (—) or ivermectin (—) on days 0 (grouping and inoculation), 22 (before treatment), 29 (three days after first treatment) and 36 (at dissection or three days after second treatment).

9.4.1.2. Effect of extracts on adult *H. bakeri*

Figure 9.3 shows the effect of plant extracts on adult *H. bakeri*. At the average dose level of 250 mg/kg BW, crude water extract of *Adenia* sp. resulted in TWCR of 78% ($P < 0.0001$) compared to deionized water-treated group. Similarly, at the average dose level of 219 mg/kg BW, *C. ruspolii* tended to reduce worm burdens ($P = 0.096$) resulting in a TWCR of 55%. Ivermectin, at an average dose rate of 0.15 mg/kg BW, showed a highly significant TWCR of 99.6% ($P < 0.0001$). The TWCR observed for *Adenia* sp. tended to be greater than for *C. ruspolii* ($P = 0.086$).

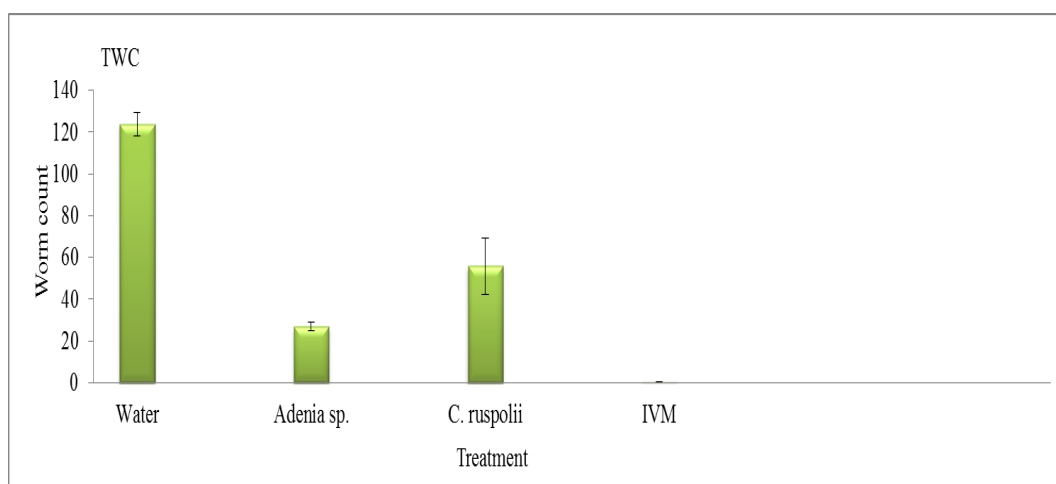


Figure 9.3. The effect of extracts on total worm burden in mice infected with *H. bakeri*.

The mean numbers of *H. bakeri* recovered by gender are shown in Figure 9.4. The effect of plant extracts on worm count reduction was more pronounced for female than for male worms, with variation between the plant extracts used. *Adenia* sp. extract resulted in 89.9% (six average female worm count with range of 5-8) and 67.4% (twenty one average male worm count with range of 18-24) worm reductions while the *C. ruspolii* extract also exhibited 71.1% (seventeen average female worm count with range of 16-29) and 40.6% (thirty nine average male worm count with range of 34-42) worm reductions compared to the water treated group. The positive control, ivermectin, resulted in 99.8% female and 99.5% male worm reductions compared to the water treated group. The average male and female worm count for positive control was less one as no worm was recovered from some mice in this treatment group. The negative control had average male and female worm counts of 66 and 58 with worm counting ranges of 56-71 and 40-61 respectively.

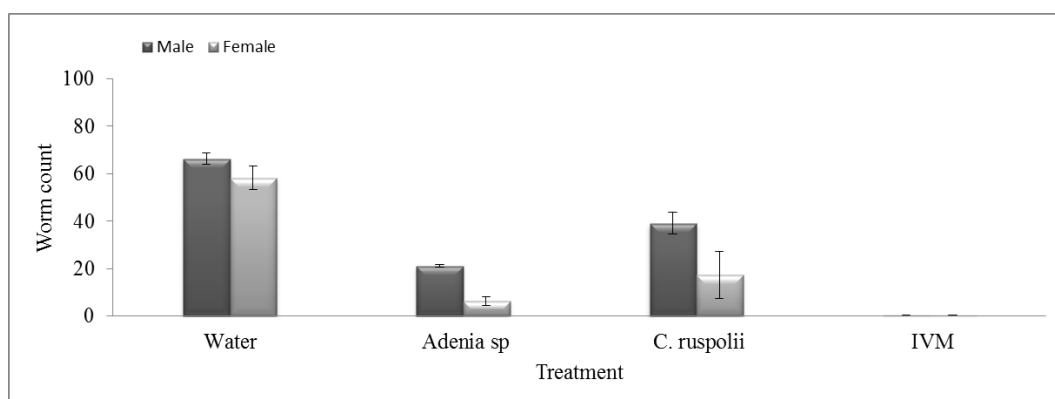


Figure 9.4. The effect of extracts on male and female worms in mice infected with *H. bakeri*.

9.4.2. Body weight measurement

The mouse BW is shown in Figure 9.5. All treatment groups showed a slight increase in BW from grouping and infection date (day 0) to full establishment of infection (day 22). Then, BW more or less remained the same from first treatment till to the end of the experiment (dissection stage). There was no significant effect of treatment on BW, or BW gain ($P > 0.05$) at any time during the study.

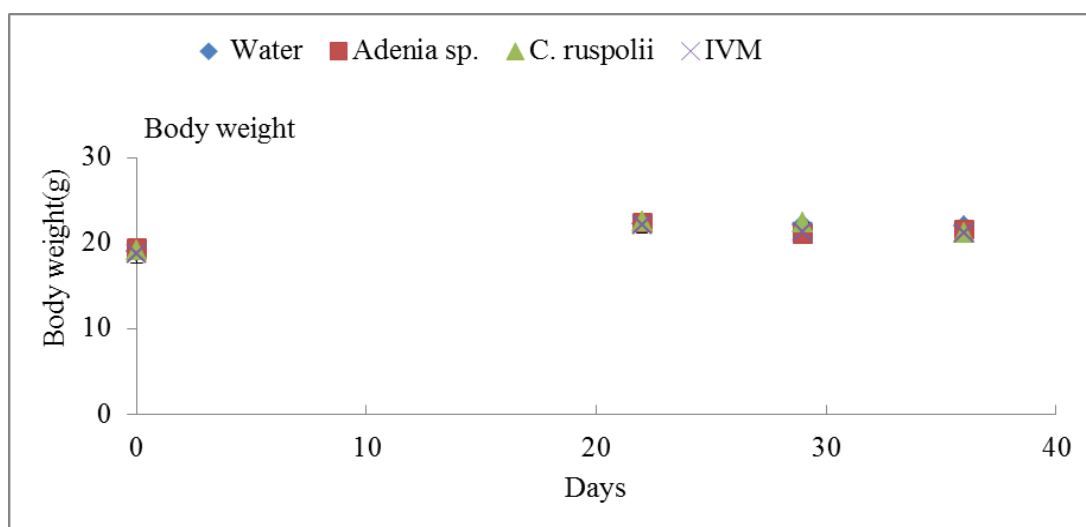
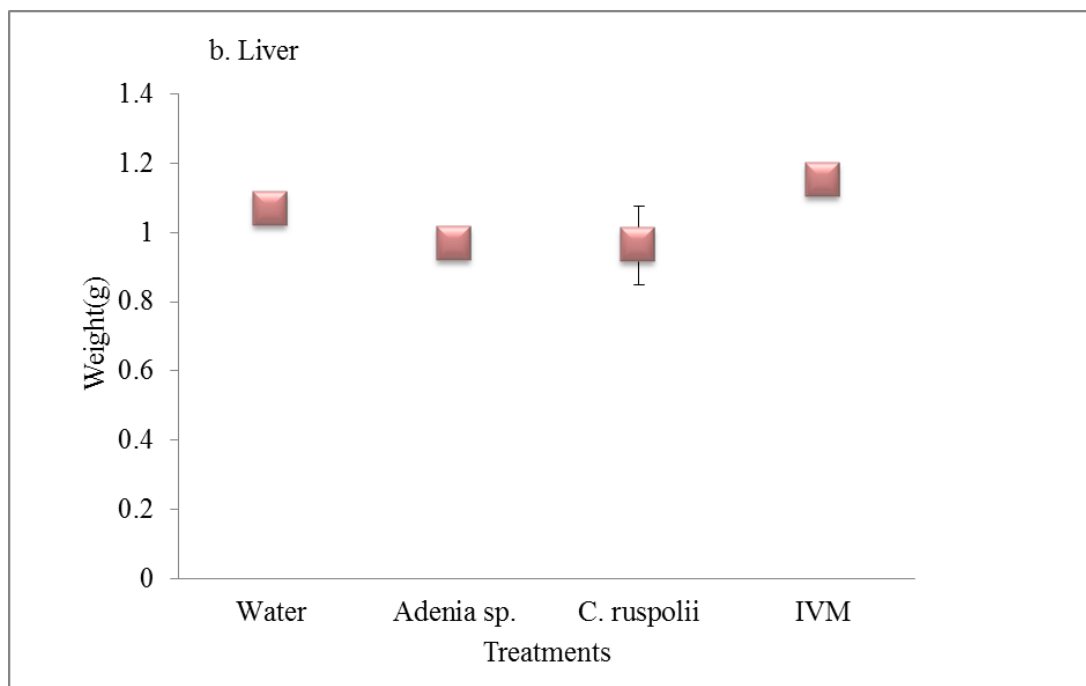
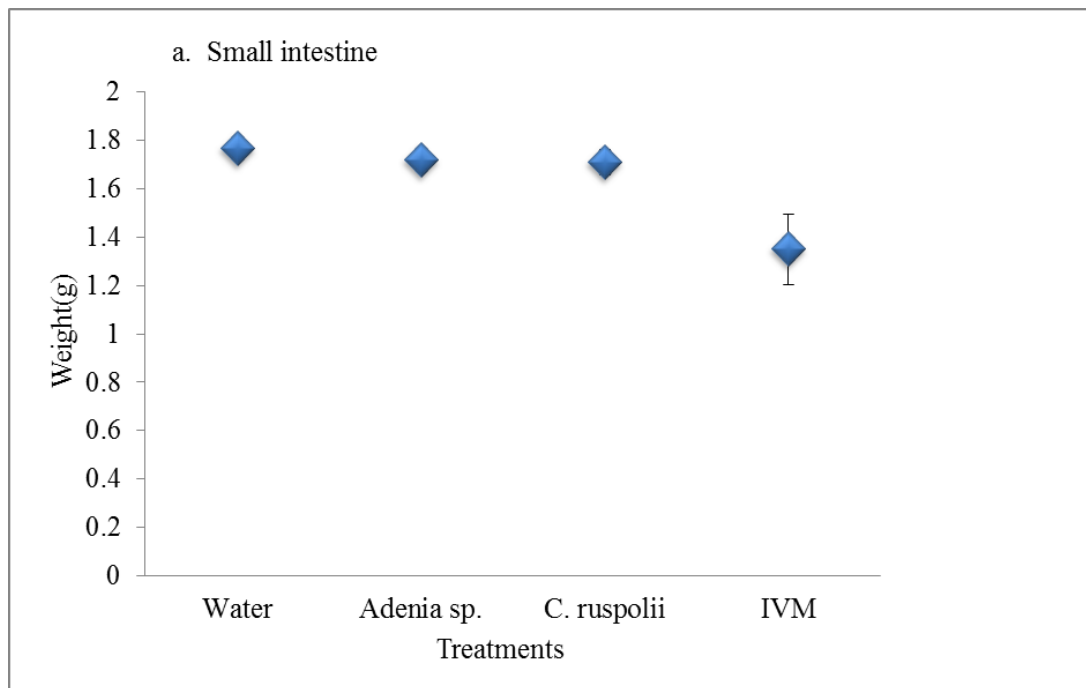


Figure 9.5. The effect of extracts on mice body weight infected with *H. bakeri*. Orally treated with water (♦), *C. ruspolii* (▲), *Adenia* sp.(■) or ivermectin (×) on days 0 (grouping and inoculation), 22 (before treatment), 29 (three days after first treatment) and 36 (at dissection, three days after second treatment).

9.4.3. Organ weight measurement

The gross morphologies of all recovered vital organs looked normal. Figure 9.6 shows the weights of small intestine, liver, spleen and kidneys. Treatments with water extracts of both *Adenia* sp. and *C. ruspolii* did not significantly affect weights of intestine, liver and kidneys ($P > 0.05$) when compared to the control although kidneys weight was clearly numerically increased for both *Adenia* sp. and *C. ruspolii* treated groups. However, spleen weight in *Adenia* sp. treated mice was significantly greater than that in control mice ($P < 0.05$). The greatest intestine weight was recorded for water group while the smallest was recorded for ivermectin treated group ($P < 0.05$).



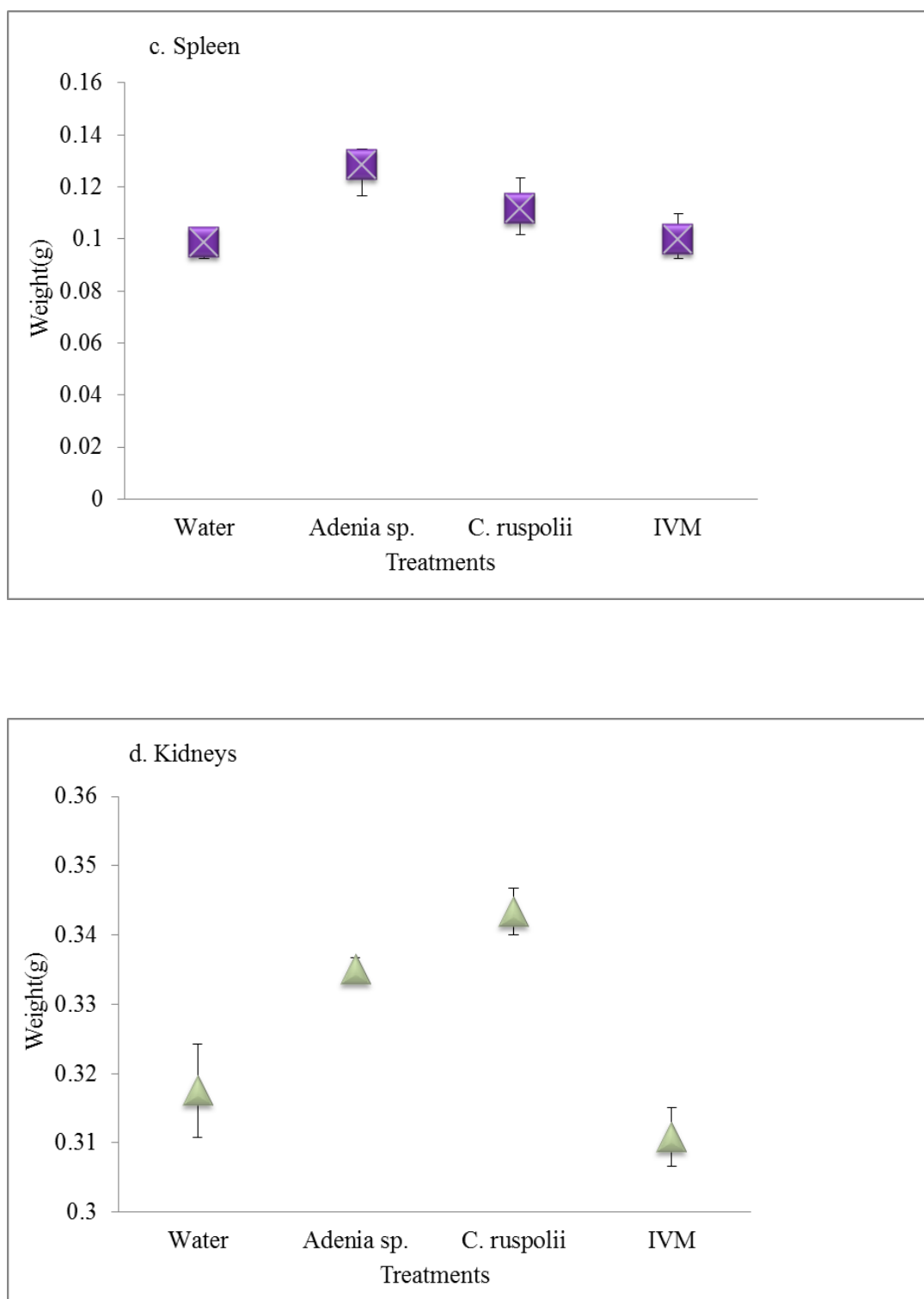


Figure 9.6. The effect of extracts on organ weight in mice infected with *H. bakeri*. After oral treatment with water, *C. ruspolii*, *Adenia* sp. or ivermectin. Small intestine (a), liver (b), spleen (c) and kidney (d).

9.4.4. Effects of extracts on haematological parameters

Before treatment, the concentration of red blood cells, and percentage of lymphocytes, segmented neutrophils, monocytes, eosinophils and basophils averaged $5.4 \pm 0.09 \times 10^{12}/L$, and $61.1 \pm 1.47\%$, $24.7 \pm 0.78\%$, $8.8 \pm 0.74\%$, 5.3 ± 0.39 and $0.1 \pm 0.03\%$, respectively. At dissection, these overall figures had changed to $7.7 \pm 0.09 \times 10^{12}/L$, $86.0 \pm 0.66\%$, $10.3 \pm 0.54\%$, $3.0 \pm 0.22\%$, $0.6 \pm 0.08\%$ and $0 \pm 0.0\%$, respectively. Thus, the proportion of neutrophils, monocytes and eosinophils were significantly ($P < 0.05$) reduced, whilst that of lymphocytes, as well as total RBC counts increased significantly ($P < 0.05$) across treatments. Table 9.2 shows the haematology of the different groups at dissection.

Table 9.2. Total and differential blood counts at dissection.

		Treatments				s.e.m.
		Water	<i>Adenia</i>	<i>Cissus</i>	IVM	
RBC	$\times 10^{12}/L$	7.32	8.63*	7.94	6.94	0.46
Lymphocytes	%	85.6	87.9	75.9*	91.6	2.87
Neutrophils	%	10.9	7.2	18.2*	6.5	2.46
Monocytes	%	2.7	4.2	4.9	1.8	1.02
Eosinophils	%	0.7	0.8	1.0	0.1	0.43

*Different from water ($P < 0.05$)

A significant increase in RBCs count ($P < 0.05$) was observed for *Adenia* sp. extract treated group compared to the water treated group. Furthermore, a significantly decreased percentage of lymphocytes and significantly increased percentage of neutrophils ($P < 0.05$) were observed for *C. ruspolii* extract treated group compared to the negative (water treated) control group.

9.5. Discussion

Anthelmintic efficacy evaluation of *Adenia* sp. and *C. ruspolii* water crude extract *in vivo* was based following a series of intensive *in vitro* anthelmintic efficacy experiments (Chapter Three) and strong claims by traditional healers as folkloric medicinal plants. In this study, powdered roots of both plants were extracted by maceration in de-ionized water. The freeze-dried water extract reconstituted in de-ionized water and tested for their anthelmintic properties *in vivo*. The anthelmintic efficacy of these extracts were evaluated by monitoring the deparasitization rate in mice, through faecal sample analysis after each treatments and post-mortem adult worm count to assess reduction in FEC and TWC, respectively. Both crude water extracts of *C. ruspolii* and *Adenia* sp. possessed significant anthelminthic properties against egg excretion and total worm count. At tested dose rate, *Adenia* sp. and *C. ruspolii* extracts resulted in total worm count reduction by 78% and 55% respectively compared to de-ionized water treated group (negative control).

Using the same model, Enejoh *et al.* (2015) reported that *Citrus aurantifolia* (Christmann) fruit locally used as an anthelmintic in Nigeria, showed 80.5% TWCR in mice orally treated with water juice of the plant at 800 mg/kg BW. They also revealed that the plant extract exhibited dose-dependent anthelmintic activity. Therefore, selection of the plant based on its ethno-medicine use, use of *H. bakeri* infected mouse as model animal, water as a vehicle, oral route of administration, and dose-dependent efficacy of the extract used are strongly in agreement with our experimental design and findings. Treatment of mice infected with *H. bakeri* with *Rauwolfia vomitoria* (Apocynaceae) at 3200 mg/kg BW showed a highly significant anthelmintic effects with 76% FECR and 80% TWCR efficacies after 7 days post-

treatment (Yondo *et al.*, 2013). Similarly, Udoha *et al.* (2015) also reported that oral administration of ethanol extract of *Ocimum gratissimum* reconstituted in water to *H. bakeri* infected mice at dose levels of 100, 200 and 400 mg/kg BW resulted in 30%, 47% and 67% FECR after 21 days of treatments respectively, while the 800 mg/kg BW of the extract achieved 100% FECR and TWCR by the 12 days post treatment. On the contrary, there are a number of medicinal plant extracts that showed highly significant EHI and/or LMI properties *in vitro* but had no effect against *H. bakeri in vivo* (Githiori *et al.*, 2004). For instance, leaf extracts of *Ficus exasperata* exhibited significant larvicidal activity on the infective stage larvae of *H. bakeri in vitro* but showed no activity on the same parasite *in vivo* (Nweze *et al.*, 2013). Such variability in the efficacies and/or toxicities of plant extracts could be associated with chemotaxonomic and phytochemical profile of the target plant, method of plant selection, site and season of collection, methods of processing and extraction, solvent type and polarity used for extraction and dose levels used.

In this study, it was observed that the initial dose level of 500 mg/kg BW was potentially toxic to mice, particularly for *C. ruspolii*, although this dose level is considerably lower compared to maximum dose levels used in some of the aforementioned studies. The reduction in the number of female worm counts compared to males could be associated with greater susceptibility of females to plant extracts and ivermectin (positive control). Apart from the cuticle and epithelium tissues as target sites of anthelmintics in both sexes, female nematodes have genital pore (vulva) covered by flap through which sperm enter the uterus and oviduct as well as embryonated and non-embryonated eggs are released (Carta *et al.*, 2009). Thus, it might be hypothesised that in female worms during eggs expulsion, the

active constituents of plant extracts and ivermectin could be absorbed through ovijector and cause ovicidal, ovulation/embryo development inhibition or nematocidal effect on female nematodes. The significant FECRs observed for plant extracts and ivermectin are also supporting these arguments.

At the dose levels used that did not exceed humane endpoints, body weight data did not show a significant effect of plant extracts ($P>0.05$). However, longer term experiments and inclusion of non-infected controls, are needed to assess whether the reduction in worm burdens result in performance benefits.

In addition to testing for pathogen reductions, *in vivo* studies also importantly provides opportunity to assess the effects of xenobiotics on specific organs. For many organs, this is done through macroscopic examination of the organs, measuring organ weight and histopathologic examination of the tissue. Organ weight can be a first indicator of an effect of an experimental compound/plant extract, as significant differences in organ weight between treated and untreated (control) animals may occur in the absence of any morphological changes.

In this study, upon removal of vital organs during dissection, no detectable abnormality was revealed. All recovered vital organs appeared grossly morphologically normal. However, IVM treated group (positive control) showed a numerical increase in liver weight and a significant decrease in intestine weights. The slight increment in liver weight might be due to inflammation and swollen up of the liver that caused by ivermectin toxicity (Kang *et al.*, 2016) or ivermectin stimulated hepatic enzyme-induced synthesis of compounds (Maronpot *et al.*, 2010). There was a decrease in small intestine weight observed for IVM treated compared to other

groups. This small intestine weight reduction could be associated with extremely insignificant remaining worm burden that resulted in very low residual mucus production from intestinal wall (Athanasiadou *et al.*, 2015). The largest small intestine weight recorded for water treated group could be associated with oedema and large amount of mucus production from the intestinal wall due to high worm burden.

The *Adenia* sp. treated group showed a significant increase in spleen weight. The spleen is a major lymphoid organ that plays a critical role in the primary humoral and secondary immune system (Al-Fararjeh *et al.*, 2013). This increase in spleen weight could be associated with migration of partially matured B lymphocytes from bone marrow to white pulp of spleen to complete their maturation or enlargement of spleen due to extract toxicity. If the spleen enlargement was due to the migration of partially matured B lymphocytes to the white pulp of spleen, then the *Adenia* extract might have immune stimulatory effect that boost the immune system. This is because the plant is also claimed for its wound healing properties by the traditional healers. The averaged absolute weights of kidneys of both *Adenia* sp and *C. ruspolii* treated groups were slightly increased compared to the control groups; although this was not statistically significant, it might indicate that the plant extracts may have some toxicity on this vital organ. These slight increments could be associated with nephrotoxicity because renal system actively involves in drugs or xenobiotics elimination from body through renal filtration processes, proximal tubule secretion and distal tubule reabsorption (Modaresi *et al.*, 2011). Hence, it cannot be excluded that the bioactive constituents of these plants may induce some renal inflammation or damage. In general, the organ weight is an important indicator of physiological and

pathological state both in humans and animals. Its weight is used as a fundamental diagnosis whether the organ was exposed to injury/damage or not. Analysis of organ weight in toxicology studies is an important end point for identification of potentially harmful effects of plant extracts, drugs or other chemicals. Differences in vital organ weight between treatment groups are likely to accurately detect target organ toxicity (Bailey *et al.*, 2004).

Blood is a vital and special circulatory tissue composed of cells suspended in an intercellular fluid substance known as plasma with the major function of maintaining homeostasis (Provan *et al.*, 2015; Isaac *et al.*, 2013). According to these authors, RBC is involved in oxygen and carbon dioxide transport. Thus, reduced RBC count implies a reduction in the level of oxygen that would be carried to the tissues as well as the level of carbon dioxide returned to the lungs. The main functions of WBC and its differentials are to fight infections, defend the body by phagocytosis against invasion by foreign organisms and to produce or at least to transport and distribute antibodies in immune response. Thus, animals with low WBCs may have increased risk of disease or infection while those with high WBC counts may be more capable of generating antibodies in the process of phagocytosis and have high degree of resistance to disease (Soetan *et al.*, 2013).

The results of haematological parameters revealed that there were significant changes in differential neutrophils and lymphocytes counts. RBC counts increased for *Adenia* sp. compared to water treatment. This increment may be associated with *Adenia* sp. extract stimulated production of RBC in bone marrow and stored as a reserve in red pulp of spleen, since *Adenia* sp. treated group also showed greater spleen weight compared to other treatment groups. The significant decrease in

lymphocytes percentage in *C. ruspolii* extract treated group might be associated with the cell specific adverse effect of the constituent(s) of the extract on lymphocytes whereas the significant increase in neutrophils percentage might be indicator of infection or inflammation. However, these changes are in the same direction in all groups. The magnitude of the changes in WBC, WBC differentials and RBCs counts are dependent on the sampling techniques and site of collection (Schnell *et al.*, 2000). Overall, *Adenia* sp. appeared to be stimulating the RBC production whereas *C. ruspolii* extract seemed to have adverse effect on lymphocytes. However, to generate conclusive evidence on effects of extracts on haematological and biochemical parameters, further and more detailed studies are needed.

Chapter Ten: Overall discussion, conclusions and future work

10.1. Introduction

Infections with gastrointestinal nematodes represent a major constraint in small ruminants. For many years, the control of these parasites has solely relied on the intensive and indiscriminate use of synthetic anthelmintics (Zajac, 2006). However, the emergence of resistant gastrointestinal nematode populations and the increasing concern of consumers for drug residues in animal products have provided a strong impetus towards the development of alternative strategies to control nematodes in livestock. Amongst those alternatives, the use of medicinal plant extracts to deworm infected small ruminants received prime attention in the last decades (Wink, 2012). The anthelmintic effects observed in response to the plant extracts screened against economically important parasites both *in vitro* and *in vivo* are believed to be associated to plant secondary metabolites (such as alkaloids, saponins, tannins and other polyphenols) that are contained in the tested plants (Bauri *et al.*, 2015).

In Ethiopia, livestock productivity is very low due to poor livestock health care in pastoral and agro-pastoral communities arising from lack of adequate clinics, veterinarians and supply of drugs. Besides, most modern drugs are inaccessible and/or not affordable by the majority of Ethiopian farmers and pastoralists. Therefore, they rely, as they have done for centuries, on their indigenous knowledge, practices and locally available plant materials for the management of diseases of their domestic animals (Bekele and Reddy, 2015; Giday and Teklehaymanot, 2013). Screening of such ethno-medicinal plants that highly utilized and claimed by the traditional healers assists to validate their efficacy and to identify active constituents

responsible for the observed activities (Kinghorn *et al.*, 2011). This was the objective of my thesis for selected Ethiopian plants.

10.2. Effects of crude extracts on nematode egg hatching and larvae motility

These experiments were basically designed to verify the hypothesis that extracts prepared from selected plants based on their ethno-medicinal uses in livestock will show anthelmintic activity *in vitro* against the free living stages of small ruminant nematodes such as *T. circumcincta*. In the *in vitro* anti-parasitic screening experiment (Chapter Three), EHI tests of crude extracts from four Ethiopian medicinal plants (*Euphorbia thymifolia*, *Ipomoea eriocarpa*, *Cissus ruspolii* and *Adenia* sp.) were conducted using a standard anthelmintic evaluation method on *T. circumcincta* eggs. LMI properties of *C. ruspolii* and *Adenia* sp. crude extracts were also assessed against third stage larvae of the same nematode using real time cell analyser (RTCA) equipment. Generally, EHI properties of plant extracts increased with increasing of extract doses, although these increases varied in magnitude between the type of plant and solvent polarity used for extraction. For instance, at 10 mg/ml concentration, 70% MeOH extract of *C. ruspolii* and water extracts of both *C. ruspolii* and *Adenia* sp. completely inhibited *T. circumcincta* egg hatching. In contrast, *E. thymifolia* extracts using all solvent systems, at each tested concentration, showed less than 30% EHI activity. For *I. eriocarpa*, only the 70% MeOH extract at 10 mg/ml showed greater than 70% EHI.

The water and 70% MeOH extracts of *C. ruspolii* and water extract of *Adenia* sp. also significantly reduced L₃ motility at 10 mg/ml compared to controls (PBS with L₃) and exhibited almost the same readouts as for positive control wells, i.e. dead L₃

with plant extracts and PBS only. In contrast, the acetone extract of *Adenia* sp. did not show any larval motility inhibition as there was a constant increase in mean motility observed throughout experiments similar to the L₃ incubated in PBS (negative control).

The *in vitro* assays used thus revealed that the four medicinal plants have variable degrees of anti-parasitic properties. Such variability in the efficacies of extracts could be associated with chemotaxonomic and phytochemical profile of the target plant, solvent type and polarity used for extraction and dose levels used. However, these *in vitro* experiments verified the stated hypothesis, validated the ethno-medicinal uses of the four medicinal plants used in this study and also assisted us to choose water extracts of *C. ruspolii* and *Adenia* sp. for further bioassay guided phytochemical studies.

There are a number of similar *in vitro* findings on medicinal plants and plant extracts that have been screened against economically important parasites and exhibited strong anthelmintic activities that support our findings. For instance, in Cameroon at 5 mg/ml, the water extracts of *Nauclea latifolia* exhibited 62.7 and 21.7% of *H. bakeri* embryo development and egg hatching inhibition rates, respectively (Josué *et al.*, 2012). They also reported 89.3 and 77.5% larvicidal activity against *H. bakeri* L₁ and L₂, respectively. Water extracts of leaves of *Carissa spinarum* and *Azadirachta indica* showed 100% EHI at concentration of 0.5 mg/ml, whilst water extracts of *Acacia tortilis* and *Phytolacca dodecandra* exhibited 100% and 99.4% EHI of *H. contortus* at concentration of 2 mg/ml (Mohammed *et al.*, 2013). Our findings are further in agreement with these outcomes because as in our study, these researchers selected target plants based on their ethno-medicinal uses, used water solvent system

to prepare extracts and screened these extracts against eggs from trichostrongylid nematodes. Moreover, their findings also support the general principle that plants selected based on their ethno-medicinal uses are more likely to contain the active components of medicinal interest, as argued at the outset of this thesis.

10.3. Effects of crude extract physico-chemical treatments on their EHI properties

These experiments were aimed at assessment of the nature (molecular size, thermal stability and polarity) of active constituents of water crude extracts and how their bioactivities are affected by physicochemical treatments. In the physico-chemical studies and EHI properties of crude extracts (Chapter Four), the active constituents of water crude extracts of *C. ruspolii* and *Adenia* sp. were characterized physico-chemically by membrane dialysis, thermal stability testing and solvent partition. After dialysis, external solutions recovered from first dialysis (low molecular weight) of both plant samples showed significantly greater EHI activities than the sac contents (high molecular weight). This effect was stronger for *C. ruspolii* than for *Adenia* sp. ($P < 0.001$). The modest EHI activities exhibited by high molecular weight fractions might be due to incomplete removal of active low molecular weight constituents during further dialysis or some high molecular weight fractions might have EHI properties. At comparable concentration, it was observed that the EHI exhibited by membrane separated fractions was lower than the crude extract. The smaller percentage of EHI exhibited by membrane separated fractions of both plants compared to the crude extract (positive control) at comparable tested concentrations might be due to loss of low molecular weight active constituents during further dialysis, the crude extract may contain both low and high molecular weight active

constituents or the solubility of the recovered samples in deionized water during reconstitution for bioassay might have been compromised. The smaller percentage of EHI activities exhibited by membrane separated low molecular constituents compared to the crude extract might also be due to the 19-30% low molecular weight constituents lost during further dialysis. In general, this study shown that low molecular weight constituents are largely responsible for the observed anthelmintic activities of both extracts.

The EHI activities of heat treated water crude extracts of both plants were decreased with increased heating time ($P < 0.001$). The decrease in EHI properties of extracts with increased heating time is an indicator that the anthelmintic constituents of extracts are at least partially thermal degradable. The fluorescent spots under UV-light at 366 nm for *C. ruspolii* and thymol and molybdate stained concentrated spots for *Adenia* sp. (Chapter Four) may be among the likely active heat stable or slightly thermo-labile constituents that survived the complete thermal degradation or only partially degraded during boiling. Our heat stability findings are in agreement with the findings of many researchers. Cheng *et al.* (2014) reported that phenolic compounds in water solution such as protocatechuic acid partially degraded partially at 200°C and completely decomposed at 300°C upon heating for 20-60 minutes. Thus, the blue fluorescing constituents of *C. ruspolii* at 366 nm could be phenolic compounds such as flavonoids that survived prolonged heating or partially degraded at 100°C for an hour. Önning *et al.* (1994) also reported that oat saponins (avenacosides) were stable when heated at 100°C for 3 h. Also, *Adenia* sp. water extract was highly foamy, suggesting that it might be rich in saponins. Hence, the two close and slow migrating spots on TLC that stained well with thymol and

molybdate could be saponins that are either stable or only partially degraded at 100°C upon heating for 1 h. Thus, both plant extracts contained active constituents that could either survived or partially degraded at 100°C for an hour and hence exhibit EHI activity. So, the active principles of both plants are moderately heat-labile.

Solvent partition is an indication of the polarity of the extract as well as the compounds present in that extract. The EHI tests followed by chromatogram analyses of solvent partitioned fractions (Chapter Four) revealed that the water extracts of *Adenia* sp. and *C. ruspolii* contained both hydrophilic and amphiphilic constituents that preferentially partitioned into water, butan-1-ol, ethylacetate fraction or three of them. However, the water fractions of both plants were more bioactive than their organic counterparts implying that the major active anthelmintic component(s) are largely hydrophilic and preferentially partitioned into water phase. The preferential partitioning of constituents of crude extracts into one of the solvent system in the mixture may not only dependent on solvent polarity (dielectric constant) but also on the affinity and selectivity of the solvent. For instance, the blue and yellow fluorescent compounds at 366 nm in *C. ruspolii* were partitioned into both water and organic phases. However, the fast migrating yellow fluorescing constituent seems largely partitioned into butan-1-ol (Chapter Four). Similarly, the two major and closely migrating spots of *Adenia* sp. also partitioned into both water and organic phases. Thus, both plants could contain hydrophilic and amphiphilic constituents that may partition either into water, organic or both based on the solvent affinity and selectivity. Thus, it can be concluded that the major constituents of both

plant extracts responsible for the EHI activities observed are highly polar and preferentially water-soluble molecules.

In general, the overall result of physico-chemical studies showed that major active constituents of both plant extracts responsible for the EHI activities observed are highly polar, water-soluble, small and moderately heat-labile molecules.

10.4. Bioassay-guided fractionations of crude extracts and chromatographic profiling of Bio-Gel P-2 fractions

The aim of bioassay-guided fractionations of *C. ruspolii* and *Adenia* sp. water crude extracts on Bio-Gel P-2 (Chapters Five and Six) was to separate constituents of these extracts into discrete fractions based on their molecular sizes and then to identify active fraction(s) based on their EHI properties. The EHI tests of GPC fractions of both plants revealed that active constituents of these extracts were partitioned into a small number of fractions based on their molecular sizes. Chromatograms examined under UV-light at both shorter and longer wavelengths shown that *C. ruspolii* extract contained constituents that fluoresce at 366 nm. However, the *Adenia* sp. extract did not contain any fluorescent spots. Such a result could happen because of the method of extraction employed, polarity incompatibility between the solvent and fluorescing compound (not soluble in water), the extraction condition used (not soluble at room temperature) or the plant may not synthesise metabolites with UV-active chromophore functional groups.

For *Adenia* sp. runs 1 and 2, it was noted that the void volumes (V_0) correspond to fraction 8 and 12 respectively. These fractions were among those active fractions pooled as ASPA and thus presumably are small molecules. Bio-Gel P-2 is

“supposed” to retard small molecules, however, some active constituents of *Adenia* sp., more likely small molecules with anomalous behaviour possibly detergent-like molecules such as saponins that form big micelles in water solution, might be eluted in V_0 . Thus, the $V_0=V_i$ observed here implies that the general principle of separation of constituents of medicinal plant crude extracts on GPC based only on molecular size may not necessarily be effective. The GPC separation of constituents of a mixture based only on molecular size may work for biomolecules (primary metabolites) but may not work for plant secondary metabolites which are known for their diverse physicochemical properties. These diverse physicochemical properties could be related to the diverse phytochemical classes they belong to and the functional groups in their structures that influence their elution behaviour on GPC.

During the chromatogram profiling of Bio-Gel P-2 fractions of *C. ruspolii* and *Adenia* sp. (run-1), glucose and sucrose were components of the marker mixture for TLC development. These two common plant sugars are expected to exist as free sugar molecules in most of plant crude extracts. Surprisingly, none of the separated bands in the fractions of both plants matched with either of the bands. This result implies that these sugars are not present as free sugar molecule in the water extracts as prepared from both plants. The absence of these common sugars may be related to the parts of the plants used, as both plants may not synthesise and/or store these sugars in their root or they may exist as glycosides rather than free monosaccharide sugars.

From the chromatogram profiling of Bio-Gel P-2 fractions of both plants, it was also observed that the active and inactive fractions had distinct patterns of separated spots. Such detailed information assists to pool active fractions based on their similar

spot patterns for further isolation and purification. For Bio-Gel P-2 (runs 1 and 2) of a given extract, it was also noted that there was a strong correlation between discrete fractions with significant EHI activities and their spot patterns on chromatograms. This bio-assay guided fractionation and chromatogram profiling of Bio-Gel P-2 fractions helped us to categorize and merge the main active Bio-Gel P-2 fractions into pools based on their similar EHI efficacy and spot patterns on chromatogram. This is because merging of these partially purified active fractions into a small number of active pools enriches pools in active constituents, which makes further bioassay-guided isolation and purification more quantitative (i.e. reasonable amount of target compound(s) recovered that may be enough for physical, chemical and biological assays) and also minimize time and cost of purification.

The chromatogram profiling of Bio-Gel P-2 fractions also revealed that fractions containing V_0 and V_i eluates were influenced by nature and sample volume loaded, column bed volume, the volume of fractions collected and flow rate during fractionation. It was observed that simultaneous increase in sample size and column bed volume and decrease in volume of fraction collected and flow rate resulted in partitioning of active constituents into a number of neighbouring fractions. The chromatogram profiling also revealed that *C. ruspolii* extract fractionations on Bio-Gel P-2 were more influenced by the change in sample size and column parameters compared to *Adenia* sp. extract fractionations. This difference might be related to the physicochemical properties of their constituents. Overall, optimizing of the column parameters during fractionations followed by EHI tests and TLC profiling helped us to better identify active and inactive fractions and to merge the active fractions into a small number of pools for further bioassay guided isolation and purification (Chapter

Seven). Thus, pooling of Bio-Gel P-2 fractions into pools A, B and C for *C. ruspolii* (CRPA, CRPB and CRPC) and for *Adenia* sp. (ASPA, ASPB and ASPC) were done based on their combined EHI and TLC profiles.

10.5. Isolation and purification of compounds from active pooled fractions

In Chapter Seven, a number of chromatographic techniques were employed with the objective of isolation, purification and profiling of constituents from active pooled fractions of *C. ruspolii* and *Adenia* sp. For instance, paper chromatography (PC) was used to assess the presence and nature of fluorescent compound(s) in the active pooled fractions of both plants using arbitrary marker mixture containing ferulic and caffeic acids. PC was also assessed for its suitability as preparative chromatographic technique to isolate and purify constituents of the active pooled fractions using the ASPC sample. However, the constituents of ASPC did not migrate far from the origin as only the band recovered from the origin exhibited significant EHI activity ($P < 0.05$). This is because papers are made up of cellulose, which has numerous hydroxyl (-OH) functional groups that could form strong covalent bond with various constituents of water pooled fractions. Therefore, PC was not found a suitable chromatographic technique for quantitative isolation and purification of bioactive plant secondary metabolites from active pooled fractions. However, it was used to detect the presence of fluorescent compounds in one of the *C. ruspolii* active pooled fractions (CRPC), whilst none such fluorescent compounds were observed in *Adenia* sp. active pooled fractions.

High voltage paper electrophoresis (HVPE) was also used to qualitatively characterise and semi-quantitatively estimate the constituent in *C. ruspolii* water crude extract that stains yellow with molybdate using standard sodium dihydrogen

phosphate dihydrate as a marker. This yellow-stained constituent with molybdate may be inorganic phosphate or an organic compound with the same R_F -value and ionic mobility like sodium dihydrogen phosphate dihydrate. Its concentration in the crude extract of *C. ruspolii* was semi-quantitatively determined to be about 48 mM.

For isolation and purification of active pooled fractions, Sephadex LH-20 and reversed phase C_{18} columns followed by PTLC were intensively used. In Sephadex LH-20 and C_{18} purification, the gradient elution method was used. Water was the first eluent used in both techniques. The major constituents of pooled fractions of both plants were eluted in water fractions on both Sephadex LH-20 and C_{18} columns. This is because the crude extract was prepared in water solvent system and the Bio-Gel P-2 fractionations also done using an isocratic elution method in which de-ionized water was used as eluent. Therefore, it was less likely to partition the major constituents of pooled fractions into less polar solvents such as methanol gradients or absolute methanol. Monitoring of the column parameters and sequential applications of column chromatography followed by PTLC resulted in the isolation and purification of three compounds with R_F -values of 0.13, 0.58, and 0.68 from CRPA; one compound with R_F -value of 0.73 from CRPB; a blue fluorescent compound under UV-light at 366 nm with R_F -value of 0.53 from CRPC and two compounds from ASPA, one with R_F -value of 0.23 and one with R_F -value of 0.27.

A number of PSM with anthelmintic properties with different chemical structures and functions have been screened, separated, fractionated, purified or analyzed using various adsorbents and eluents through column chromatography and thin layer chromatography. For instance, a new cycloartane-type saponin and monoterpenoid glucoindole alkaloids with antiprotozoal activities were isolated from 70% MeOH

extract of aerial part of *Mussaenda luteola* (Rubiaceae) on Sephadex LH-20 in absolute methanol eluent (Mohamed *et al.*, 2016). Wangchuk *et al.* (2016) reported that out of six phytochemicals isolated and purified from *Corydalis crispera* and *Pleurospermum amabile*, two Bhutanese medicinal plants tested for anthelmintic properties, two compounds (isomyristicin and bergapten) showed significant anthelmintic activity against *Schistosoma mansoni* and *Trichuris muris* with bergapten being the most efficacious compound against both parasites at average IC_{50} of 9.1 μ g/ml. They also reported that these two compounds induced tegumental damage to *S. mansoni* and affected the cuticle, bacillary bands and bacillary glands of *T. muris*. The phytochemical characterization of a hydro-alcoholic leaf extract of *Combretum mucronatum* and bioassay-guided fractionation, isolation and purification led to the identification of epicatechin and oligomeric proanthocyanidins as the active compounds with a dose-dependent *in vitro* anthelmintic activity against the model nematode *Caenorhabditis elegans* (Spiegler *et al.*, 2015).

10.6. Proposed structures of compounds isolated from active fraction(s)

This experiment was fundamentally intended to prove the hypothesis that the major active phytochemical groups isolated from active fractions of these selected plants may belong to plant secondary metabolites known for their anthelmintic activity, such as tannins, flavonoids, saponins and alkaloids. In Chapter Eight, analytical and spectroscopic characterizations of compounds isolated from two medicinal plants were attempted to elucidate or propose their structures. However, for reasons discussed in Chapter Eight, only the structures of two triterpenoid saponins (A and B) isolated from *Adenia* sp. were most successfully proposed based on MS data and TLC of TFA hydrolysates of samples containing compounds A and B with

supportive data from NMR, physicochemical properties of A and B, literature and bioassay data. These two compounds may have closely similar oleanane type core structures and the same trisaccharide attached to the hydroxyl group at C-3 although compound A may have a galactose unit attached to its C-28 carboxyl functional group. The trisaccharide common to both A and B consisted of rhamnose, xylose and an unknown sugar, which may be quinovose, an epimer of rhamnose.

10.7. *In vivo* validation of water crude extracts in mice

This experiment was essentially designed to corroborate the hypothesis that extracts from selected plants that show anthelmintic activity *in vitro* will show anthelmintic activity *in vivo*. The main objective of the *in vivo* experiment (Chapter Nine) was to assess the efficacy of crude water extracts of *C. ruspolii* and *Adenia* sp. by determination of faecal egg count and total worm count reductions and safety through their effect on body and vital organ weights and haematological parameters in a mice model. This *in vivo* efficacy and safety assessment of these extracts was designed based on the efficacy observed during intensive *in vitro* EHI tests and their ethno-medicinal use in the treatment of gastrointestinal nematodes in livestock.

Heligmosomoides bakeri is a trichostrongylid nematode found in small rodents including mice (*Mus musculus*). It is an important laboratory model for chronic nematode infections, especially for small intestinal nematodes due to its persistence in mice for at least 46 weeks (ten months) following a single infection (Behnke *et al.*, 2009). The nematode *H. bakeri* is a good model to assess the efficacy of medicinal plant extracts claimed for anti-parasitic properties. In this respect, *H. bakeri* resembles hookworms of humans (*Ancylostoma duodenale*) and gastrointestinal nematodes of livestock such as *H. contortus* and *T. circumcincta* of sheep (Geets *et*

al., 2000). Therefore, the *H. bakeri* mouse model is commonly used in anthelmintic screening of plant extracts with purported anti-parasitic properties against endo-parasitic nematodes of humans and livestock.

10.7.1. The effect of extracts on FEC and TWC

At an averaged oral dose of 219 and 250 mg/kg body weight water extracts of *C. ruspolii* and *Adenia* sp. reduced mice faecal egg counts by 55 and 54% respectively ($P < 0.05$). The *Adenia* sp. and *C. ruspolii* extracts also reduced worm burdens by 78 and 55%, respectively ($P < 0.05$). Both extracts exhibited greater degree of worm burden reductions in adult female worm than male worms. For instance, *Adenia* sp. and *C. ruspolii* extract resulted in 89.9% and 71.1% reduction in female worms, respectively, whilst this was 67.4% and 40.6% for male worms, respectively, in comparison to the water-treated negative control group. These significant FEC and TWC reductions ($P < 0.05$) exhibited by these plant extracts could be associated with the PSMs that interfere with the life cycle of the target parasite. This is because bioactive PSMs in medicinal plant extracts with anthelmintic properties often interfere with central targets in parasites, such as DNA (intercalation, alkylation), membrane integrity, microtubules polymerization, energy production and neuronal signal transduction (Wink, 2012). For instance, tannin containing plant extracts have anthelmintic properties against nematodes by interfering with three key biological stages, i.e. inhibit L₃ exsheathment, interfere with energy production, and ovicidal or larval development inhibition (Hoste *et al.*, 2012). Plant extracts with optimum alkaloids content may interfere with neurotransmitter molecules or regulatory enzymes involved neuromuscular system of nematodes. Flavonoids and polyphenols inhibit key enzymes of glycolysis and glycogenolysis of nematodes (Bauri *et al.*,

2015). According to Francis *et al.* (2002), saponins showed anthelmintic activities due to the intercalation of the hydrophobic portions of the saponins in cell membranes that resulted in the formation of pores in the tegument of helminths. The hydrophobicity of essential oils disrupts the structure and affects its fluidity. Thus, the anthelmintic properties observed for both plants may be due to the presence of one or more of such classes of phytochemical groups (PSMs).

10.7.2. The effect of extracts on body weight, organ weight and haematological parameters

At the dose levels used that did not exceed humane endpoints, no significant body weight change ($P>0.05$) was observed. The insignificant effect of plant extracts on mice body weight could be associated either with the short experiment duration that did not allow to see the performance benefit and/or penalties of extracts or the eight weeks old mice used were fully grown and significant body weight gain might not be expected. Nevertheless, drenching with *Adenia* sp. increased spleen weight and red blood cell concentrations, whereas drenching with *C. ruspolii* increased segmented neutrophil and reduced lymphocyte percentages. In addition, both plants resulted in a numerically increased kidneys weight when compared with the water-treated group. The increment in RBC concentrations may be associated with *Adenia* sp. extract stimulated production of RBC in bone marrow and stored as a reserve in red pulp of spleen, since *Adenia* sp. treated group also showed greater spleen weight compared to other treatment groups. The spleen is also a major lymphoid organ in immune system network that plays a critical role in the primary humoral and secondary immune system (Al-Fararjeh *et al.*, 2013). This increase in spleen weight could also be associated with migration of partially matured B lymphocytes from bone marrow

to white pulp of spleen to complete their maturation. If the spleen enlargement was due to the migration of partially matured B lymphocytes to the white pulp of spleen, then, the *Adenia* extract might have immune stimulatory effect that boost the immune system of mice. On the contrary, the likelihood of extracts to, toxicity to spleen cannot be excluded and hence further study is needed to generate a conclusive evidence to support either the safety or toxicity of these extracts. This is further supported by the observation that at initially used dose of 500 mg/kg BW a number of mice, especially for *C. ruspolii* had to be euthanased as their near moribund behaviour exceeded the humane endpoints set for the trial.

The significant decrease in lymphocytes percentage in *C. ruspolii* extract treated group might be associated with the cell specific adverse effect of the constituent(s) of the extract on lymphocytes whereas the significant increase in neutrophils percentage might be indicator of infection or inflammation. Overall, *Adenia* sp. appeared to be stimulating the RBC production whereas *C. ruspolii* extract seemed to have adverse effect on lymphocytes. However, to generate conclusive evidence on effects of extracts on body weight, haematological and biochemical parameters, further and more detailed studies are needed.

In general, these *in vivo* data reaffirmed the anthelmintic efficacies of the extracts observed during *in vitro* experiment, validated the traditional healers' claims and, also supporting the ethno-medicinal use of these plants as alternative plant based parasite control option in livestock.

10.8. Conclusions

The conclusions of my thesis can be summarised as follows.

- The data generated from the intensive *in vitro* EHI and preliminary LMI assays support the view that tested medicinal plants have anti-parasitic properties and validated their ethno-medical uses. These data also proved that the general principle of plants selected based on their ethno-medicinal uses are more likely contain the active components of medicinal interest. The *in vivo* data also revealed that *Adenia* sp. and *C. ruspolii* extracts had anthelmintic properties thus supporting the ethno-medicinal use of these plants.
- Physico-chemical characterization of water crude extracts of *Adenia* sp. and *Cissus ruspolii* revealed that the active constituents of both plants are highly polar, water-soluble, small and moderately heat-labile molecules.
- Bioassay guided fractionations of crude extracts and merging of the partially purified active fractions based on their EHI and TLC profiling in to few numbers of pools enrich the pools with active constituents.
- Planar or column chromatography can be used for isolation and purification of compounds from active pooled fractions. In this study, sequential applications of Sephadex LH-20, reversed phase C-18 column followed by PTLC resulted in the isolation and purification of compounds from active pooled fractions of both plants.
- The structures of two triterpenoid saponins (A and B) isolated from *Adenia* sp. were successfully proposed based on MS data, sugar chromatograms of

TFA hydrolysates of samples containing compounds A and B with supportive data from NMR, physicochemical properties of A and B, literature and bioassay data.

10.9. Future directions

From the work carried out a number of possible future research directs have emerged. These can be summarised as follows.

- The bioassay-guided phytochemical study of these plants may continue as part of my post-doctoral work under different laboratory settings.
- Detailed *in vivo* assays may be carried out by adjusting the dose level of the crude extracts that allow to dose appropriate number of mice per treatment repeatedly over certain duration to further validate the ethno-medicinal uses and for detail assessment of safety of these plants.
- Longer term benefit on worm resistance and resilience may be assessed through mouse model experiments.
- Field trials may be conducted to verify the impact of plant extracts on parasitism in collaboration with the end-users (smallholder farmers and traditional healers).
- The efficacies of active constituents may be assessed in the presence of competitive inhibitors (antagonists).
- Extraction techniques other than maceration may be employed to prepare crude extracts using a range of solvent polarities and their combinations.
- Apart from anti-parasitic activities, the plant samples may be assessed against range of medicinally important micro-organisms for both livestock and humans.
- The extracts or purified compounds may also be evaluated for their cytotoxicity using different cell lines.

- Different solvent systems used for TLC development, fractionation, isolation and purification may result in identification of different active ingredients.
- Using a larger array of detailed chemical and chromatographic screenings may assist to inform optimal isolation and purification technique(s) to be employed.
- Reasonable amount of starting materials may be used to recover quantitative amount of purified compounds that are sufficient for physical, chemical and biological assays. This approach may allow a wider array of chromatographic, analytical and spectroscopic techniques to be employed for structural characterization and elucidation of isolated compounds from active fractions of these and other such plants.

11. References

- Abebe R, Tatek M, Megersa B, Sheferaw D, 2011. Prevalence of small ruminant ecto-parasites and associated risk factors in selected districts of Tigray Region, Ethiopia. *Global Veterinaria* **7**:433-437.
- Abera B, 2014. Medicinal plants used in traditional medicine by Oromo people, Ghimbi district, southwest Ethiopia. *Journal of Ethnobiology and Ethnomedicine*, **10**:40.
- Acikara BÖ, Citoglu SG, DallAcqua S, Özbek H, Cvacka J, Zemlicka M, Smejkal K, 2014. Bioassay-guided isolation of the antinociceptive compounds motiol and β -sitosterol from *Scorzonera latifolia* root extract. *Pharmazie*, **69**:711-714.
- Adamu M, Naido V, Eloff JN, 2013. Efficacy and toxicity of thirteen plant leaf acetone extracts used in ethnoveterinary medicine in South Africa on egg hatching and larval development of *Haemonchus contortus*. *BMC Veterinary Research*, **9**:38-53.
- Ademola IO, Eloff JN, 2011. Anthelmintic efficacy of cashew (*Anarcadium occidentale*) on *in vitro* susceptibility the ova and larvae of *Haemonchus contortus*. *African Journal of Biotechnology*, **10**:9700-9705.
- Agrawal AA, Janssen A, Bruin J, Posthumus MA, Sabelis MW, 2002. An ecological cost of plant defence: attractiveness of bitter cucumber plants to natural enemies of herbivores. *Ecology Letter*, **5**:377-385.
- Aguoru CU, Ameh SJ, Olasan O, 2014. Comparative phytochemical studies on the presence and quantification of various bioactive compounds in the three major organs of okoho plant (*Cissus populnea*) in Benue state north central Nigeria,

- western Africa. *European Journal of Advanced Research in Biological and Life Sciences*, **2**:2056-5984.
- Akkol EK, Süntar I, Keleş H, Sezik E, Gürler G, 2015. Bioassay-guided isolation and characterization of wound healer compounds from *Morus nigra* (Moraceae). *Record of Natural Products*, **9**:484-495.
- Anulika NP, Ignatius EO, Raymond ES, Osasere OI, Abiola AH, 2016. The chemistry of natural product: plant secondary metabolites. *International Journal of Technology Enhancements and Emerging Engineering Research*, **4**:ISSN2347-4289.
- Al-Fararjeh MA, Jaber MH, Abdelrahman YS, 2013. Evaluation of immune-modulatory, effects of antiepileptic drug phenytoin. *Jordan Journal of Biological Sciences*, **6**:328-333.
- Álvarez-Sánchez MÁ, Mainar-Jaime RE, Pérez García J, Rojo-Vázquez FÁ, 2002. A review of the methods for the detection of anthelmintic resistance. *Revista Ibérica de Parasitología*, **62**:51-59.
- Alzahrani F, Al-Shaebi EM, Dkhil MA, Quraishy SA, 2016. *In vivo* anti-*Eimeria* and *in vitro* anthelmintic activity of *Ziziphus spina-christi* leaf extracts. *Pakistan Journal of Zoology*, **48**:409-413.
- Amin MR, Mostofa M, Hoque ME, Sayed MA, 2009. *In vitro* anthelmintic efficacy of some indigenous medicinal plants against gastrointestinal nematodes of cattle. *Journal of the Bangladesh Agricultural University*, **7**:57-61.
- Amr A, Al-Tamimi E, 2007. Stability of the crude extracts of *Ranunculus asiaticus* anthocyanins and their use as food colorants. *International Journal of Food Science and Technology*, **42**:985–991.

- Argaw S, Beyene D, Abebe B, 2014. Prevalence of abomasal nematodes in sheep and goats slaughtered at Haramaya municipal abattoir, Eastern Hararghe, Ethiopia. *Journal of Biology, Agriculture and Healthcare*, **6**: 81-87.
- Argentieri PM, D'Addabbo T, Tava A, Agostinelli A, Jurzysta M, Avato P, 2008. Evaluation of nematicidal properties of saponins from *Medicago sativa* spp. *European Journal of Plant Pathology*, **120**:189-197.
- Asami DK, Hong YJ, Barrett DM, Mitchell AE, 2003. Comparison of the total phenolic and ascorbic acid content of freeze-dried and air-dried marionberry, strawberry, and corn grown using conventional, organic, and sustainable agricultural practices. *Journal Agriculture and Food Chemistry*, **51**:1237-1241.
- Atanasov AG, Waltenberger B, Pferschy-Wenzig EM, Linder T, Wawrosch C, Uhrin P, Temml V, Wang L, Schwaiger S, Heiss EH, Rollinger JM, Schuster D, Breuss JM, Bochkov V, Mihovilovic MD, Kopp B, Bauer R, Dirscha VM, Stuppner H, 2015. Discovery and resupply of pharmacologically active plant-derived natural products: A review. *Biotechnology Advances*, **33**:1582–1614.
- Atawodi SE, Atawodi JC, Idakwo P, Pfundstein B, Haubner R, 2009. Evaluation of the polyphenol composition and antioxidant activity of African variety of *Dacryodes edulis* fruit. *Journal Medicine and Food*, **6**: 1321-1325.
- Athanasiadou S, Kyriazakis I, 2004. Plant secondary metabolites: antiparasitic effects and their role in ruminant production systems. *Proceedings of the Nutrition Society*, **63**:631-639.
- Athanasiadou S, Kyriazakis I, Jackson F, Coop RL, 2001. Direct anthelmintic effects of condensed tannins towards different gastrointestinal nematodes of sheep: *in vitro* and *in vivo* studies. *Veterinary Parasitology*, **99**:205–219.

- Athanasiadou S, Tolossa K, Debela E, Tolera A, Houdijk JGM, 2015. Tolerance and resistance to a nematode challenge are not always mutually exclusive. *International Journal for Parasitology*, **45**:277-82.
- Atienzar FA, Tilmant K, Gerets HH, Toussaint G, Speeckaert S, Hanon E, Depelchin O, Dhalluin S, 2011. The use of real-time cell analyzer technology in drug discovery: defining optimal cell culture conditions and assay reproducibility with different adherent cellular models. *Journal of Biomolecular Screening*, **16**:575-587.
- Azando EVB, Hounzangbe-Adote MS, Olounlade PA, Brunet S, Fabre N, Valentin A, Hoste H, 2011. Involvement of tannins and flavonoids in the *in vitro* effects of *Newbouldia laevis* and *Zanthoxylum zanthoxyloides* extracts on the exsheathment of third-stage infective larvae of gastrointestinal nematodes. *Veterinary Parasitology*, **180**:292–297.
- Azwanida NN, 2015. A review on the extraction methods use in medicinal plants: principle, strength and limitation. *Medicinal and Aromatic Plants*, **4**:196.
- Bahrami Y, Zhang W, Chataway T, Franco C, 2014. Structural elucidation of novel saponins in the sea cucumber *Holothuria lessona*. *Marine Drugs*, **12**:4439-4473.
- Bailey SA, Zidell RH, Perry RW, 2004. Relationships between organ weight and body weight in the rat: What is the best analytical endpoint? *Toxicologic Pathology*, **32**:448-466.
- Bajpai VK, Majumder R, Park JG, 2016. Isolation and purification of plant secondary metabolites using column-chromatographic technique. *Bangladesh Journal Pharmacology*, **11**:844-848.

- Bart HJ, 2011. Extraction of natural products from plants: Introduction (a book chapter) on industrial scale natural extraction, first edition. Edited by Hans-Jörg Bart, Stephan Pilz., published by Wiley-VCH Verlag GmbH and Co. KGaA:1-26.
- Bauri RK, Tigga MN, Kullu SS, 2015. A review on use of medicinal plants to control parasites. *Indian Journal of Natural Product Resource*, **6**:268-277.
- Behnke JM, Buttle DJ, Stepek G, Lowe A, Duce IR, 2008. Developing new anthelmintics from plant cysteine proteinases (review). *Parasitology Vectors* **1**:29.
- Behnke J, Harris P, 2009. *Heligmosomoides bakeri* or *Heligmosomoides polygyrus*? *American Society of Tropical Medicine*, **80**:684-685.
- Behnke JM, Menge DM, Noyes H, 2009. *Heligmosomoides bakeri*: a model for exploring the biology and genetics of resistance to chronic gastrointestinal nematode infections. *Journal of Parasitology*, **136**:1565–1580.
- Bekele G, Reddy PR, 2015. Ethnobotanical study of medicinal plants used to treat human ailments by Guji Oromo tribes in Abaya district, Borana, Oromia, Ethiopia. *Universal Journal of Plant Science*, **3**:1-8.
- Bell EA, 2003. Non-protein amino acids of plants: significance in medicine, nutrition, and agriculture. *Journal of Agricultural and Food Chemistry*, **51**:2854–2865.
- Berenbaum M, 1995. Phototoxicity of plant secondary metabolites: insect and mammalian perspectives. *Archives of Insect Biochemistry and Physiology*, **29**:119-134.

- Bernhoft A, 2010. In proceedings on bioactive compounds in plants –benefits and risks for man and animals: a brief review on bioactive compounds in plants. *The Norwegian Academy of Science and Letters*, Oslo, 13 – 14 November, 11-17.
- Bersissa K, Ajebu N, 2008. Comparative efficacy of albendazole, tetramisole and ivermectin against gastrointestinal nematodes in naturally infected sheep in Hawassa, southern Ethiopia. *Revue Méd. Vét.*, **159**:593-598.
- Bhattacharya A, Sood P, Citovsky V, 2010. The roles of plant phenolics in defence and communication during *Agrobacterium* and *Rhizobium* infection. *Molecular Plant Pathology*, **11**:705–719.
- Bhellum BL, 2012. Taxonomic studies on genus *Ipomoea* (*Convolvulaceae*) in the flora of Jammu and Kashmir State. *Journal of Plant Biology Research*, **1**:29-35.
- Bigoniya P, Singh CS, Shukla A, 2011. Pharmacognostical and physicochemical standardization of ethnopharmacologically important seeds of *Lepidium sativum* and *Wrightia tinctoria*. *Indian Journal of Natural Products and Resources*, **2**:464-471.
- Blackie S, 2014. Review of the epidemiology of gastrointestinal nematode infections in sheep and goats in Ghana. *Journal of Agricultural Science*, **6**:109-118.
- Bonikowski R, Paoli M, Szymczak K, Krajewska A, Bonikowska AW, Tomi F, Kalembe D, 2016. Chromatographic and spectral characteristic of some esters of common monoterpene alcohols. *Flavour and Fragrance Journal*, **31**:290-292.

- Bosman AA , Combrinck S, Roux-van der Merwe R, Botha BM, McCrindle RI, 2004. Isolation of an anthelmintic compound from *Leucosidea sericea*. *South African Journal of Botany*, **70**: 509–511.
- Botura MB, Santos JDG, Silva GD, Lima HG, Oliveira JVA, Almeida MAO, Batatinha MJM, Branco A, 2013. *In vitro* ovicidal and larvicidal activity of *Agave sisalana* on gastrointestinal nematodes of goats. *Veterinary Parasitology*, **192**:211–217.
- Bryant V, 1973. Life cycle of *Heligmosomoides polygyrus*. *Journal of Helminthology*, **3**:263-268.
- Bunglavan SJ, Dutta N, 2013. Use of tannins as organic protectants of proteins in digestion of ruminants. *Journal of Livestock Sciences*, **4**:67-77.
- Buttle DJ, Behnke JM, Bartley Y, Elsheikha HM, Bartley DJ, Garnett MC, Donnan AA, Jackson F, Lowe A, Duce IR, 2011. Oral dosing with *papaya latex* is an effective anthelmintic treatment for sheep infected with *Haemonchus contortus*. *Parasites and Vectors*, **4**:36.
- Carta LK, Handoo ZA, Hoberg EP, Eric F, Erbe EF, Wergin WP, 2009. Evaluation of some vulval appendages in nematode taxonomy. *Comparative Parasitology*, **76**: 191–209.
- Carvalho CO, Chagas AS, Cotinguiba F, Furlan M, Britod LG, Chaves FCM, Stephan MP, Bizzo HR, Amarante AFT, 2012. The anthelmintic effect of plant extracts on *Haemonchus contortus* and *Strongyloides venezuelensis*. *Veterinary Parasitology*, **183**:260–268.

- Cheng Y, Xu Q, Liu J, Zhao C, Xue F, Zhao Y, 2014. Decomposition of five phenolic compounds in high temperature water. *Journal Brazilian Chemistry Society*, **25**:2102-2107.
- Chiejina SN, Behnke JM, 2011. The unique resistance and resilience of the Nigerian west African dwarf goat to gastrointestinal nematode infections. *Parasites and Vectors*, **4**:12.
- Choche T, Shende S, Kadu P, 2014. Extraction and identification of bioactive components from *Aloe barbadensis*. *Journal of Pharmacognosy and Phytochemistry*, **2**:14-23.
- Çitoğlu GS, Acıkara ÖB, 2012. Column chromatography for terpenoids and flavonoids, chromatography and its applications, Sasikumar Dhanarasu (Ed.), ISBN: 978-953-51-0357-8.
- Colegate SM and Molyneux RJ (Eds.), 2007. Bioactive natural products: Detection, isolation and structural determination, Book, CRC press, Taylor and Francis Group, London
- Coles GC, Baier C, Borgsteede HM, Geerts S, Klef TR, Taylor MA, Waller PJ, 1992. World Association for the Advancement of Veterinary Parasitology (WAAVP). Methods for the detection of anthelmintic resistance in nematodes of veterinary importance. *Veterinary Parasitology*, **44**:35-44.
- Coles GC, Jackson F, Pomroy WE, Prichard RK, Samson-Himmelstjerna GV, Silvestre A, Taylor MA, Vercruysse J, 2006. The detection of anthelmintic resistance in nematodes of veterinary importance. *Veterinary Parasitology*, **136**:167–185.

- Coyne MJ, Smith G, Johnstone C, 1991. Fecundity of gastrointestinal *Trichostrongylid* nematodes of sheep in the field. *American Journal of Veterinary Research*, **52**:1182-1188.
- Cunha L, de Moraisa S, de Aquino F, Changa R, de Oliveira A, Martins M, Martins C, Sousa L, Barros T, da Silva C, do Nascimento E, 2017. Bioassay-guided fractionation and antimicrobial and cytotoxic activities of *Cassia bakeriana* extracts. *Brazilian Journal of Pharmacognosy*, **27**:91–98.
- Dahare DK, Jain A, 2010. Ethnobotanical studies on plant resources of Tahsil Multai, district Betul, Madhya Pradesh, India. *Ethnobotanical Leaflets*, **14**:694-705.
- Dai J, Mumper RJ, 2010. Plant phenolics: extraction, analysis and their antioxidant and anticancer properties. *Molecules*, **15**:7313-7352.
- D'Angelo F, Poné W, Jeannette Y, Claire KM, Vittori S, Mbida M, 2014. Evaluation of ovicidal and larvicidal activities of methylene chloride-methanol extract of *Annona Senegalensis* (Annonaceae) stem bark on *Heligmosomoides Bakeri* (Nematoda, Heligmosomatidae). *Global Journal of Science Frontier Research*, **14**:29-39.
- Das B, Tandon V, Lyndem LL, Gray AI, Ferro VA, 2009. Phytochemicals from *Flemingia vestita* (Fabaceae) and *Stephania glabra* (Menispermaceae) alter cGMP concentration in the cestode *Raillietina echinobothrida*. *Comparative Biochemistry and Physiology*, **149**:397–403.
- Das TK, Banerjee D, Chakraborty D, Pakhira MC, Shrivastava B, Kuhad RC, 2012. Saponin role in animal system. *Journal of Veterinary World*, **5**:248-254.

- Dauda U, Mudi SY, 2013. Screening and bioassay-guided isolation of antimicrobial components from *Laggera mollis*. *Journal of Pure and Applied Sciences*, **6**:152–158.
- de Moraes J, Nascimento C, Yamaguchi LF, Kato MJ, Nakano E, 2012. *Schistosoma mansoni* *in vitro* schistosomicidal activity and tegumental alterations induced by pipartine on schistosomula. *Experimental Parasitology*, **132**:222-227.
- De S, Dey YN, Ghosh AK, 2010. Phytochemical investigation and chromatographic evaluation of the different extracts of tuber of *Amorphaphallus paeoniifolius* (Aaraceae). *International Journal on Pharmaceutical and Biomedical Research*, **1**:150-157.
- Debebe Y, Tefera M, Mekonnen W, Abebe D, Woldekidan S, Abebe A, Belete Y, Menberu T, Belayneh B, Tesfaye B, Nasir I, Yirsaw K, Basha H, Dawit A, Debella A, 2015. Evaluation of anthelmintic potential of the Ethiopian medicinal plant *Embelia schimperi* *in vivo* and *in vitro* against some intestinal parasites. *BMC Complementary and Alternative Medicine*, **15**:187.
- Delhaize E, Randall PJ, 1995. Characterization of a phosphate-accumulator mutant of *Arabidopsis thaliana*. *Plant Physiology*, **107**:207-213.
- Demeler J, Kleinschmidt N, Küttler U, Koopmann R, von Samson-Himmelstjerna G, 2012. Evaluation of the egg hatch assay and the larval migration inhibition assay to detect anthelmintic resistance in cattle parasitic nematodes on farms. *Journal of International Parasitology*, **61**:614-618.
- Denayer T, Stöhr T, MaartenVanRoy M, 2014. Animal models intranational medicine: validation and prediction of new horizons in translational medicine, **2**:5–11

- Dent M, Dragovi-Uzelac V, Penić M, Brnčić M, Bosiljkov T, Levaj B, 2013. The effect of extraction solvents, temperature and time on the composition and mass fraction of polyphenols in Dalmatian wild sage (*Salvia officinalis*) extracts. *Food Technology and Biotechnology*, **51**:84-91.
- Dewick PM, 2002. The biosynthesis of C₅–C₂₅ terpenoid compounds. *Natural Product Report*, **19**:181–222.
- Diaz AMA, Acosta TJFJ, Castro SCA, Hoste H, 2010. Tannins in tropical tree fodders fed to small ruminants: a friendly foe? *Small Ruminants Research*, **89**:164–173.
- Doligalska M, Józwicka K, Kiersnowska M, Mroczek A, Paczkowski C, Janiszowska W, 2011. Triterpenoid saponins affect the function of P-glycoprotein and reduce the survival of the free living stages of *Heligmosomoides bakeri*. *Veterinary Parasitology*, **179**:144–151.
- Domke AVM, Chartier C, Gjerde B, Höglund J, Leine N, Vatn S, Stuen S, 2012. Prevalence of anthelmintic resistance in gastrointestinal nematodes of sheep and goats in Norway. *Parasitology Research*, **111**:185–193.
- Driver GC, Bilgener M, 1989. Herbivores and plant tannins. *Advances in Ecological Research*, **19**:263–302.
- Dryden MW, Payne PA, Ridley R, Smith V, 2005. Comparison of common faecal flotation techniques for the recovery of parasite eggs and oocytes. *Veterinary Therapeutics*, **6**:14–28.
- Dykes L, Rooney LW, 2006. Review sorghum and millet phenols and antioxidants. *Journal of Cereal Science*, **44**:236–251.

- Eguale T, Tadesse D, Giday M, 2011. *In vitro* anthelmintic activity of crude extracts of five medicinal plants against egg-hatching and larval development of *Haemonchus contortus*. *Journal of Ethnopharmacology*, **137**:108-113.
- Eguale T, Tilahun G, Debelli A, Feleke A, Makonnen E, 2007. *In vitro* and *in vivo* anthelmintic activity of crude extracts of *Coriandrum sativum* against *Haemonchus contortus*. *Journal of Ethnopharmacology*, **110**:428-433.
- Ellenby C, 1968. Desiccation survival of the infective larva of *Haemonchus contortus*. *Journal of Experimental Biology*, **49**:469-475.
- Enejoh OS, Suleiman MM, Ajanusi JO, Ambali SF, 2015. Anthelmintic activity of extracts of *Citrus aurantifolia* (christmann) fruit peels against experimental *Heligmosomoides bakeri* in mice. *Journal of Advanced Scientific Research*, **6**:29-32.
- Engström M, 2016. Understanding of the bioactivity of plant tannins: developments in analysis methods and structure-activity studies. Doctoral thesis, Department of Chemistry, University of Turku, Turku, Finland.
- Esmacili N, Ebrahimzadeh H, Abdi K, Safarian S, 2011. Determination of some phenolic compounds in *Crocus sativus* corms and its antioxidant activities study. *Pharmacognosy Magazine*, **7**:74-80.
- Esposito D, Munafo JP, Lucibello T, Baldeon M, Komarnytsky S, Gianfagna TJ, 2013. Steroidal glycosides from the bulbs of Easter lily (*Lilium longiflorum*) promotedermal fibroblastmigration *in vitro*. *Journal of Ethnopharmacology*, **148**:433-440.

- FAO, 2002. A systematic review on cattle and small ruminant production systems in Sub-saharan Africa. Livestock information sector analysis and policy branch, FAO agriculture department 1-81.
- Fernandes G, Banu J, 2012. Medicinal properties of plants from the genus *Cissus*: A review. *Journal of Medicinal Plants Research*, **6**:3080-3086.
- Ferreira AA, Amaral FA, Duarte IDG, Oliveira PM, Alves RB, Silveira D, Azevedo AO, Raslan DS, Castro MSA, 2006. Antinociceptive effect from *Ipomoea cairica* extract. *Journal of Ethnopharmacology*, **105**: 148-153.
- Ferreira JFS, Luthria DL, Sasaki T, Heyerick A, 2010. Flavonoids from *Artemisia annua* L. as antioxidants and their potential synergism with artemisinin against malaria and cancer. *Molecules*, **15**:3135–3170.
- Ferreira LE Castro PMN, Chagas ACS, França SC, Beleboni RO, 2013. *In vitro* anthelmintic activities of water leaf extract of *Annona muricata* (Annonaceae) against *Haemonchus contortus* from sheep. *Experimental Parasitology*, **134**:327–332.
- Filice M, Palomo JM, 2012. Monosaccharide derivatives as central scaffolds in the synthesis of glycosylated drugs. *RSC Advances*, **2**:1729–1742.
- Fleming SA, Craig T, Kaplan RM, Miller JE, Navarre C, Rings M, 2006. Anthelmintic resistance of gastrointestinal parasites in small ruminants. *Journal of Veterinary Internal Medicine*, **20**:435–444.
- Foster JG, Cassida KA, Turner KE, 2011. *In vitro* analysis of the anthelmintic activity of forage chicory (*Cichorium intybus*) sesquiterpene lactones against a predominantly *Haemonchus contortus* egg population. *Veterinary Parasitology*, **180**:298–306.

- Francis G, Kerem Z, Makkar HPS, Becker K, 2002. The biological action of saponins in animal systems: a review. *British Journal of Nutrition*, **88**:587–605.
- Fukushi E, 2006. Advanced NMR approaches for detailed analysis of natural products-review. *Journal of Bioscience, Biotechnology and Biochemistry*, **70**:1803-1812.
- Fuloria NK, Fuloria S, 2013. Structural elucidation of small organic molecules by 1D, 2D and multidimensional-solution NMR spectroscopy. *Journal of Analytical and Bioanalytical Techniques* S11: 001. doi:10.4172/2155-9872.S11-001.
- Fürstenberg-Hägg J, Zagrobelny M, Bak S, 2013. Plant defense against insect herbivores. *International Journal of Molecular Sciences*, **14**:10242–10297.
- Gajbhiye NA, Makasana J, Kumar S, 2015. Accumulation of three important bioactive compounds in different plant parts of *Withania somnifera* and its determination by the LC–ESI-MS-MS method. *Journal of Chromatographic Science*, doi:10.1093/chromsci/bmv088.
- Gana JJ, Makun H, Chiezey NP, Tekdek LB, 2015. Epidemiological study on abomasal nematodes in slaughtered small ruminants raised in the guinea savannah zone of Nigeria. *Sokoto Journal of Veterinary Sciences*, **13**:26-33.
- Gebresilassie L, Tadele BA, 2015. Prevalence of ovine haemonchosis in Wukro, Ethiopia. *Journal of Parasitology Research*. Article ID 635703.
- Geets S, Gryseels B, 2000. Drug resistance in human helminths: Current situation and lessons from livestock. *Clinical Microbiology Reviews*, **13**:207–222.

- Ghareeb MA, Shoeb HA, Madkour HMF, Refahy LA, Mohamed MA, Saad AM
2013. Radical scavenging potential and cytotoxic activity of phenolic compounds from *Tectona grandis*. *Global Journal of Pharmacology*, **7**:486-497.
- Ghasemzadeh A, Ghasemzadeh N, 2011. A review on flavonoids and phenolic acids: role and biochemical activity in plants and human. *Journal of Medicinal Plants Research*, **5**:6697-6703.
- Ghisalbert EL, 2008. Detection and isolation of bioactive natural products. Chapter two in bioactive natural products: Detection, isolation and structural determination. Second edition. Colegate SM and Molyneux RJ (editors). CRC Press, Boca Raton, USA. ISBN 9780849372582:11-76.
- Loftsson T, 2014. Drug stability for pharmaceutical scientists. Chapter three in drug degradation in aqueous solution due to hydrolysis. First edition. Elsevier Academic press ISBN:9780124115484
- Gibbons S, 2012. An introduction to planar chromatography and its application to natural products isolation. In a book edited by Sarker SD and Nahar L (eds.), *Natural Products Isolation, Methods in Molecular Biology*. Springer, **864**:117-153.
- Gibbs HC, 1986. Hypobiosis in parasitic nematodes—an update. *Advances in Parasitology*, **25**:129–174.
- Giday M, Teklehaymanot T, 2013. Ethnobotanical study of plants used in management of livestock health problems by Afar people of Ada'ar district, Afar Regional State, Ethiopia. *Journal of Ethnobiology and Ethnomedicine*, **9**:8.

- Gill SS, Anjum NA, Gill R, Jha M, Tuteja N, 2015. DNA damage and repair in plants under ultraviolet and ionizing radiations. *The Scientific World*. <http://dx.doi.org/10.1155/250158>.
- Githiori JB, Höglund J, Waller PJ, Baker RL, 2003. The anthelmintic efficacy of the plant, *Albizia anthelmintica*, against the nematode parasites *Haemonchus contortus* of sheep and *Heligmosomoides polygyrus* of mice. *Veterinary Parasitology*, **116**:23–34.
- Githiori JB, 2004. Evaluation of anthelmintic properties of ethnoveterinary plant preparations used as livestock dewormers by pastoralists and small holder farmers in Kenya. Doctoral thesis, Swedish University of Agricultural Sciences, Uppsala, Sweden. ISSN1401-6257, ISBN 91 576 6666 0.
- Glish GL, Vachet RW, 2003. The basics of mass spectrometry in the twenty-first century. *Nature Reviews Drug Discovery*, **2**:140-150.
- Gogoi J, Nakhuru KS, Rudragoud S, Policegoudra RS, Chattopadhyay P, Rai AK, Veer V, 2016. Isolation and characterization of bioactive components from *Mirabilis jalapa*. *Journal of Traditional and Complementary Medicine*, **6**:41-47.
- Grunewald W, van Noorden G, Isterdael GV, Beeckman T, Gheysen G, Mathesiussc U, 2009. Manipulation of auxin transport in plant roots during rhizobium symbiosis and nematode parasitism. A review. *The Plant Cell*, **21**:2553–2562.
- Guiochon G, 2001. Basic principles of chromatography in: Handbook of anal. tech. Eds. Günzler H and Williams A, 1:173-198. Wiley-VCH Verlag GmbH, Weinheim, Germany.

- Hancock RD, Hogenhout S, Foyer CH, 2015. Mechanisms of plant–insect interaction. *Journal of Experimental Botany*, **66**:421-424.
- Haouas D, Halima-Kamel MB, Hamouda MHB, 2008. Insecticidal activity of flower and leaf extracts from *Chrysanthemum* species against *Tribolium confusum*. *Tunisian Journal of Plant Protection*, **3**:89-94.
- Haralampidis K, Trojanowska M, Osbourn AE, 2002. Biosynthesis of triterpenoid saponins in plants. *Advance Biochemistry, Engineering and Biotechnology*, **75**:31–49.
- Harris N, Jou JM, Devoto G, Lotz J, Pappas J, Wranovics D, Wilkinson M, Fletcher SR, Kratz A, 2005. Performance evaluation of the ADVIA 2120 haematology analyser: An international multicentre clinical trial. *Laboratory Haematology*, **11**:62-70.
- Hearn DJ, 2006. *Adenia* (family *Passifloraceae*) and its adaptive radiation: phylogeny and growth form diversification. *Systematic Botany*, **31**:805-821.
- Hemalatha M, Thirumalai T, Saranya R, Elumalai EK, David E, 2013. A review on antimicrobial efficacy of some traditional medicinal plants in Tamilnadu. *Journal of Acute Disease*:99-105.
- Hijwegen T, 1963. Lignification, a possible mechanism of active resistance against pathogens. *Netherlands Journal of Plant Pathology*, **69**:314-317.
- Hoareau L, 1999. Medicinal plants: a re-emerging health aid. *Electronic Journal of Biotechnology* ISSN:0717-3458.
- Hopkins RJ, van Dam NM, van Loon JJA, 2009. Role of glucosinolates in insect-plant relationships and multitrophic interactions. *Annual Review of Entomology*, **54**:57-83.

- Hossain MA, Salim AL-Raqmi KA, AL-Mijizy ZH, Weli AM, Al-Riyami Q, 2013. Study of total phenol, flavonoids contents and phytochemical screening of various leaves crude extracts of locally grown *Thymus vulgaris*. *Asian Pacific Journal of Tropical Biomedicine*, **3**:705-710.
- Hoste H, Jackson F, Athanasiadou S, Thamsborg SM, Hoskin SO, 2006. The effects of tannin rich plants on parasitic nematodes in ruminants. *Trends in Parasitology*, **22**:253–261.
- Hoste H, Martinez-Ortiz-De-Montellano C, Manolaraki F, Brunet S, Ojeda-Robertos N, Fourquaux I, Torres-Acosta JFJ, Sandoval-Castro CA, 2012. Direct and indirect effects of bioactive tannin-rich tropical and temperate legumes against nematode infections. *Veterinary Parasitology*, **186**:18–27.
- Hoste H, Torres-Acosta JFJ, 2011. Non-chemical control of helminths in ruminants: adapting solutions for changing worms in a changing world. *Veterinary Parasitology*, **180**:144–154.
- Howell JS, 2009. Evaluation of three *in vitro* bioassays for measuring the anthelmintic activity of plant extracts containing condensed tannins. MSc Thesis, Athens, Georgia.
- <http://www.ville-e.ch/musinfo/bd/cjb/africa/details.php> date June 2017.
- https://en.wikipedia.org/wiki/Hydrog-deuterium_exchange dated December 2016.
- <http://www.scops.org.uk> dated June 2017
- Hrckova G, Velebny S, 2013. Pharmacological potential of selected natural compounds in the control of parasitic diseases, Springer, *Briefs in Pharmaceutical Science and Drug Development* (Book chapter), **125**:29-99.

- Hsieh MK, Shyu CL, Liao JW, Franje CA, Huang YJ, Chang SK, Shih PY, Chou CC, 2011. Correlation analysis of heat stability of veterinary antibiotics by structural degradation, changes in antimicrobial activity and genotoxicity. *Veterinarni Medicina*, **56**:274–285.
- Ibrahim GI, Jalal AF, Ibrahim BM, 2013. Evaluation of antioxidant activity, phenolic, flavonoid and ascorbic acid contents of three edible plants from Kurdistan. *Tikrit Journal of Pure Science*, **18**:1813–1662.
- Iloki-Assanga SB, Lewis-Luján LM, Lara-Espinoza CL, Gil-Salido AA, Fernandez-Angulo D, Rubio-Pino JL, Haines DD, 2015. Solvent effects on phytochemical constituent profiles and antioxidant activities, using four different extraction formulations for analysis of *Bucida buceras* L. and *Phoradendron californicum*. *BMC Research Notes*, **8**:396.
- Ingle KP, Deshmukh AG, Padole DA, Dudhare MS, Moharil MP, Khelurkar VC, 2017. Phytochemicals: Extraction methods, identification and detection of bioactive compounds from plant extracts. *Journal of Pharmacognosy and Phytochemistry*, **6**:32-36.
- Intisar AMO, Goreish I, Shaddad S, Elamin T, Eltayeb IB, 2015. *In vitro* and *in vivo* anthelmintic activity of *Peganum harmala* seeds against *H. contortus* in goats. *Journal of Applied and Industrial Sciences*, **3**:67-71.
- Isaac LJ, Abah G, Akpan B, Ekaette IU, 2013. Haematological properties of different breeds and sexes of rabbits. *Proceedings of the 18th of Annual Conference of Animal Science Association of Nigeria*:24-27.

- Jamil M, Haq IU, Mirza B, Qayyum M, 2012. Isolation of antibacterial compounds from *Quercus dilatata* through bioassay guided fractionation. *Annals of Clinical Microbiology and Antimicrobials*, **11**:11.
- Jasmer DP, Goverse A, Smant G, 2003. Parasitic nematode interactions with mammals and plants. *Annual Review of Phytopathology*, **41**:245-270.
- Jatau ID, Abdulganiyu A, Lawal AI, Okubanjo OO, Yusuf KH, 2011. Gastrointestinal and haemoparasitism of sheep and goats at slaughter in Kano, northern-Nigeria. *Sokoto Journal of Veterinary Science*, **9**:7-11.
- Jawale CS, 2014. Larvicidal activity of some saponin containing plants against the Dengue vector *Aedes aegypti*. *International Journal of Trends in Biotechnology Research*, **3**:2320-0421.
- Jayashree D, 2013. Phytochemical analysis and TLC fingerprinting of methanolic extracts of three medicinal plants. *International Research Journal of Pharmacy*, **4**:123-126.
- Jenkins SN, Behnke JM, 1977. Impairment of primary expulsion of *Trichuris muris* in mice concurrently infected with *Nematospiroides dubius*. *Parasitology*, **75**:71-78.
- Jensen KB, 1956. Isolation by paper chromatography of unknown glycosides from *Digitalis purpurea* and their transformation into the known cardiac glycosides. *Acta Pharmacology and Toxicology*, **12**:20-26.
- Jilani G, Saxena RC, 1990. Repellent and deterrent effects of turmeric oil, sweetflag oil, neem oil, and a neem-based insecticide against lesser grain borer (*Coleoptera: Bostrychidae*). *Journal of Economic Entomology*, **83**:629-634.

- Jork HH, Funk W, Fischer W, Wimmer H, 1990. Thin-layer chromatography reagents and detection methods, volume 1a: Physical and chemical detection methods: fundamentals, reagents, VHC, Weinheim, Germany
- Joshi DD, 2012. Herbal drugs and finger prints. *Evidence Based Herbal Drugs* (ebook). Springer London:ISBN 978-81-322-0804-4.
- Jothy SL, Zakaria Z, Chen Y, Lau YL, Latha LY, Shin LN, Sasidharan S, 2011. Bioassay-directed isolation of active compounds with anti-yeast activity from a *Cassia fistula* seed extract. *Molecules*, **16**:7583-7592.
- Józwiak GW, Hajnos MW, 2007. Preparative-layer chromatography of an extract of alkaloids from *Fumaria officinalis*. *Acta chromatographica*, **18**:207-218.
- Josué WP, Payne VK, Alidou MN, Claire KM, Jeannette Y, Gertrude MT, Mbida M, Bilong CFB, 2012. *In vitro* ovicidal and larvicidal activities of water and ethanolic extracts of stem bark of *Nauclea latifolia* (Rubiaceae) on *H. bakeri* (Nematoda, Heligmosomatidae). *Journal of Medicinal Plants*, **4**:1-6.
- Juhnke J, Miller, Hall JO, Provenza FD, Villalba JJ, 2014. Preference for condensed tannins by sheep in response to challenge infection with *Haemonchus contortus*. *Veterinary Parasitology*, **188**:104–114.
- Jurasek ME, Bishop-Stewart JK, Storey BE, Kaplan RM, Kent ML, 2010. Modification and further evaluation of a fluorescein-labeled peanut agglutinin test for identification of *Haemonchus contortus* eggs. *Veterinary Parasitology*: **169**:209–213.
- Kabaka WM, Gitau GK, Kitala PM, Maingi N, Vanleeuwen JA, 2012. Risk factors associated with gastrointestinal nematode infections of cattle in Nakuru and

- Mukurweini districts of Kenya. *Bulletin of Animal Health and Production*, **60**:413–419.
- Kabaka WM, Gitaub GK, Kitalaa PM, Maingic N, VanLeeuwend JA, 2013. The prevalence of gastrointestinal nematode infection and their impact on cattle in Nakuru and Mukurweini districts of Kenya. *Ethiopian Veterinary Journal*, **17**:95-104.
- Kakar SA, Tareen RB, Sandhu Z, Kakar MA, Kakar SR, Iqbal Z, Jabeen H, 2013. *In vitro* and *in vivo* anthelmintic activity of *Ferula costata* against gastrointestinal nematodes of sheep. *Pakistan Journal of Botany*, **45**:263-268.
- Kang NX, Zhu YJ, Zhao JP, Zhu WF, Liu YL, Xu QM, Zhuge HX, Khan IA, Yan SL, 2016. Antischistosomal activity of hederacochiside C against *Schistosoma japonicum* harboured in experimentally infected animals. *Journal of Asian Natural Product Research*:1-14,
- Karayil S, Chandran KPS, Sudeesh PS, Veraiah K, 2014. Isolation and structural elucidation of novel bioactive molecule-coumarin from traditionally used medicinal plant *Ceropegia juncea*. *Journal of Pharmacy and Biological Sciences*, **9**:19-22.
- Karthika K, Jamuna S, Paulsamy S, 2014. TLC and HPTLC fingerprint profiles of different bioactive components from the tuber of *Solena amplexicaulis*. *Journal of Pharmacognosy and Phytochemistry*, **3**:198-206.
- Kaschny M, Demeler J, Janssen IJ, Kuzmina TA, Besognet B, Kanellos T, Kerboeuf D, Samson-Himmelstjerna G, Krücken J, 2015. Macrocyclic lactones differ in interaction with recombinant P-Glycoprotein-9 of the parasitic nematode

- cylicocylus elongates and ketoconazole in a yeast growth assay. *PLOS pathogens* DOI:10.1371/journal.ppat.1004781
- Kennedy DO, Wightman EL, 2011. Herbal extracts and phytochemicals: plant secondary metabolites and the enhancement of human brain function. *Advances in Nutrition*, **2**:32–50.
- Kerboeuf D, Blackhall W, Kaminsky R, von Samson-Himmelstjerna G, 2003. P-glycoprotein in helminths: function and perspectives for anthelmintic treatment and reversal of resistance. *International Journal of Antimicrobial Agents*, **22**:332-346.
- Kerboeuf D, Riou M, Neveu C, Issouf M, 2010. Membrane drug transport in helminths. *Anti-infective Agent in Medicinal Chemistry*, **9**:113–129.
- Khan A, Tak H, Nazir R, Lone BA, 2016. *In vitro* and *in vivo* anthelmintic activities of *Iris kashmiriana* Linn. *Journal of the Saudi Society of Agricultural Sciences*. <http://dx.doi.org/10.1016/j.jssas.2016.05.001>.
- Khoo LT, Abdullah JO, Abas F, Tohit ERM, Hamid M, 2015. Bioassay-guided fractionation of *Melastoma malabathricum* leaf solid phase extraction fraction and its anticoagulant activity. *Molecules*, **20**:3697-3715.
- Kimani D, Kareru PG, Karanja JM, Njonge FK, Githira PN, Kutima HL, Mercy G, Nyagah GC, 2014. *In vivo* activity of two herbal plant mixtures against gastrointestinal nematodes in ruminants. *Journal of Applied Chemistry*, **7**:21-28
- Kinghorn AD, Pan L, Fletcher JN, Chai H, 2011. The relevance of higher plants in lead compound discovery programs. *Journal of Natural Product*, **74**:1539–1555.

- Klongsiriwet C, Quijada J, Williams AR, Mueller-Harvey I, Williamson EM, Hoste H, 2015. Synergistic inhibition of *Haemonchus contortus* exsheathment by flavonoid monomers and condensed tannins. *International Journal for Parasitology: Drugs and Drug Resistance*, **5**:127-134.
- Kotze AC, 2012. Target-based and whole-worm screening approaches to evaluate botanicals. *Journal of Drug Information*, **32**:513–524.
- Kumsa B, Tolera A, Nurfeta A, 2007. Comparative efficacy of seven brands of albendazole against naturally acquired gastrointestinal nematodes in sheep in Hawassa, southern Ethiopia. *Turkish Journal of Veterinary and Animals Sciences*, **34**:417-425.
- Kwan EE, Huang SG, 2008. Structural elucidation with NMR spectroscopy: Practical strategies for organic chemists. *European Journal of Organic Chemistry*:2671–2688.
- Ladan Z, Amupitan OA, Oyewale OA, Ayo RG, Temple E, Ladan EO, 2014. Phytochemical screening of the leaf extracts of *Hyptis spicigera* plant. *African Journal of Pure and Applied Chemistry*, **8**:83-88.
- Lalrinzuali K, Vabeiryureilai M, Jagetia GC, 2015. Phytochemical and TLC profiling of *Oroxylum indicum* and *Milletia pachycarpa*. *Journal of Plant Biochemistry and Physiology* **3**:152. doi:10.4172/2329-9029.1000152.
- Lamy E, Van Harten S, Sales-Baptista E, Guerra MM, Almeida AM, 2012. Factors influencing livestock productivity: environmental stress and amelioration in livestock production. Book chapter (edited by Sejian V, Naqvi SMK, Ezeji T, Lakritz J, Lal R), 19-51.

- Lemma D, Abera A, 2013. Prevalence of ovine gastrointestinal nematodes in and around Asella, south eastern Ethiopia. *Journal of Veterinary Medicine and Animal Health*, **5**: 222-228.
- Lespine A, Ménez C, Bourguinat C, Prichard RK, 2012. P-glycoproteins and other multidrug resistance transporters in the pharmacology of anthelmintics: Prospects for reversing transport-dependent anthelmintic resistance. *International Journal for Parasitology: Drugs and Drug Resistance*, **2**:58–75.
- Lorimer SD, Perry NB, Foster LM, Burgess EJ, Douch PGC, Hamilton MC, Donaghy MJ, McGregor RA, 1996. A nematode larval motility inhibition assay for screening plant extracts and natural products. *Journal of Agriculture and Food Chemistry*, **44**:2842–2845.
- Kusiluka L, Kambarage D, 1996. Diseases of small ruminants in sub-Saharan Africa. A hand book funded by overseas development administration animal health programme. ISBN 0952229951 edited and published by VETAID Centre for Tropical Veterinary Medicine.
- Lulekal E, Asfaw Z, Kelbessa E, Damme PV, 2014. Ethnoveterinary plants of Ankober district, north shewa zone, Amhara region, Ethiopia. *Journal of Ethnobiology and Ethnomedicine*, **10**:21.
- Ludvik B, Waldhausl W, Prager R, Kautzky-Willer A, Pacini G, 2003. Mode of action of *Ipomoea batatas* in type 2 diabetic patients. *Metabolism*, **52**: 875-880.
- Macedo ITF, Bevilaqua CML, de Oliveira LMB, Camurca-Vasconcelos ALF, Vieira SL, Oliveira FR, Queiroz-Junior EM, Tomé RA, Nascimento NRF, 2010. Anthelmintic effect of *Eucalyptus staigeriana* essential oil against goat gastrointestinal nematodes. *Veterinary Parasitology*, **173**:93–98.

- Macel M, 2011. Attract and deter: a dual role for pyrrolizidine alkaloids in plant–insect interactions. *Phytochemistry Reviews*, **10**:75–82.
- McLafferty FW, Turecek F, 1993. Interpretation of mass spectra, 4th edition, Mill Valley, California.
- Magalhães LG, de Souza JM, Wakabayashi KAL, Rosangela da S. Laurentiz Vinhólis AHC, Rezende KCS, Simaro GV, Bastos JK, Rodrigues V, Esperandim VR, Ferreira DS, Crotti AEM, Cunha WR, Silva MLA, 2012. *In vitro* efficacy of the essential oil of *Piper cubeba* (Piperaceae) against *Schistosoma mansoni*. *Parasitology Research*, **110**:1747–1754.
- Malešev D, Kunti V, 2007. Investigation of metal–flavonoid chelates and the determination of flavonoids via metal–flavonoid complexing reactions (a review). *Journal of Serbian Chemical Society*, **72**:921–939.
- Maronpot RR, Yoshizawa K, Nyska A, Harada T, Flake G, Mueller G, Singh B, Ward JM, 2010. Hepatic enzyme induction-histopathology. *Journal of Toxicologic Pathology*, **38**:776-795.
- Martin D, Jonathan G, Jörg B, 2003. Induction of volatile terpene biosynthesis and diurnal emission by methyl jasmonate in foliage of Norway spruce. *Plant Physiology*, **132**:1586–1599.
- Martin RJ, 1997. Modes of action of anthelmintic drugs. *Veterinary Journal*, **154**:11–34.
- Martin RJ, Pennington AJ, 1989. Patch-clamp study of effects of dihydroavermectin on *Ascaris* muscle. *British Journal of Pharmacology*, **98**:747-756.

- Mavrot F, Hertzberg H, Torgerson P, 2015. Effect of gastro-intestinal nematode infection on sheep performance: a systematic review and meta-analysis. *Parasites and Vectors*, **8**:557.
- Max RA, 2010. Effect of repeated wattle tannin drenches on worm burdens, faecal egg counts and egg hatchability during naturally acquired nematode infections in sheep and goats. *Veterinary Parasitology*, **169**:138–143.
- Mazid M, Khan TA, Mohammad F, 2011. Role of secondary metabolites in defense mechanisms of plants. *Biology and Medicine*, **3**:232-249.
- Mbaya AW, Ogwiji M, 2014. *In vivo* and *in vitro* activities of medicinal plants on ecto, endo and haemoparasitic infections: a review. *Current Clinical Pharmacology*, **9**:271-82.
- Masoko P, Nemudzivhadi V, 2015. Isolation and chemical structural characterization of the mixture of two related phytosterols from *Ricinus communis* (*Euphorbiaceae*) leaves. *European Journal of Medicinal Plants*, **10**:1-12.
- McLaughlin JL, Rogers LL, Anderson JE, 1998. The use of biological assays to evaluate botanicals. *Journal of Drug Information*, **32**:513–524.
- McPartland TJ, Patil RA, Malone MF, Roberts SC, 2013. Liquid-liquid extraction for recovery of paclitaxel from plant cell culture: solvent evaluation and use of extractants for partitioning and selectivity. *Biotechnology Progress*, **28**:990–997.
- Meira M, Silva EP, David JM, David JP, 2012. Review of the genus *Ipomoea*: traditional uses, chemistry and biological activities. *Brazilian Journal of Pharmacognosy*, **22**:682-713.

- Mendonça-Lima FW, Santos RB, Santos LC, Zacharias F, David JM, David JP, Lopez JA, 2016. Anthelmintic activity of *Cratylia mollis* leaves against gastrointestinal nematodes in goats. *Brazilian Journal of Animal production*, **17**:753-762.
- Mesfin F, Demissew S, Teklehaymanot T, 2009. An ethnobotanical study of medicinal plants in Wonago Woreda, SNNPR, Ethiopia, *Journal of Ethnobiology and Ethnomedicine*, **5**:28.
- Michelle S. Tierney MS, Smyth TJ, Rai DK, Vila AS, Croft AK, Brunton N, 2013. Enrichment of polyphenol contents and antioxidant activities of Irish brownmacroalgae using food-friendly techniques based on polarity and molecular size. *Food Chemistry*, **139**:753-761.
- Mierziak J, Kostyn K, Kulma A, 2014. Flavonoids as important molecules of plant interactions with the environment. *Molecules*, **19**:16240-16265.
- Mirzaei M, Mirzaei A, 2013. Comparison of the *Artemia salina* and *Artemia uramiana* bioassays for toxicity of four Iranian medicinal plants. *International Research Journal of Biological Sciences*, **2**:49-54.
- Miyagawa H, 2009. Studies on nitrogen-containing secondary metabolites playing a defensive role in plants. *Journal of Pesticide Science*, **34**:110–112.
- Mfotie Njoya E, Weber C, Hernandez-Cuevas NA, Hon CC, Janin Y, Kamini MFG, Moundipa PF, Guillen N, 2014. Bioassay-Guided fractionation of extracts from *Codiaeum variegatum* against *Entamoeba histolytica* discovers compounds that modify expression of ceramide biosynthesis related genes. *PLoS Neglected Tropical Diseases*, **8**:e2607.

- Modaresi M, Pour MG, Tabeidian SA, Jalalizand A, 2011. Study of histopathologic changes of the effect of zingiber extract on mice kidneys. *International Conference on Food Engineering and Biotechnology*, **9**:16-20.
- Młodzińska E, 2009. Survey of plant pigments: molecular and environmental determinants of plant colours. *Acta Biologica Cracoviensia Series Botanica*, **51**:7–16.
- Mohamed SM, Backheet EY, Bayoumi SA, Ross SA, 2016. New cycloartane saponin and monoterpenoid glucoindole alkaloids from *Mussaenda luteola*. *Fitoterapia*, **110**:129–134.
- Mohammed A, Wossene A, Giday M, Tilahun G, Kebede N, 2013. *In vitro* anthelmintic activities of four medicinal plants against *Haemonchus contortus*. *African Journal of Plant Science*, **7**:369-373.
- Moinuddin MA, Begum N, Akhter S, Biswas PG, 2011. *In vitro* study of factors related to the hatching of eggs of *Oesophagostomum columbianum*. *Journal Bangladesh Agriculture University*, **9**:55–60.
- Molan AL, Faraj AM, 2010. The effects of condensed tannins extracted from different plant species on egg hatching and larval development of *Teladorsagia circumcincta* (Nematoda: *Trichostrongylidae*). *Folia Parasitologica*, **57**:62–68.
- Molan AL, Waghorn GC and McNabb WC, 1999. Condensed tannins and gastrointestinal parasites in sheep. *Proceedings of the New Zealand Grassland Association*, **61**:57–61.
- Molento MB, Fortes FS, Pondelek DAS, de Almeida Borges F, de Souza Chagas AC, Torres-Acosta JFJ, Geldhof P, 2011. Challenges of nematode control in ruminants: Focus on Latin America. *Veterinary Parasitology*, **180**:126–132.

- Moraes J, Nascimento C, Yamaguchi LF, Kato MJ, Nakano E, 2012. *Schistosoma mansoni in vitro* schistosomicidal activity and tegumental alterations induced by pipartine on schistosomula. *Experimental Parasitology*, **132**:222-227.
- Moshi MJ, Otieno DF, Weisheit A, 2012. Ethnomedicine of the Kagera region, north western Tanzania. Part 3: plants used in traditional medicine in Kikuku village, Muleba district. *Journal of Ethnobiology and Ethnomedicine* **8**:14.
- Mueller-Harvey I, 2006. Unravelling the conundrum of tannins in animal nutrition and health. *Journal of Science, Food and Agriculture*, **86**:2010–2037.
- Murugan R, Parimelazhagan T, 2014. Comparative evaluation of different extraction methods for antioxidant and anti-inflammatory properties from *Osbeckia parvifolia*– An *in vitro* approach. *Journal of King Saud University Science*, **26**:267–275.
- Mutembei J, Kareru P, Njonge F, Peter G, Kutima H, Karanja J, Kimani D, 2015. *In vivo* anthelmintic evaluation of a processed herbal drug from *Entada leptostachya* and *Prosopis juliflora* against gastrointestinal nematodes in sheep. *IOSR Journal of Polymer and Textile Engineering*, **2**:6-10.
- Mwale M, Masika PJ, Materechera SA, 2014. Effect of medicinal plants on haematology and serum biochemical parameters of village chickens naturally infected with *Heterakis gallinarum*. *Bangladesh Journal of Veterinary Medicine*, **12**:99-106.
- Nandi B, Roy S, Bhattacharya S, Sinha Babu SP, 2004. Free radicals mediated membrane damage by the saponins acaciaside A and acaciaside B. *Phytotherapy Research*, **18**:191–194.

- Ngarivhume T, Klooster CV, deJong JM, Westhuizen JV, 2015. Medicinal plants used by traditional healers for the treatment of malaria in the Chipinge district in Zimbabwe. *Journal of Ethnopharmacology*, **159**:224–237.
- National Research Council, 2011. Guide for the care and use of laboratory animals. (8th Edition). Washington, DC: The National Academies Press.
- Ntie-Kang F, Lifongo LL, Mbaze LM, Ekwelle N, Owono LO, Megnassan E, Judson PN, Sippl W, Efange SMN, 2013. Cameroonian medicinal plants: a bioactivity versus ethnobotanical survey and chemotaxonomic classification. *BMC Complementary and Alternative Medicine*, **13**:147.
- Ntonifor HN, Shei SJ, Ndaleh NW, Mbunkur GN, 2013. Epidemiological studies of gastrointestinal parasitic infections in ruminants in Jakiri, Bui Division, North West Region of Cameroon. *Journal of Veterinary Medicine and Animal Health*, **5**:344-352,
- Nweze NE, Ogidi A, Ngongeh LA, 2013. Anthelmintic potential of three plants used in Nigerian ethnoveterinary medicine. *Pharmaceutical Biology*, **53**:311-315.
- Ogugua VN, Anaduaka EG, Egba SI, Apeh VO, Nriagu MC, 2013. Does *Cissus Quadrangularis* contain nutritive and medicinal constituents? *World Journal of Pharmacy and Pharmaceutical Sciences*, **2**:4404-4414.
- Önning G, Juillerat MA, Fay L, Asp NG, 1994. Degradation of oat saponins during heat processing-effect of pH and metal catalysts at different temperatures. *Journal of Agriculture and Food Chemistry*, **42**:2578-2582.
- Onguéné PA, Ntie-Kang F, Lifongo LL, Ndom JC, Sippl W, Mbaze LM, 2013. The potential of anti-malarial compounds derived from African medicinal plants.

- Part I: A pharmacological evaluation of alkaloids and terpenoids. *Malaria Journal*, **12**:449 DOI: 10.1186/1475-2875-12-449..
- Ortutu SC, Aremu MO, 2016. Antioxidant capacity and free radical scavenging effects on Nigerian pineapple (*Ananas cormosus*) and orange (*Citrus sinensis*) pulp extracts at different levels of ripeness. *Open Pharmaceutical Sciences Journal*, **3**:25-30.
- Osbourn A, Gross RJM, Field RA, 2011. Saponins-polar isoprenoids with important and diverse biological activities. *Natural Product Report*, **28**:1261-1268.
- Osbourn A, 1996. Saponins and plant defence—a soap story. *Trends Plant Science*, **1**:4–9
- Özbilgin S, Saltancitoğlu G, 2012. A review on uses of some *Euphorbia* species in traditional medicine in Turkey and their biological activities. *Turkish Journal Pharmaceutical Sciences*, **9**:241-256.
- Paolini V, Frayssines A, Farge FD, Dorchie P, Hoste H, 2003. Effects of condensed tannins on established populations and on incoming larvae of *Trichostrongylus colubriformis* and *Teladorsagia circumcincta* in goats. *Veterinary Research*, **34**:331–339.
- Patel SS, Soni H, Mishra K, Singhai AK, 2011. Recent updates on the genus *Passiflora*: A review. *International Journal of Research in Phytochemistry and Pharmacology*, **1**:1-16.
- Pathomwichaiwat T, Ochareon P, Soonthornchareonnon N, Ali Z, Khan IA, Prathanturarug S, 2015. Alkaline phosphatase activity-guided isolation of active compounds and new dammarane-type triterpenes from *C. quadrangularis* hexane extract. *Journal of Ethnopharmacology*, **160**:52-60.

- Pessoa LM, Morais SM, Bevilaqua CML, Luciano JHS, 2002. Anthelmintic activity of essential oil of *Ocimum gratissimum* Linn. and eugenol against *Haemonchus contortus*. *Veterinary Parasitology*, **109**:59–63.
- Pena-Espinoza M, Boas U, Williams AR, Thamsborg SM, Simonsen HT, Enemark HL, 2015. Sesquiterpene lactone containing extracts from two cultivars of forage chicory (*Cichorium intybus*) show distinctive chemical profiles and in-vitro activity against *Ostertagia ostertagi*. *International Journal for Parasitology: Drugs and Drug Resistance*, **5**:191-200.
- Pfarr KM, Qazi S, Fuhrman JA, 2001. Nitric oxide synthase in filariae: demonstration of nitric oxide production by embryos in *Brugia malayi* and *Acanthocheilonema viteae*. *Experimental Parasitology*, **97**:205–214.
- Picot CMN, A. Subratty AH Mahomoodally MF, 2014. Inhibitory potential of five traditionally used native antidiabetic medicinal plants on α -amylase, α -glucosidase, glucose entrapment, and amylolysis kinetics *in vitro*. *Advances in Pharmacological Sciences*, Hindawi Publishing Corporation, <http://dx.doi.org/10.1155/2014/739834>
- Praman S, Mulvany MJ, Williams DE, Andersen RJ, Jansakul C, 2013. Crude extract and purified components isolated from the stems of *Tinospora crispa* exhibit positive inotropic effects on the isolated left atrium of rats. *Journal of Ethnopharmacology*, **149**:123–132.
- Provan D, Baglin T, Dokal I, de Vos J, 2015. Oxford handbook of clinical Haematology (4thed), Oxford University Press, print ISBN-13: 9780199683307.

- Qadir S, Dixit AK, Dixit P, 2010. A review on use of medicinal plants to control *Haemonchus contortus* infection in small ruminants. *Veterinary World*, **3**:515-518.
- Quintanilla-Licea R, Morado-Castillo R, Gomez-Flores R, Laatsch H, Verde-Star MJ, Hernández-Martínez H, Tamez-Guerra P, Tamez-Guerra R, Rodríguez-Padilla C, 2012. Bioassay-guided isolation and identification of cytotoxic compounds from *Gymnosperma glutinosum* leaves. *Molecules*, **17**:11229-11241.
- Rahman G, Seip H, 2006. Alternative strategies to prevent and control endo- parasite diseases in organic sheep and goat farming systems: a review of current scientific knowledge. *Ressortforschung für den ökologischen landbau*: 49-90.
- Ramazani A, Zakeri S, Sardari S, Khodakarim N, Djadid ND, 2010. *In vitro* and *in vivo* anti-malarial activity of *Boerhavia elegans* and *Solanum surattense*. *Malaria Journal*, **9**:124.
- Rao FV, Andersen OA, Vora KA, DeMartino JA, van Aalten DMF, 2005. Methylxanthine drugs are chitinase inhibitors: investigation of inhibition and binding modes. *Brief Communication Chemistry and Biology*, **12**:973–980.
- Rebiai A, Lanez T, 2012. Chemical composition and antioxidant activity of *Apis mellifera* bee pollen from northwest Algeria. *Journal Fundamental Applied Sciences*, **4**:155-163.
- Regassa F, Sori T, Dhuguma R, Kiros Y, 2006. Epidemiology of gastrointestinal parasites of ruminants in western Oromia, Ethiopia. *International Journal of Applied Research in Veterinary Medicine*, **4**:51-57.

- Rocha RP, Melo EC, Radünz LL, 2011. Influence of drying process on the quality of medicinal plants: a review. *Journal of Medicinal Plants Research*, **5**:7076–7084.
- Roeber F, Jex AR, Gasser RB, 2013. Advances in the diagnosis of key gastrointestinal nematode infections of livestock with an emphasis on small ruminants. *Biotechnology Advances*, **31**:1135–1152.
- Rossanigo CE, Grunner L, 1995. Moisture and temperature requirements in faeces for the development of free living stages of gastrointestinal nematodes of sheep, cattle and deer. *Journal of Helminthology*, **69**:357-362.
- Roy EA, Hoste H, Beveridge I, 2004. The effects of concurrent experimental infections of sheep with *Trichostrongylus colubriformis* and *T. vitrinus* on nematode distributions, numbers and on pathological changes. *Parasite Journal*, **11**:293-300.
- Runners LD, 2004. Key to cholesterol's role in nematode development. *PLoS biology*, **2**:345.
- Saeidian S, Rashidzadeh B (2013). Optimum temperature and thermal stability of crude polyphenol oxidase in green small cherry tomatoe (*Solanum Lycopersicum*). *International Research Journal of Applied and Basic Sciences*, **4**:3306-3311.
- Saewan N, Jimtaisong A, 2013. Photo protection of natural flavonoids. *Journal of Applied Pharmaceutical Science*, **3**:129-141.
- Salifou S, Daga DF, Attindehou S, Deguenon R, Biaou CF, 2013. Antiparasitic effects of the water extract from *Chenopodium ambrosioides*

- (*Chenopodiaceae*) against some gastrointestinal nematodes in West African long legged goats. *Journal of Parasitology and Vector Biology*, **5**:13-16.
- Sandoval-Castro CA, Torres-Acosta JJ, Hoste H, Salem AZM, Chan-Pérez JI, 2012 Using plant bioactive materials to control gastrointestinal tract helminths in livestock. *Animal Feed Science and Technology*, **176**:192–201.
- Sarker SD, Latif Z, Gray AI, 2006. Natural products isolation, 2nd edition, Humana Press, Totowa, New Jersey.
- Schmelzer GH, Gurib-Fakim A (eds), 2008. Plant resources of tropical Africa. PROTA Foundation. Wageningen, Netherlands/ CTA, Wageningen, Netherlands:34-43.
- Schnell MA, Hardy C, Hawley M, Propert KJ, Wilson (2002). Effect of blood collection technique in mice on clinical pathology parameters. *Human Gene Therapy*, **13**:155-162.
- Shabbir M, Khan MR, Saeed N, 2013. Assessment of phytochemicals, antioxidant, anti-lipid peroxidation and anti-hemolytic activity of extract and various fractions of *Maytenus royleanus* leave. *BMC Complementary and Alternative Medicine*, **13**:143.
- Shah U, 2011. *Cissus quadrangularis*: Phytochemicals, traditional uses and pharmacological activities. *International Journal of Pharmacy and Pharmaceutical Sciences*, **3**: ISSN- 0975-1491.
- Shai LJ, Bizimenyera ES, Bagla V, McGaw LJ, Eloff JN, 2009. *Curtisia dentata* (*Cornaceae*) leaf extracts and isolated compounds inhibit motility of parasitic and free-living nematodes. *Journal of Veterinary Research*, **76**:249–256.

- Shalaby HA, 2013. Anthelmintics resistance; how to overcome it? *Iranian Journal of Parasitology*, **8**:18-32.
- Sharma V, Paliwal R, 2013. Isolation and characterization of saponins from *Moringa oleifera* (Moringaceae) pods. *International Journal of Pharmacy and Pharmaceutical Sciences*, **5**:179-183.
- Siegmund-Schultze M, Rischkowsky B, da Veiga JB, King JM, 2007. Cattle are cash generating assets for mixed smallholder farms in the eastern Amazon. *Agricultural Systems*, **94**:738–749.
- Simon MK, Nafanda WD, Obeta SS, 2012. *In vivo* evaluation for anthelmintic effect of alkaloids extracted from the stem bark of *Afzelia africana* in rats. *Journal of Advanced Scientific Research*, **3**:100-104.
- Siqueira EP, Souza-Fagundes EM, Sobral MEG, Almeida Alves TM, Rabello A, Zani CL, 2010. Leishmanicidal activities of the extract from *Blepharocalyx salicifolius*, *Myrtaceae*. *Brazilian Journal of Pharmacognosy*, **20**:416-421.
- Sissay MM, Ugglä A, Waller PJ, 2007. Epidemiology and seasonal dynamics of gastrointestinal nematode infections of sheep in a semi-arid region of eastern Ethiopia. *Veterinary Parasitology*, **143**:311-321.
- Sinha Babu SP, Sarkar D, Ghosh NK, Saha A, Sukul NC, Bhattacharya S, 1997. Enhancement of membrane damage by saponins isolated from *Acacia auriculiformis*. *Japan Journal of Pharmacology*, **75**:451–454.
- Singh R, 2016. Chemotaxonomy: a tool for plant classification. *Journal of Medicinal Plants Studies*; **4**:90-93.
- Sleigh JN, 2010. Functional analysis of nematode nicotinic receptors. *Bioscience Horizons*, **3**:29-39.

- Smout MJ, Kotze AC, McCarthy JS, Loukas A, 2010. Novel high through put assay for anthelmintic drug screening and resistance diagnosis by real-time monitoring of parasite motility. *PLoS Neglected Tropical Diseases*, **4**:e885.
- Smyth JD, 1994. Introduction to animal parasitology (Book), third edition published by Cambridge University press. ISBN 0521417708
- Soetan KO, Akinrinde AS, Ajibade TO, 2013. Preliminary studies on the haematological parameters of cockerels fed raw and processed guinea corn (*Sorghum bicolor*). *Proceedings of 38th Annual Conference of Nigerian Society for Animal Production*:49-52.
- Soriano IR, Riley IT, Potter MJ, Bowers WS, 2004b. Phytoecdysteroids: a novel defense against plant-parasitic nematodes. *Journal of Chemical Ecology*, **30**:1885-1899.
- Spiegler V, Sendker J, Petereit F, Liebau E, Hensel A, 2015. Bioassay-guided fractionation of a leaf extract from *Combretum mucronatum* with anthelmintic activity: oligomeric procyanidins as the active principle. *Molecules*, **20**:14810-14832.
- Squires JM, Ferreira JFS, Lindsay DS, Zajac AM, 2011. An effect of artemisinin and Artemisia extracts on *Haemonchus contortus* in gerbils (*Meriones unguiculatus*). *Veterinary Parasitology*, **175**:103–108.
- Srivastava P, Raut HN, Puntambekar HM, Upadhye AS, Desai AC, 2010. Stability studies of crude plant material of *Bacopa monnieri* and its effect on free radical scavenging activity. *Journal of Phytology*, **2**:103-109.

- Stadalienė I, Petkevičius S, Šarkūnas M, 2014. The impact of grazing management on seasonal activity of gastrointestinal parasites in goats. *Helminthologia*, **51**:103–111.
- Stein KK, Golden A, 2015. The *C. elegans* eggshell. WormBook, editors (Labouessee M and Moerman DG) .The *C. elegans* research community, Worm Book: <http://www.wormbook.org>.
- Steppek G, Alowe AE, Buttle DJ, Duce IB, Behnke JM, 2006. Anthelmintic action of plant cysteine proteinases against the rodent stomach nematode, *Protospirura muricola*, *in vitro* and *in vivo*. *Parasitology*, **134**:103–112.
- Storey B, Marcellino C, Miller M, Maclean M, Mostafa E, Howell S, Sakanari J, Wolstenholme A, Kaplan R, 2014. Utilization of computer processed high definition video imaging for measuring motility of microscopic nematode stages on a quantitative scale: “the worminator”. *International Journal for Parasitology: Drugs and Drug Resistance*, **4**:233–243.
- Sun H, Fang WS, Wang WZ, Hu C, 2006. Structure-activity relationships of oleanane- and ursane type triterpenoids. *Journal of Botanical studies*, **47**:339-368.
- Sykes AR, 1994. Parasitism and production in farm animals. *Journal of Animal Production*, **59**:155-172.
- Tanaka Y, Sasaki N, Ohmiya A, 2008. Biosynthesis of plant pigments: anthocyanins, betalains and carotenoids. *Plant Journal*, **54**:733-49.
- Tandon V, Yadav AK, Roy B, Das B, 2011. Phytochemicals as cure of worm infections in traditional medicine systems. *Emerging Trends in Zoology* (Edited

- by: U.C. Srivastava and Santosh Kumar), Narendra Publishing House:351–378.
- Tang Z, Qin J, Xu X, Shi G, Yang H, Liang Y, 2011. Applying silica gel column chromatography to purify resveratrol from extracts of *Morus alba* L. Leaf. *Journal of Medicinal Plants Research*, **5**:3020-3027.
- Taylor MA, Coop RL, Wall RL, 2007. *Veterinary Parasitology*. 3rd edition. Oxford UK: Blackwell Publishing.
- Tayo GM, Poné JW, Marie MC, Yondo J, Ngangout AM, Mbida M, 2014. Anthelmintic activity of *Moringa oleifera* leaf extracts evaluated *in vitro* on four developmental stages of *H. contortus* from Goats. *American Journal of Plant Sciences*, **5**:1702-1710.
- Tesfalem N, 2016. Prevalence of ovine gastrointestinal nematodes in Meskan district, Gurage zone, southern Ethiopia. *International Journal of Advanced Multidisciplinary Research*, **3**:22-30.
- Tholl D, 2006. Terpene synthases and the regulation, diversity and biological roles of terpene metabolism. *Current Opinion in Plant Biology*, **9**:1–8.
- Tholl D, 2015. Biosynthesis and biological functions of terpenoids in plants. *Advanced Biochemistry, Engineering and Biotechnology*, **148**:63–106
- Thornton PK, 2010. Livestock production: recent trends, future prospects. *Philosophical Transaction of Royal society of Biological Science*, **365**:2853–2867.
- Tiwari P, Kumar B, Kaur M, Kaur G, Kaur H, 2011. Phytochemical screening and Extraction: A Review. *Internationale Pharmaceutica Scientia*, **1**:98-106.

- Tiwari P, Mishra BN, Sangwan NS, 2014. Phytochemical and pharmacological properties of *Gymnema sylvestre*: An important medicinal plant. *Biomedical Research International*. <http://dx.doi.org/10.1155/2014/830285>
- Tolossa K, Debela D, Athanasiadou S, Tolera A, Ganga G, Houdijk JGM, 2013. Ethno-medicinal study of plants used for treatment of human and livestock ailments by traditional healers in South Omo, southern Ethiopia. *Journal of Ethnobiology and Ethnomedicine*, **9**:32.
- Tomass Z, Imam E, KifleYohannes T, Tekle Y, Weldu K, 2013. Prevalence of gastrointestinal parasites and *Cryptosporidium* species in extensively managed pigs in Mekelle and urban areas of southern zone of Tigray region, Northern Ethiopia. *Veterinary World*:433-439.
- Treutter D, 2006. Significance of flavonoids in plant resistance: a review. *Environmental Chemistry Letter*, **4**:147-457.
- Trojanowska M, Osbourn AE, 2002. Biosynthesis of triterpenoid saponins in plants. *Advanced Biochemistry, Engineering and Biotechnology*, **75**:31-49.
- Turina AV, Nolan MV, Zygodlo JA Perillo MA, 2006. Natural terpenes: self-assembly and membrane partitioning. *Biophysical Chemistry*, **122**:101–113.
- Uddin R, Saha MR, Subhan N, Hossain H, Jahan IA, Akter R, Alam A, 2014. HPLC-analysis of polyphenolic compounds in *Gardenia jasminoides* and determination of antioxidant activity by using free radical scavenging assays. *Advanced Pharmaceutical Bulletin*, **4**:273-281.
- Udoha MU, Okolie NJ, Ijioma SN, 2015. Anthelmintic activity of *Ocimum gratissimum* leaf extract in *Heligmosomoides bakeri* infected experimental mice. *Annals of Biological Sciences*, **3**:1-7.

- Veeresham C, 2012. Natural products derived from plants as a source of drugs. *Journal of Advanced Pharmaceutical Technological Research*, **3**:200–201.
- Visht S, Chaturvedi S, 2012. Isolation of natural products. *Journal of Current Pharmaceutical Research*, **2**:584-599.
- Voutquenne L, Guinot P, Thoison O, Sevenet T, Lavaud C, 2003. Oleanolic glycosides from *Pometia ridleyi*. *Phytochemistry*, **64**:781-789.
- Waksmundzka-Hajnos M, Sherma J, Kowalska T, 2008. Thin layer chromatography in phytochemistry. *Chromatographic Science Series*, 99, CRC press:527.
- Wangchuk P, Giacomini PR, Pearson MS, Smout MJ, Loukas A, 2016. Identification of lead chemotherapeutic agents from medicinal plants against blood flukes and whipworms. *Scientific Reports*, **6**:32101 DOI: 10.1038/srep32101 2
- Wang G, Han J, Feng T, Li F, Zhu B, 2009. Bioassay-guided isolation and identification of active compounds from *Fructus arctii* against *Dactylogyrus intermedius* (*Monogenea*) in goldfish (*Carassius auratus*). *Parasitology Research*, **106**:247-255.
- Wang J, Yue YD, Tang F, Sun J, 2012. TLC screening for antioxidant activity of extracts from fifteen Bamboo Species and identification of antioxidant flavone glycosides from leaves of *Bambusa. textilis* McClure. *Molecules*, **17**:12297-12311.
- War AR, Paulraj MG, Ahmad T Buhroo AA, Hussain B, Ignacimuthu S, Sharma HC, 2012. Mechanisms of plant defence against insect herbivores. *Plant Signalling and Behaviour*, **7**:1306-1320.
- Waterman PG, 1999. The tannins - an overview. In Brooker JD (ed) tannins in livestock and human nutrition. *Proceedings of International Workshop*,

Adelaide, Australia, *Australian Centre for International Agricultural Research*: 10–13.

Williams AR, Ropiak HM, Fryganas C, Desrues O, Mueller-Harvey I, Thamsborg SM, 2014. Assessment of the anthelmintic activity of medicinal plant extracts and purified condensed tannins against free-living and parasitic stages of *Oesophagostomum dentatum*. *Parasites and Vectors*, **7**:518.

Williams AR, Peña-Espinoza MA, Boas U, Simonsen HT, 2016. Anthelmintic activity of chicory (*Cichorium intybus*): *in vitro* effects on swine nematodes and relationship to sesquiterpene lactone composition. *Journal of Parasitology*, **143**:770-777.

Williamson SM, Robertson AP, Brown L, Williams T, Woods DJ, Martin RJ, Sattelle DB, Wolstenholme AJ, 2007. The nicotinic acetylcholine receptors of the parasitic nematode *Ascaris suum*: Formation of two distinct drug targets by varying the relative expression levels of two subunits. *PloS Pathogens*, **5**, e1000517.

Wink M, 1988. Plant breeding: importance of plant secondary metabolites for protection against pathogens and herbivores. *Theoretical Applied Genetics*, **75**:225-233.

Wink M, 2012. Medicinal Plants: a source of anti-parasitic secondary metabolites. A review. *Molecules*, **17**:12771-12791.

Wink M, 2015. Modes of action of herbal medicines and plant secondary metabolites. *Medicines*, **2**:251-286.

Wilar G, Kusuma SAF, Ridwan Y, Amni F, 2014. *In vivo* anthelmintic activities of ethanol extract of Croton (*Codiaeum variegatum*) against tapeworm

- Hymenolepis microstoma*. *Scholars Academic Journal of Pharmacy*, **3**:108-115.
- Willcox M, Bodeker G, Bourdy G, Dhingra V, Falquet J, Ferreira JF, 2004. *Artemisia annua* as a traditional herbal antimalarial. *Traditional Medicinal Plants and Malaria*:43–59.
- Xie G, Schepetkin IA, Siemsen DW, Kirpotina LN, Wiley JA, Quinn MT, 2008. Fractionation and characterization of biologically-active polysaccharides from *Artemisia tripartita*. *Phytochemistry*, **69**:1359–1371.
- Yondo J, Komtangi MC, Wabo JP, Bilong CF, Kuate JR, Mpoame M, 2013. Nematicidal efficacy of methanol and methylene chloride extract of *Rauwolfia vomitoria* (Apocynaceae) on *Heligmosomoides bakeri* (Nematoda, Heligmosomatidae) parasite of the white mouse (*Mus musculus*). *Journal of Medicinal Plant Research*, **7**:3220-3225.
- Zagrobelny M, Bak S, Rasmussen AV, Jørgensen B, Naumann CM, Møller BL, 2004. Cyanogenic glucosides and plant–insect interactions. A review. *Phytochemistry*, **65**:293–306.
- Zajac AM, 2006. Gastrointestinal nematodes of small ruminants: Life cycle, anthelmintics, and diagnosis. *The Veterinary Clinics of North America, Food and Animal Practice*, **22**:529-541.
- Zielińska-Pisklak MA, Kaliszewska D, Stolarczyk M, Kiss AK, 2015. Activity-guided isolation, identification and quantification of biologically active isomeric compounds from folk medicinal plant *Desmodium adscendens*. *Journal of Pharmaceutical and Biomedical Analysis*, **102**:54-63.

12. Publications

Full papers

1. **Tolossa K**, Debela E, Athanasiadou S, Tolera A, Ganga G, Houdijk JGM, 2013. Ethno-medicinal study of plants used for treatment of human and livestock ailments by traditional healers in South Omo, Southern Ethiopia. *Journal of Ethnobiology and Ethnomedicine* **9**:32.
2. Athanasiadou S, **Tolossa K**, Debela E, Tolera A, Houdijk JGM, 2015. Tolerance and resistance to a nematode challenge are not always mutually exclusive. *International Journal for Parasitology* **45**, 277-282.

Conference proceedings contributions (Oral presentations)

1. Athanasiadou S, Terry S, Tolera A, Debela E, **Tolossa K**, Connelley T, Burgess S, Houdijk JGM, 2013. *In vitro* validation of the antiparasitic properties of medicinal Ethiopian plant extracts. *Advances in Animal Bioscience* **4**:46.
2. Athanasiadou S, Debela E, Tolera A, **Tolossa K**, Terry S, Houdijk JGM, 2013. *In vitro* validation of the anthelmintic properties of Ethiopian medicinal plant extracts. *Proceedings of the 24th International Conference of the World Association for the Advancement of Veterinary Parasitology*: 615.
3. Athanasiadou S, Debela E, Tolera A, Debela E, **Tolossa K**, Burgess S, Connelley T, Terry S, Houdijk JGM, 2013. *In vitro* validation of Ethiopian

- medicinal plant extracts against ticks and mites. *Proceedings of the 24th International Conference of the World Association for the Advancement of Veterinary Parasitology*: 475.
4. **Tolossa K**, Debela E, Athanasiadou S, Tolera A, Houdijk JGM, 2013. Assessment of ethno-medicinal plants used for treatment of livestock ailments by traditional healers in southern Ethiopia. *Proceedings of the 24th International Conference of the World Association for the Advancement of Veterinary Parasitology*: 630-631.
 5. **Tolossa K**, Debela E, Athanasiadou S, Tolera A, Ganga G, Houdijk JGM, 2013. Ethno-medicinal study of plants used for treatment of human and livestock ailments by traditional healers in South Omo, Southern Ethiopia. *Proceedings of the First Workshop 'Identification, investigation and implementation of plant based parasite control strategies'*. Compiled by Nurfeta, A and Regassa A. Hawassa University, Ethiopia: 7-26.
 6. Athanasiadou S, Debela E, Regassa A, Tolera A, Nurfeta A, **Tolossa K**, Terry S, Houdijk JGM, 2014. Anthelmintic Ethiopian medicinal plants for small ruminants: *in vitro* and *in vivo* studies. *Proceedings of the 13th International Conference for Parasitology*; A2187.
 7. Athanasiadou S, Tolera A, Debela E, **Tolossa K**, Terry S, Regassa A, Nurfeta A, Houdijk JGM, 2014. *In vivo* validation of the antiparasitic properties of medicinal plants. *Advances in Animal Biosciences* **5**, 156.
 8. Nurfeta A, Tolera A, Debela E, Regassa A, Athanasiadou S, **Tolossa K**, Bokore T, Banerjee S, Houdijk JGM, 2014. Evaluation of anthelmintic

- properties of Itacha (*Dodonea angustifolia*) leaves in goats. *Proceedings of the 13th International Conference for Parasitology*; A2746.
9. **Tolossa K**, Fry SC, Athanasiadou S, Loake GJ, Houdijk JGM, 2015. Physico-chemical study and anti-parasitic properties of aqueous *Cissus ruspolii* and *Adenia* sp. extracts. *Advances in Animal Biosciences* **6**:72.
 10. Athanasiadou S, Debela E, Tolera A, **Tolossa K**, Burgess STG, Terry S, Houdijk JGM, 2015. Validation of acaricidal activity of medicinal plants: *in vitro* and *in vivo* studies. *Advances in Animal Biosciences* **6**:73.
 11. **Tolossa K**, Fry SC, Athanasiadou S, Loake GJ, Houdijk JGM, 2015. *In vitro* screening of anti-parasitic properties of four Ethiopian medicinal plant extracts. *Advances in Animal Biosciences* **6**:92.
 12. **Tolossa K**, Fry SC, Athanasiadou S, Loake GJ, Houdijk JGM, 2015. Bio-assay guided fractionation of crude aqueous extracts of *Cissus ruspolii* and *Adenia* sp. *Advances in Animal Biosciences* **6**:94.
 13. **Tolossa K**, Fry SC, Athanasiadou S, Loake GJ, Houdijk JGM, 2015. Bioassay-guided purification of anti-parasitic compounds from indigenous Ethiopian medicinal plants. *25th International Conference of the World Association for the Advancement of Veterinary Parasitology*:pp 174.
 14. Athanasiadou S, Regassa A, Debela E, **Tolossa K**, Nurfeta A, Tolera A, Houdijk JGM, 2015. *In vitro* and *in vivo* validation of bioactive plants for parasite control. *25th International Conference of the World Association for the Advancement of Veterinary Parasitology*: pp 199.